Information Series 110

Downhole Geophysics Project 1986–1990

Final Report

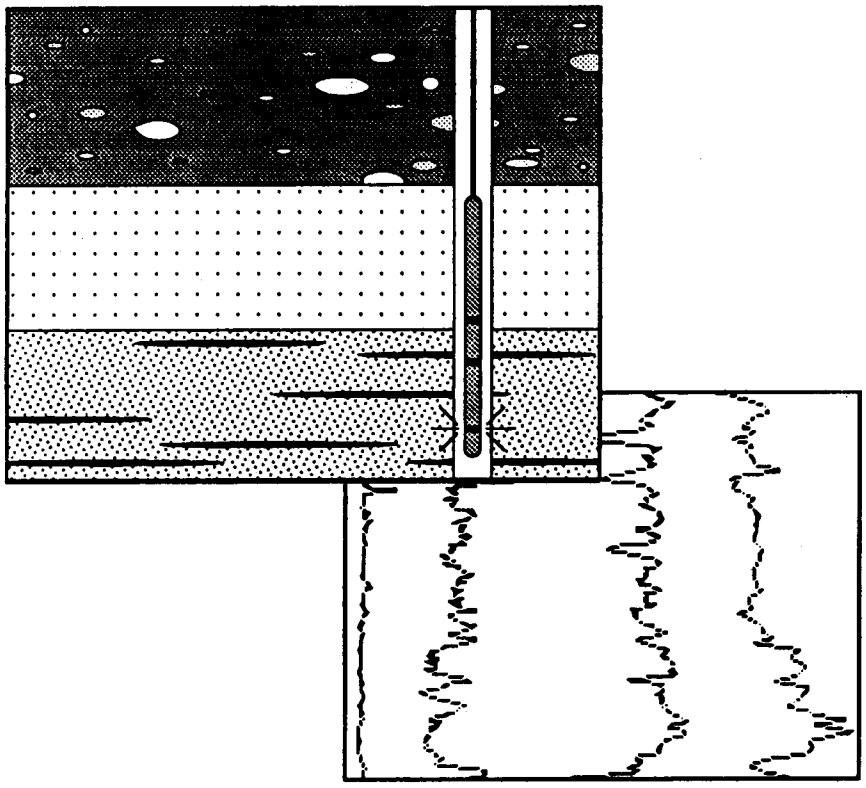

ALBERTA RESEARCH COUNCIL
Environmental Research and Engineering

DOWNHOLE GEOPHYSICS PROJECT
1986 - 1990
FINAL REPORT

compiled and edited
by
Georgia L. Hoffman [1]
Mark M. Fenton [2]
and
John G. Pawlowicz [2]

on behalf of
TransAlta Utilities Corporation
and
a Joint-Venture Group of Companies

December 31, 1990
(Revised January 31, 1991)

Western Economic Diversification file #89-W-04
Alberta Office of Coal Research and Technology file #2835-SP-86/1
Supply and Services Canada file #04SQ.23440-6-9175

[1] G. Hoffman Consulting Services Ltd.
[2] Alberta Research Council

This report will be available for public release March 1, 1992
through the Alberta Research Council as Information Series No. 110.

Copies of this publication can be obtained from:

Alberta Research Council
Publication Sales
250 Karl Clark Road
P.O. Box 8330, Postal Station F
Edmonton, Alberta
T6H 5X2

Phone: (403) 450-5390

DISCLAIMER

The research project for which this report is submitted was funded, in part, from the Alberta/Canada Energy Resources Research Fund, a fund jointly established by the Government of Canada and Government of Alberta, and administered by the Alberta Office of Coal Research and Technology; in part, by CANMET: Energy, Mines and Resources through Supply and Services Canada; and in part, by the Western Diversification Program through the Department of Western Economic Diversification.

LIST OF ABBREVIATIONS

Terms and Units of Measurement	
API	American Petroleum Institute standard units
BRD	bed resolution density (short spaced)
cm	centimetre
g	gram
m	metre
KeV	thousand electron volts
kHz	kilohertz
km	kilometre
LSD	long spaced density
-L	long spaced
-M	medium spaced
mA	milliamperes
MeV	million electron volts
microsec/ft	microsecond per foot
microsec/m	microsecond per metre
mCi	millicurie
MHz	megahertz
min.	minute(s)
mm	millimetre
ms	milliseconds
O.D.	outside diameter
ohm-m	ohm-metres
NN	dual-spaced neutron
ppm	parts per million
r	revolutions
s	second(s)
-S	short spaced
sdu	standard density units
SP	spontaneous potential
snu	standard neutron units
vs	versus
Z	atomic number

ABBREVIATIONS (continued)

Organization and Place Names	
A/CERRF	Alberta/Canada Energy Resources Research Fund
AECL	Atomic Energy of Canada Ltd.
AGS	Alberta Geological Survey
AOCRT	Alberta Office of Coal Research and Technology
ARC	Alberta Research Council
BPB	BPB Wireline Services
BV	Big Valley
CANMET	Energy Mines and Resources Canada (EMR) through Supply and Services (Canada)
CMRC	Coal Mining Research Company
ERED	Environmental Research and Engineering Department
EMR	Energy, Mines and Resources Canada
GSC	Geological Survey of Canada
HV	Highvale
SCL	Syncrude Canada Ltd.
TAU	TransAlta Utilities Corp.
U of A	University of Alberta
UBC	University of British Columbia
U of C	University of Calgary
WED	Western Economic Diversification

Additional abbreviations used in Sect. 3, 6 and 7 are explained in those sections.

ACKNOWLEDGEMENTS

Funding for this four-year research project has been provided by the companies and government agencies listed in Table I, and their support is gratefully acknowledged. Approximately half of the total funding came from industry. The remaining half was shared between the following Provincial and Federal agencies:

the Alberta/Canada Energy Resources Research Fund, a fund jointly established by the Government of Canada and Government of Alberta, and administered by the Alberta Office of Coal Research and Technology;

CANMET: Energy, Mines and Resources, through Supply and Services Canada; and

the Western Diversification Program, through the Department of Western Economic Diversification.

The project was founded by TransAlta Utilities Corporation, which acted as lead company for the joint-venture. Without the efforts of Dennis Nikols, then with TransAlta, who established the joint-venture, and Andrew Hickinbotham who chaired the project through to its completion, this research would not have been possible.

Because of the wide scope of the research, many people from the participating companies contributed to the project during its four year-history; they are listed in Table II. Their participation and assistance are gratefully acknowledged.

The project has benefitted greatly from the guidance of the members of the expert review panels who are indicated in Table II. They deserve much credit, but none of the blame for any of the mistakes that may remain. The suggestions and efforts of W. Scott Keys were particularly helpful and inspiring to the researchers.

This report has been compiled and edited by Georgia L. Hoffman, Mark M. Fenton, and John G. Pawlowicz. Authors of individual report chapters are cited in the introductions to their sections.

Thanks also goes to Kathy Gates, Jennifer Maltby and Tracy Miller for their help in preparing this manuscript.

Table I. Project participants.

Name	Company	Phase 1	2	3a	3b
Balfour, John	Piteau Engineering		•		
Balych, Maurice A.	Manalta Coal				•
Bishop, Richard †	BPB Wireline	•	•	•	
Brawner, Chuck †	UBC	•	•		
Cochrane, Kathryn J.	AOCRT			•	•
Cuddy, Graham	Syncrude			•	•
Dabrowski, Tom	Piteau Engineering	•	•		
Das, B. Manas	EMR Canada	•	•	•	•
Elkington, Peter A.S. †	BPB Instruments				•
Fenton, Mark M.	ARC		•	•	•
Fraser, Edwin	Suncor	•	•		
Gillespie, Ken	Klohn Leonoff		•		
Graham, Peter	Manalta Coal			•	•
Hickinbotham, Andrew	TAU	•	•	•	•
Hoffman, Georgia L.	CMRC/Consultant	•		•	•
Hulatt, Edgar †	BPB Wireline				•
Jenkins, Geoff	Manalta Coal	•	•	•	
Keys, W. Scott †	GeoKeys	•	•	•	•
Kahn, Farrukh Z.	Terracon Geotechnique	•	•		
Killeen, Pat G. †	Geological Survey of Canada	•	•		
Leach, Andrew	Klohn Leonoff	•			
Lobb, Gerry D.	Syncrude	•	•	•	•
Lyons, Brian	Monenco Consultants			•	
Mills, Don	Fording Coal	•	•		
Moran, Steve	ARC		•		
Morgenstern, N. †	U of A	•			
Mwenifumbo, C.J. †	Geological Survey of Canada	•	•	•	•
Nichols, Lee	Terracon Geotechnique	•	•		
Nikols, Dennis	TAU/ARC	•	•		
Nowak, Robert L.	Consultant	•			
Nyland, Edo †	U of A	•			
Pauls, David	ARC	•			
Pawlowicz, John G.	ARC		•	•	•
Pitts, Lloyd	Monenco Consultants	•			
Rozier, Ian	Golder Associates	•			
Scott, Don	U of A	•	•		
Sneddon, Don T.	AOCRT	•	•	•	
Soonawala, Nash	AECL	•			
Trudell, Mark	ARC	•			
Wade, Neil H.	Monenco Consultants	•	•	•	•
Waterhouse, Roger	BPB Wireline			•	
Wilson, Robert A.	CMRC	•	•	•	
Worsely, Neil	Saskatchewan Power	•	•	•	

† Denotes member of expert review panel.

Table II. Funding organizations.

Organization	Phase 1	2	3a	3b
Alberta/Canada Energy Resources Research Fund (A/CERRF) through Alberta Office of Coal Research & Technology (AOCRT)	•	•	•	
Alberta Research Council (ARC), Environmental Research & Engineering Department (ERED)	•	•	•	•
Atomic Energy of Canada Ltd. (AECL), Whiteshell Nuclear Research Establishment	•			
BPB Wireline Services (BPB)			•	•
CANMET: Energy, Mines & Resources Canada (EMR) through Supply & Services Canada	•	•		
Coal Mining Research Company (CMRC)		•	•	
Fording Coal Ltd.	•	•		
Golder Associates	•			
Klohn Leonoff Ltd.	•	•		
Manalta Coal Ltd.	•	•	•	•
Monenco Consultants Ltd.		•	•	•
N. Wade Holdings			•	•
Saskatchewan Power Corporation	•	•	•	
Suncor Inc., Oil Sands Division	•	•		
Syncrude Canada Ltd.	•	•	•	•
Terracon Geotechnique Ltd.	•	•		
TransAlta Utilities Corporation Ltd. (TAU)	•	•	•	•
University of Alberta (U of A)	•			
Western Diversification Program through Department of Western Economic Diversification (WED)				•

SUMMARY

The Downhole Geophysics Project has been a joint venture of coal and oilsands mining operators, consultants, geophysical companies, research organizations, and government agencies. From 1986 to 1990 project researchers studied the practical application of downhole geophysics to the quantitative determination of geotechnical and hydrogeological parameters in overburden materials. The ultimate objective was to identify and refine methods that will improve the collection of geotechnical and hydrological data for coal and oilsands mines in western Canada. Ultimately, this will lead to improved levels of confidence for mine design, generating benefits in such diverse areas as operating costs, mine safety, and environmental impact.

After an initial literature review, sets of geophysical, geotechnical and hydrological data from Alberta coal and oilsands mines were needed to test the correlations between geophysical log responses and the parameters of interest. Geophysical logs were reviewed to find sets from drillholes in which geotechnical parameters had been determined on samples taken from known depths within those holes, or where hydrological tests had been conducted over a specified interval. Much of the data proved to be unsuitable for quantitative analysis however, and the number and size of the usable data sets was much smaller than originally envisioned, especially for hydrological data.

Extracting the data and organizing it into unified databases proved to be much more difficult than expected. Problems included depth mismatches between the geophysical logs and the geotechnical and hydrological information; differences in data reporting units between different logging and laboratory contractors; and variations due to calibration and correction routines that had been applied to the logs. In many cases it was difficult to extract complete data sets, and multiple extractions and recombination were required. It became apparent that better data handling and analysis procedures would be needed before operating mines could make practical use of quantitative log analysis, so much subsequent work was devoted to those aspects.

Despite the above difficulties, preliminary analysis of the geotechnical and groundwater data sets indicated that there were correlations between a number of the parameters of interest and the responses of some of the geophysical logs. Those correlations were refined and strengthened during the subsequent work. The conclusions and recommendations are :

• Data related to geotechnical and groundwater problems can be derived from geophysical logs, and can be used to supplement data obtained by more expensive conventional means such as core testing.

• The relationships between log response and geotechnical and hydrologic factors are site-specific and have to be substantiated at each new site.

• One of the most important techniques available for log analysis today is the use of computers to: (1) correct log suites for depth and other variables; (2) crossplot data obtained from logs against data from other logs, core analyses, or tests; and (3) analyze these data both graphically and statistically. Quantitative log analysis by computer can and should be used to provide information that is not available from standard visual inspection of paper log charts.

• Log interpretations and correlations should be made by someone who is thoroughly familiar with the algorithms used and local geology and hydrology of the site in order to avoid misleading conclusions.

• A number of steps must be taken to ensure reasonable accuracy of the data if geophysical logs are to be interpreted quantitatively: (1) the equipment must be properly calibrated and standardized to ensure that log response is reproducible and can be related to environmental units such as density or percent porosity; (2) logs must be checked for extraneous effects such as hole diameter changes and beds that are too thin to be resolved correctly; and (3) corroborating core samples must be taken carefully after examination of the geophysical logs, so that their depth correlation with thicker, uniform beds shown by the logs is known with certainty.

• Before quantitative log analysis can start: (1) depths must be corrected so that corresponding points on each log and core sample are at consistent depths; (2) effects produced by drilling fluids, changes in borehole diameter, and well construction techniques must be corrected; and (3) beds that are thinner than the limits of resolution of the instruments should be excluded from consideration or corrected. Log data that cannot be corrected for the above factors are unsuitable for quantitative analysis.

• All logs should be provided by the logging contractor both as a paper print and in digital form. A paper print of each log must be provided in the field. The digital data may be provided later and should be an ASCII file on a 3-1/2 inch floppy disk, with a space-delimited columnar format, and the depth values and each corresponding set of log values in separate labelled columns.

• During this research project, satisfactory quantitative correlations were obtained between several types of standard geophysical logs (sonic, density, neutron, gamma caliper and resistivity) and a variety of geotechnical parameters including moisture content, liquid and plastic limits, bulk and dry density, plasticity index, and uniaxial compressive strength.

• The sonic log gave the best indication of water table in both clay-rich and sandy material. Resistivity, neutron and density logs could also detect the water table under some conditions. Generally the water table could be more readily detected (1) in coarse-grained (sandy) sediment than in fine-grained (clayey) sediments, and (2) by using a suite of logs together rather than individual logs separately. It is recommended that, for increased confidence in recognizing the water table, a suite of logs including sonic, resistivity, neutron and density should be run and interpreted together.

• Glacially deformed bedrock is a geotechnically weakened material that is significant to exploration and mining activities in the Alberta Plains because of its impact on highwall stability, coal recovery, etc. Geophysical data from the sonic, density, neutron, and dipmeter logs were applicable to the identification of deformed bedrock. The dipmeter data may allow glacially deformed bedrock to be divided into deformed and undeformed units over intervals as thin as 1 m. It is recommended that sonic, density, neutron, and caliper logs, and if possible dipmeter and acoustic-televiewer logs, should be run and interpreted together for the detection and evaluation of glacially deformed bedrock.

• The spectral gamma log proved to be capable of identifying bentonite and montmorillonitic clays that cause problems for pit-wall stability. It was more effective than ordinary total-count gamma logs for determining clay content or shaliness. The spectral gamma ray logging tool should be used: (1) for better lithologic correlations between holes; and (2) where a detailed understanding of mineralogy and clay content is required.

• The assessment of other new tools indicated that: (1) the full-wave sonic log can provide data to calculate rock properties applicable in mining and geotechnical engineering; and (2) the acoustic-televiewer can provide high-resolution information on the strike and dip of bedding, and on the location, orientation and character of secondary porosity such as fractures and solution openings. New small-diameter logging tools, digital surface equipment and software are becoming available which will provide the quality of data approaching that of the more expensive oilfield tools.

• To implement a program of quantitative log interpretation, a mine should begin

building a database that can be used to establish the relationships between log response and geotechnical or hydrological parameters for their site(s), by: (1) obtaining their geophysical log data in digital form; (2) ensuring that log quality is suitable for quantitative analysis as described in Sec. 2; and (3) ensuring that core samples (or hydrological tests) are taken with reference to the geophysical logs, so that the depth correspondence between them is known with certainty.

Recommendations for future research are:

- Research on the relationship between geophysical log response and parameters of interest to mining should continue. Future research should extend the correlations to include: (1) a wider range of lithologies and locations; (2) other geotechnical parameters such as grain size, strengths from triaxial tests, and consolidation test parameters; (3) other hydrological parameters such as hydraulic conductivity; and possibly (4) other factors such as coal quality or oilsands grade.

- Additional data from full-wave sonic logs should be obtained for correlation with the various geotechnical parameters including Poisson's ratio, Young's modulus, shear modulus, and bulk modulus.

- Continuous spectral-gamma logging tools of the type provided by service companies should be tested to determine their correlations between natural radioisotope content and clay content, clay mineralogy and/or geotechnical index properties.

- Geophysical logs, core samples and/or groundwater data for future studies should be taken at a site that has: (1) well-documented geology; and (2) good drilling characteristics so that core recovery can be maximized and hole caving can be minimized. The drillers should be instructed that both core recovery and hole condition have high priorities. The holes should be continuously cored, there should be sufficient logging time available to test variations in logging speed and related factors, and there should be provision for complete laboratory analysis of core samples. Log response must be used to select the core samples, because the the correspondence between the two must be known with certainty. If the water table is of interest, it should be known from piezometer data to be stable at a depth greater than 4 m. The research should be conducted at an active mine, so that when mining eventually proceeds into the study area, production rates and problems can be compared with those anticipated from the study results; project funding and timing must be sufficient to allow for this task.

TABLE OF CONTENTS

6. USE OF SPECTRAL GAMMA FOR CLAY MINERALOGY

C. Jonathan Mwenifumbo and John G. Pawlowicz

7. POTENTIALLY APPLICABLE NEW TOOLS

W. Scott Keys, C. Jonathan Mwenifumbo and Edgar W. Hulatt

8. CONCLUSIONS

9. RECOMMENDATIONS

LIST OF FIGURES

Figures (continued)

Figures (continued)

Figures (continued) Page

Figures (continued) Page

Figures (continued) Page

LIST OF TABLES

1. INTRODUCTION

Georgia L. Hoffman and Robert A. Wilson

1.1 TECHNICAL SIGNIFICANCE

The Downhole Geophysics Project began in 1986 as a joint venture of coal and oilsands mining operators, consultants, geophysical companies, research organizations and government agencies. The group has studied the use of downhole geophysics to determine geotechnical and hydrological parameters in overburden materials. The ultimate objective has been to decrease costs and increase data availability, continuity and accuracy for coal and oilsands exploration, open-pit mine planning and operations.

Engineers must address a variety of problems when designing and operating surface mines. These include stability of highwalls and spoil piles; diggability of overburden materials; the ability of overburden and pit-floor materials to support mine equipment; and the impact of groundwater on the mining operations and materials handling. Geological, geotechnical and hydrological factors play major roles in solving these problems.

In the mining industry, downhole geophysical logs have rarely been used to obtain geotechnical and hydrological data. However, a suite of natural gamma, resistivity, density and caliper logs is normally run in most coal and oilsands exploration drilling programs in western Canada and in some instances supplementary neutron, sonic and dipmeter logs are also run. The logs are used primarily qualitatively, to determine geological stratigraphy and to verify the depth and thickness of ore zones. Extending the use of the logs to the quantitative determination of geotechnical and hydrological information would have immediate practical and economic benefits, as would identifying new logging tools that should be applied to these problems.

1.2 OBJECTIVE

The ultimate objective has been to develop downhole geophysical techniques that will reduce the cost of open-pit mining through improved mine design, by providing more abundant, continuous and reliable and less costly geotechnical and hydrological information about the overburden materials that occur with western Canada's coal and oilsands deposits.

1.3 PROJECT HISTORY AND ORGANIZATION

1.3.1 Formation of the Project

During the spring of 1985, the western Canadian coal and oilsands mining community held meetings to consider the potential for a program of research on the use of borehole geophysical logs to obtain geotechnical and hydrological information. The success of a surface geophysics research project conducted by a group of plains coal producers suggested that a cooperative research venture was a viable approach. After several exploratory meetings, a working group was formed under the leadership of Dennis Nikols, then with TransAlta Utilities. That group developed an outline of the project objectives, scope and management structure. The outline was submitted to the Coal Mining Research Company in the fall of 1985 for the development of a firm project proposal, budget, and work plan.

The interested companies established a formal joint-venture under the leadership of TransAlta Utilities, and sought matching funds from government agencies. Because of Federal and Provincial jurisdictional arrangements regarding coal and oilsands, two separate proposals were developed with complimentary work plans and budgets, and a single unified reporting system and management structure. Those proposals were submitted to the Alberta Office of Coal Research and Technology (coal proposal), and to Supply and Services, Canada under the sponsorship of CANMET (oilsands proposal) in March of 1986.

The research strategy was to utilize the broad spectrum of expertise, information and data that was available through the coal and oilsands mining operators, consultants, geophysical companies, research organizations and government agencies that formed the joint venture. Individuals with appropriate backgrounds in mining engineering, geology, geophysics or groundwater were assigned to the project according to the objectives of each phase, and tasks were divided amoung the individuals or subcommittees. A review panel of experts was also established.

1.3.2 Phase 1

The proposals for funding and the first year's work plan were accepted by the funding agencies in the summer of 1986. The associated contracts were finally signed in November 1986. The objective of Phase 1 (November 1986 to March 1987) was "to examine the current state of the art and the published literature concerning the use of downhole geophysics to obtain various geotechnical and hydrological parameters".

A list of keywords was developed and used to search for potentially relevant publications. References were also submitted by participants. The resulting list included 1435 citations, from which 326 were selected for detailed review by the subcommittees. A summary of each paper was included in the two-volume Phase 1 report, "A Review of Potential Applications" (TransAlta Utilities, 1987). The most relevant references are cited in the References (Section 10) of the current report.

1.3.3 Phase 2

The proposals for Phase 2 were submitted in the fall of 1986 and work commenced upon approval in May, 1987. The objective was "to evaluate the techniques identified in Phase 1 to obtain various geotechnical and hydrological parameters from downhole geophysics; and to review which tools, not currently in use in Alberta, might have potential to provide the desired parameters".

Work was divided amoung participants with appropriate technical backgrounds. Geophysical logs from some of the participants' mines were reviewed to find sets from drillholes in which geotechnical parameters had been determined on samples taken from known depths within those holes, or where hydrological tests had been conducted over specified intervals. The number and size of the resulting data sets proved to be much smaller than originally envisioned, especially for hydrological data.

Extracting the data and organizing it into unified databases proved to be much more difficult than expected. Problems included depth mismatches between the geophysical logs and the geotechnical and hydrological core and test data; differences in data reporting units between different logging and laboratory contractors; and variations due to calibration and correction routines that had been applied to the logs. Some companies found that the data extraction routines of their in-house databases were not capable of directly extracting the complete data set, and multiple extractions and recombination were required. Reformatting was usually required before the data could be transferred between the various researchers in a usable form. The extra work necessitated revisions to the work plan and budget. It became apparent that better data handling procedures would be needed before operating mines could make practical use of quantitative log analysis, so much subsequent work was devoted to those aspects.

The most complete geotechnical data sets came from TransAlta's Highvale coal mine near Edmonton, and Syncrude's oilsands mine near Fort McMurray (Fig. 1-1). The hydrological data sets were from an Alberta Research Council study of the groundwater environments at the Highvale Mine and in the Battle River Region.

The literature review had identified several significant correlations between geophysical log values and geotechnical or hydrological parameters, and these were tested on the Highvale and Syncrude data sets. Because of the delays caused by the data extraction problems, the data sets were used as received, without any corrections or depth adjustments. These initial trials indicated that several of the correlations had promise in the local geological setting, and it was felt that these correlations could be strengthened by detailed editing of the data sets to eliminate erroneous data, to correct depth mismatch between the logs and the laboratory data, and to refine the geophysical value averaging over the corresponding laboratory sampling intervals. The Phase 2 report "Correlations of Existing Data" (TransAlta Utilities, 1988) recommended that this be done during Phase 3.

Newly developed or otherwise untested geophysical tools were also reviewed in detail during Phase 2. The full-wave sonic tool, the Geological Survey of Canada's instruments, and others were designated for testing if suitable opportunities arose.

1.3.4 Phase 3A

The proposal for Phase 3 was split into two years (3A and 3B) in response to the Phase 2 recommendations and changes in the funding support from government and industry, as described in the Phase 3A report (TransAlta Utilities, 1989). The objective of Phase 3A was "to further enhance the data sets and the resulting correlations by the inclusion of more data and by careful refinement of the assumptions used in Phase 2 for interval selection. Further evaluation of the newly available full-wave sonic tool and other new instruments [was] also part of the Phase 3A objectives".

Work was again divided amoung the participants. Several participants found relatively inexpensive software packages that they felt were effective for handling and analyzing log and laboratory data from shallow, non-petroleum drillholes. By the end of Phase 3A it had become much easier for researchers and experts to exchange and analyze the data sets.

A careful review of geophysical logging principles and tool responses at bed boundaries led to a refinement in the selection of geophysical log intervals to be matched against the geotechnical and hydrological data. This improved the correlations for many of the parameters.

In October 1988 there was an opportunity to collect new data specifically targeted for this project. As a result, project representatives supervised the logging, sampling, and

laboratory analysis for several holes at TransAlta Utilities' Big Valley site near Stettler (Fig. 1-1). Piezometers were set near several holes so that the water table could be monitored. This very carefully documented data set was used to evaluate the changes in data collection methods that had been suggested by the earlier work.

Evaluation of new tools also continued during Phase 3A. This included preliminary evaluation and testing of a full-wave sonic tool, and field trials of the Geological Survey of Canada's spectral gamma, resistivity, temperature and other devices in the summer of 1988. A preliminary review of the results was completed by the end of February 1989 and included in the Phase 3A progress report.

1.3.5 Phase 3B

Changes in funding delayed the start of the last phase until August 1989. The objective of Phase 3B was "to finalize the correlations between the geophysical logs and the desired geotechnical and hydrological parameters; to formalize the procedures by which mine operators can make use of these suitable correlations; to document the suitability of new geophysical tools for the collections of geotechnical and hydrological information; and to provide a Final Report on the entire four-year project". The Phase 3B tasks were completed by the summer of 1990, and this report describes the final results and conclusions of the project.

1.3.6 Geology of the Test Sites

The work described in this report was conducted at the Highvale Coal Mine, Big Valley, and the Syncrude Oilsands Mine (Fig. 1-1). At Highvale, the study involved the overburden layers immeadiately on top of the mineable coal seams of the Ardley coal zone (Fig. 1-2). Those strata are of lowermost Tertiary (Paleocene) age and consist of poorly consolidated, clay-rich sandstones, siltstones, mudstones, bentonitic mudstones, and bentonites. The work at Big Valley extended into the strata below the Ardley zone, which are lithologically very similar to those above it. Montmorillonite, an expanding clay which poses problems for slope stability, is a common clay mineral at both sites, particularly in the bentonitic units. Some of the bedrock in both areas was deformed by ice movement during the Pleistocene, which increased its weakness.

The work at Syncrude involved the weak, poorly indurated marine mudstones and shales of the Lower Cretaceous Clearwater Formation (Flach, 1984) which overlie the ore zone in much of the mine area (Fig. 1-3). The Clearwater strata also contain montmorillonite, and pose problems for mining operations.

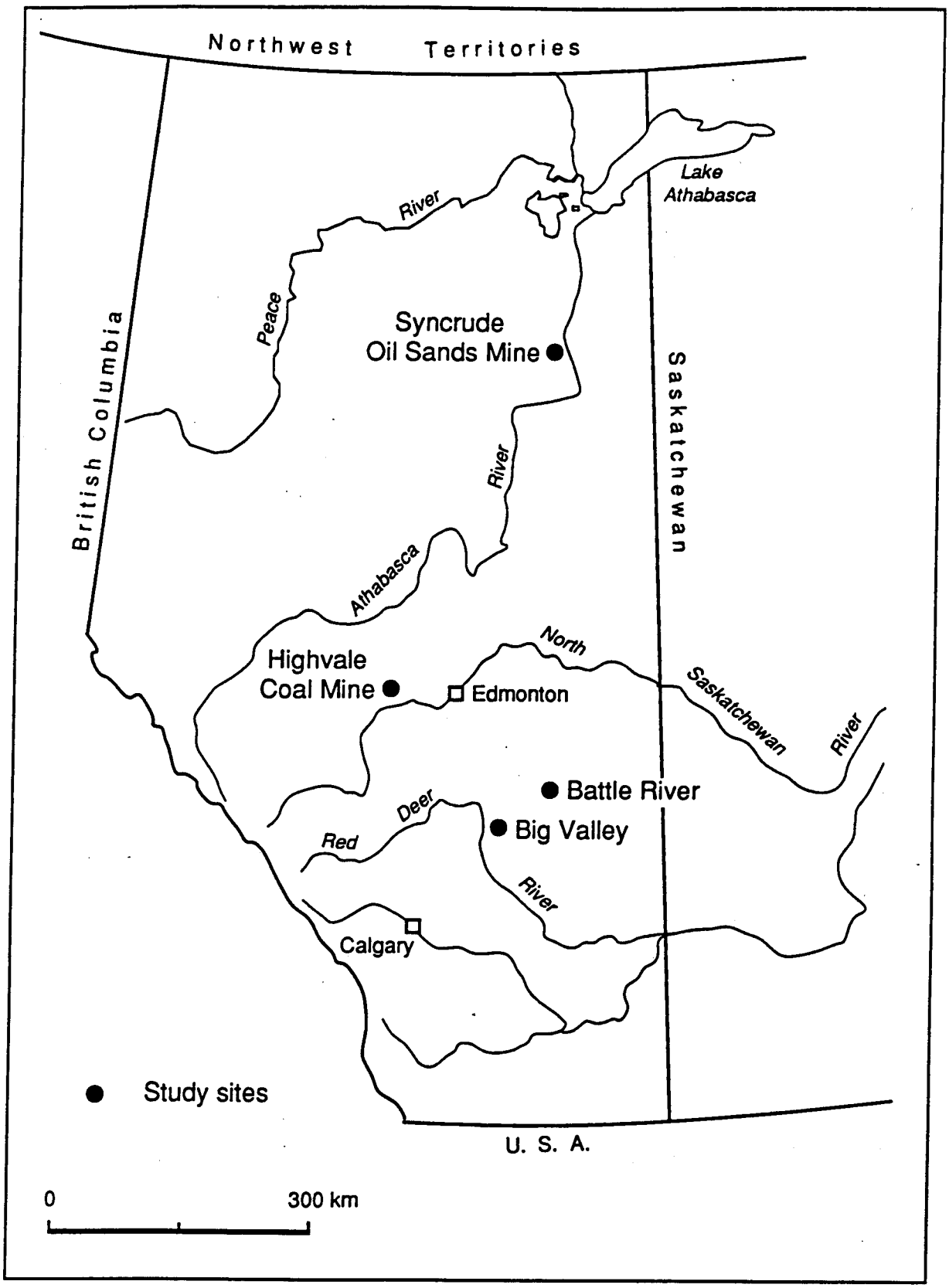

Figure 1-1. Location of study sites in Alberta.

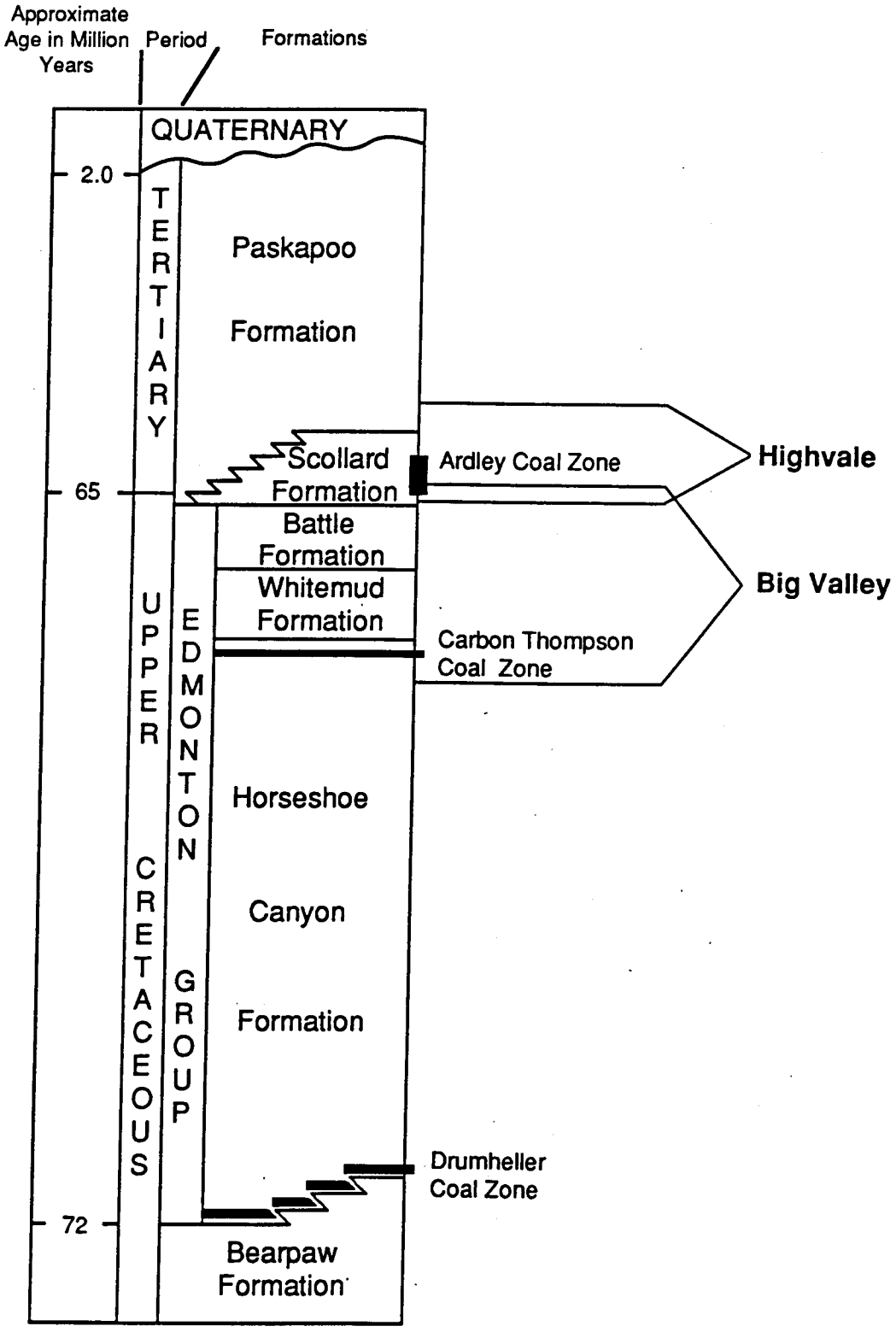

Figure 1-2. Stratigraphy of Highvale and Big Valley sites (modified from Irish, 1970).

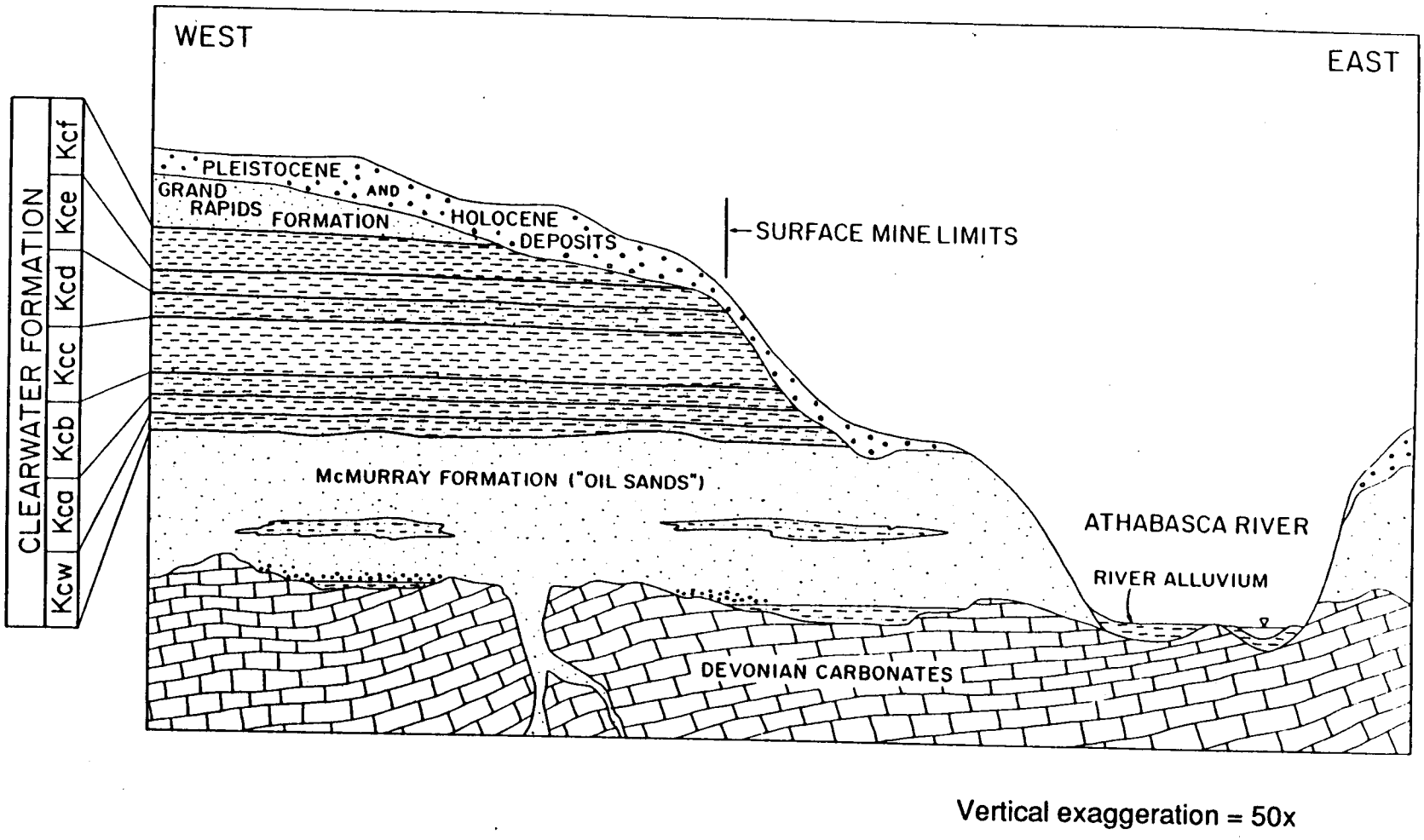

Figure 1-3. Stratigraphy and geology of the Syncrude site.

2. GENERAL METHODS OF ANALYZING GEOPHYSICAL LOGS AND CORE DATA

W. Scott Keys, Georgia L. Hoffman and John G. Pawlowicz

Problems with inconsistent data quality proved to be a major obstacle in the early stages of the research. Uncertainties about core sampling and the original geophysical field procedures, data acquisition, and correction procedures rendered the majority of the available data sets unsuitable for quantitative analysis. Data handling was also a problem, and at first large amounts of time had to be spent editing, reformatting, rearranging and replotting log and laboratory data before any relationships could be isolated or evaluated. The discussions below provide some recommendations that should help the reader avoid many of the common pitfalls.

It is assumed that the reader is familiar with the most common types of geophysical logging devices: caliper, density (gamma-gamma), sonic, neutron, and resistivity; if not, descriptions may be found in Keys (1989a) and Hoffman et al. (1982).

2.1 DATA ACQUISITION

2.1.1 Recording the Geophysical Data

A geoscientist who understands the project objectives and the local geology and hydrology must observe and make suggestions to improve the procedures and results in the logging truck, until the equipment operator is completely familiar with the logging parameters needed for that site. The observer usually makes preliminary interpretations of the logs as they come off the recorder so that reruns can be requested immediately if problems are suspected. A few symptoms can be recognized during logging that may suggest equipment malfunctions; these include periodic oscillations, nonlinear response, temperature drift, noisy sections, or rapid transients. So many factors must be remembered by the observer to help control the quality of logs that many major oil companies provide a quality control check-list. An example of such a list is found in Keys (1989a). The observer should ensure that all of the factors that will be needed for quantitative interpretation of the logging data have been measured, including the resistivity, density and temperature of the drilling fluid. Repeatability should be tested by logging selected intervals of the hole a second time.

Depth readout needs to be checked against the analog record periodically and at the depth reference point for the well when the probe returns to the surface. A uniformly

distributed error can be corrected easily in a computer; random, unknown corrections by the operator cannot be reconstructed. Depth errors that are not consistent throughout a suite of logs often can be recognized by a careful correlation of anomalies between logs and readily corrected by a computer. Core data may provide some information on correct log depths; however, errors on core depths are very common.

The selection of the horizontal and vertical scales that will provide the most useful data and the required resolution without "noise" is difficult; these are among the most important aspects of log quality control. Many commercial logs are run on a horizontal scale that is too compressed, in the interest of simplifying the logs by eliminating multiple back-up curves. To some degree, the ability to digitize logs on-site permits more latitude in the selection of scales because the digitized logs later can be replotted at more suitable scales.

Sample interval and sample time need to be correctly selected for the on-site digitizing of logs. Sample intervals of 0.1 m may be adequate for some studies; however, for detailed investigations, intervals as small as 0.01 m may be necessary. If too many samples of the data are recorded, every other or every tenth sample can be used, and the data can be averaged or smoothed. If not enough samples are recorded, needed information may be lost. Sample time is the duration of time over which a single digital sample is recorded. Sample time may be milliseconds or less for analog voltages but may be 1 s or longer for pulse signals from a nuclear logging probe. Digital sample time is important to the proper recording of all nuclear logs; it should not be too short in order to reduce statistical error.

The digital data may be printed or plotted while the log is being run, but for the true analog recording to be replaced by a digital playback is not recommended. Watching a log develop on a chart type recorder is one of the best ways to avoid major errors in logging and to optimize probe and data input configurations. The analog record may show more detail than the digital record because of sample interval or the elimination of the step function present in many plots of digital data. Information on the digital record always is listed on the log heading of the analog chart. This information includes the label on the recording medium, file number, sample interval, sample time, and depth interval recorded, and any calibration information pertinent to the digital record. The digital-recording medium needs to be write-protected and labeled, as soon as it is removed from the recorder. These valuable records need to be backed up by copying as soon as they are received in the office.

To have logs digitized commercially, certain specifications or instructions should be provided to the company with the purchase order. What recording medium will be used, and who will provide it? Usually 7- or 9-track magnetic tape is used by major companies, and floppy disks are used for smaller data sets. The format and bits per inch must be specified. The types of logs to be digitized must be listed, along with the specific curve on each log, the depth interval, the sample interval, and vertical and horizontal scales. If editing of logs is to be done, it must be specified. Editing would include such changes as depth shifts up or down in specified depth intervals, removing cycle skips from acoustic-velocity logs, or eliminating off-scale deflections. In addition to the computer-compatible recording medium, the customer can specify a printout of all digital data and check plots of the logs. If the check plots are on the same scale as the original, they can be overlaid to verify the accuracy of digitizing.

2.1.2 Calibration and Standardization

If logs are to be used for any type of quantitative analysis or used to measure changes in a groundwater system with time, they need to be properly calibrated and standardized. For example, the gamma log is most widely used for identification of lithology and stratigraphic correlation; in addition studies in various sedimentary basins throughout the world have demonstrated local relations to grain size distribution and to permeability. Such relations cannot be demonstrated unless the logs used have a standardized response. A gradual change in gamma response across a depositional basin may be the result of a change in the percentage of clay and silt, or the result of equipment drift.

Calibration is considered to be the process of establishing environmental values for log response in a semi-infinite model that closely simulates natural conditions. Environmental units are related to the physical properties of the rock, such as porosity or acoustic velocity. Probe output may be recorded in units, such as pulses per second, that can be converted to environmental units with calibration data. Calibration usually is carried out before going to the field to log.

Standardization is the process of checking response of the logging probes in the field, usually before and after logging. Standardization uses some type of a portable field standard that usually is not infinite and may not simulate environmental conditions. Field standards need to be checked before and after each log and the values placed on the log if the data are to be used quantitatively. Frequent standardization of probes provides the basis for correcting for system drift in output with time or temperature. Repeatability is best ensured by logging selected depth intervals a second time; equipment drift is indicated by changes in response as a function of time or

temperature.

2.1.3 Cored Drillholes

Borehole cores that have been carefully recovered and analyzed quantitatively may also be used to calibrate logging probes. Because of the matrix effect, calibration in one rock type may not ensure accurate porosity or bulk density scales in another rock type. For this reason, if the rocks being logged are not the same as those in which the equipment was calibrated, core analyses are needed to check values on the logs.

The use of core data is fundamental to identifying or confirming relationships between log response and geotechnical parameters, coal quality data, etc., and it is of course essential that the position of the core sample be correlated precisely with the correct interval on the logs. To reduce depth errors, core recovery in calibration holes needs to approach 100 percent for the intervals cored. Log response should be used to select the core samples for laboratory analyses, and the logs should be compared to the core in the field immediately after they have been run. Discussions of the use of logs to select coal core sample intervals are included in BPB (1981), Hoffman et al. (1982), and Sec. 3 and 4.

Because of the possibility of depth errors in both core and logs, and of bed thickness errors, samples should be selected in thicker units, where the bed is thicker than the vertical resolution capability of the probe (Sec. 2.2 and 2.3), and where the log response is consistent and free of bed boundary effects. This problem is illustrated in Fig. 2-1 where the mean and standard deviation of the log data for the depth intervals corresponding to core depths (shown as bars) indicate that correlation coefficients with core data are likely to be very poor. Note that several of the samples were taken across depth intervals where the density log indicated a gradational change in lithology.

2.2 DATA HANDLING

Obtaining quantitative data on mining and groundwater characteristics of rocks is a major objective of the logging programs described in this report. In order for the logs to be interpreted quantitatively a number of steps must be taken to ensure reasonable accuracy of the data. The repeat curve should be inspected, and then the scales on logs in environmental units (e.g., percent porosity, bulk density in grams per cubic centimetre (g/cm^3), or resistivity in ohm metres (ohm-m)) need to be checked. Even if the procedures described under log calibration and standardization are followed carefully, corroborating data from core samples are needed for the particular rocks and

wells logged at each site. Before any log data are used quantitatively, they must be checked for extraneous effects, such as hole diameter changes or thin beds that are not accurately resolved. Log data are of questionable value when they are from depth intervals where hole diameter is significantly greater than bit size, or from intervals where bed thickness is equal to, or less than, the vertical dimension of the volume of investigation for the probe.

2.2.1 Depth Correction of Logs

The computer is suited ideally for correcting logs and plotting them with calibrated scales. Depth correction is required on a very large number of logs, and it can be carried out at the same time the computer is being used to make the first plot of digitized data. The most common correction needed is a consistent depth shift for the entire log to make it correlate with other logs of the same well or with core data. A technique for the computer correlation of log and core data is described by Jeffries (1966), and most log analysis software provides methods for depth correction. Sometimes all of the logs in a suite will require some shifting to agree with a preselected datum. Sudden changes in depth may occur randomly in the log, because of a sticking probe or because of changes cranked in manually by the operator when a magnetic cable marker is detected. These types of errors are best avoided, if possible, but need to be noted on the log when they occur. Different corrections for specific depth intervals will produce either overlap or missing data sections that will require editing. VIEWLOG (Sec. 2.4) includes an elastic stretch or compress transform that greatly simplifies the correction of varying depth errors between logs.

2.2.2 Calibration of Log Scales

Few logs measure the quantity shown on the horizontal scale directly; for example, the neutron log does not measure porosity; it responds chiefly to hydrogen content. The difference between porosity and hydrogen content can lead to a large porosity error where bound water or hydrocarbons are present. Thus, a knowledge of the principles of log-measuring systems is a prerequisite to the accurate quantitative analysis of logs.

Data from probe calibration can be entered in the computer to produce a log in the appropriate environmental units such as density or porosity. Most probes output a pulse frequency or a voltage that is related to the desired parameter by an equation. For example, most density logs are recorded in pulses per second, which can be converted to bulk density by a computer, if proper calibration and standardization data are available.

Replotting logs to produce scales best suited for the intended purpose is a simple matter with a computer. Correcting for nonlinear response or changing from a linear to a logarithmic scale are also simple procedures with some log analysis software packages such as VIEWLOG. Logs can also be plotted at several different scales to keep the full data range on the paper and, at the same time, to resolve small but significant changes.

2.2.3 Borehole Effects

The manner in which a test hole or well is drilled, completed, and tested has a significant effect on geophysical logs made in that well. One of the objectives of logging is to obtain undisturbed values for such rock properties as porosity, bulk density, acoustic velocity, and resistivity, but the drilling process disturbs the rock near the drillhole to varying degrees. Borehole effects on geophysical logs can be divided into those produced by the drilling fluids, borehole diameter, and well construction techniques. All these procedures can be controlled to produce better logs, if that is a high-priority objective.

2.2.3.1 Drilling Fluid Effects

The hydrostatic pressure of the fluid column is an important factor in preventing caving in poorly consolidated materials. This same pressure can cause invasion of the rocks by the mud filtrate and the development of a filter cake or mud cake on the wall of the hole. Coal, oilsand, groundwater and geotechnical drillholes are much shallower than typical oil and gas holes, so lower pressures are used and drilling time is shorter; these effects may therefore be reduced but not necessarily eliminated. Mud cake may reduce permeability and, thus, change results obtained from various flow logging devices or packer tests. The thickness of mud cake often is related to the permeability and porosity of the rocks penetrated. A comparison of a log that measures material close to the hole, such as microresistivity, with a deeper investigating log, such as focused resistivity, will indicate the amount of invasion that has taken place. The relation between the conductivity of the fluid in the borehole and in the adjacent rocks will determine the magnitude and direction of deflection on a spontaneous potential log. Invasion by drilling fluids may change the conductivity of the pore water and reduce porosity and permeability in the vicinity of the borehole. Hydraulic fractures can be induced in hard rocks by overpressure during drilling. Drilling-induced fractures commonly are observed on acoustic-televiewer logs (Sec. 7.3); these fractures not only may affect log response, but may also increase vertical permeability.

2.2.3.2 Hole Diameter Effects

Although many logs are titled "borehole compensated" or "borehole corrected", almost all logs are affected to some degree by significant changes in borehole diameter. All boreholes, except those drilled in very hard rocks like granite, have thin intervals where hole diameter exceeds bit size sufficiently to cause anomalous log response. For this reason drilling needs to be planned to minimize changes in hole diameter, and high resolution caliper logs need to be run to detect such changes. For purposes of log interpretation, hole diameter changes can be subdivided into those caused by bit size, where only the average diameter is affected, and thin intervals of high rugosity, caused by a combination of drilling technique and lithology. Logs usually can be corrected for average hole diameter, but thin zones of different diameter spanned by the logging tools are difficult to correct.

Many borehole compensated probes employ two detectors at different distances from the source of the signal, and the log is based on the ratio of output of these detectors. In theory, the different length of the paths traveled to these detectors allows cancellation of some of the effect of near-borehole cavities or washouts. The short-spaced detector is supposed to be affected by the cavity; the long-spaced detector is not. The accuracy of such techniques over a wide range of borehole conditions is questionable and it is desirable to obtain the unprocessed data from both detectors rather than just the calculated log.

From the standpoint of quantitative log analysis, the best procedure is to eliminate from consideration those depth intervals that demonstrate diameter changes that are significant with respect to the borehole diameter response of the logging tool. Determining the significance of changes might be done in several ways. Test data on a specific probe might indicate the magnitude of hole diameter response. If the log being analyzed has deflections that closely match the intervals where the caliper log shows hole diameter changes, those intervals can be eliminated from quantitative analysis. Although such changes in hole diameter might be caused by lithology, log response caused by a change in lithology is very difficult to separate from that caused by a change in borehole diameter. Also, not all hole diameter changes are caused by drilling. Solution openings, open fractures, and vesicles can exist to great depths, and they are an intrinsic part of the rock fabric to be considered during log analysis. An acoustic-televiewer can be particularly useful for distinguishing such primary features from drilling-induced hole enlargements. Changes in hole diameter behind casing will have a significant, but undetermined, effect on through-the-casing logs. Thus, a caliper log needs to be made before casing is installed, if possible.

2.2.3.3 Volume of Investigation

The volume of investigation needs to be considered in evaluating log data and in log analysis, because it has a significant effect on response to borehole characteristics and to beds of different thickness. The size and shape of the volume of investigation change in response to changing borehole conditions and to the physical properties and geometry of boundaries in the rock matrix. Decentralized, side-collimated, dual-detector probes are often called "borehole compensated" because they may reduce the percentage of the total signal coming from the borehole and the mudcake.

In general, longer spacing between the source of energy and the detector increases the radius of investigation and reduces borehole effects, because the volume of investigation encompasses a larger volume of undisturbed rock. However, if a bed is thinner than the vertical dimension of the volume of investigation or thinner than the spacing, the bed will not be resolved correctly, and the log seldom provides accurate measurement of its thickness or physical properties. Under these conditions, the volume of investigation includes some of the adjacent beds, so that the signal or data recorded as a log is an average of the data from several lithologic units.

A radiation detector will begin to receive some data from a bed before it arrives at that bed. When the detector is centered on the contact between two beds of sufficient thickness, roughly half the signal will be derived from one unit, and half from the other; selection of contacts at half amplitude for nuclear logs is based on this model. If a nuclear or other slow-responding log is run too fast, contacts will be hard to pick and apparently will be displaced upward. If a bed is too thin with respect to the probe spacing, it may not cause any response on the log; this becomes a problem at high logging speeds.

2.3 DATA ANALYSIS AND INTERPRETATION

After logs have been properly recorded and the data have been processed to reduce errors, logs can be analyzed qualitatively or quantitatively to provide predictive information on the rocks and their contained fluids. For either type of analysis, borehole conditions need to be known, because they can alter log response significantly.

2.3.1 Qualitative Interpretation

Qualitative log analysis is based mostly on knowledge of the local geology and hydrology, rather than on log response charts or computer plots. Examination of outcrops, core and drill cuttings, coupled with an understanding of log response, will permit the identification and correlation of rock units and aquifers. Logs should be interpreted as an assemblage of data, not singly, to increase the accuracy of analysis. The accuracy of qualitative interpretation usually improves with an increase in the number of wells that are logged in an area and the amount of core data that is available. Continuous core or a large number of core samples from one test hole is more useful than a few nonrepresentative samples scattered throughout the stratigraphic section. If continuous coring of one hole is not economically feasible, then logs of a nearby hole can be used to select representative depth intervals for coring.

2.3.2 Quantitative Interpretation

Obtaining quantitative data on rock or water characteristics is an important objective of the logging programs discussed here, and computer analysis can contribute significantly to the effectiveness of log interpretation. The very large amount of data in a suite of well logs cannot easily be collated or condensed in the human mind so that all interrelations can be isolated and used. Computer analysis makes this possible.

Probably the most important technique available for log analysis today is the computer plotting of data obtained from logs against data from other logs, core analyses, or tests. The most commonly used technique is the crossplot, which compares the response of two different types of logs. Fig. 2-2 shows a crossplot of the gamma and neutron logs for a borehole from the Highvale Mine. Coal, sandstone, mudstone and bentonite are clearly distinguished as clusters of points in this crossplot. Several software packages are available commercially for the analysis of geophysical logs, in addition to those used by the logging service companies for their own logs. VIEWLOG was used for Fig. 2-2. Interactive programs used by a geoscientist familiar with the local geology and hydrology are likely to produce more accurate analysis than sending logs to be analyzed by an organization that is not familiar with the area. Computer log analysis performed by service companies should not be used without knowing the basis for the algorithms.

The technique of studying the different types of logs as a group, rather than one at a time, is important to develop. For this purpose the complete suite of logs for one well are located side by side, as in Fig. 2-3, making the appropriate corrections for depth

errors. Locating logs with similar response, like neutron and density, side by side, makes depth errors and differences in response easier to identify and analyze with a computer program like VIEWLOG. Plotting any core data or lithologic descriptions on the same vertical scale as the logs is helpful, but these data often will require vertical displacement with respect to the logs because the depth datum may be different. It is helpful to draw correlation lines across a suite of logs at contacts or water tables that are apparent on several logs, as was done in Fig. 4-1 in Sec. 4.

Replotting logs at different vertical or horizontal scales, using a computer, may bring out features not previously obvious. The suite of logs needs to be examined for similarities and differences, and explanations need to be sought for log response that departs from that anticipated, based on the available background data. When searching for explanations for anomalous log response, first examine the caliper log to determine if hole diameter increase offers a possible reason. Well construction information also may explain anomalous response, as may information on the mineral or chemical composition of the rock. The output from synergistic log analysis depends to a large degree on the input from other data sources and a complete understanding of what the various logs respond to.

The final goal of using geophysical logs to predict mining and groundwater parameters is usually based on the calculation of correlation coefficients between laboratory analyses of selected core samples and the response of geophysical logs in a carefully matched depth interval. Depth correction techniques are described in Sec. 2.2.1 and 3.4.2.1. Less common techniques such as multiple linear and curvilinear regression analyses are now easily applied to sets of log and core data with spreadsheet programs like Lotus 1-2-3 (Sec. 2.4). Log analysis software programs such as VIEWLOG permit rapid calculation of correlation matrices of up to 20 logs and sets of core data. VIEWLOG also provides a means for principal component analysis (PCA), which is a mathematical technique for describing the relationships of a suite of logs to geologic parameters, such as those that might be measured on core. PCA is described in detail be Davis (1986) and PCA as applied to geophysical logs is described in Doveton (1986). Regardless of the analytical technique used to demonstrate the relationship of log response to geotechnical and hydrologic factors important to mining, these relationships will have to be substantiated at each new site.

2.4 SOFTWARE AND DATA FORMAT

Without appropriate software and consistent data format, the task of organizing, plotting, displaying, comparing and analyzing geophysical log and laboratory data

becomes exceedingly time-consuming and impractical. Preferences for software and format vary according to an individual's or company's specific objectives, and to some extent according to personal preference and work habits. The software discussed below proved helpful to some of the research groups for achieving the goals of this project, but the reader should bear in mind that newer versions and new packages will become available with time.

2.4.1 LAS Log Data Format

With the widespread use of personal computers, both in the field for recording the data and in the office for processing the data, it would appear that data files in ASCII format are the most convenient. The floppy disk committee of the Canadian Well Logging Society designed a standard format for log data on floppy disks called the LAS format (Log ASCII Standard), which it is hoped will be widely accepted by both oilfield service companies and oil companies. If the slimhole service companies and coal companies also adopt this format there is the opportunity to finally have a unique standard for geophysical log data across the well logging industry. BPB is offering this format from its slimline units. The details of LAS format are presented in Appendix A.

2.4.2 Lotus 1-2-3

Data analysis in the geotechnical portion of this report (Sec. 3) was performed using the software Lotus 1-2-3 (Lotus Development Corp., 55 Cambridge Parkway, Cambridge, MA., U.S.A., 02142) on an IBM-compatible computer. Lotus 1-2-3 is a spreadsheet-type program that originally was intended for business applications, but it can be used effectively for managing and processing the core and geophysical log data, and creating the graphics for illustrations (Keys, 1986). Fig. 3-1, 3-2, 3-5, 3-6, 3-7 and 3-19 in Sec. 3 are examples of the different plots that can be created using Lotus 1-2-3.

2.4.3 VIEWLOG

VIEWLOG (VIEWLOG Systems, #301 421 Eglinton Ave. West, Toronto, Ontario, Canada M5N 1A2), known in the United States as Analytical Compu-Log, was written specifically for the purpose of geophysical log analysis. VIEWLOG is easy to use and is well-suited for groundwater and mining applications. Up to 20 logs and core data in ASCII format are readily input to VIEWLOG using Lotus as the interface, and data can be easily output to Lotus. VIEWLOG data can be transferred to CAD programs such as Autocad for drawing cross-sections and fence diagrams, and a utility allows extraction of data for contouring and surface analysis.

VIEWLOG is menu-driven and most of the manipulations of logs and other data are performed using a mouse. It supports most graphics systems up to and including VGA, and more than 100 different printers. Log editing, such as depth shifting, stretching, smoothing and averaging are easily performed. Crossplots of logs or logs and core data can be made interactively with labeled depth intervals. Statistical analysis and principal component analysis are included in the software along with a large number of mathematical functions. Contacts, lithologic descriptions and symbols are easily added to sets of logs. Logs from up to 20 wells may be combined into a cross-section and contacts drawn using a mouse. Fig. 2-1, 2-2, and 2-3 in this section and Fig. 4-1, 4-2, and 4-4 to 4-7 in Sec. 4 are examples of plots made with VIEWLOG.

2.4.4 Data Desk

The program Data Desk, version 3.0 (Odesta Corporation, 4084 Commercial Ave., Northbrook, Illinois, U.S.A., 60062) was used in Sec. 4 and 5. Data Desk is a statistical program that runs on a Macintosh computer and offers a graphical approach to understanding data. Use of the mouse provides easy interface with the displays on the computer screen. The program's ability to link data displayed in different plots and diagrams greatly facilitated the understanding of the relationships in the data. For example, an anamolous cluster of data points selected from a crossplot display would also be highlighted throughout the entire database and in the other diagrams. The program supports a wide range of statistical computations that can be presented in graphical or numerical form. Data Desk is not ideally suited to the analysis of geophysical log data, but because of its ease of use, high speed, visual interface and data import/export abilities it proved to be very useful for exploring the data. Fig. 4-10, 4-11, 5-12, 5-13 and 5-19 in this report are examples of plots made with Data Desk.

2.4.5 Other Programs

Other programs used during this study included Microsoft Excel (v2.2; spreadsheet and data editing), Deneba Canvas (v2.1; illustrations), Cricket Graph (v1.3; plotting graphs), WriteNow (v2.2; word processing and data editing), Microsoft Word (v4.0; word processing and data editing), Wordperfect (v5.2; word processing), Wordstar (v5.5; word processing) and SAS (v5.16; statistical analysis). The WriteNow and Word 4 software proved useful in the initial conversion and preparation of the log data files.

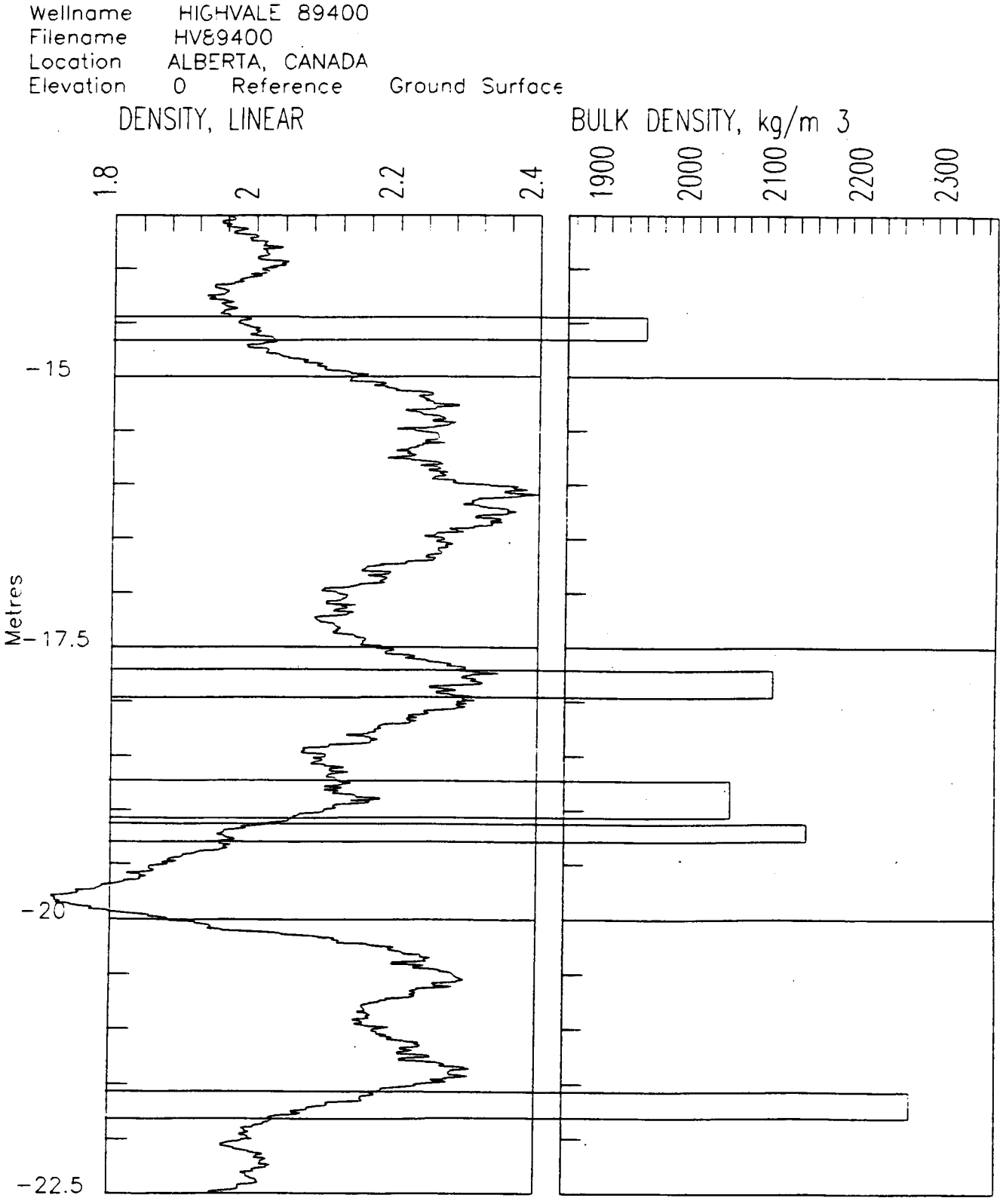

Figure 2-1. Linear density log and core bulk density samples, HV89-400. Depth interval of core sample is shown by thickness of bar.

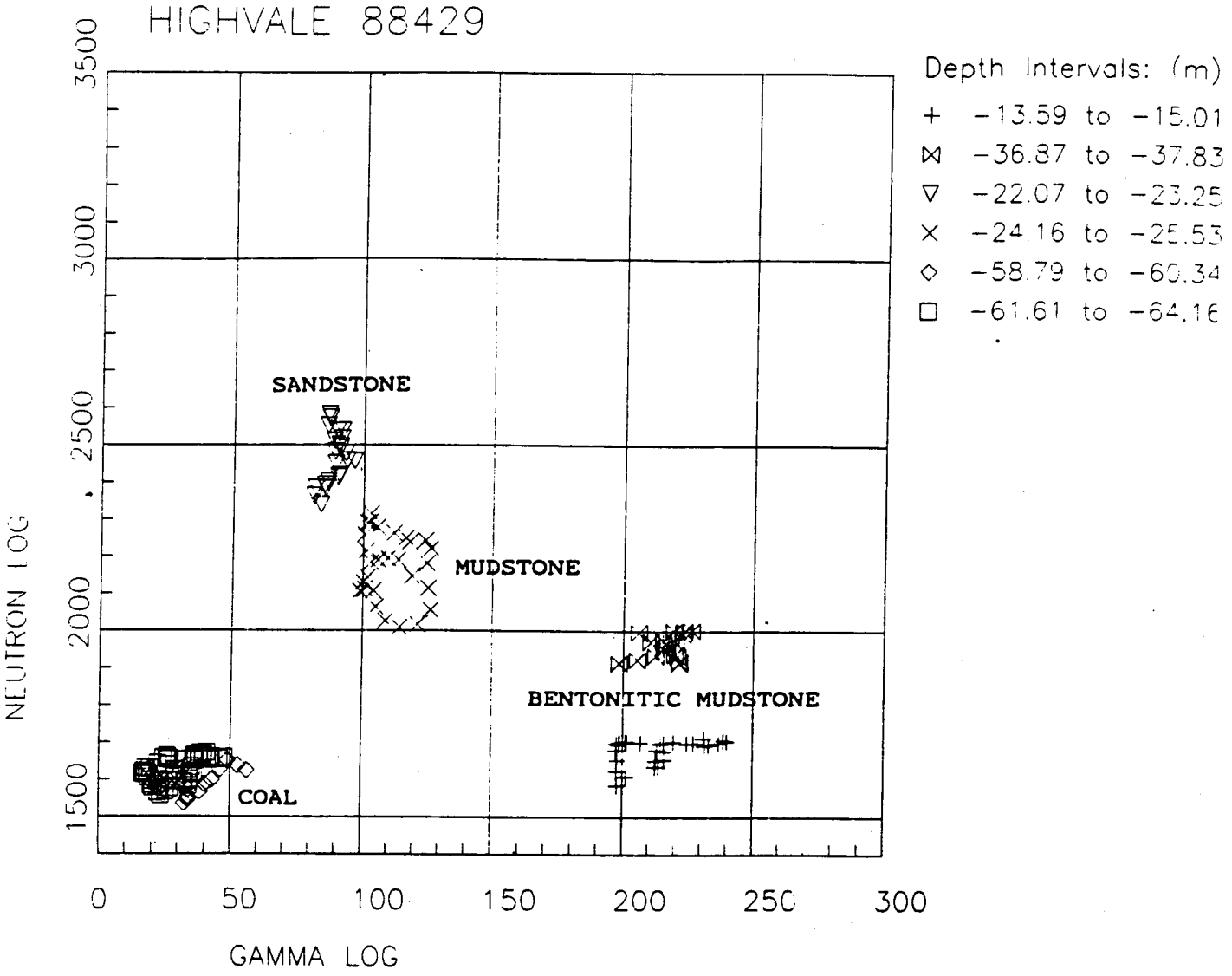

Figure 2-2. Neutron log and gamma log crossplot, HV88-429.

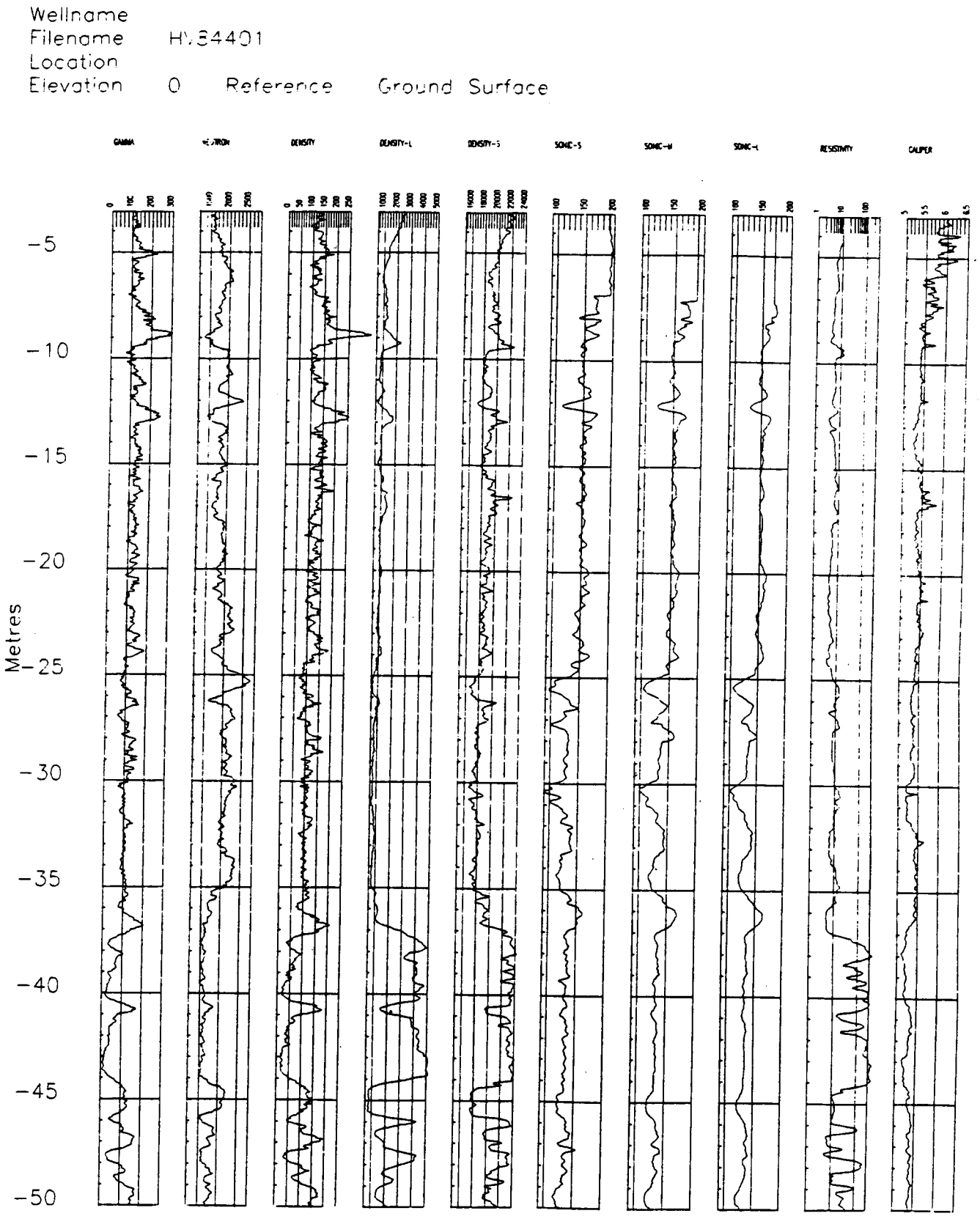

Figure 2-3. Plot of complete suite of logs, HV84-401.

3. GEOTECHNICAL PARAMETERS

Neil H. Wade

The discussion below covers the continuation of the work summarized in previous reports, in particular the Phase 2 Report (TransAlta, 1988) and the Phase 3A Report (TransAlta, 1989). Although the geotechnical and geophysical data utilized were, as in the earlier studies, from the Syncrude and Highvale Mines (Fig. 1-1), additional data collected in 1989 from Highvale were made available for the final phase of this study.

Work on the Highvale data was conducted, in part because of their long association and familiarity with the project, by Monenco Consultants Limited. Dr. N. H. Wade was engaged to evaluate the Syncrude data on an individual consulting basis.

3.1 OBJECTIVE

The objective of the present study was to use the existing and new data to extend, if possible, the number of plausible correlations between geotechnical parameters and individual or multiple geophysical logs and, by careful scrutiny and selection of data, to enhance the correlations obtained in previous studies.

3.2 AVAILABLE DATA

A list of abbreviations used for the geotechnical correlations is presented in Table 3-1.

3.2.1 Syncrude Data

The geotechnical and geophysical information studied in Phase 3B is from a single drillhole in the existing tailings pond area a few kilometres northwest of the main Syncrude Mine complex. The data gathered are representative of the poorly indurated units comprising the Clearwater Formation (Fig. 1-3) which overlies the ore zone in much of the Ft. McMurray area. It was considered expedient to use data from only one drillhole for a number of reasons, namely:

- this was the only drillhole available for study for which the geotechnical samples had been carefully depth-aligned with the geophysical logs by Syncrude geologists;

Table 3-1. Abbreviations used for geotechnical correlations.

% clay	-	% finer than 2 microns
A-line	-	empirical line on Plasticity Chart separating silts and organic soils from inorganic clays
Activity	-	ratio of PI to % Clay
avg	-	average
BWE	-	Bucketwheel Excavator
c	-	cohesion (MPa) - (total stress basis)
c'	-	cohesion (MPa) - (effective stress basis)
coef	-	coefficient
deg	-	degrees
e	-	base of natural logarithms
err	-	error
intcp	-	intercept
LI	-	liquidity index = (MC-PL)/PI (%)
LL	-	liquid limit (%)
ln	-	natural logarithm
log	-	common logarithm
MC	-	moisture content (%)
MPa	-	megapascals
n/a	-	not available
n	-	number of observations
phi	-	friction angle (degrees) - (total stress)
phi'	-	friction angle (degrees) - (effective stress)
PI	-	plasticity index = (LL-PL) (%)
PL	-	plastic limit (%)
Qu	-	uniaxial compressive strength (MPa)
R	-	correlation coefficient
Ru	-	ratio of porewater pressure to overburden pressure at given point
sbrdu	-	standard bed resolution density units
SCL	-	Syncrude Canada Ltd.
sdu	-	standard density units
snu	-	standard neutron units
sqrt	-	square root
sst	-	sandstone
std	-	standard

- sample-to-log depth alignment procedures were considered less workable for the Syncrude drillholes than for the Highvale and Big Valley drillholes, due to the presence of well-defined lithological horizons and hardband marker beds in the latter;

- this was one of a limited number of Syncrude holes logged by BPB Wireline Services, the same company that logged the Highvale and Big Valley drillholes. It was anticipated that errors associated with different tools and processing procedures would be minimized by using data generated by a single logging company.

3.2.1.1 Syncrude Geotechnical Database

The geotechnical test data from Syncrude used in this study consisted of the following:

- natural moisture contents
- liquid and plastic limits
- bulk densities
- grain size data

3.2.1.2 Syncrude Geophysical Database

The geophysical database consisted of the following geophysical logs:

Log	Sonde No.	Units
Natural Gamma	118	API
Caliper	118	inches
Linear Density	118	g/cm^3
Dual-Spaced Neutron	515	snu
Resistivity (focussed)	232	ohm-m

KIM drilling mud was used as the drillhole fluid during logging and casing was installed to a depth of 11.5 m.

3.2.2 Highvale Data

Geotechnical and geophysical data from Highvale Mine were obtained from drillholes put down through overburden overlying the coal seams of the Ardley coal zone in the active mine area. The overburden materials are composed of gently dipping sequences of mudstones, siltstones and sandstones of lowermost Tertiary age (Fig. 1-2). Overlying

this succession are Pleistocene deposits consisting of clay till containing ice-thrusted blocks of Tertiary rock (Sec. 5).

3.2.2.1 Highvale Geotechnical Database

The geotechnical data used in the study were available from Monenco files and from the computerized database maintained by TransAlta Utilities Corporation, the owner of the Highvale Mine. The database contains data from geotechnical tests on core samples from over 300 drillholes, which over the years had been performed by numerous reputable laboratories including Hardy-BBT Limited and their predecessor firms, Thurber Consultants, EBA Consultants and Golder Associates. Some data from tests on samples from TransAlta's Big Valley property in central Alberta were also used in the correlation study. The test parameters used were derived from the following geotechnical tests on core samples:

- natural moisture content
- liquid and plastic limits
- bulk density
- uniaxial compression
- direct shear

3.2.2.2 Highvale Geophysical Database

Geophysical logging of geotechnical drillholes at Highvale Mine was performed by BPB Wireline Services. The following geophysical logs had been run in the drillholes from which the geotechnical samples were recovered:

- natural gamma (API)
- caliper (cm)
- long-spaced density (sdu)
- bed-resolution density (sbrdu)
- linear density (g/cm^3)
- focussed electric (ohm-m)
- short-spaced sonic (micro-sec/ft)
- medium-spaced sonic (micro-sec/ft)
- long-spaced sonic (micro-sec/ft)
- short-spaced neutron (snu)

All holes were logged uncased with water as the drillhole fluid. A summary of the holes

included in the database for this phase of the work and the geophysical sondes used in logging of each hole are listed in Appendix B.

3.3 METHODOLOGY

3.3.1 Syncrude Data

3.3.1.1 Syncrude Geotechnical Data

The geotechnical data, received on floppy disk in Lotus 1-2-3 format (Sec. 2.4), were edited to remove missing data gaps and checked for consistency by conventional crossplots. One such consistency plot is the Plasticity Chart, shown on Fig. 3-1, wherein the plasticity index is plotted against the corresponding liquid limit values. Linear regression analyses of these classification data yielded a coefficient of correlation, R, equal to 0.999 which indicates very good consistency for all the geological units studied.

The relationship between three independent classification test parameters can be demonstrated by plotting the data on a three dimensional graph. An example of such a graph is shown on Fig. 3-2 where moisture content, clay content and plasticity index data are plotted. This method of data presentation is sometimes useful when comparing materials from different localities. The procedure and formulae used to develop a three-parameter graph utilizing Cartesian (or x-y) co-ordinates are outlined in Appendix C.

3.3.1.2 Syncrude Geophysical Data

Since the geotechnical samples had been carefully depth-aligned with the geophysical logs prior to receipt of the data, no modifications or adjustments to the geophysical data were carried out.

3.3.2 Highvale Data

3.3.2.1 Highvale Geotechnical Data

Crossplots of the geotechnical data were generated to confirm consistency of the data. An example of the good correlation between plasticity index and liquid limit for the Highvale data is shown on the Plasticity Chart where the computed R value is essentially equal to unity (Fig. 3-3). A comparison of the Plasticity Charts (Fig. 3-1 and

3-3) illustrates that the Highvale materials exhibit a greater range in liquid limits than the Syncrude materials. The three-dimensional plot of moisture content, clay content and plasticity index (Fig. 3-4) also indicates that the Highvale data set contains materials with a wider range in clay content than the materials in the Syncrude data set (Fig. 3-2).

Adjustment of the geotechnical sample depths was found to be necessary, however, to improve correlations between geotechnical parameters and geophysical logs. The approach adopted took advantage of the fact that both extremely hard sandstone lenses (hardbands) and weak bentonitic seams are present in the overburden formations at Highvale. These strata not only were extensively sampled geotechnically but also exhibited pronounced sonic log signatures. By selecting samples with uniaxial compressive strengths greater than 10 MPa and plotting the digitized short-spaced sonic log readings over a depth interval 0.5 m above and below the recorded sample depth, it was possible to realign the sample with the characteristic trough or low transit time on the sonic log as indicated on Fig. 3-5. A similar approach was used for very low strength (less than 2 MPa) bentonitic seams except that the sample was aligned with the peak or high transit time on the short-sonic curve. Depth corrections were generally not possible for specimens having compressive strengths intermediate between 2 and 10 MPa since a characteristic peak or trough on the curve was rarely present. The magnitude of depth corrections applied to uniaxial compression test samples varied from 0 to a maximum of 0.7 m as depicted on Fig. 3-6 and 3-7.

A second method of sample depth alignment was used in which the laboratory-determined sample bulk density and linear density log values were compared to obtain the depth of best match. A histogram of depth corrections applied on a density log basis is illustrated on Fig. 3-8. This procedure resulted in enhanced correlations especially between moisture content and density logs as indicated on Fig. 3-9 and 3-10. The unadjusted data from Highvale plotted on Fig. 3-9 exhibit a coefficient of correlation, R, of 0.77 whereas the depth-adjusted moisture content samples from both the Highvale and Big Valley sites yield an R of 0.96. The data on Fig. 3-10 are replotted on Fig. 3-11 with sample clay content emphasized and confirm that high moisture content and low density are associated with high clay content. However, a second replot (Fig. 3-12) indicates no well-defined trend in resistivity with density for the various lithologies correlated.

For correlations with the uniaxial compressive strength, average values of each of the sonic logs (short, medium and long sonic) were used for samples having strengths less than 10 MPa, whereas minimum sonic values were used for samples with strengths

greater than 10 MPa since the hardbands were generally thin. For all other correlations, the various geophysical logs over depth intervals corresponding to the corrected geotechnical sample depths were downloaded from the database and the average, maximum and minimum values, respectively, computed for each log and depth interval. These average, maximum and minimum values were in turn correlated with each geotechnical parameter. Except for a few cases where scatter plots with relatively low correlation coefficients are included for discussion purposes, only those correlations with an R value greater than 0.70 were plotted and included in the report.

3.3.2.2 Highvale Geophysical Data

Based on the results of the Phase 3A study, it was concluded that the depth alignment between individual logs from each drillhole did not need correction, that the standard 9 m/min logging rate is satisfactory, and that the natural gamma log would be excluded from further correlations between geotechnical and geophysical data. Preliminary correlations for natural gamma data had been poor, presumably due to variations in clay mineralogy and chemistry (TransAlta, 1989).

3.4 CORRELATIONS

3.4.1 Syncrude Data

3.4.1.1 General

After compilation and editing in tabular form, the geotechnical and geophysical parameters were correlated using the linear regression procedures in version 3.0 of the Lotus 1-2-3 program (Sec. 2.4). Both single and multiple regression analyses were conducted.

In addition, a few crossplots of geotechnical parameters were prepared to illustrate the degree of consistency within the data set. Apart from those relations discussed in the preceding paragraphs, another conventional method of comparing geotechnical samples is with the Activity Chart wherein the plasticity index is plotted against the clay content. The empirical gridlines on the Chart suggest that calcium montmorillonite and illite are the predominate clay minerals in the Syncrude materials (Fig. 3-13). Regression analyses indicate a good correlation between data points, indicating a formation with few erratic changes in clay mineral composition (Fig. 3-14).

3.4.1.2 Single Linear Regression Correlations for Syncrude Data

A summary of all correlations attempted using single linear regression analysis techniques is listed in Table 3-2. The number of observations and the computed R value are shown for each pair of parameters correlated. Those correlations with R values equal to or greater than 0.70 have been compiled separately, along with the equations for the best-fit line, in Table 3-4. Graphs for each set of relationships in Table 3-4 which has the highest R value are included in Appendix D.

Table 3-2. Summary of single regression analyses - SCL hole 01.

Geotechnical Parameter	n	Correlation Coefficients res	logres	loglogres	gamma	denpor	neupor
Activity	54	0.77	0.79	0.79	0.25	0.31	0.57
MC	54	0.51	0.57	0.61	0.20	0.64	0.71
LI	54	0.29	0.29	0.28	0.22	0.38	0.37
LL	54	0.81	0.86	0.89	0.23	0.46	0.66
PI	54	0.82	0.87	0.89	0.24	0.45	0.65
% Clay	54	0.79	0.83	0.84	0.15	0.48	0.58
% Silt	54	0.75	0.77	0.77	0.37	0.27	0.46
% Sand	54	0.08	0.11	0.12	0.43	0.40	0.24
log Activity	54	0.77	0.77	0.76	0.22	0.27	0.53
log LL	54	0.86	0.86	0.86	0.18	0.42	0.60
log MC	54	0.51	0.57	0.61	0.17	0.65	0.68
log PI	54	0.84	0.85	0.85	0.18	0.39	0.57
log % Clay	54	0.80	0.82	0.81	0.12	0.44	0.53

denpor - density porosity (%)
gamma - gamma log (API)
LI - liquidity index (%)
LL - liquid limit (%)
MC - moisture content (%)
n - number of observations
neupor - neutron porosity (%)
PI - plasticity index (%)
res - resistivity log (ohm-m)

3.4.1.3 Multiple Linear Regression Correlations for Syncrude Data

Since poor correlations were generally found between the classification test parameters and some of the geophysical logs for the Syncrude data, a number of multiple linear regressions were run to determine if better correlations could be achieved with groups of, rather than individual, geophysical logs. The multiple regression analysis used, along with the linear regression method, forms part of the Lotus 1-2-3 version 3 software. The results of these analyses are depicted in Table 3-3. Those correlations with computed R values in excess of 0.70 are also listed in Table 3-4. Graphs are included in Appendix D.

3.4.2 Highvale Data

3.4.2.1 General

As with the Syncrude data, crossplots of selected geotechnical parameters from the Highvale data set were prepared to assess data consistency. These plots included the Plasticity Chart (Fig. 3-3) and 3-parameter plot (Fig. 3-4) discussed previously as well as the Activity Chart (Fig. 3-15), a graph of specimen dry density versus moisture content (Fig. 3-16) and finally a plot of uniaxial compressive strength versus secant modulus (Fig. 3-17).

Unlike the corresponding chart for Syncrude materials, the Activity Chart for Highvale materials (Fig. 3-15) indicates a much wider range in clay mineral composition encompassing both sodium and calcium montmorillonite as well as illite and kaolinite. The relatively high concentration of sodium montmorillonite denotes a potentially active material with an affinity for water and a potential for high change in volume with change in moisture content. The effects on geophysical log responses of varying montmorillonite content within a formation are difficult to predict.

The relationship between dry density and moisture content determined in the laboratory using representative core samples shows a good correlation on a semi-log plot (Fig. 3-16). Another interesting, if not unexpected, relationship is the very good correlation between the uniaxial compressive strength and the secant modulus shown on Fig. 3-17. The secant modulus is defined as the ratio of the compressive strength to the strain required to cause failure, i.e., the slope of the line running from the origin to the point of failure on the stress-strain curve.

The geophysical data for the desired geotechnical sample depth intervals were manually downloaded from the VAX database and manipulated to obtain the

Table 3-3. Summary of multiple linear regressions - SCL hole 01.

Geophysical Log						R for Geotechnical Parameter				
RES	GAM	DEN	NEU	CAL	llRES	MC	LL	PI	% Clay	Activity
x	x					0.52	0.82	0.82	0.79	0.78
x	x	x				0.74	0.86	0.86	0.84	0.78
x	x	x	x			0.79	0.88	0.88	0.85	0.81
x		x	x			0.79	0.88	0.88	0.85	0.81
x		x				0.73	0.85	0.85	0.84	0.78
x			x			0.74	0.88	0.88	0.83	0.81
		x	x			0.76	0.67	0.63	0.60	0.57
	x	x				0.65	0.49	0.48	0.48	0.37
	x		x			0.71	0.66	0.65	0.58	0.58
x		x	x	x		0.79	0.89	0.89	0.85	0.82
x			x	x		0.74	0.88	0.88	0.83	0.82
	x				x	0.62	0.89	0.89	0.84	0.79
	x	x			x	0.77	0.90	0.90	0.86	0.79
	x	x	x		x	0.80	0.91	0.91	0.86	0.80
		x	x		x	0.80	0.91	0.91	0.86	0.80
		x			x	0.77	0.90	0.90	0.86	0.79
			x		x	0.75	0.91	0.90	0.85	0.80
	x	x				0.65	0.49	0.48	0.48	0.37
		x	x	x	x	0.80	0.91	0.91	0.86	0.81
			x	x	x	0.75	0.91	0.91	0.85	0.81

Legend:

CAL = Caliper Log (in)
DEN = Density Porosity (%)
GAM = Gamma Log (API)
llRES = loglog (Resistivity Log, ohm-m)
LL = liquid limit (%)
MC = moisture content (%)
NEU = Neutron Porosity (%)
PI = plasticity index (%)
R = coefficient of correlation
RES = Resistivity Log (ohm-m)

Notes: i) No. of Observations = 54
ii) Geological units included in the correlations are a, b, c & w.

Table 3-4. Summary of satisfactory correlations - SCL hole 01.

Parameters Y	X	Equation Obtained	R
MC	NEU	$Y = 0.4 + 0.35X$	0.71
MC	llRES,DEN,NEU	$Y = -2 - 14X_1 + 0.4X_2 + 0.2X_3$	0.80
LL	RES	$Y = 222 - 20X$	0.81
LL	logRES	$Y = 300 - 260X$	0.86
LL	loglogRES	$Y = 48 - 415X$	0.89
LL	llRES,DEN,NEU	$Y = -20 - 354X_1 + 0.8X_2 + 1.2X_3$	0.91
% Clay	RES	$Y = 90 - 6.2X$	0.79
% Clay	loglogRES	$Y = 35 - 127X$	0.84
% Clay	loglogRES,DEN	$Y = 16 - 116X_1 + 0.8X_2$	0.86
Activity	RES	$Y = 2.3 - 0.14X$	0.77
Activity	loglogRES	$Y = 1.1 - 2.9X$	0.79
Activity	loglogRES,NEU	$Y = 0.8 - 2.5X_1 + 0.007X_2$	0.80
PI	loglogRES	$Y = 30 - 375X$	0.89
PI	llRES,DEN,NEU	$Y = -26 - 324X_1 + 0.9X_2 + 0.7X_3$	0.91

Legend:

DEN = Density Porosity (%)
llRES = loglog(Resistivity Log, ohm-m)
LL = liquid limit (%)
MC = moisture content (%)
NEU = Neutron Porosity (%)
PI = plasticity index (%)
R = coefficient of correlation
RES = Resistivity Log (ohm-m)

Note:

i) No. of Observations = 54
ii) Geological units included in the correlations are a, b, c & w.

maximum, minimum and average values for each log and depth interval. Upon tabulating and aligning with the geotechnical data in Lotus 1-2-3 format, the correlation procedure commenced.

3.4.2.2 Regression Correlations for the Highvale Data

A significant number of satisfactory (R = 0.7 to 0.8) to very good (R = 0.9+) correlations were obtained for the Highvale data from the regression analyses conducted. Most correlations were derived from computerized linear regression analyses, although two relations were obtained manually from curvilinear analysis. A summary of satisfactory correlations is given in Table 3-5. The good correlation between uniaxial compressive strength and short-spaced sonic transit time is illustrated on Fig. 3-18 and comparable relations by other investigators are shown on Fig. 3-19. Graphs for the remaining correlations listed in Table 3-5 are included in Appendix E.

3.5 DISCUSSION

The lack of consistent relationships between the Syncrude and Highvale data sets for the same pairs of geotechnical and geophysical parameters frustrated attempts to establish unique, universal correlations which were not site specific. For example, a reasonably good correlation was found between liquid limit and resistivity for the Syncrude data (Fig. 3-20) whereas the Highvale data with a similar range in liquid limit values indicated that the liquid limit was practically independent of resistivity (Fig. 3-21). When the full range of liquid limit values was plotted, an apparent trend was observed only for highly bentonitic samples with liquid limits greater than 200% (Fig. 3-22). A second example occurs with the moisture content versus density log plot. The Syncrude data plotted on Fig. 3-23 have a coefficient of correlation of 0.65 whereas the corresponding Highvale and Big Valley data (Fig. 3-10) indicate a strong correlation with a coefficient of 0.96.

As a result of the inconsistencies between the two sites, other correlation approaches were investigated. One which showed some success involved the 3-parameter plot referred to in Sec. 3-3. On Fig. 3-24, the three parameters, resistivity, ln(% Clay) and ln(Plasticity Index), for the Syncrude data set are plotted on the triangular graph and yield a best-fit line with R=0.99. Although the triangular plot has been shifted away from the origin of the x-y axes for clarity of presentation, the equations for transforming the three variables to Cartesian co-ordinates, as well as the equation for the best-fit line through the data points, are based on coincident origins.

Table 3-5. Summary of satisfactory correlations - Highvale data.

Parameters Y	X	Equation Obtained	n	R
i) Geotechnical/Geophysical Correlations				
Bulk Den	NEUT	Y = 1137 + 0.48X	127	0.78
Bulk Den	LSD	Y = 2605 - 0.44X	88	0.75
Bulk Den	LD	Y = 1.043 - 0.108X	46	0.98
Bulk Den	SS	Y = 3180 - 2.1X	120	0.81
Bulk Den	logSS	Y = 7434 - 1969X	120	0.79
log Bulk Den	SS	Y = 3.53 - 0.0004X	120	0.80
MC	SS	Y = 0.3X - 27.2	121	0.76
MC	S-WAVE	Y = 20.67 + 0.01X	14	0.96
lnMC	LD	Y = 9.12 - 2.92X	45	0.96
lnMC	LD	Y = 9.8 - 3.33X	128	0.77
lnMC	ln{LDxRES/MC}	Y = 2.95 - 0.53lnX	45	0.91
loglogMC	logRES	Y = 0.68 - 0.61X	123	0.77
lnMC	lnNEUT	Y = 33.7 - 4.07X	127	0.79
% Clay	LD	Y = 203 - 74X	43	0.79
ln(% Clay)	LD	Y = 8.06 - 2.03X	43	0.84
Qu	SS	Y = 153-0.65X+0.00068X^2	104	0.89
Qu	SS	Y = e^(7.88 - 0.018X)	104	0.95
lnQu	lnSS	Y = 38.42 - 6.35X	104	0.94
1000lnQu/SS	SS	Y = 29.20 - 0.063X	104	0.96
1000lnQu/SS	lnSS	Y = 139.93 - 22.88X	104	0.98
Qu	LS	Y = e^(7.31 - 0.015X)	59	0.87
lnQu	lnLS	Y = 32.04 - 5.10X	59	0.85
1000lnQu/LS	LS	Y = 30.87 - 0.067X	59	0.93
1000lnQu/LS	lnLS	Y = 140.39 - 22.82X	59	0.95
Qu	logRES	Y = 52.8X - 49.2	92	0.77
Qu (sst only)	logRES	Y = 26.4X - 54.5	44	0.87
Sec Mod	SS	Y = 5707 - 10.98X	85	0.73
Sec Mod	SS	Y = 17394-65.2X+0.061X^2	85	0.84
Sec Mod	lnSS	Y = 25294 - 11512X	85	0.78
ln Sec Mod	lnSS	Y = 23.51 - 10.09X	85	0.85
ln Sec Mod	SS	Y = 6.72 - 0.0104X	85	0.86

Table 3-5. (Continued)

Parameters Y	X	Equation Obtained	n	R
ii) Geophysical Cross-Plots				
avg LS	avg SS	Y = 63.53 + 0.903X	59	0.97
min LS	min SS	Y = 58.65 + 0.920X	59	0.95
avg SS	avg LS	Y = 2.64 + 0.975X	2711*	0.89
min SS	avg SS	Y = 0.998X - 8.717	66	1.00
iii) Geotechnical Cross-Plots				
Dry Den	MC	Y = 23.10 - 0.255X	73	0.94
Dry Den	log MC	Y = 33.75 - 12.51X	73	0.95
PI	LL	Y = 0.95X - 20.5	74	1.00
Qu	Sec Mod	Y = 0.0086X + 1.609	106	0.96
log Qu	log Sec Mod	Y = 0.926X - 1.672	106	0.98

* Data from one hole only.

Legend:

avg	= Log value averaged over a particular depth
Bulk Den	= laboratory determined bulk density (g/cm^3)
Dry Den	= laboratory determined dry density (kN/cu.m.)
LD	= Linear Density Log (g/cm^3)
LL	= liquid limit (%)
ln	= natural logarithm
log	= common logarithm
LSD	= Long Spaced Density Log (sdu)
LS	= Long Spaced Sonic Log (micro-sec/m)
MC	= moisture content (%)
min	= minimum Log value over a particular depth
n	= No. of observations
NEUT	= Neutron Log (snu)
PI	= plasticity index (%)
Qu	= uniaxial compressive strength (MPa)
R	= coefficient of correlation
RES	= Resistivity Log (ohm-m)
Sec Mod	= Secant Modulus (MPa)
SS	= Short Spaced Sonic Log (micro-sec/m)
sst	= sandstone
S-WAVE	= Shear Wave Transit Time (micro-sec/m)

Another method of representing three independent variables in two dimensions is as follows:

- consider three mutually perpendicular axes which correspond to the three variables;

- the conditions which occur when all the variables are of equal value can be represented by a straight line extending from the origin into space; this line is called the space diagonal;

- any plane which intersects the space diagonal at right angles is termed a right section;

- an x-y graph with its origin coincident with the space diagonal outcrop can be plotted on a right section once the equations relating x & y to the three variables are established from geometrical considerations.

Such a graph has been plotted on Fig. 3-25 and indicates a best-fit line with the same slope and R value as shown on the preceding triangular plot. However, the y-intercept is different on each figure as a result of differing graph geometries. Although the three independent variables are not as apparent when viewing Fig. 3-25, the data points are less congested than in the triangular plot.

An extension of the above graphical procedures is possible by plotting the distance from the origin that the data points lie along the space diagonal, represented by parameter N, against their perpendicular distance from the space diagonal, denoted by parameter T. The equations relating T and N to the three independent variables are given on Fig. 3-26 along with the plotted data.

Some degradation in R values occurs in the correlations shown on Fig. 3-24 and 3-25 when the Highvale and Big Valley data are incorporated into the data set (Fig. 3-27 and 3-28) although R value enhancement is indicated on the T versus N plot (Fig. 3-29). A summary of the correlations employing three variables is given in Table 3-6 and graphs of those correlations not already discussed are included in Appendix F.

Appendix G contains a few examples of unsatisfactory ($R < 0.7$) correlations for illustration only.

Table 3-6. Summary of correlations between three variables.

Parameters Correlated A	B	C	Equation Obtained	n	R
i) SCL Hole 01					
RES	ln %Clay	ln PI	y = 3.99 + 0.45x	54	0.99
RES	ln %Clay	ln PI	Y = 9.44 + 0.45X	54	0.99
RES	ln %Clay	ln PI	T = 1.39N - 16.24	54	0.84
ii) HV % BV Data					
LD	RES	MC	Y = 1.00 - 1.55X	45	0.97
LD	RES	MC	T = 1.25N - 16.32	45	0.94
LD	RES	%Clay	Y = 0.85 - 1.30X	41	0.98
LD	RES	%Clay	T = 1.32N - 18.78	41	0.96
iii) HV, BV & SCL Data					
RES	ln %Clay	ln PI	y = 0.51x + 0.85	97	0.96
RES	ln %Clay	ln PI	Y = 0.51X - 0.06	97	0.96
RES	ln %Clay	ln PI	T = 1.42N - 16.75	97	0.96
RES	% Clay	LL	Y = 65.85 - 0.50X	97	0.50
RES	% Clay	LL	T = 1.08N - 51.46	97	0.99
RES	ln %Clay	ln MC	y = 0.69x - 0.13	98	0.99
RES	ln %Clay	ln MC	Y = 0.14 + 1.69X	98	0.99
RES	ln %Clay	ln MC	T = 1.5N - 15.17	98	0.99
RES	%Clay	MC	Y = 0.49 + 0.84X	98	0.71

Legend:

% Clay	= clay fraction from laboratory hydrometer test
LD	= Linear Density Log (g/cm^3)
LL	= liquid limit (%)
MC	= moisture content (%)
N	= A+B+C
n	= No. of observations
PI	= plasticity index
R	= coefficient of correlation
RES	= Resistivity Log (ohm-m)
T	= sqrt{(A-B)^2 + (B-C)^2 + (C-A)^2}
X	= 1.225(C-A)/(A+B+C)
Y	= 0.707(2B-C-A)/(A+B+C)
x	= 50(B+2C)/(A+B+C)
y	= 86.6B/(A+B+C)

3.6 APPLICATION TO MINING PROBLEMS

The geotechnical parameters generally required to address most geotechnical problems associated with surface mines can be divided into two broad categories: classification parameters and strength parameters. Classification parameters for the most part consist of:

Parameter	Laboratory Test
Moisture Content	Moisture Content
Liquid & Plastic Limits	Atterberg Limits
% Clay	Hydrometer Analysis
Bulk Density	Bulk Density

Classification parameters are used to distinguish between lithologies, compare similar geological units and predict strength parameters as well as other physical properties.

Strength parameters are further subdivided into total stress and effective stress parameters. These are as follows:

Parameter	Description	Test Used	Remarks
Qu	total stress	Uniaxial	No specimen drainage
c, phi	total stress	Triaxial	No specimen drainage
c, phi	total stress	Direct Shear	No specimen drainage
c', phi'	eff. stress	Triaxial	Specimen drained or pore pressure measured
c', phi'	eff. stress	Direct Shear	Specimen drained

The uniaxial compressive strength, Qu, and the effective stress parameters, c' and phi', from the triaxial and/or direct shear tests are conventionally employed to solve diggability and stability problems in surface mining operations (Wade et al., 1987).

A knowledge of geotechnical classification parameters, whether obtained by direct measurement in the laboratory or deduced from correlations with geophysical logs, often allows a prediction of other material properties such as formation strength. Two examples of well-established geotechnical relationships are the crossplots shown on Fig. 3-30 and 3-31. The dependence of the peak friction angle on the plasticity index in fine-grained sediments is illustrated on Fig. 3-30. The clays referred to on the graph are, in fact, poorly indurated claystones. Fig. 3-31 depicts the relationship between the residual friction angle, generally derived from direct shear tests, and the clay content of

the formation. The residual friction angle represents the steady-state strength exhibited by a material which has experienced considerable deformation along the plane of failure, e.g., gouge in a fault zone or slickensided clay seams along the seat of glacial thrusting.

The strength parameter which complements the friction angle, phi, is the cohesion parameter, c. As outlined above, both parameters can be determined from laboratory tests, but these tests are relatively expensive, somewhat time-consuming, and require intact core samples. For preliminary mine design, the number of suitable core samples available for testing, as well as the available budget, is often limited. In such circumstances, friction angles for the various lithological units can be estimated from established relationships using data from inexpensive classification tests and the cohesion computed from the expression (Underwood and Dixon, 1976):

$$c = 0.14 \text{ (uniaxial compressive strength)}$$

An illustration of the use of the strength parameters, c and phi, as well as the material bulk density or unit weight, in a typical slope stability analysis is given on Fig. 3-32. It was assumed that the rocks are horizontally bedded and composed of the lithological units listed. The groundwater level within the formation is denoted by the dotted line. The analysis indicated the potential circular arc failure surface is tangent to the top of coal and is exposed on level ground at the top of the excavated slope. This potential failure surface is termed the critical failure surface since it exhibits the lowest factor of safety of all failure surfaces through the slope.

In addition, formation diggability, or ease with which *in situ* geological materials can be excavated with a given piece of stripping equipment without blasting, is related to the uniaxial compressive strength of the material (Carroll, 1966; Hebblewhite et al., 1986; O'Regan et al., 1987; Wade et al., 1987; Wade et al., 1988). During mine planning studies for Highvale, criteria were established to assess overburden resistance to digging by various types of stripping equipment including shovels, bucketwheel excavators, and draglines. Based on the Monenco-developed criteria, the relative digging capability of different stripping equipment in terms of formation strength is compared on Fig. 3-33 with the ripping capability (Caterpillar, 1989) of various dozer models fitted with a single-shank ripper. A procedure for applying the diggability criteria and producing plans suitable for use by mine planners was also developed (Monenco, 1988; Wade, 1989; Monenco, 1990). The diggability criteria were expressed not only in terms of formation uniaxial compressive strength but also in terms of formation sonic transit time which was found from previous correlation studies to be related. The procedure for

determining those areas of the mine which required pre-blasting prior to stripping is illustrated by the flow chart on Fig. 3-34. The Lotus 1-2-3 Scanning Routine is a computer program developed by Monenco for scanning digitized sonic logs to ascertain the depth and thickness of those strata which do not meet the diggability criteria for the particular stripping equipment being considered. A copy of the program is included in Appendix H.

The uniaxial strength is also related to the focussed resistivity log, although the correlation is not as good as the Qu versus sonic relationship shown on Fig. 3-18. However, recent use was made by the writer of the Qu versus resistivity correlation obtained for sandstone at the Highvale Mine (Fig. 3-35) to make a preliminary prediction of the overburden blasting requirements for a proposed coal mine in South America where only resistivity logs were available for the site. The predicted range of strengths agreed well with the limited compressive strength data available for the cemented sandstone units at the proposed minesite.

A flow chart summarizing the application of geotechnical parameters to mining problems is illustrated on Fig. 3-36 and a partial list of specific geotechnical parameters utilized in surface mine design is provided in Table 3-7. An example of the potential use of sonic logs in predicting the competency of concrete structures, which may include applications of geophysical logs in other disciplines besides mining, is shown on Fig. 3-37.

Table 3-7. Application of geotechnical parameters to mining problems.

Geophysical Log	Geotechnical Parameter	Application to Mining
Density	Bulk Density	Input to slope stability.
Density	Moisture	Moisture content is an indication of formation clay content & degree of induration.
Density & Resistivity	% Clay	% Clay is empirically related to residual friction angle which in turn is used to characterize the strength of weak clay seams in stability analyses computations. Clay content, moisture content and types of clay minerals present are all factors which govern material stickiness and handleability.
Resistivity	Plasticity Index	Plasiticity Index is empirically related to peak friction angle which is input to slope stability analysis.
Resistivity	Activity	The activity value of a fine-grained sedimentary formation provides an indication of the dominant clay mineral present and thus material strength.
Resistivity, Sonic (short)& Sonic (long)	Qu	Magnitude of Qu is an indication of in situ formation diggability or ease with which the material can be excavated with a given pice of stripping equipment without blasting.
Sonic (short)	Secant Modulus	The Secant Modulus, in combination with Qu, permits an estimation of the magnitude of deformation at failure for a given lithological unit and thus is sometimes used to assess the relative stability of pit walls which are exhibiting signs of distress.

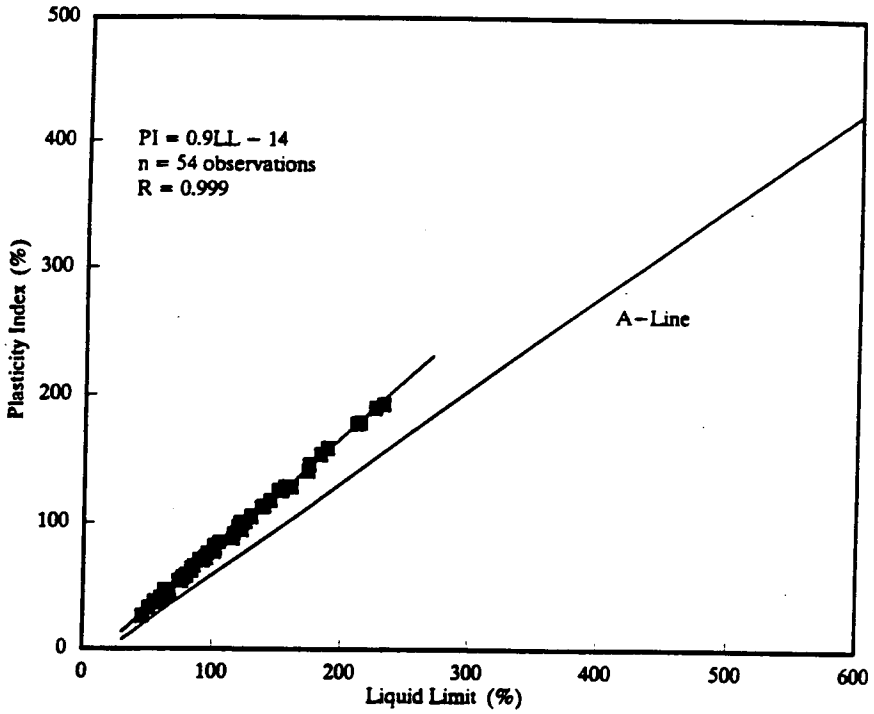

Figure 3-1. Plasticity chart - Syncrude hole 01.

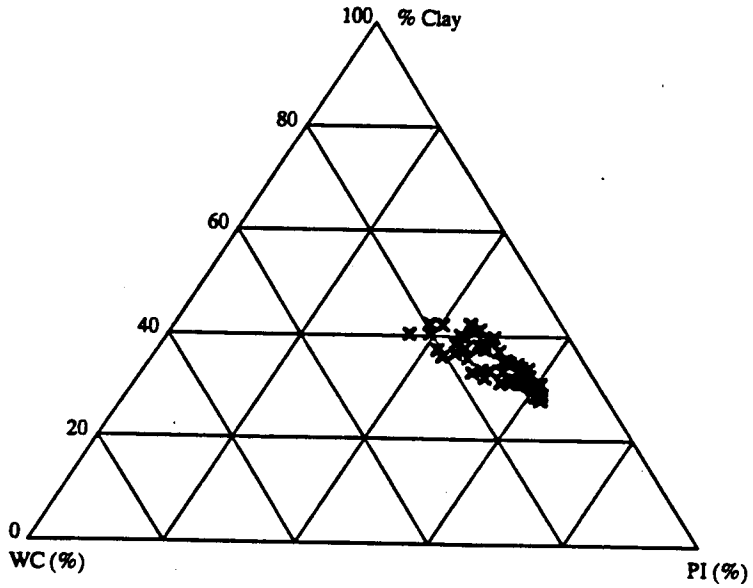

Figure 3-2. Classification parameters - Syncrude hole 01.

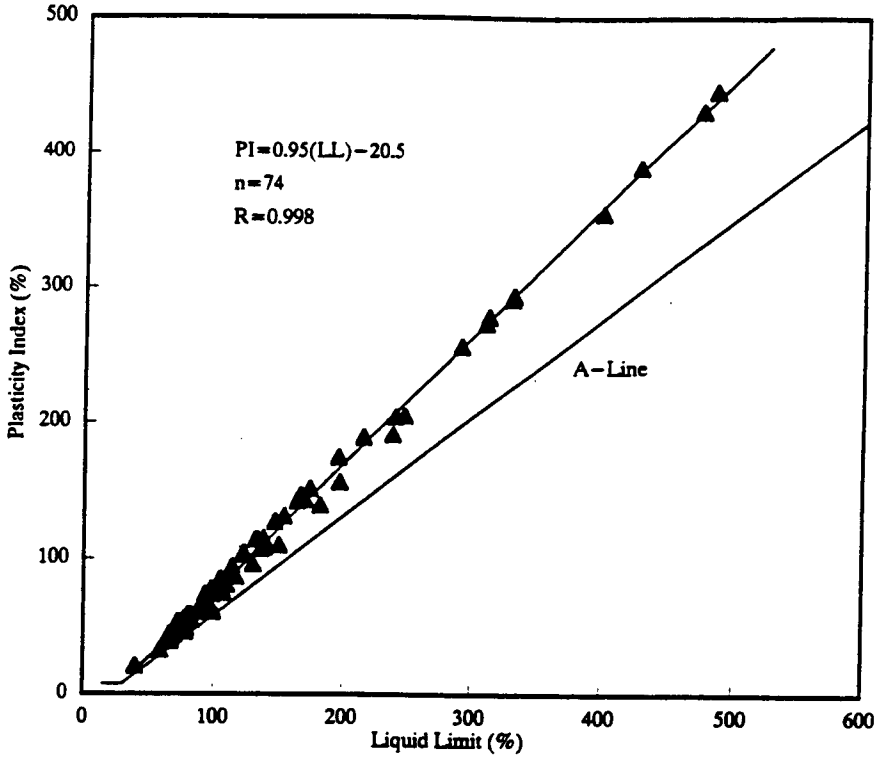

Figure 3-3. Plasticity chart - Highvale data.

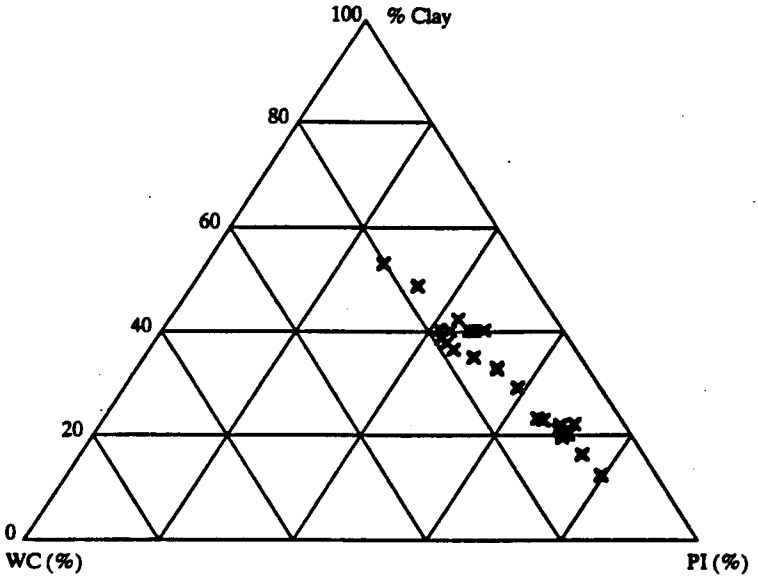

Figure 3-4. Classification parameters - Highvale data.

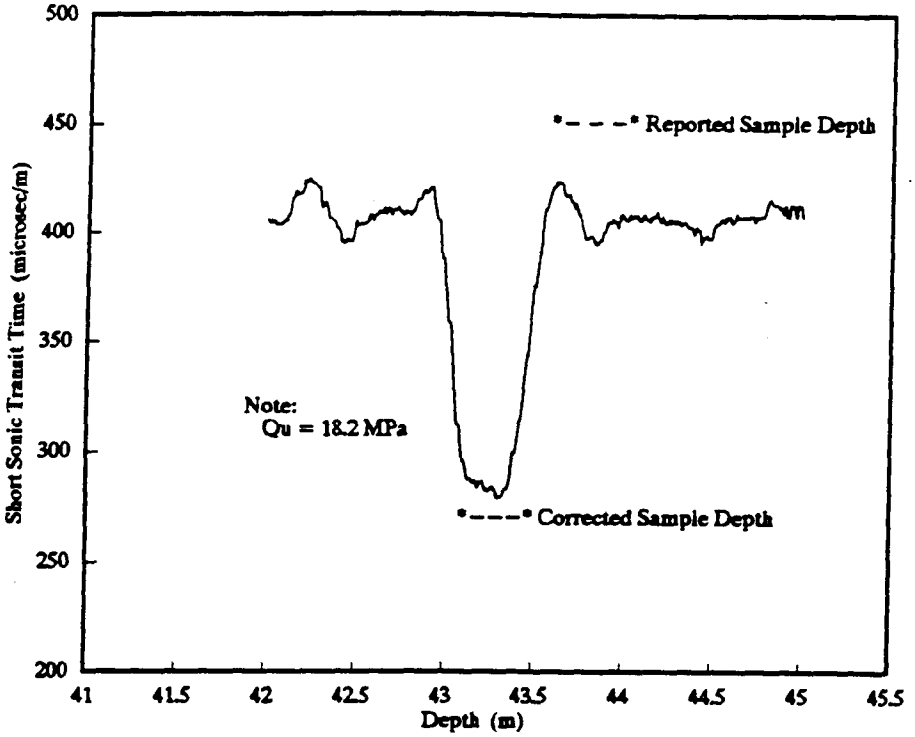

Figure 3-5. Typical depth correction for Qu specimens - HV88420.

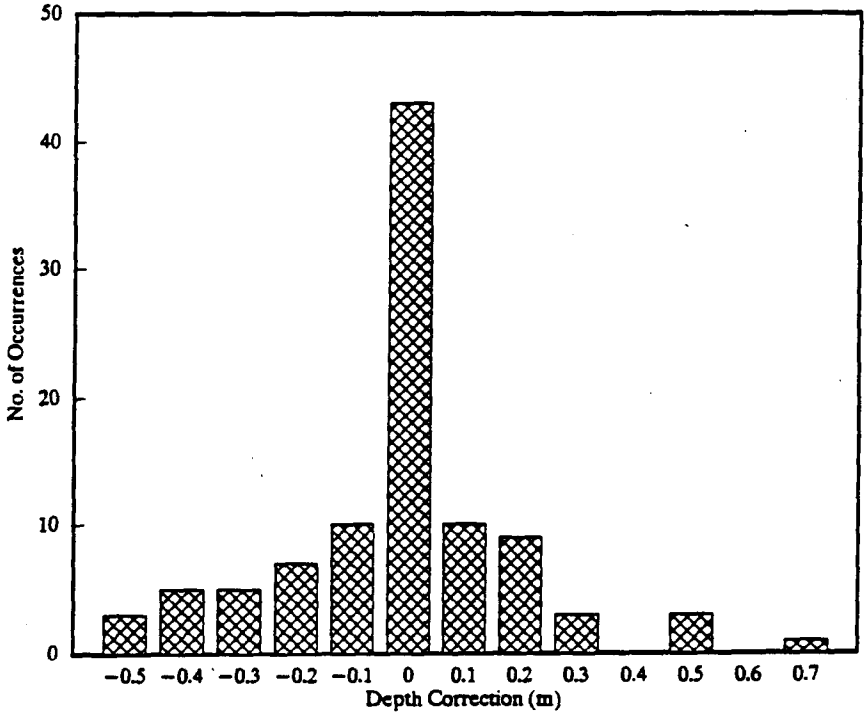

Figure 3-6. Histogram of sample depth corrections - Highvale 1987-89 data.

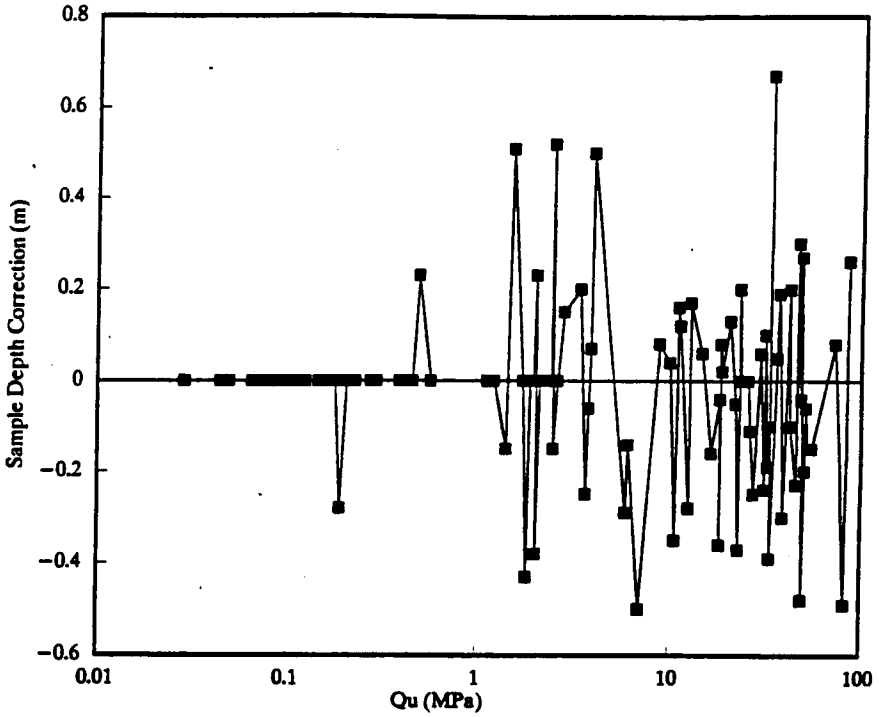

Figure 3-7. Sample depth correction vs Qu - Highvale 1987-89 data.

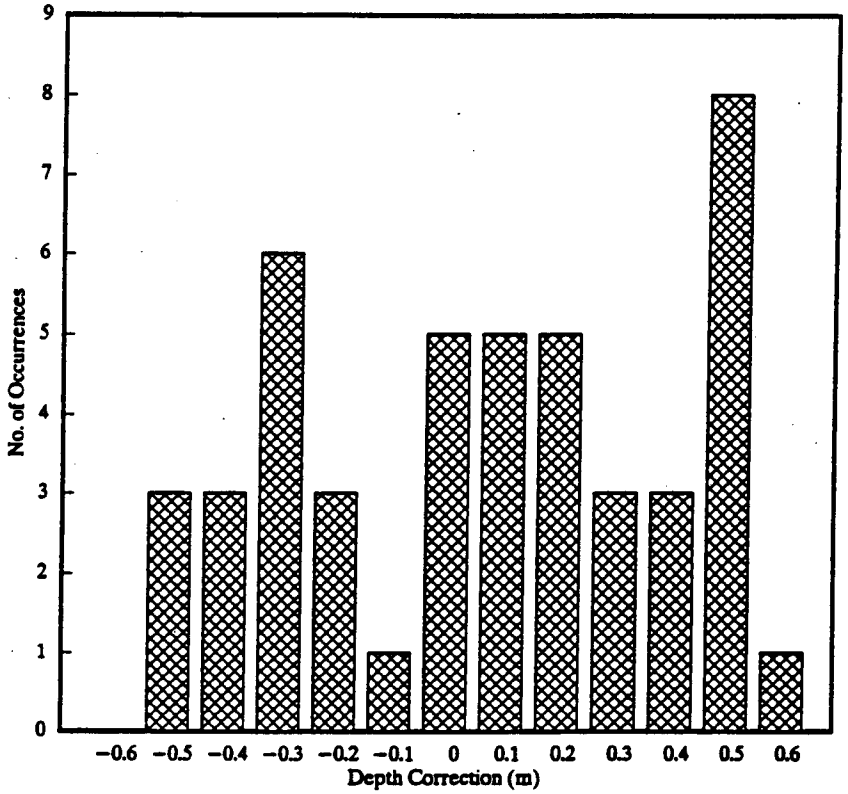

Figure 3-8. Sample depth corrections- density log basis - Highvale and Big Valley data.

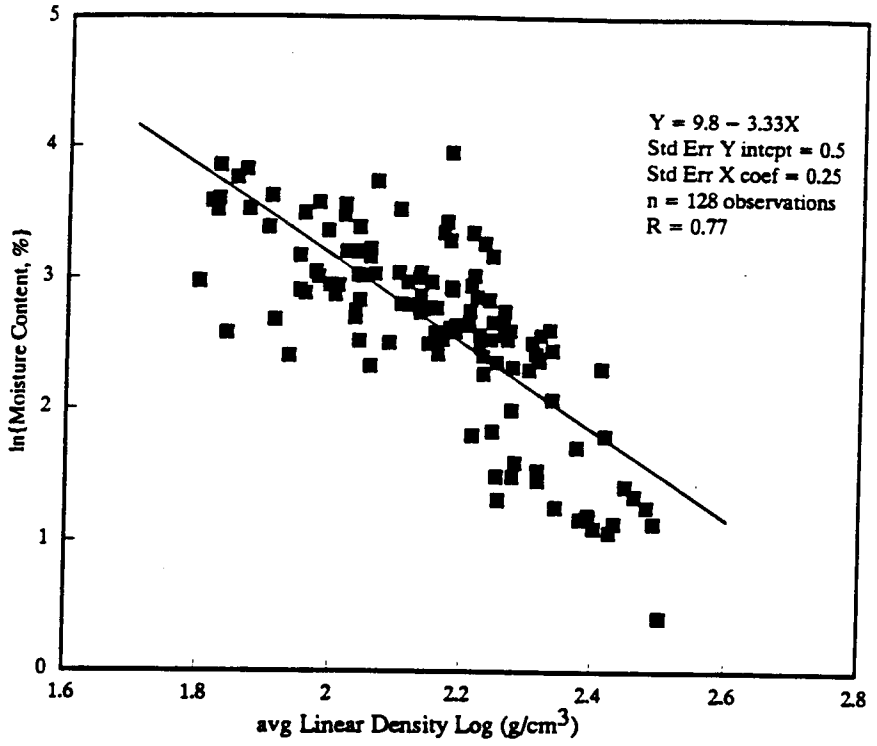

Figure 3-9. Moisture content vs linear density - Highvale 1988-89 data.

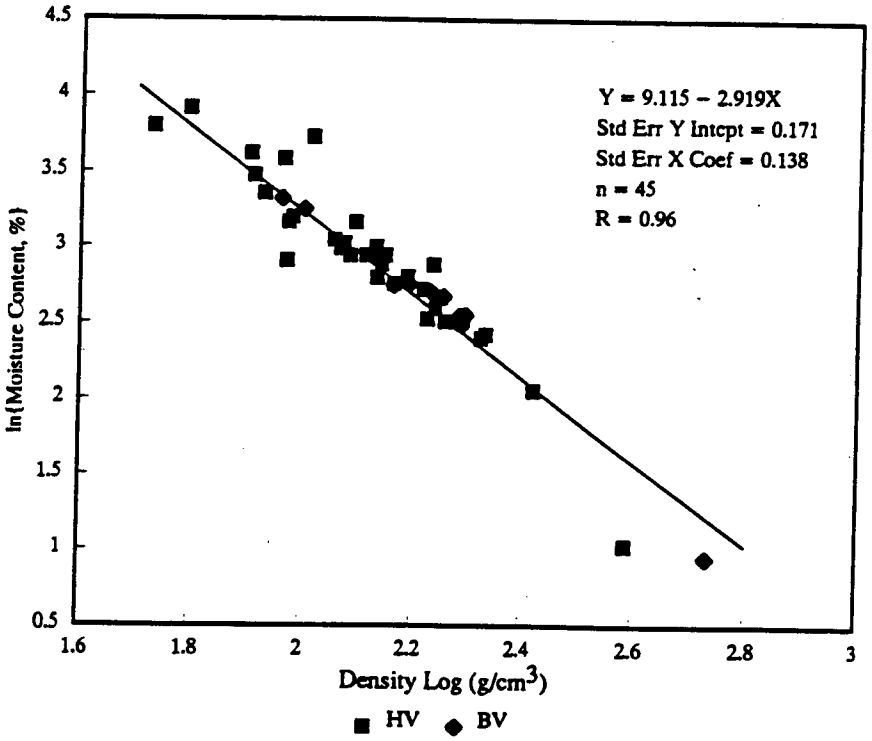

Figure 3-10. Moisture content vs density log - Highvale and Big Valley data - sheet 1.

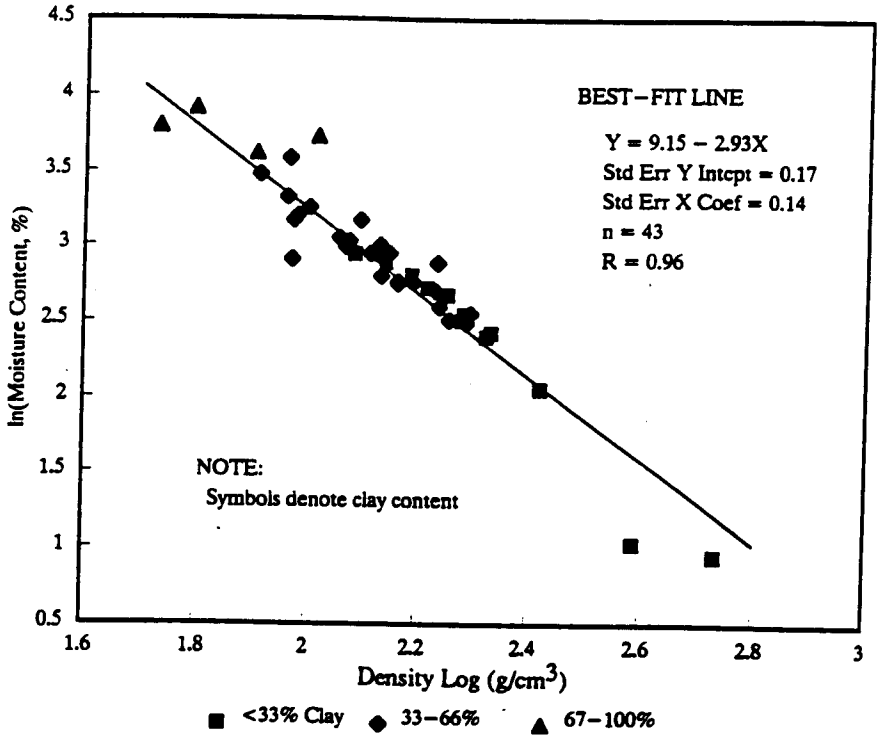

Figure 3-11. Moisture content vs density log - Highvale and Big Valley data - sheet 2.

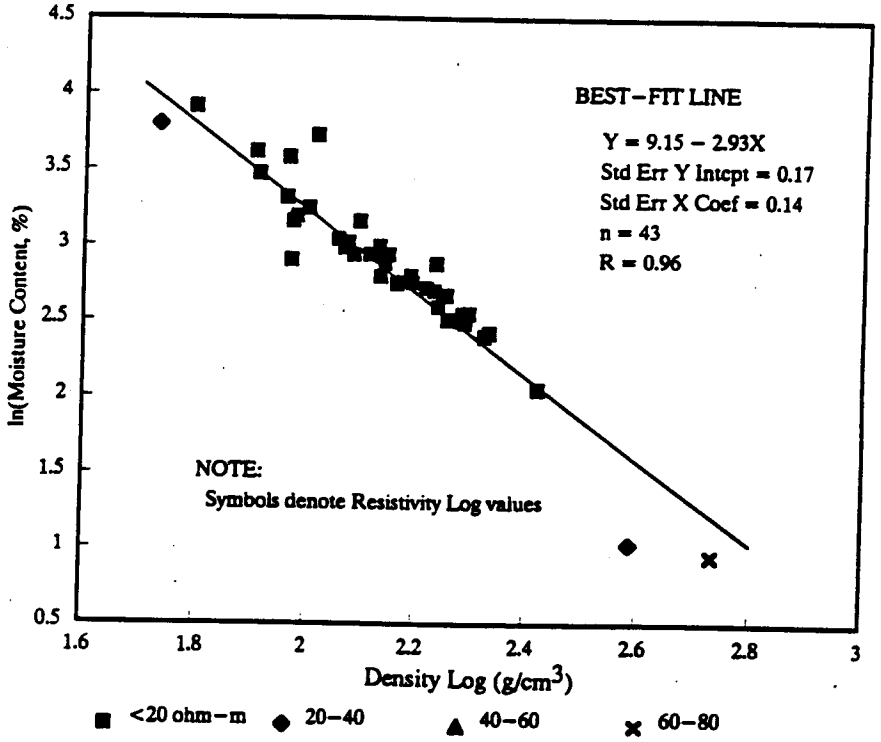

Figure 3-12. Moisture content vs density log - Highvale and Big Valley data - sheet 3.

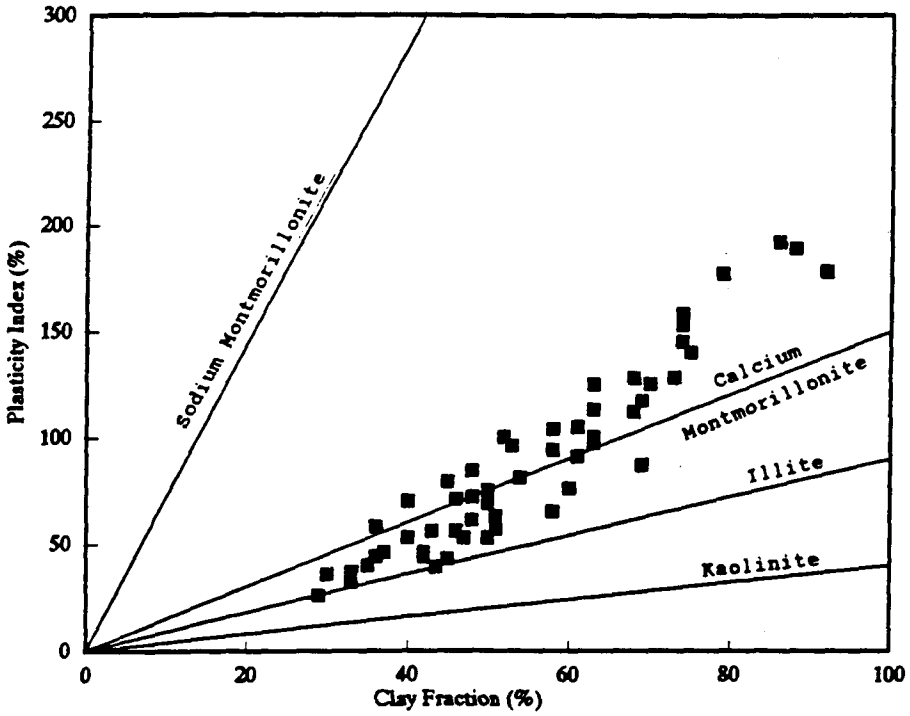

Figure 3-13. Activity chart - Syncrude data - sheet 1.

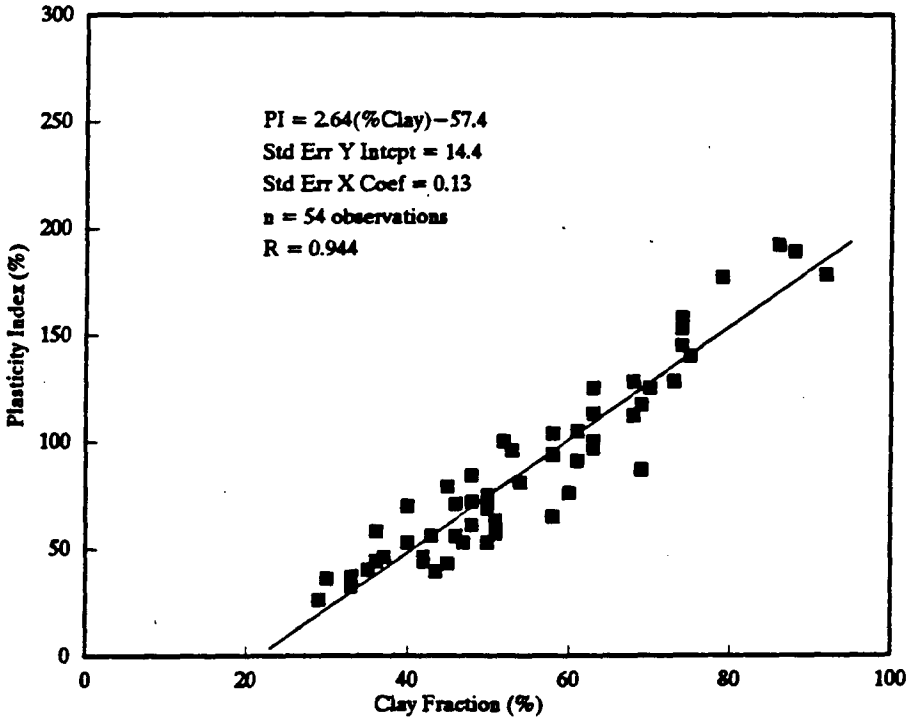

Figure 3-14. Activity chart - Syncrude data - sheet 2.

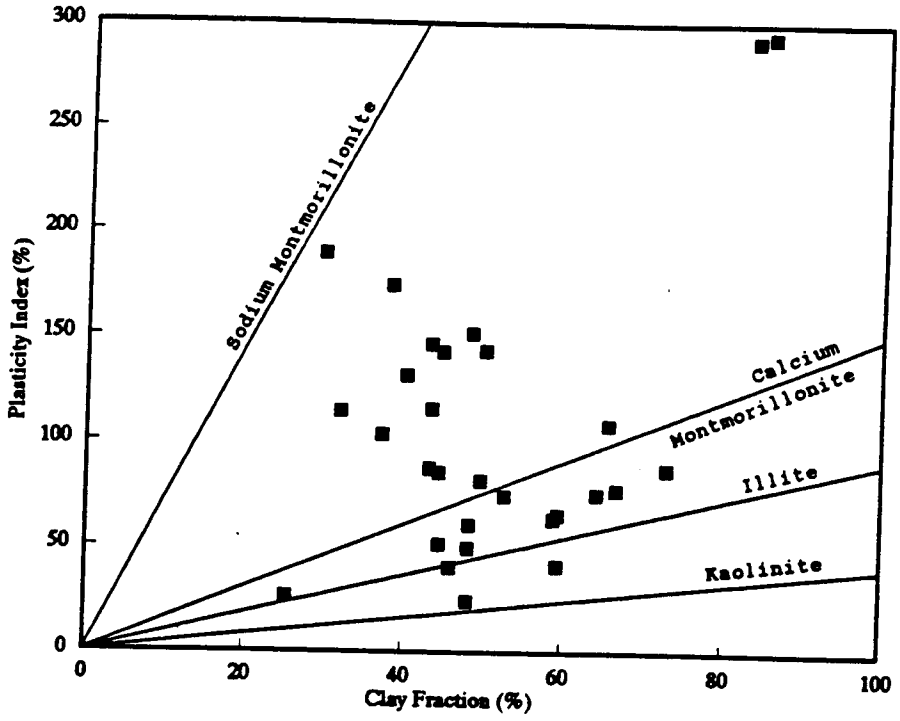

Figure 3-15. Activity chart - Highvale data.

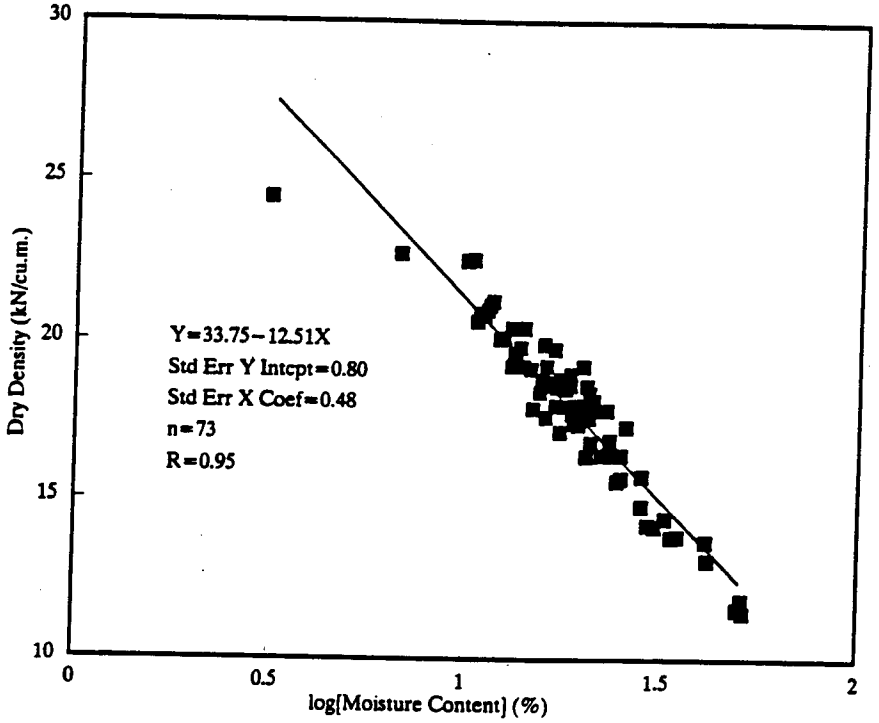

Figure 3-16. Dry density vs moisture content - Highvale 1988-89 data.

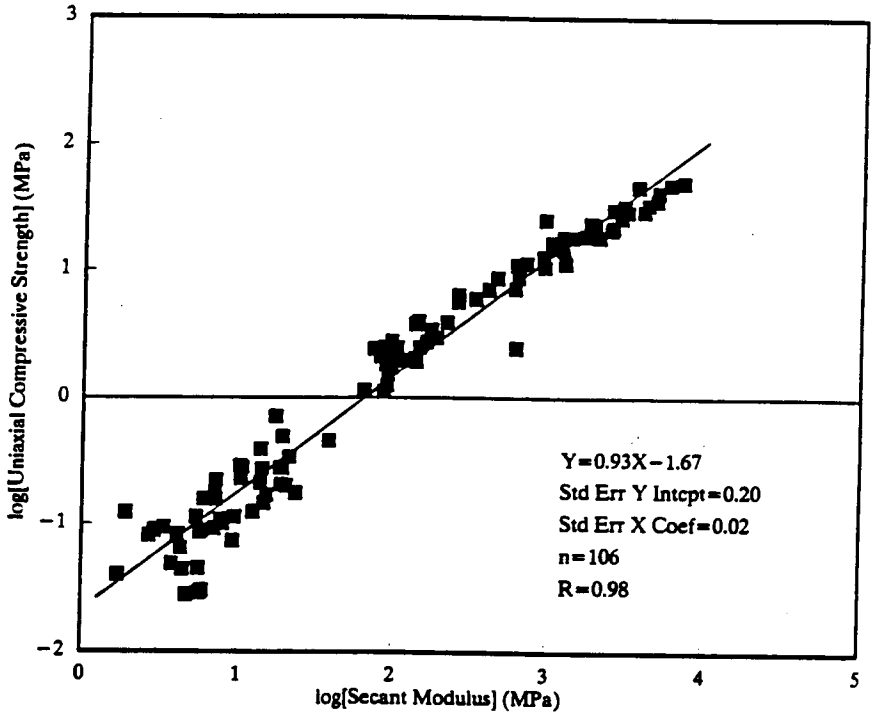

Figure 3-17. Qu vs secant modulus - Highvale 1988-89 data.

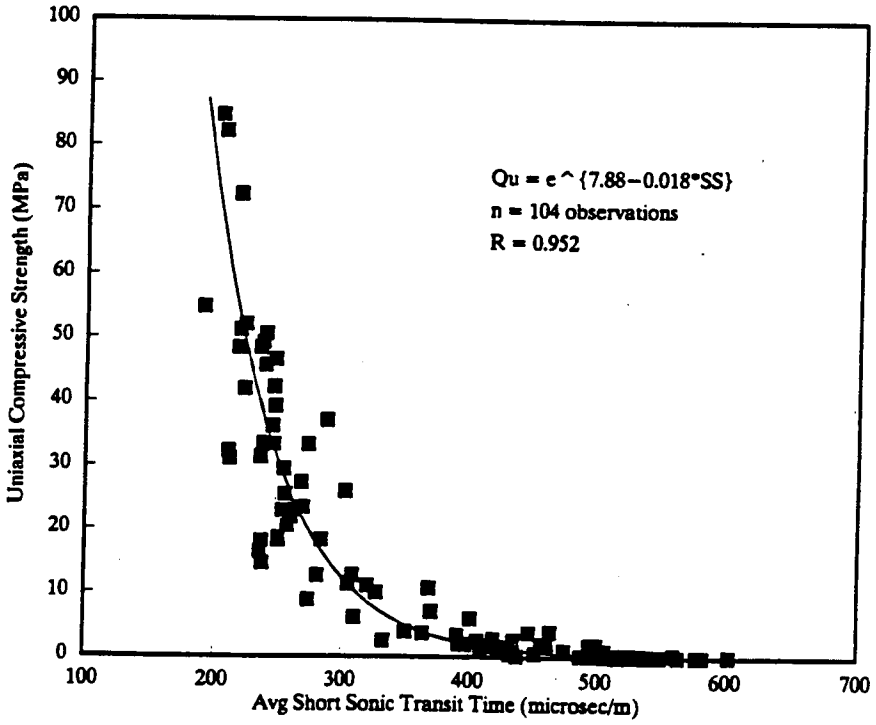

Figure 3-18. Qu vs short sonic - Highvale 1987-89 data.

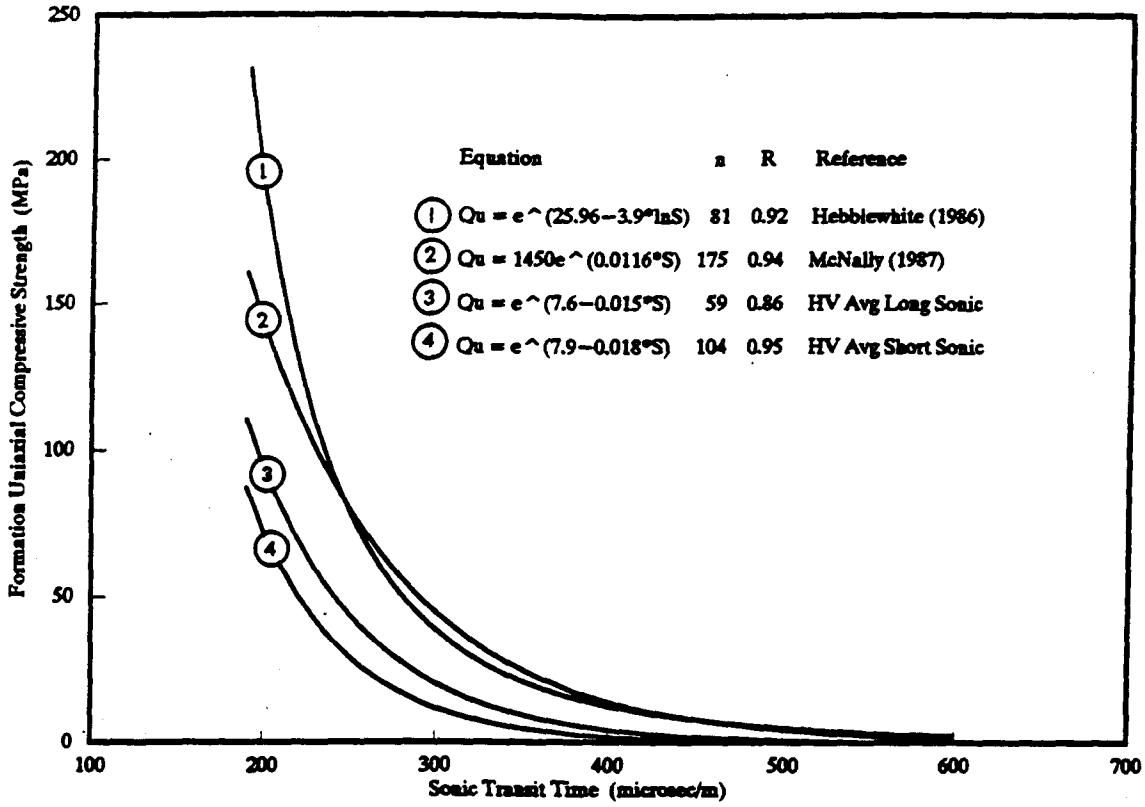

Figure 3-19. Qu vs sonic - comparative data.

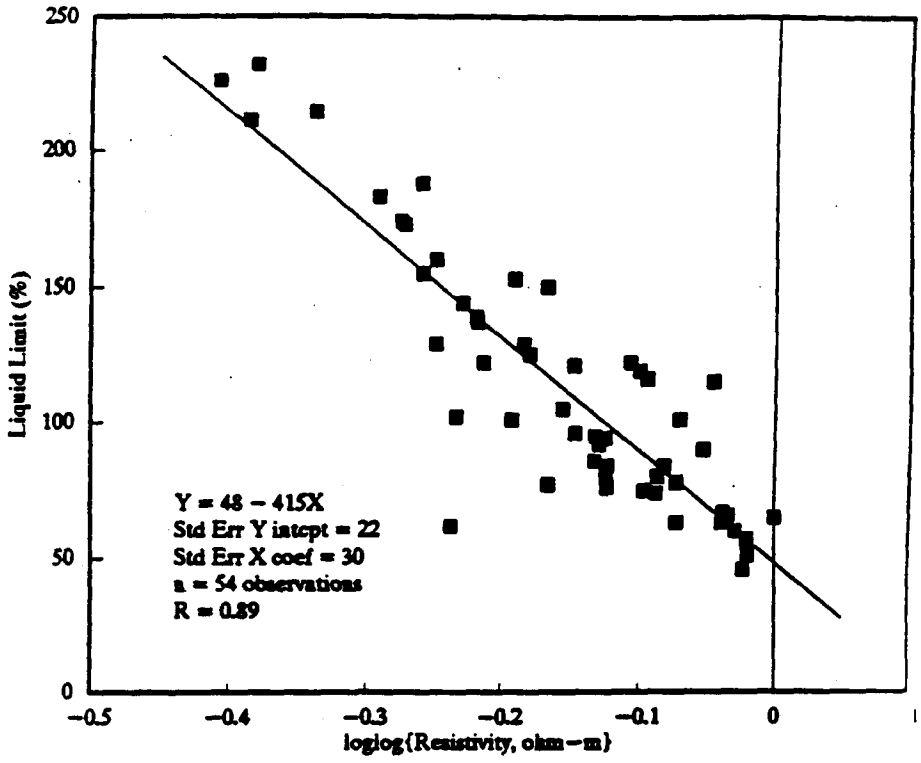

Figure 3-20. Liquid limit vs resistivity log - Syncrude hole 01.

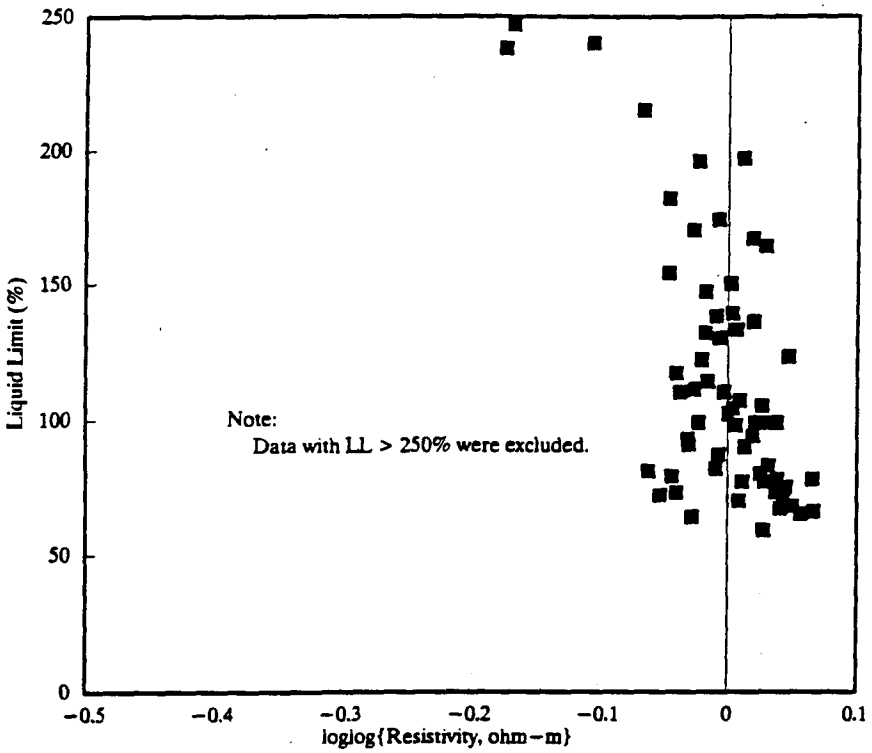

Figure 3-21. Liquid limit vs resistivity log - Highvale 1988-89 Data - sheet 1.

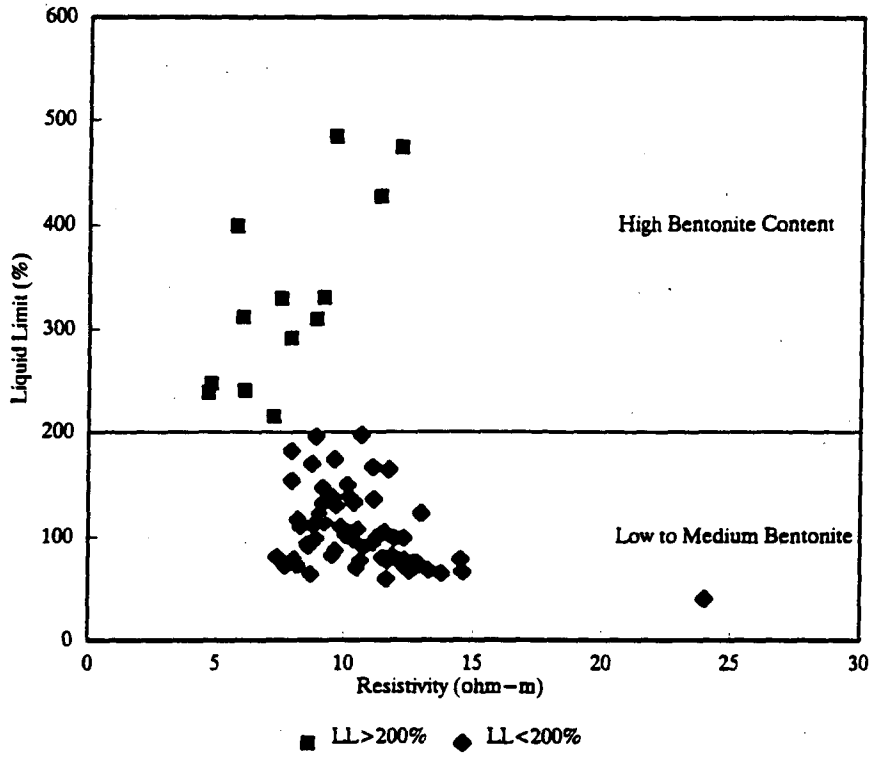

Figure 3-22. Liquid limit vs resistivity log - Highvale 1988-89 data - sheet 2.

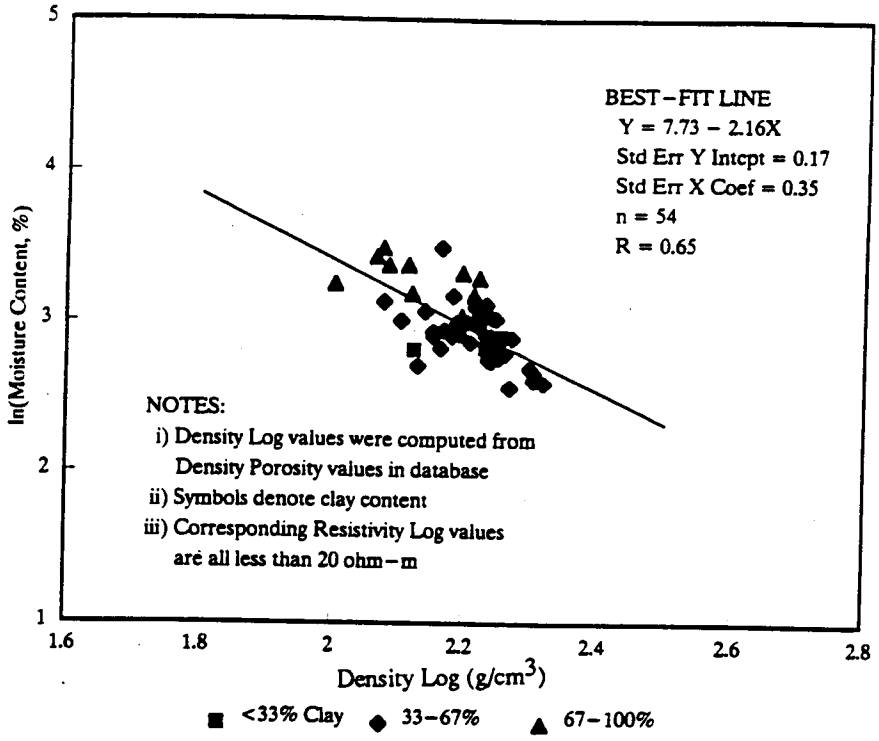

Figure 3-23. Moisture content vs density log - Syncrude hole 01.

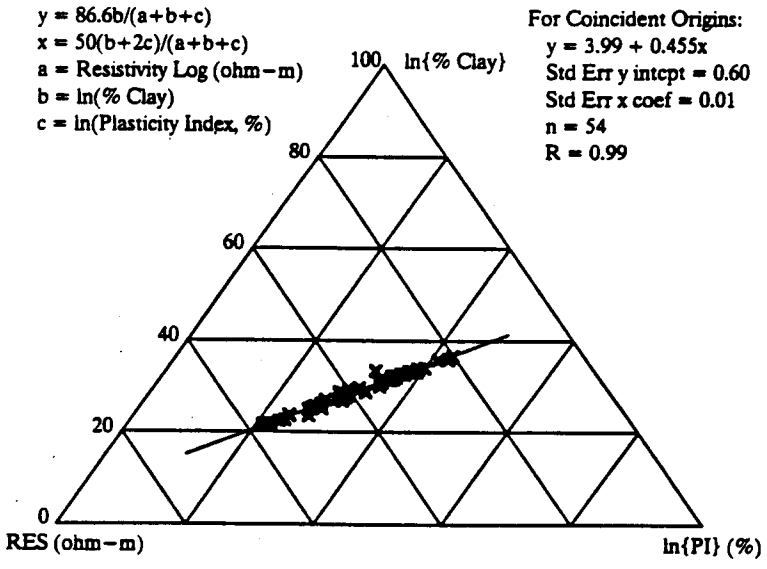

Figure 3-24. Resistivity vs % clay, Plasticity Index - Syncrude hole 01 - sheet 1.

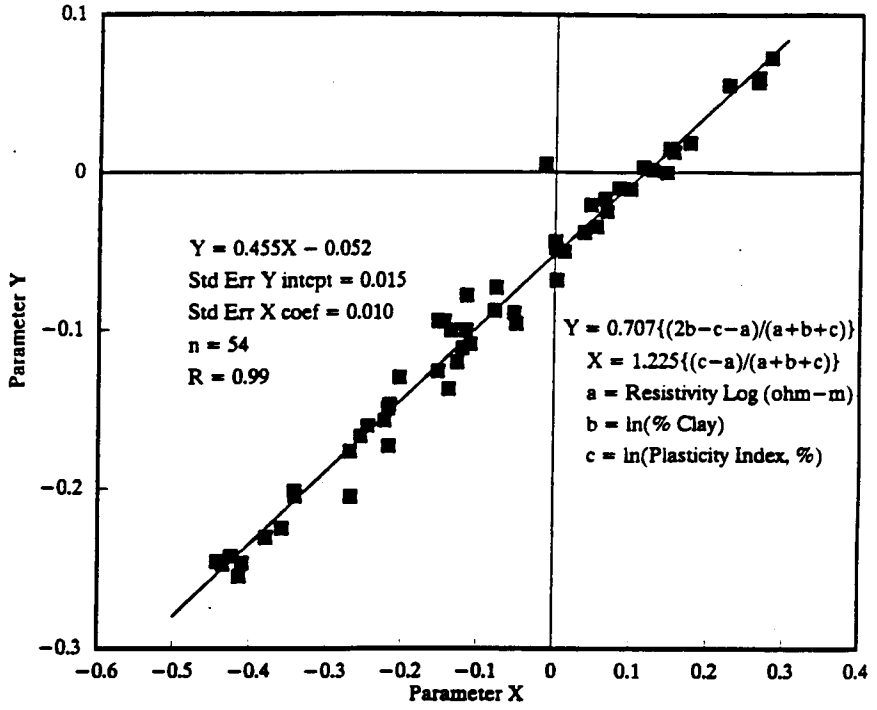

Figure 3-25. Resistivity vs % clay, Plasticity Index - Syncrude hole 01 - sheet 2.

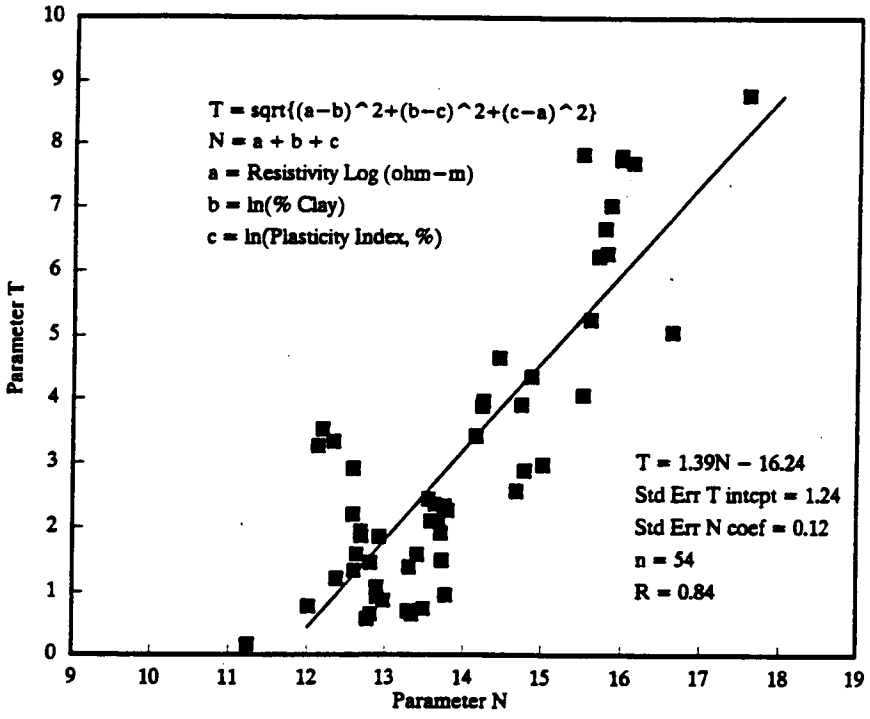

Figure 3-26. Resistivity vs % clay, Plasticity Index - Syncrude hole 01 - sheet 3.

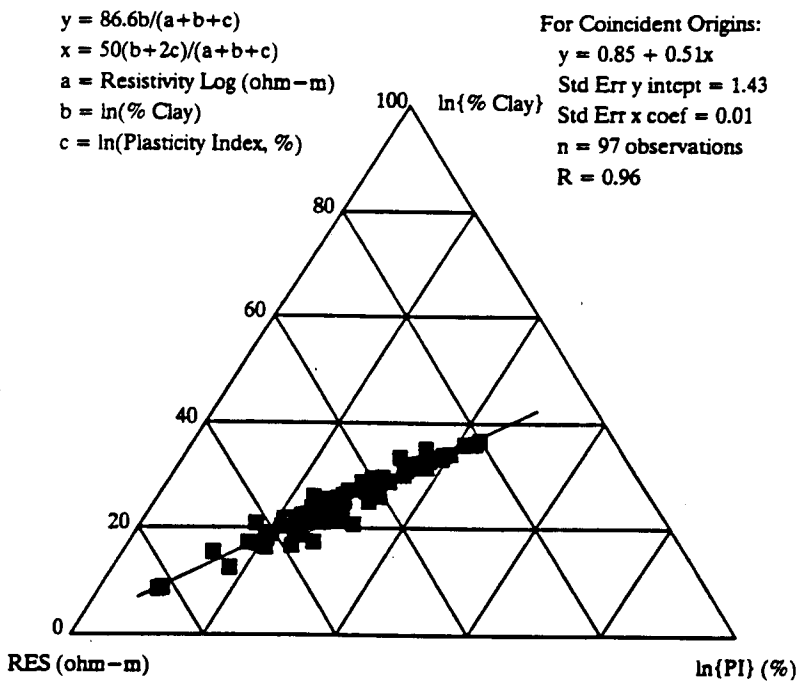

Figure 3-27. Resistivity vs % clay, Plasticity Index - Highvale, Big Valley and Syncrude data - sheet 1.

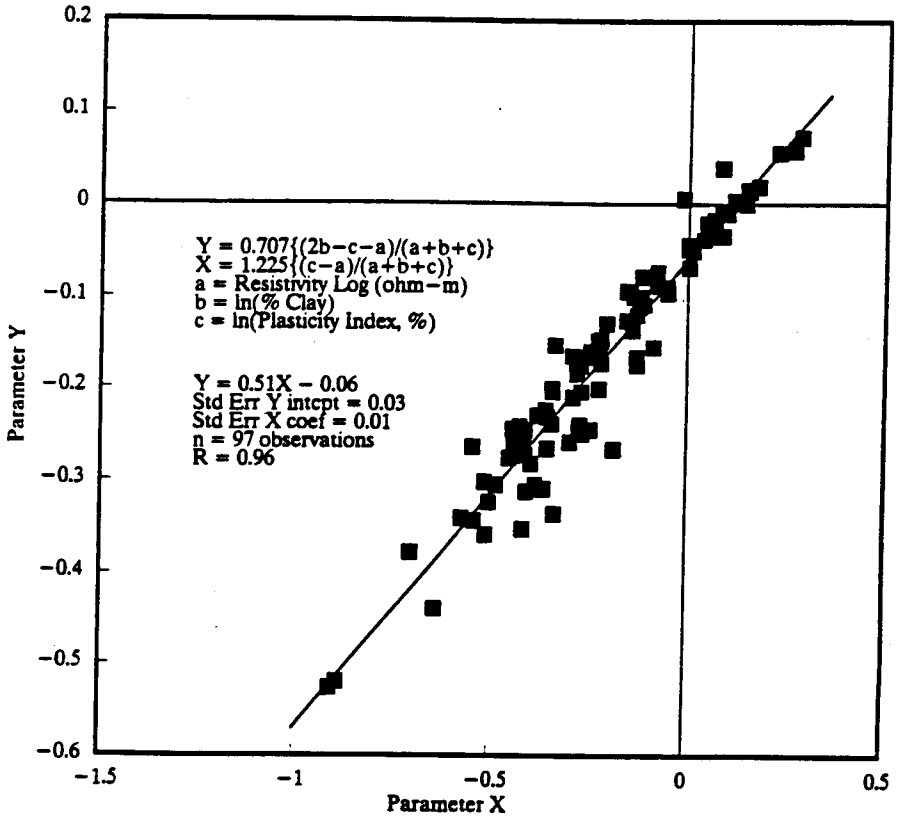

Figure 3-28. Resistivity vs % clay, Plasticity Index - Highvale, Big Valley and Syncrude data - sheet 2.

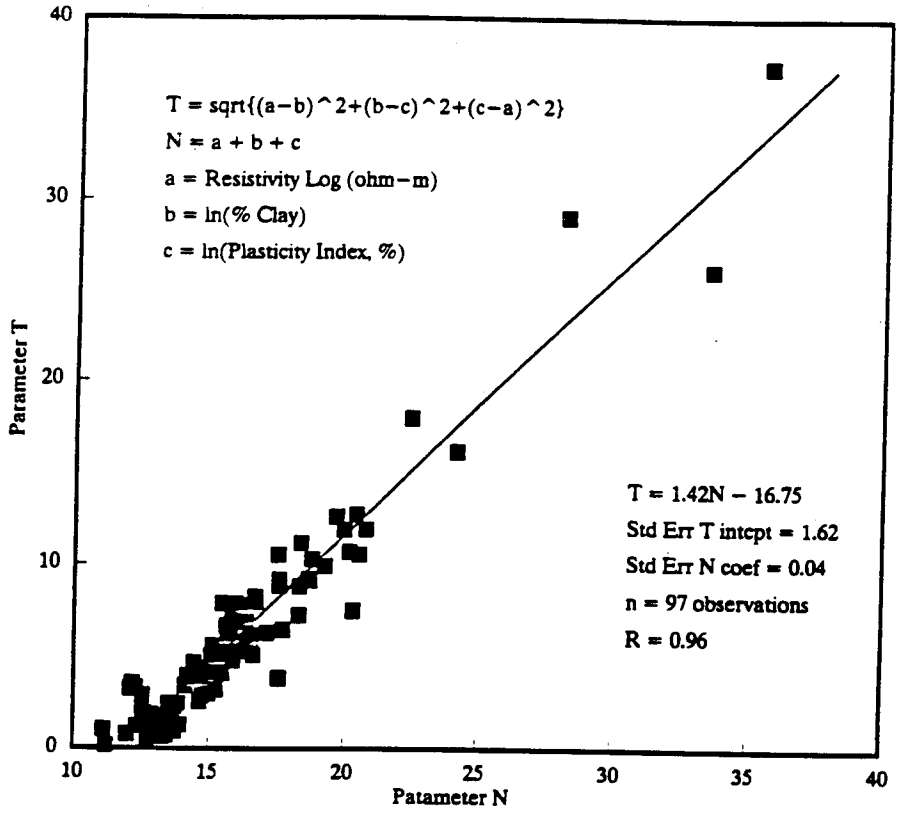

Figure 3-29. Resistivity vs % clay, Plasticity Index - Highvale, Big Valley and Sycrude data - Sheet 3.

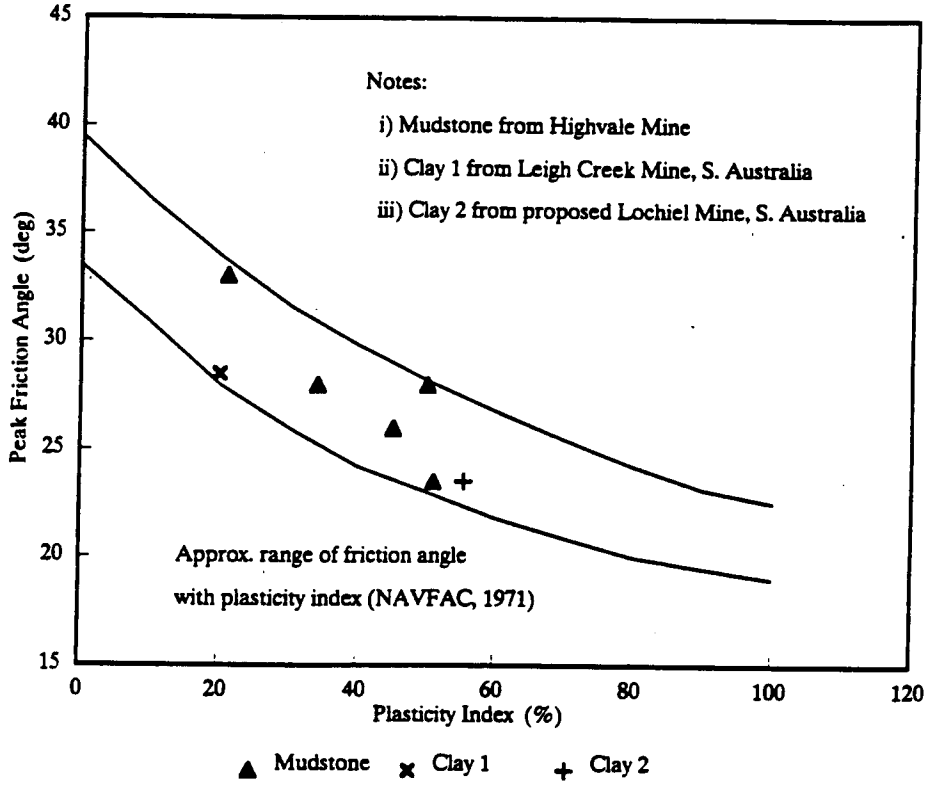

Figure 3-30. Friction Angle vs Plasticity Index.

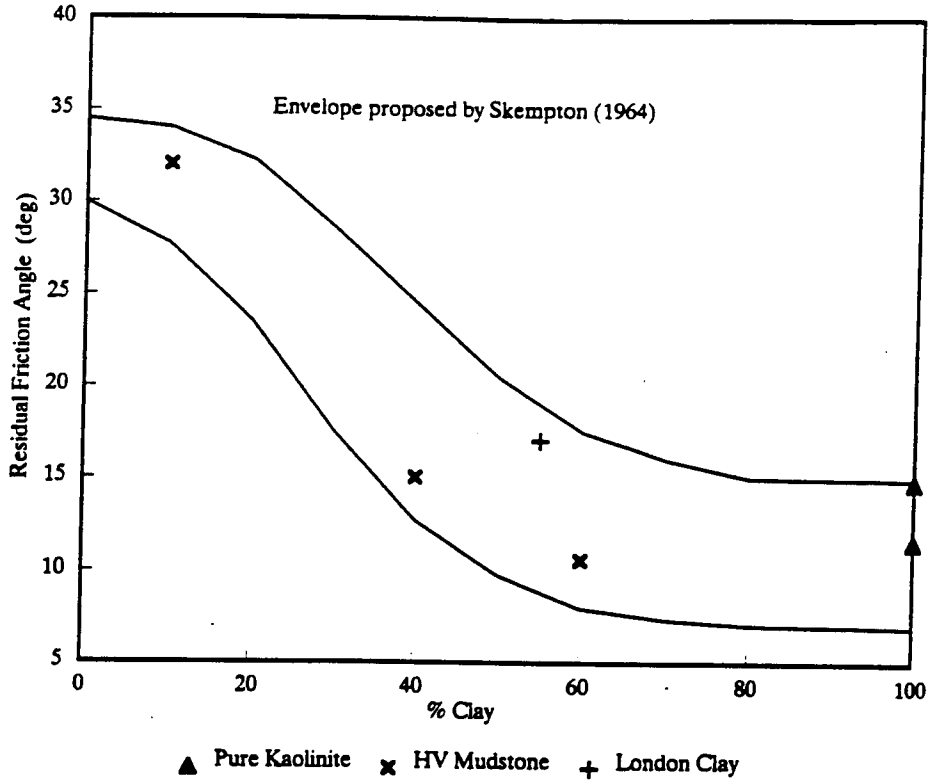

Figure 3-31. Residual friction angle vs % clay.

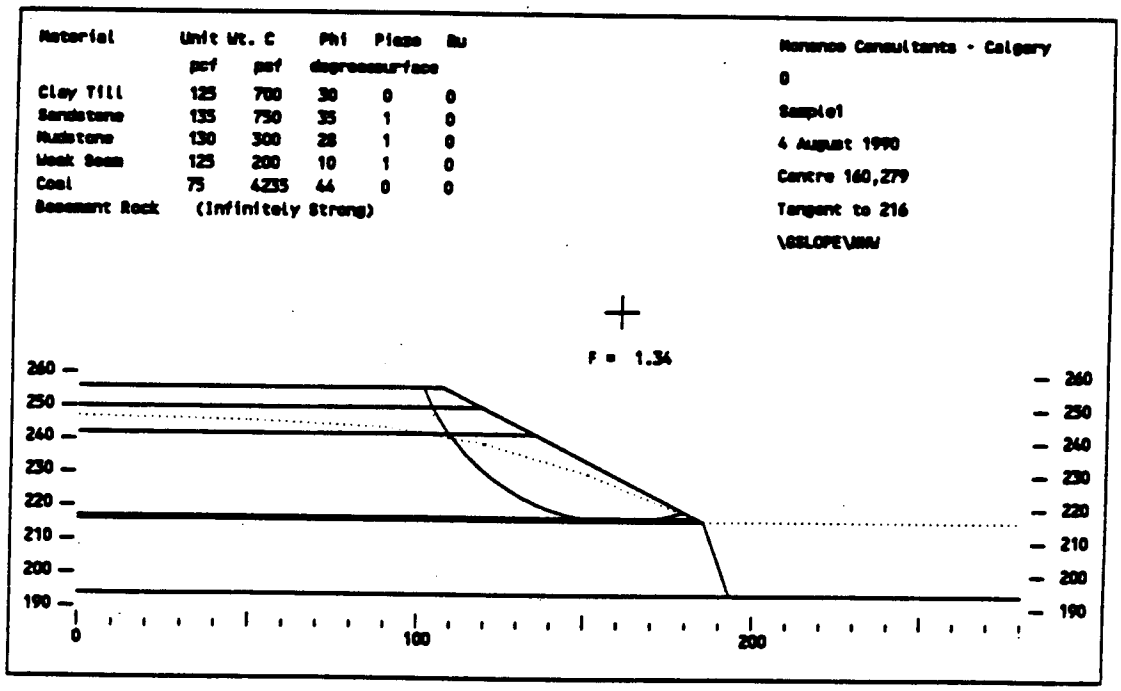

Figure 3-32. Stability analysis of a typical highwall.

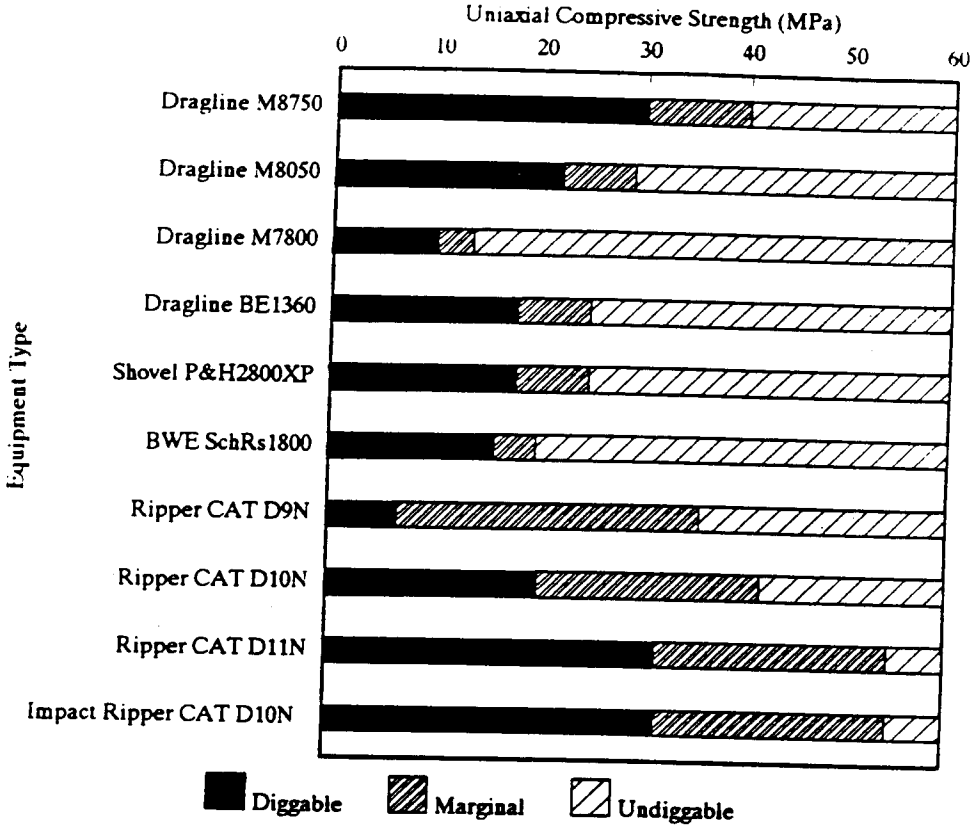

Figure 3-33. Equipment capability vs compressive strength.

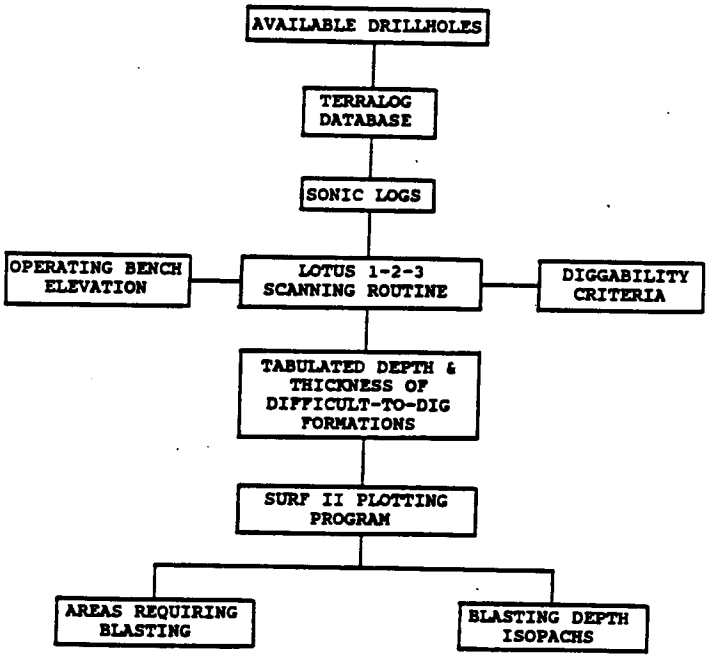

Figure 3-34. Procedure for depicting areas requiring blasting.

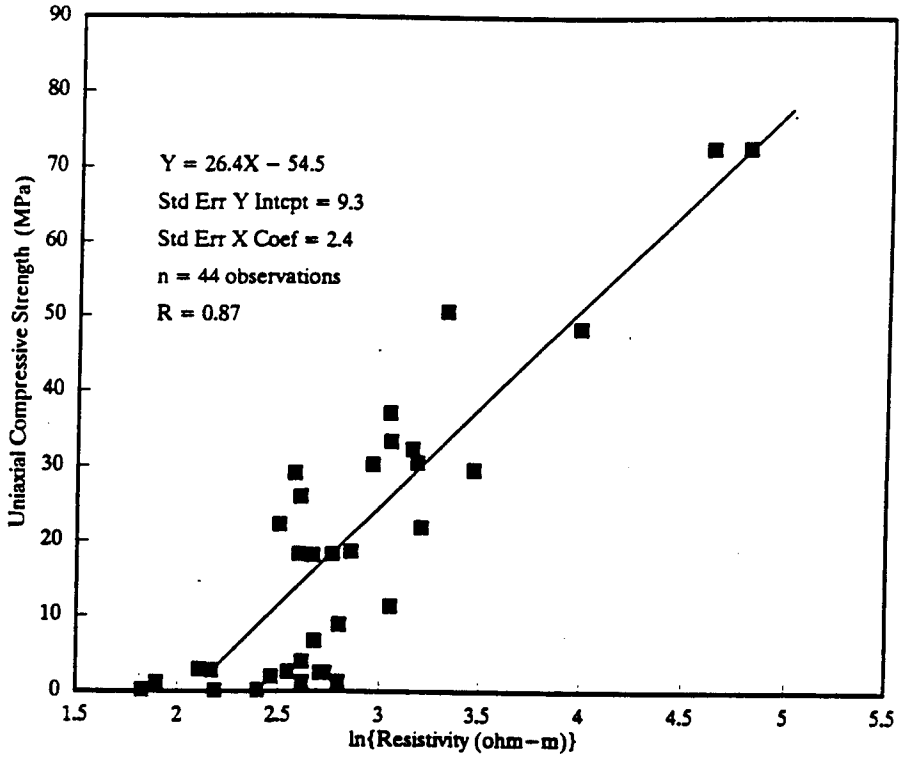

Figure 3-35. Uniaxial strength vs resistivity - Highvale data on sandstone.

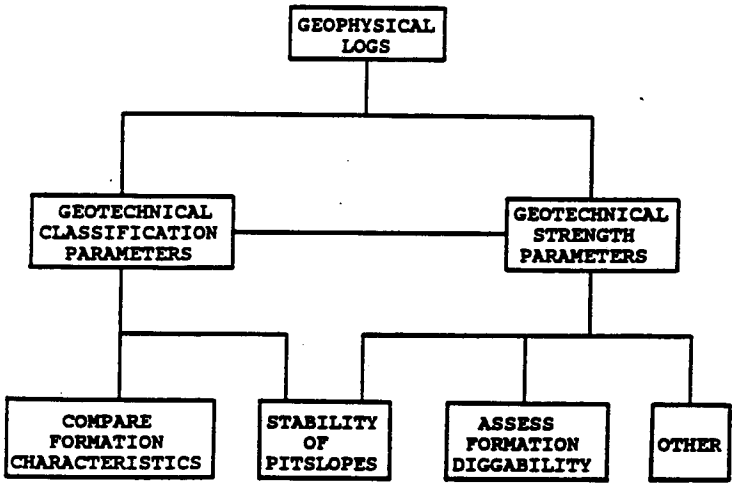

Figure 3-36. Applications to mining problems.

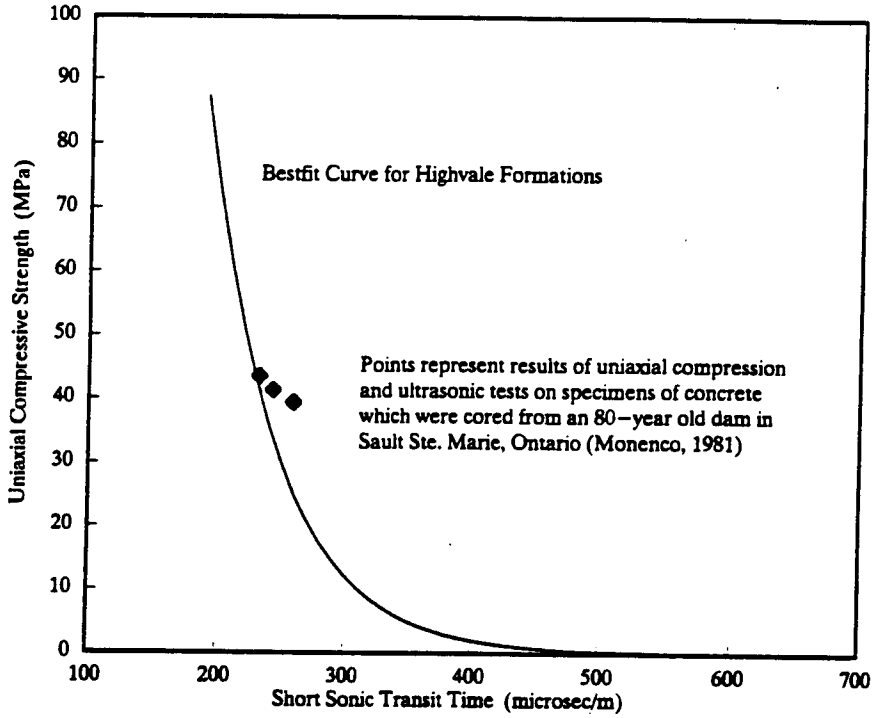

Figure 3-37. Qu vs short-spaced sonic - tests on concrete.

4. DETERMINING THE WATER TABLE

W. Scott Keys and John G. Pawlowicz

Water very strongly affects the engineering behavior of most soils and sediments, and most geotechnical engineering problems have water associated with them in various ways, either because of the water flowing through the voids and pores in the soil or rock mass, or because of the state of stress in the water in the pores (Holtz and Kovacs, 1981, p. 199). Dewatering in advance of mining is necessary to improve the stability of pit walls and floors at coal and oilsands mines. Bodies of perched water and poorly drained zones can cause problems and production delays.

Water also has a strong impact on the response of most types of geophysical logs. The discussions below focus on the use of geophysical logs to identify the water table in various types of sediments, with examples from the Highvale Mine and Big Valley area. Some work was also done on hydraulic conductivity during Phase 2 of the project. Only weak relationships were found for that parameter, but that may have been due to inconsistencies in the database and data quality (TransAlta, 1988).

4.1 WATER LEVEL AND WATER TABLE

The first problem in interpreting geophysical well logs in terms of the depth to water table is distinguishing between the water or drilling fluid level in the borehole and the water table, or top of the zone of saturation, in the rocks penetrated by the well. Fluid level and water table may coincide only under water-table conditions (non-artesian), where the well has had time to reach equilibrium and where there is a single aquifer and no bodies of perched water are present. Fluid level in the borehole may also change during logging operations so that it will appear at different depths on several logging runs. The location of saturated intervals perched above the water table may be just as important to understanding the groundwater system and to mining operations as the location of the water table.

In materials where the difference in water content between saturated and undersaturated materials is small it may not be possible to distinguish this change from lithologic changes. This is particularly true in fine-grained materials such as clay. Because most logs are affected by lithology as well as water content it may not be possible to differentiate the two unless other information is available, such as other types of logs or measurements in the well or on core or chip samples. Logs run

periodically may allow temporal changes in water content to be distinguished from lithologic changes.

In addition to lithology, well construction, borehole diameter and the actual difference in water content of the rocks above and below the water table must be considered along with the radius or volume of investigation of the logging devices used. With all of these variables to be considered it is apparent that the correct interpretation of borehole geophysical data in terms of the various water interfaces present within and adjacent to a well is not a simple matter. Because log response to these variables may be site specific the best approach is to establish useful techniques within a given hydrogeologic environment. This can best be accomplished by evaluating the response of the various logs at a site where the water table is relatively deep, possibly with perched water present. Piezometer data can be used to substantiate log interpretation, as in the examples described in Sec. 4.4 and 4.5.

4.2 BACKGROUND INFORMATION

In order to improve the accuracy of log interpretation for these purposes it is essential that information on the well drilling operations and well construction be available. The driller's log may indicate depths of water entry and lost circulation zones where the borehole diameter may be much larger than bit size. It is possible, however, that the water table or perched zones may not be noticed by the driller in low permeability materials. The following well construction information is needed because of the potential effect of these parameters on log response: drilled or reamed diameters and depths of changes; depths, types and diameter of casing; and depths where cement, bentonite or gravel pack may exist. It is also important that the water level in the well be measured at the time of logging and it is useful to have a record of changes in water level since drilling was completed. All of the parameters listed above may cause log response unrelated to the location of the tops of intervals of saturation in the rocks penetrated by a borehole. If the borehole is available for logging before casing is installed, a caliper log should be run because large washouts below the water level may appear on logs as perched water. With many types of logs it is possible to decrease borehole effects by increasing the spacing between source and detector for neutron and gamma-gamma logs or between electrodes for resistivity logs; of course this approach also decreases the vertical resolution of the logging devices.

4.3 APPLICABLE LOGS

The nuclear logs, neutron, and density, with supporting information from gamma and caliper logs, are the most useful for locating saturation under the widest range of borehole conditions. They provide information through casing regardless of type and with either air, water or drilling mud in the drillhole. Small-diameter induction probes may be used to detect saturation in air-filled, PVC-cased holes but they are not as widely available nor as frequently used as the nuclear devices. For this reason interpretation of induction logs is not based on much experience. The standard multi-electrode resistivity systems may be used if the borehole is filled with conductive fluid that is not too saline and the borehole is not cased. Sonic or acoustic velocity logs may also provide information on the water table if the borehole is filled with water above the water table.

4.3.1 Interpretation of Neutron Logs

Response of neutron logs is most closely related to the hydrogen content of materials within and adjacent to the drillhole. The standard, long-spaced neutron log shows a negative deflection or decrease in count rate when the hydrogen content within the volume of investigation is increased. When rocks are saturated the response of neutron logs can be related to porosity if no hydrocarbons or interfering elements are present. If the pore spaces are not completely filled with water, neutron log response can be related quantitatively to moisture content. The logs are widely used in agriculture to record changes in moisture content above the water table. Like most logging devices the radius or volume of investigation of neutron probes does not have a sharp boundary and materials closer to the probe influence the recorded signal more than materials farther away. Thus the water level in a larger-diameter well will probably cause a greater deflection on neutron logs than the water table located outside the casing. Neutron logs are more sensitive to small changes in water content where the total hydrogen content in the volume of investigation is small. For example, a 1% change in moisture content might be quite detectable where the total moisture is less than 5% but not detectable where the total moisture is greater than 30%.

Because both clay and hydrocarbons can significantly effect the response of neutron logs and because both are common in the coal and oilsand deposits of interest they must be identified by other means in order to improve the accuracy of locating the water table. Clay beds can frequently be identified by increased radioactivity on gamma logs and lower resistivity than adjacent sands. In contrast most hydrocarbons tend to have a low natural radioactivity and have a greater resistivity than clay or sand.

4.3.2 Interpretation of Density Logs

The count rate on density logs is inversely proportional to the electron density of materials within the volume of investigation and electron density is proportional to bulk density for most materials. Greater water content in the pore spaces increases the bulk density and thus decreases the measured count rate. By convention density logs are usually plotted with count rate increasing to the left so that they respond similarly to neutron logs under saturated conditions; porosity increases to the left. Some of the density logs from Highvale are plotted with count rate increasing to the right, however, as in Fig. 2-3. The greater water content, and thus greater bulk density, below the water table should cause density logs to deflect to the right within a rock unit with consistent lithology and porosity if there are no interfering factors such as borehole construction.

Above the water table neutron and density logs may not respond similarly. A dry sand with high porosity may produce a positive deflection on a neutron log and a negative deflection on a density log in comparison to adjacent clay beds. Density logs are usually most sensitive to small changes in water content where the bulk density is small (high porosity), which means that they may be most effective where neutron logs are least effective. Density logs are usually more sensitive to changes in borehole diameter and casing than are neutron logs.

4.3.3 Interpretation of Resistivity Logs

If lithology is constant, rocks with a greater water content will have a lower resistivity than the same rocks when dry. In some rocks this change is quite small. The standard resistivity logs require a conductive fluid in the borehole and if this fluid is too saline much of the current flow will be within the borehole and the quality of the log will be affected. With the conventional multielectrode devices the radius of investigation is increased by longer electrode spacing, which decreases the vertical resolution of the log and reduces borehole effects. Induction logs can be used in the same way as conventional resistivity logs but will operate without conductive fluid in the hole and in cased holes. Geonics, a Canadian company, produces a small-diameter induction probe that is used routinely in boreholes cased with PVC, and it is relatively insensitive to the borehole fluid.

4.3.4 Interpretation of Sonic Logs

The relationship between the transit time of the compressional wave as measured by the conventional sonic log and porosity is based on the time average equation. This

equation assumes that the measured transit time (or velocity) is an average of the transit time in the pore fluid and that of the rock matrix. Where the pore spaces are not filled with water the transit time should increase significantly. The interpretation of sonic log response at the water table is complicated by the equipment adjustment related to the threshold of compressional wave detection. The log trace may show a sharp increase in transit time to an off-scale or limited value above the water table.

4.3.5 Multiple Log Interpretation

The approach most likely to yield reliable information on the location of saturated zones is to interpret the logs mentioned above as a suite in combination with drilling and well construction information. This approach takes advantage of the synergistic nature of log response and is most efficiently carried out using a computer (Keys, 1989a). An example of this technique would be crossplotting neutron and gamma-gamma logs or plotting the ratios or differences between these two logs. This approach might emphasize dry intervals where the two logs may have a different response. Gamma log data may be used to identify depth intervals where neutron log response is related to clay rather than water content. Similarly caliper log data can be used to reduce the erroneous effect of borehole diameter increases on most logs. Keys and MacCary (1971) includes an example of the use of neutron and gamma logs to detect a body of perched water behind the casing in a relatively large-diameter well. The gamma log shows the location of a bed of clay on which the water is perched and the neutron log shows saturation above that clay bed.

4.4 CASE STUDY: HIGHVALE MINE

Data from the Highvale Mine provide examples of the response of the various logs described above. Water table depths for each borehole were taken from nearby piezometers (Table 4-1).

The logs of HV83-408 are not included in this discussion because the water table at that hole is too close to the surface; the logs stop at 2.5 to 3 m. The water table measurements were not made at the same time that the geophysical logs were run so that seasonal fluctuations and/or mining activity in the vicinity may account for some of the differences between the measured and log-derived water table reported here.

Table 4-1. Water table in depths determined from nearby piezometers.

Testhole #	Distance from testhole to piezometer (m)	Water table depth (m)
HV83-408	75	3.5
HV83-6	125	11.0
HV84-401	400	6.7
HV84-404	5	11.6
HV84-405	5	9.8

The figures referenced in this section of the report were plotted from digital log data. Fig. 4-1 shows the response of neutron, density, sonic and resistivity logs in the vicinity of the water table in borehole HV84-405. Most of the logs were terminated just above the top of the plot. The larger depth interval below the water table is plotted to show the range of log values where the rock is saturated. All four logs in Fig. 4-1 show a significant shift in average values within a metre of the water table depth from a piezometer measurement, which is shown on the figure. The response is sufficient for locating the approximate depth to the water table at this borehole in part because it is located within a thick section of rather uniform sandstone which should provide ideal conditions for the recognition of water table response. Fig. 4-2 is a similar plot for HV84-401 where the rock is mostly mudstone and all four logs show a significant shift within 0.5 m of the water table, probably because the mudstone is relatively uniform. In HV84-404 the neutron and density logs do not show a significant shift that is clearly associated with the water table even though the rock is reported to be mostly sandstone. However, the sonic and resistivity logs can be used to locate the water table in that borehole.

Fig. 4-3 is a crossplot of neutron and resistivity log response in HV84-405. The plot clearly defines two clusters of values representing the depth intervals above and below the water table. Although there is some overlap the data clusters are well defined. Crossplots of neutron - resistivity logs for other holes and resistivity - sonic logs also show distinct clusters of log values above and below the water table. Data from below the water table has a greater range of log values because of the more diversified lithology in this larger depth interval.

Fig. 4-4, 4-5, 4-6 and 4-7 are plots of the neutron, density, sonic and resistivity logs of

the four boreholes listed above. In Fig. 4-4 the neutron log of HV84-404 has a major shift at a depth of 7.5 m that probably is caused by the water level in the borehole at the time of logging. There is a smaller shift on that neutron log about 1 m above the reported water table that is consistent with the shifts seen on the other three neutron logs in the figure. In Fig. 4-5 it is clear that the density logs do not indicate the location of the water table consistently. Although there are shifts on the long-spaced sonic logs in Fig. 4-6 within 1.5 m of the water table the response is not entirely consistent. A comparison with the short-spaced sonic logs of HV84-401 and HV84-404 in Fig. 4-1 and 4-2 suggests that the short-spaced sonic log may be more effective for locating the water table than the long-spaced logs shown in Fig. 4-6. All of the resistivity logs in Fig. 4-7 show an increase in average resistivity above the water table. The three logs in Pit 03 show a gradual upward increase in resistivity starting 8 to 10 m below the water table but there is a shift near the depth where the water table was found in piezometers near HV84-404 and HV84-405.

In summary, neutron, density, sonic and resistivity logs at the Highvale Mine all indicate the location of the water table under some conditions. The approach most likely to provide the correct location, within a metre, is combined interpretation of all of the logs available. Lithology from core or cuttings description should also be used in order to eliminate lithologic variables that might be confused with log response caused by changes in water saturation.

4.5 CASE STUDY: BIG VALLEY

The Big Valley sites differ from the Highvale sites in that the water table is located in the till, rather than the bedrock. The objective here was to see if geophysical logs could detect the water table in clayey sediments.

Field work for the Big Valley study was piggy-backed onto an exploration drilling program carried out by TransAlta Utilities. Drilling and geophysical logging were funded by TransAlta, and piezometer installation, core sampling and water level monitoring were carried out by ARC personnel as part of the Downhole Geophysics Project. All drillholes were cored with a rotary drilling rig and geophysically logged by BPB. Logs were provided in both chart and digital format. The log suite consisted of gamma, focussed resistivity, caliper, sonic, density and dual-spaced neutron. A temperature log was run in one hole. Core samples were collected for geotechnical and X-ray diffraction analysis (TransAlta, 1989); the results were used in other parts of this project.

Big Valley is located approximately 130 km south of Edmonton (Fig. 1-1). Two sites were selected; Site 1 was on 25 m of drift, and Site 3 was underlain by 7 m of drift. A nest of shallow stand-pipe piezometers was installed at each site to determine depth of water table to within 0.5 m. Results of water level monitoring, shown in the hydrographs for Sites 1 and 3 (Fig. 4-8), indicate that the water table depth is about 1 m at Site 1 and 5.1 m at Site 3. Site 1 could not be used because the water table is too shallow for the geophysical logs to detect (log data stopped at 3 m).

Fig. 4-9 shows the piezometer nest installation and near-surface lithology for Site 3. The water table is located within the till, which has a high clay content with varying amounts of sand. The upper 12.5 m of the neutron, density, sonic and resistivity logs are shown in Fig. 4-10. Some of the prominent features on the logs are the spike at 7.5 m, representing a well-consolidated sandstone bed, and the coal sequence between 10 and 12.5 m. The water table however, does not cause a significant response in most of the logs, except for the sonic. The neutron log displays a very slight shift near the water table depth, but as discussed earlier, the high clay content and high moisture content of the till reduces the sensitivity of the log. The density log shows a strong positive shift at about 7 m that corresponds with the bedrock surface. Above 5.5 m the density log deflects slightly to higher density values. The depth of this shift corresponds with the water table, but the direction of the log response above the water table is opposite to what would have been expected. A similar response was noted in HV84-401 from the Highvale Mine where the near-surface lithology consisted of fairly uniform mudstone (Fig. 4-2). The sonic log appears to provide the clearest and most accurate indication of depth to water table at Site 3 (Fig. 4-10). The sonic response above the water table is artificially limited by the logging equipment and does represent the true velocity of the formation. The reason for this is not clearly understood, because the difference in moisture content above and below the water table is very small. Possibly there may be a relationship to the negative pressure of the water in the sediment above the water table. Another possible explanation for this phenomena may be related to the fact that the pore spaces must be full of water for acoustic coupling and transmission of the P-waves through the pore fluids. At Site 1 however, the sonic log shows a similar response to a depth of about 3 m, even though the water table was located at only 1 m. This may be due to a variation in water table depth over the 25 m distance between the logged borehole and the piezometers. Another factor may be the inability of the logging tool to operate properly within 3 m of the ground surface, even where the borehole is completely filled with fluid as it was at Site 1. The sonic logging tool in this case was 3 m long.

In contrast to the crossplot of logs from Highvale (Fig. 4-3), the Big Valley logs do not show two distinct groupings of values for zones above and below the water table, with the exception of plots using sonic values. The crossplots in Fig. 4-11 and 4-12 of

neutron - density, neutron - resistivity, resistivity - density and density - sonic values show the distribution of data points. It appears that in the fine-grained sediments, the neutron, density and resistivity logs are not sensitive enough to detect the water table. One of the problems in clays is that the moisture content does not change abruptly at the water table, as is the case in coarse-grained sediment. The pore spaces in the capillary fringe zone, which can extend up for several metres above the water table in clayey sediments, are virtually saturated.

In addition to the conventional geophysical logging described above, a small portable neutron moisture probe of the type used primarily for agricultural purposes, was tested for shallow moisture and density measurements at Big Valley. The test involved the collection of moisture and density data down to an depth of 10 m, which is deeper than the normal use of this tool. One of the important features of this type of neutron probe is its suitability for low-cost, long-term monitoring of changes in moisture conditions at a site. This investigation is described in the Phase 3A report (TransAlta Utilities, 1989) and briefly summarized in Appendix I of this report.

4.6 SUMMARY AND DISCUSSION

In summary, for the logs studied from Big Valley and Highvale, the sonic seems to give the best indication of water table in both clay-rich and sandy environments. The resistivity, neutron and gamma-gamma (density) logs also can detect the water table in sandy materials and should be used to support the response shown on the sonic log. Generally, the water table can be more readily detected by a suite of logs in coarse grained (sandy) sediment than in fine-grained (clayey) sediments. Crossplots of two logs can be used effectively to emphasize the difference in response above and below water table. However, other factors such as lithologic changes, borehole conditions and fluid level in the hole during logging must all be taken into consideration.

For the logs used in this study, Table 4-2 lists the relative responses to water table that work best in coarse-grained sediment. This assumes that all other factors remain constant. These log responses may not hold true where the sediment has high clay content because of bound water in the clays, and the effect of water in pore spaces of the capillary fringe zone.

Table 4-2. Relative response of applicable logs to water table in coarse-grained sediment.

Geophysical Log	Above WT	Below WT
neutron (counts)	higher	lower
neutron (apparent porosity)	lower	higher
density (counts)	higher	lower
density (g/cm^3)	lower	higher
density (apparent porosity)	lower	higher
sonic (interval transit time)	longer	shorter
resistivity (ohm-metre)	higher	lower

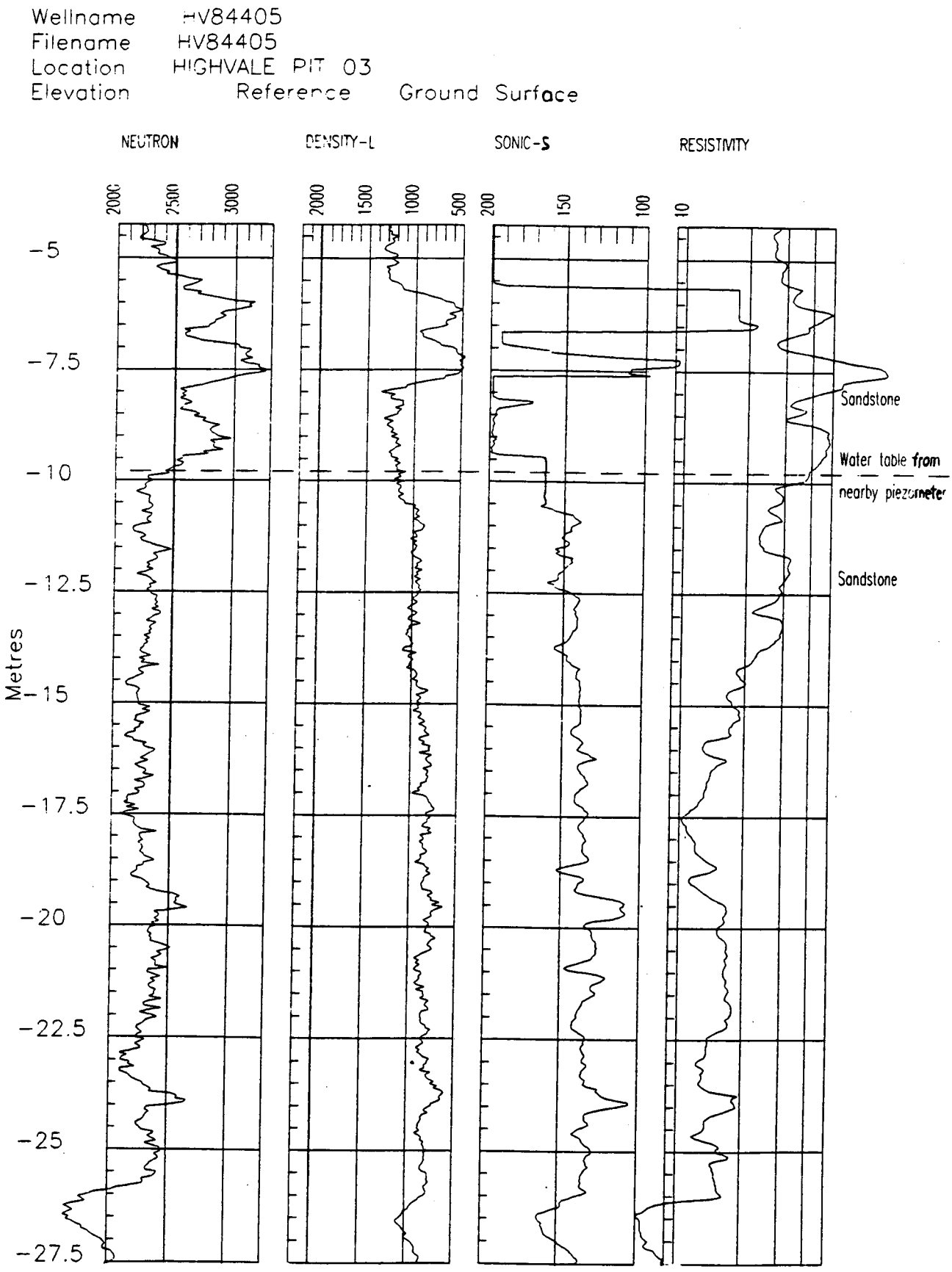

Figure 4-1. The response of neutron, density, sonic and resistivity logs in the vicinity of the water table in HV84-405 where the rock is uniform sandstone.

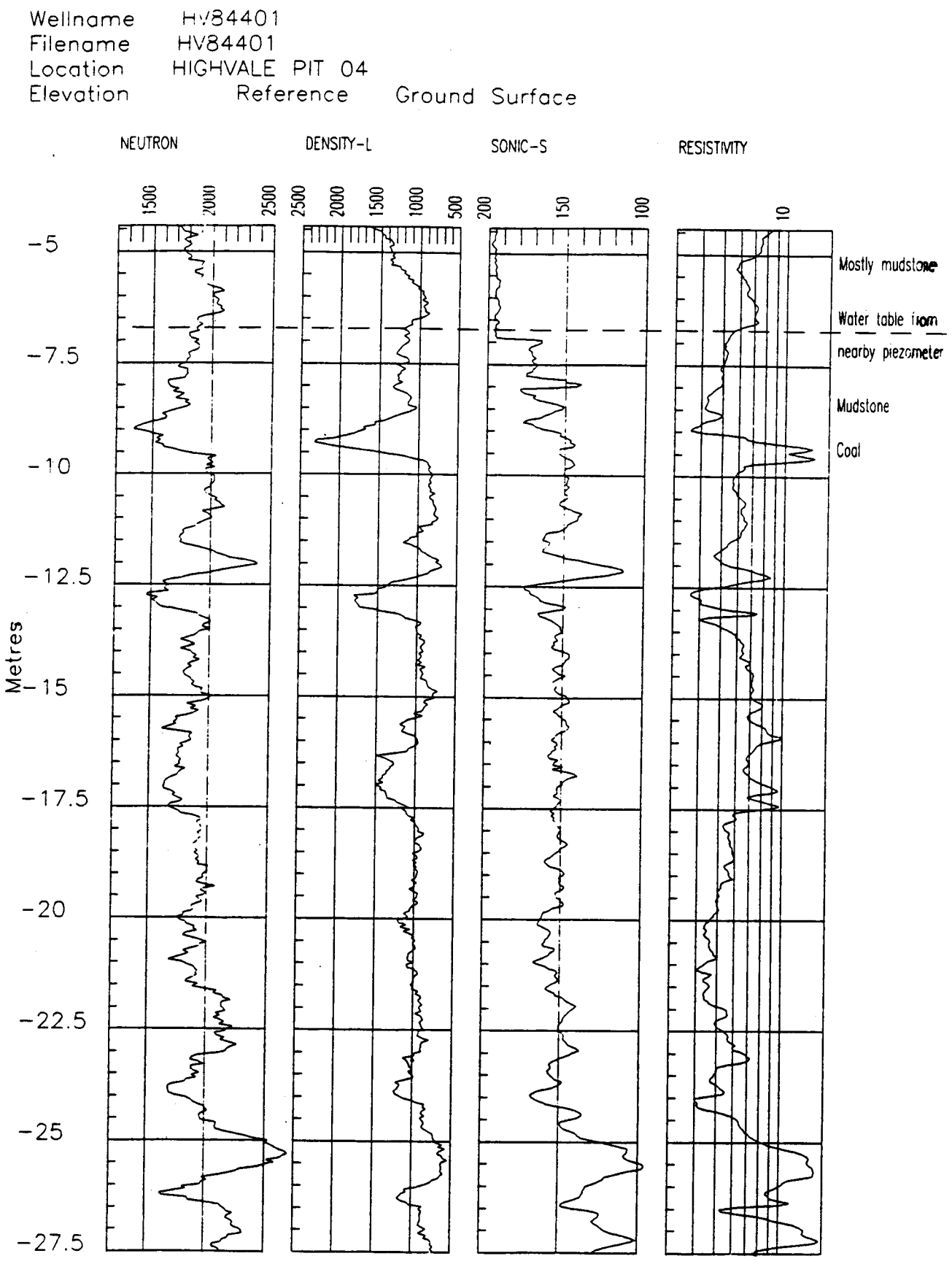

Figure 4-2. The response of neutron, density, sonic and resistivity logs in the vicinity of the water table in HV84-401 where the rock is mostly mudstone.

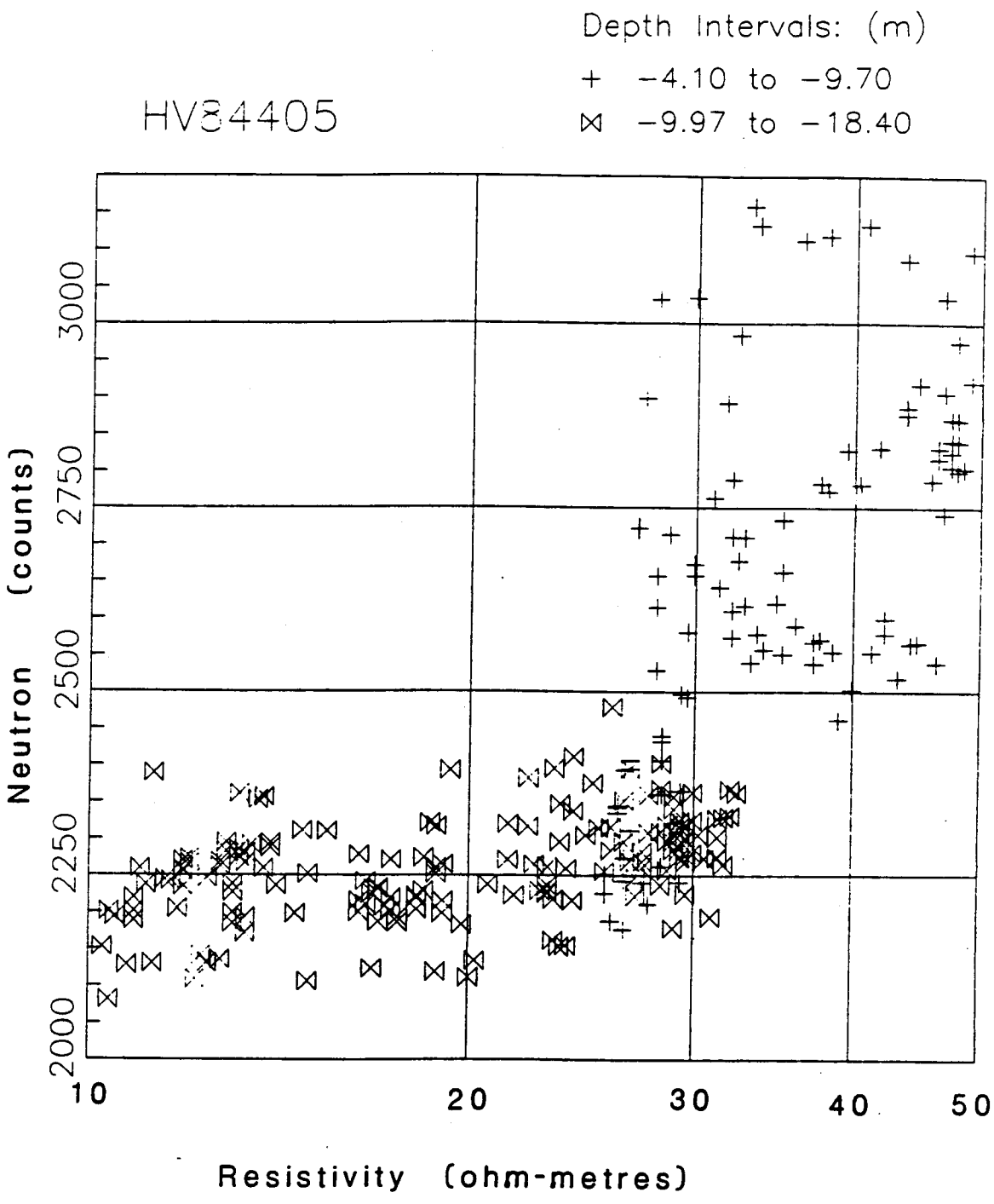

Figure 4-3. A crossplot of neutron and resistivity log response in HV84-405. The plot clearly defines two clusters of values representing the depth intervals above and below the water table, which was measured at 9.8 m in depth.

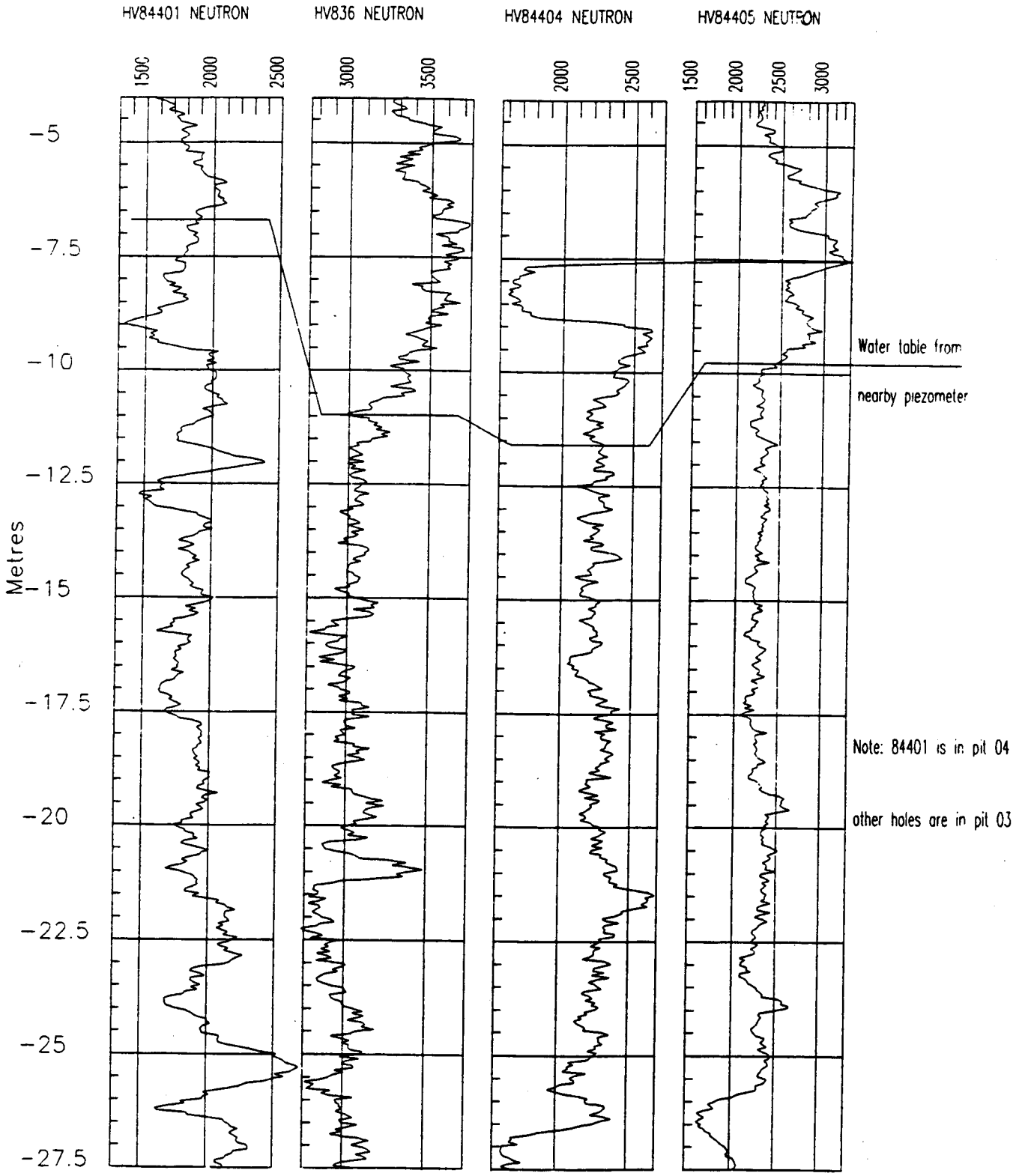

Figure 4-4. Neutron logs for holes HV84-401, HV83-6, HV84-404 and HV84-405.

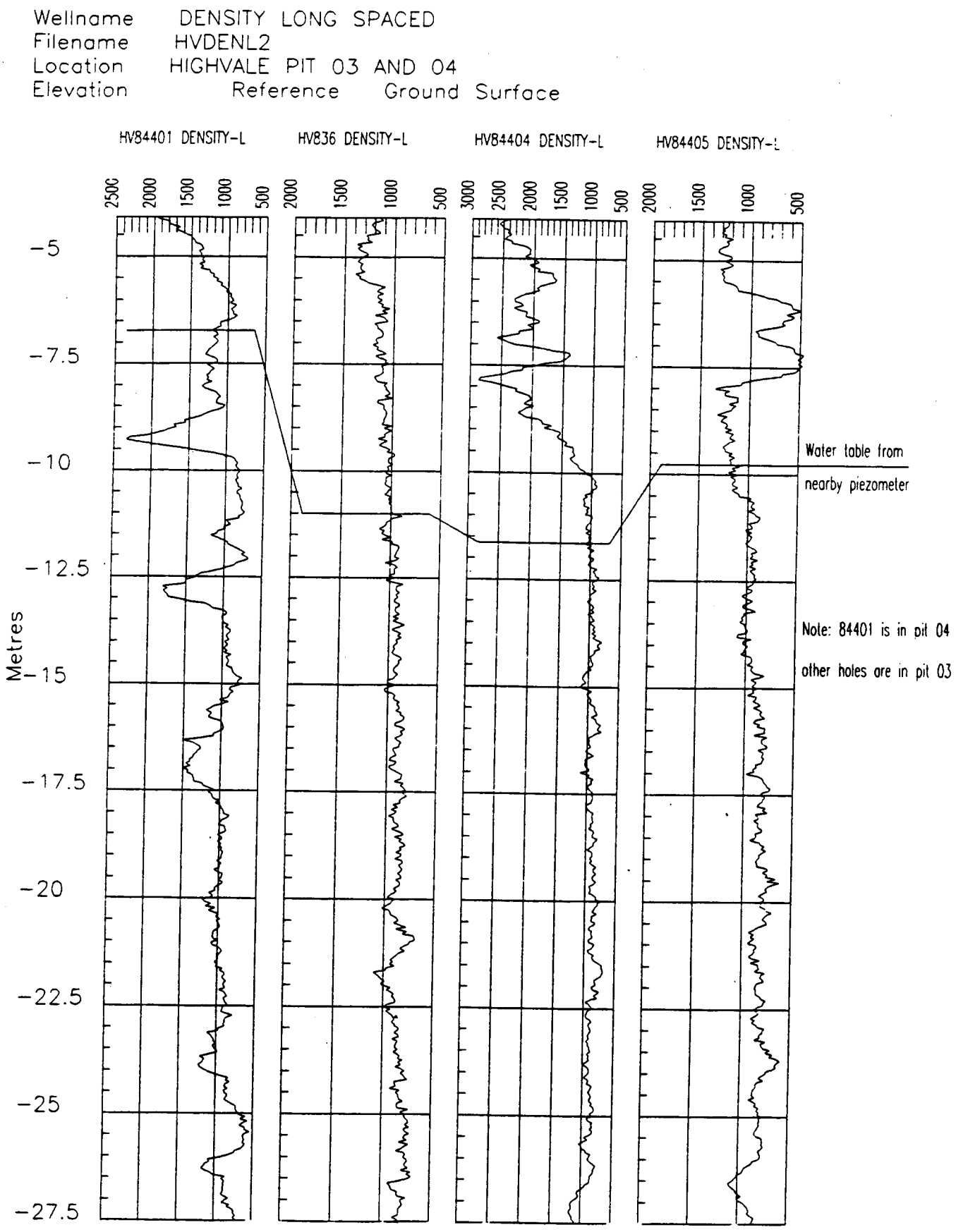

Figure 4-5. Density logs, long spaced, for holes HV84-401, HV83-6, HV84-404, HV84-405.

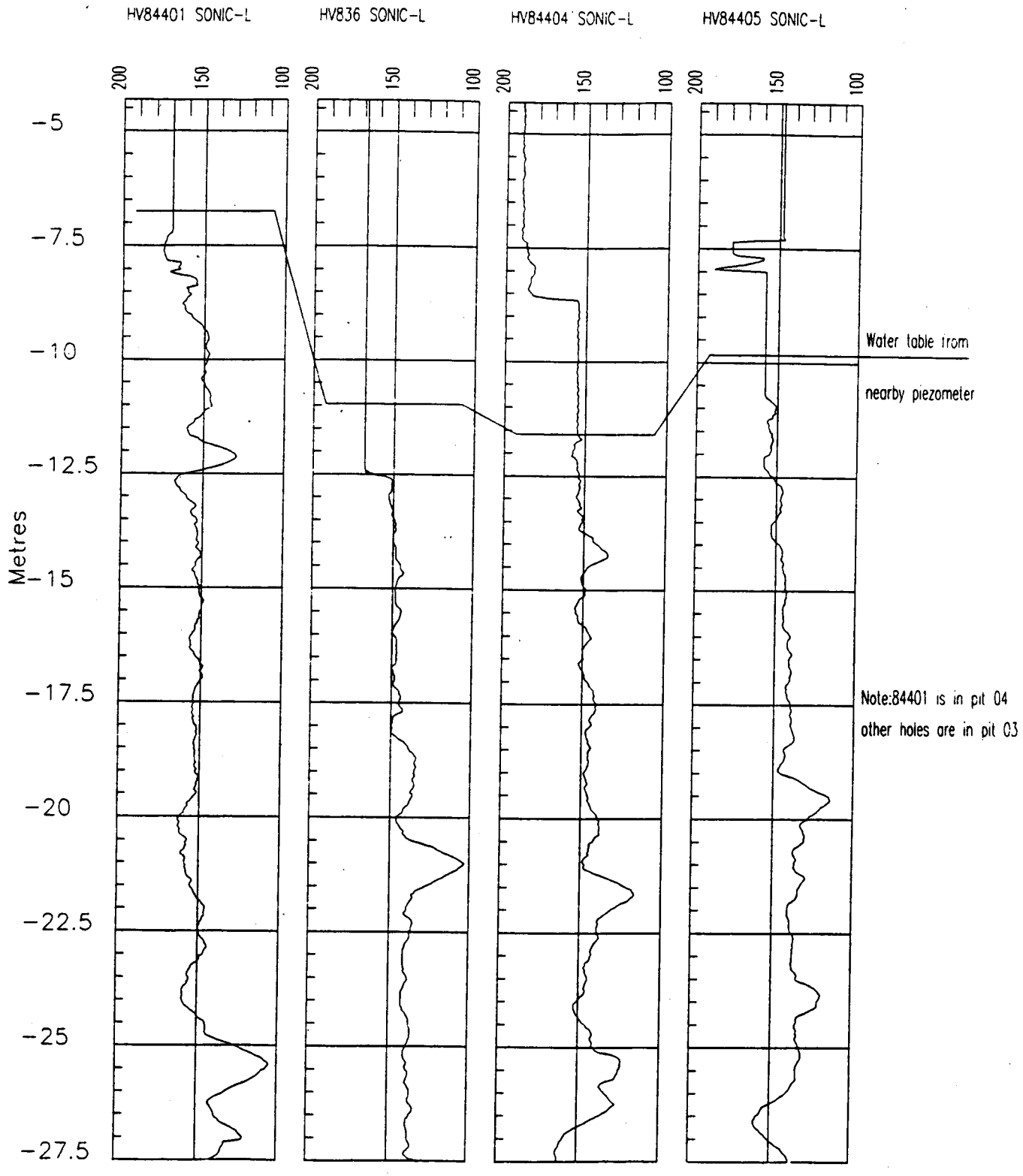

Figure 4-6. Sonic logs, long spaced, for holes HV84-401, HV83-6, HV84-404, HV84-405.

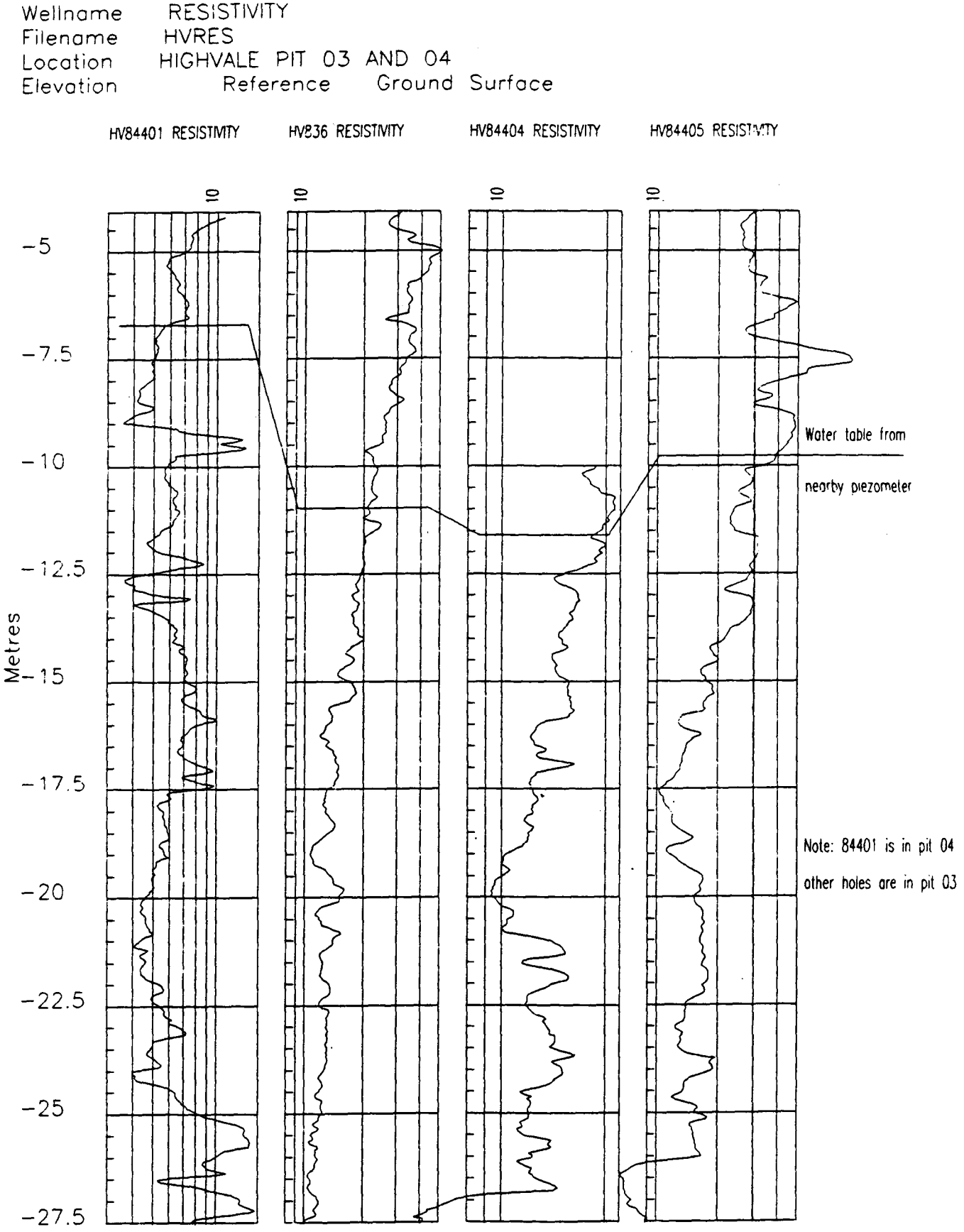

Figure 4-7. Resistivity logs for holes HV84-401, HV83-6, HV84-404, HV84-405.

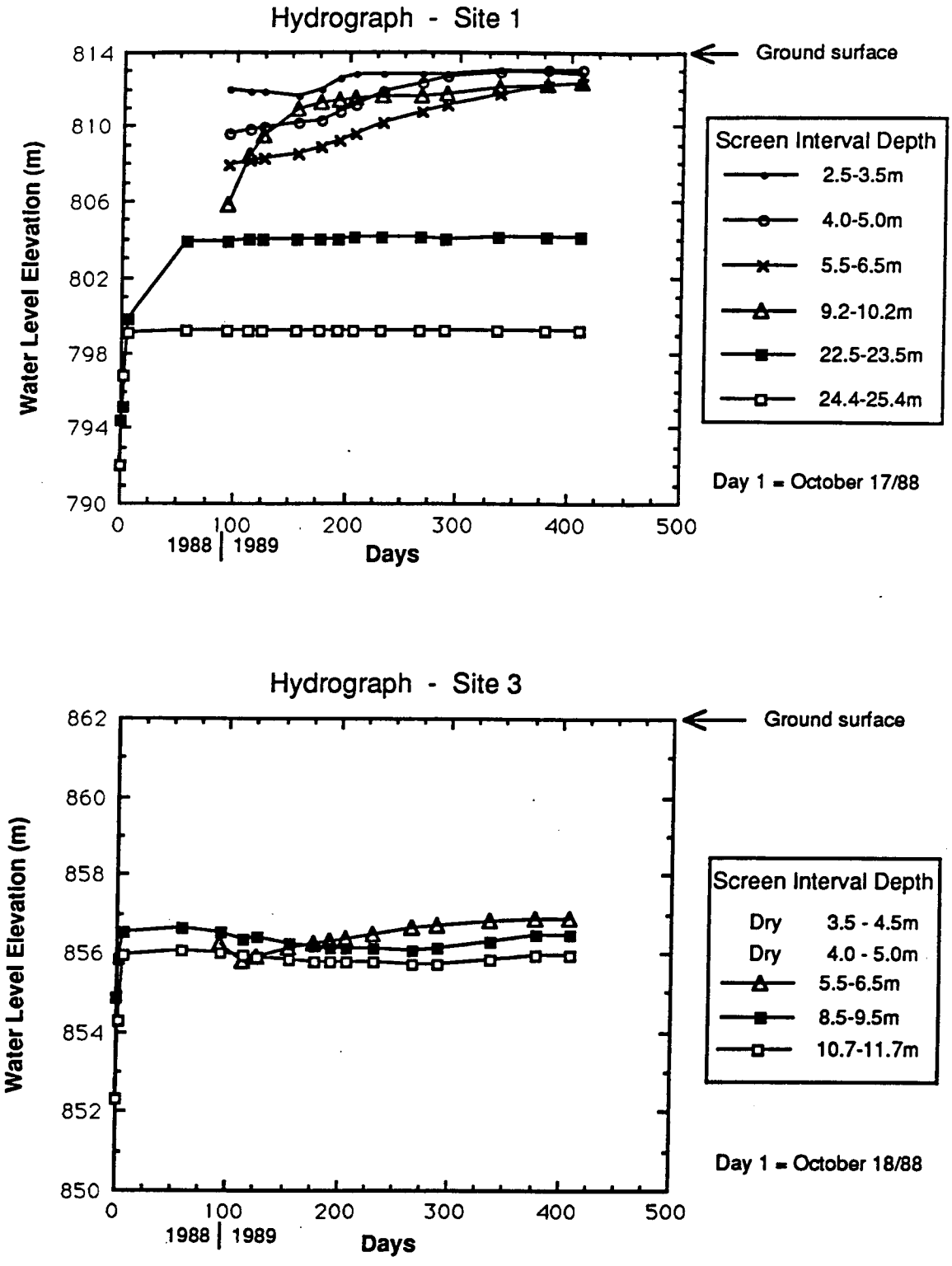

Figure 4-8. Hydrographs showing water levels from piezometer nests at Sites 1 and 3, Big Valley.

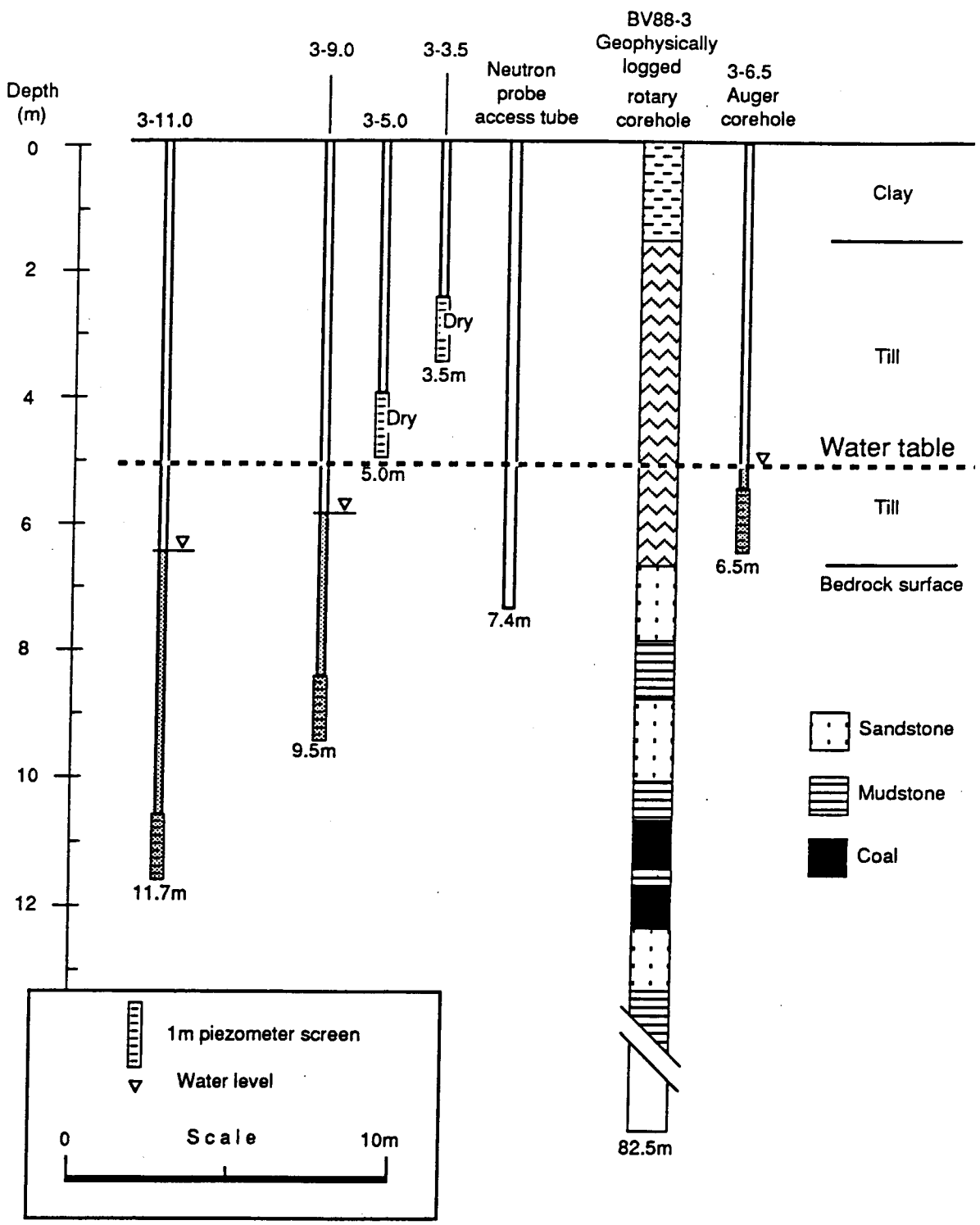

Figure 4-9. Profile of Site 3, Big Valley showing piezometer nest, lithology and water table location.

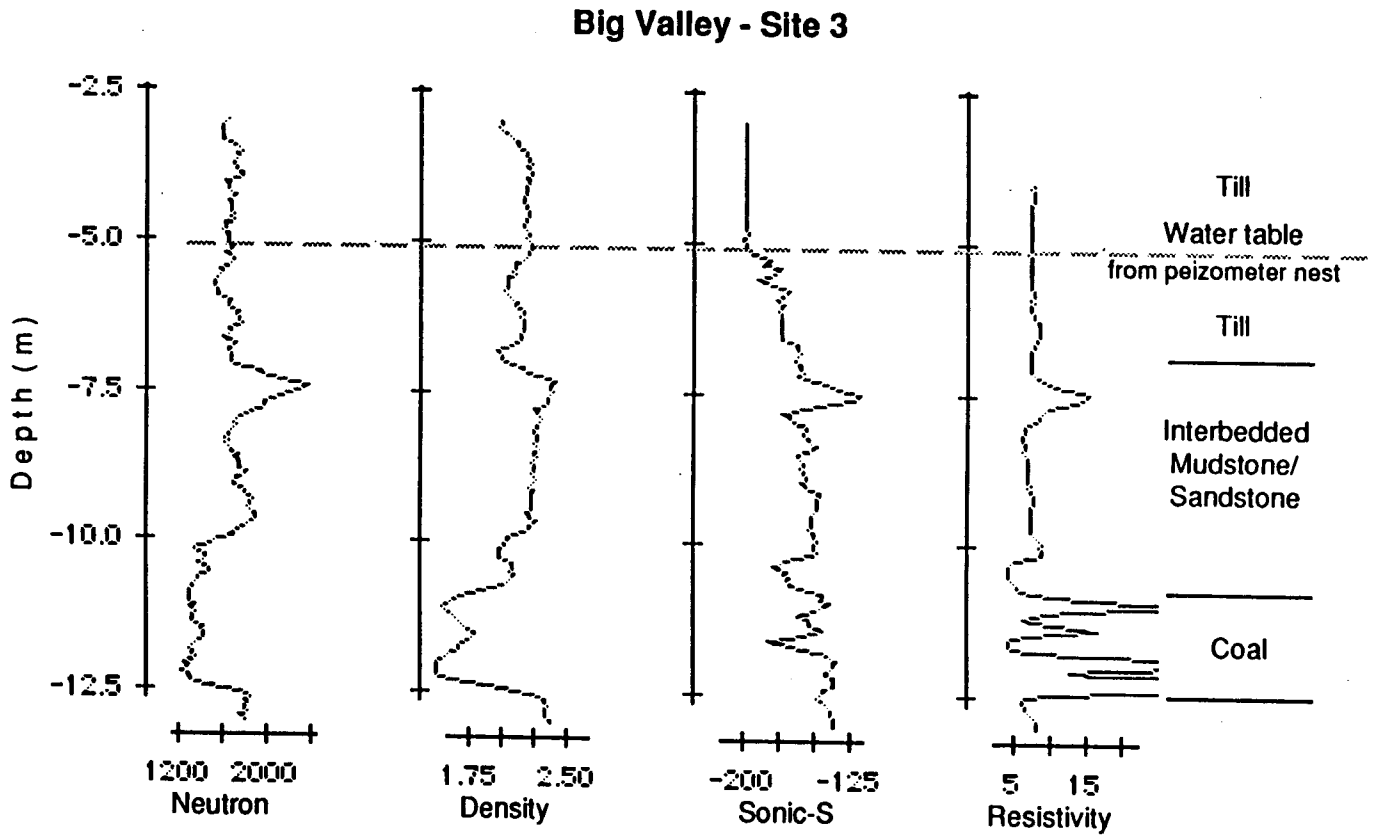

Figure 4-10. Geophysical logs and water table, Site 3, Big Valley.

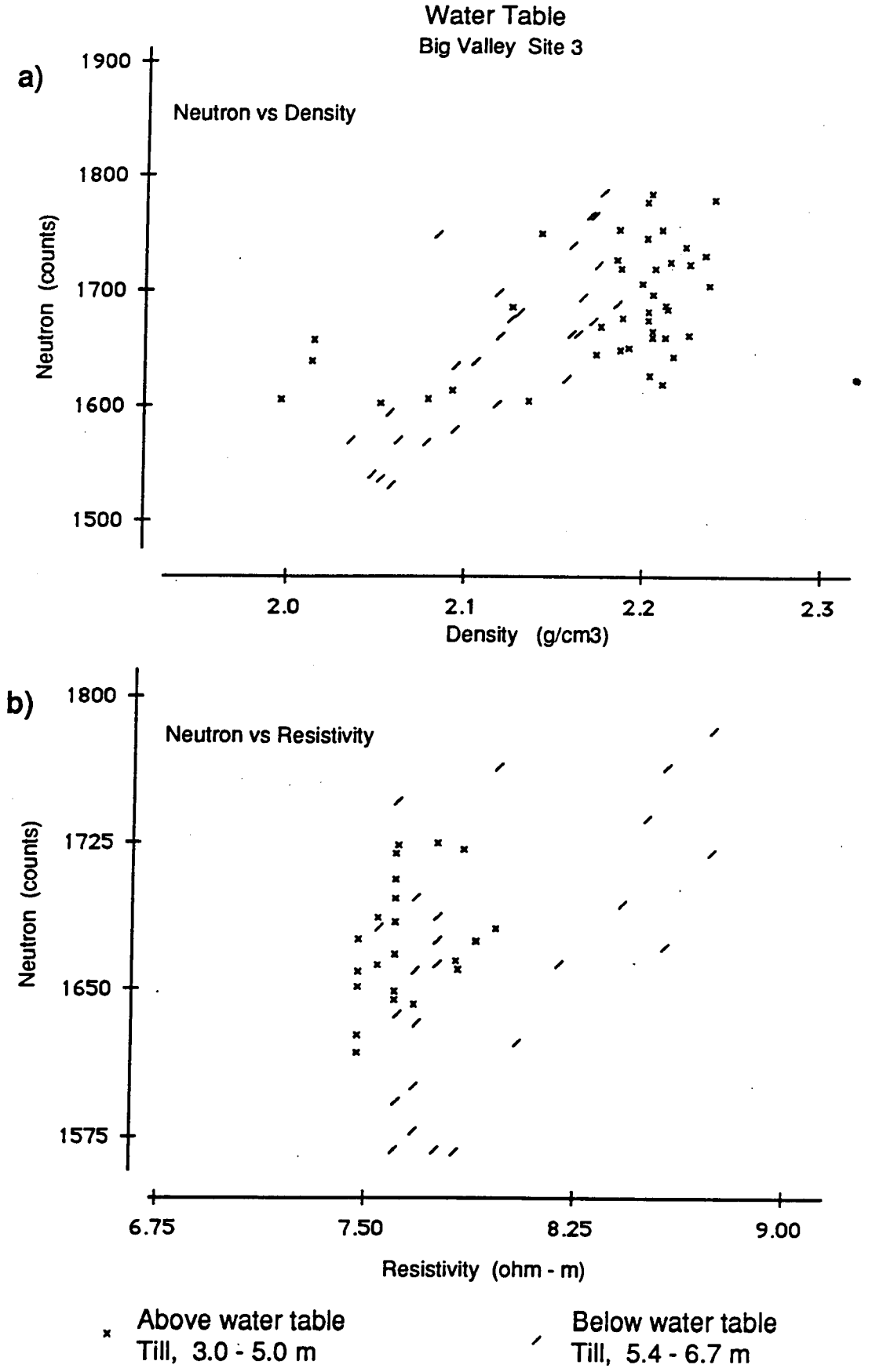

Figure 4-11. a) Crossplot of neutron and density, and b) Crossplot of neutron and resistivity.

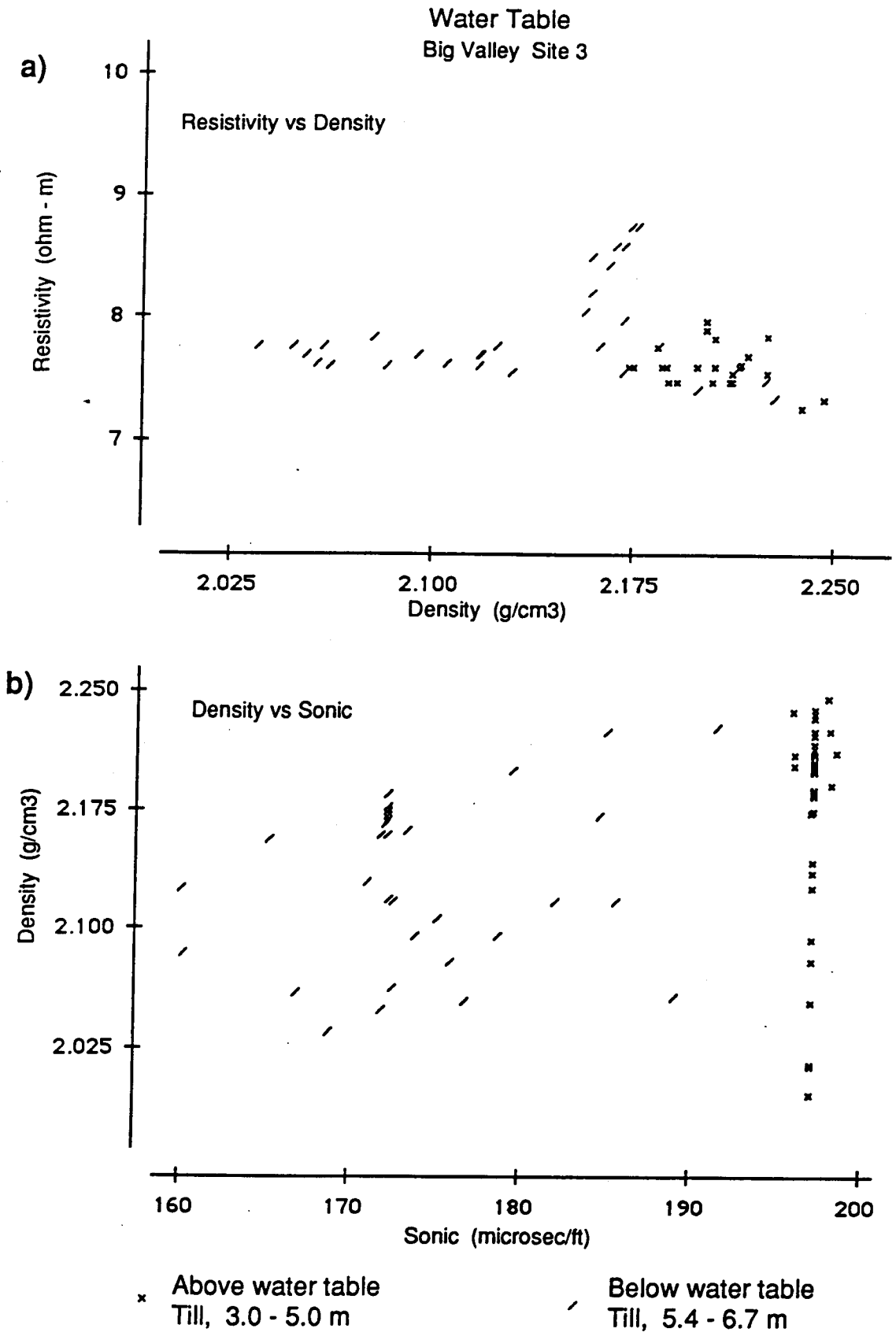

Figure 4-12. a) Crossplot of resistivity and density, and b) Crossplot of density and sonic.

5. DETECTION OF BEDROCK WEAKENED BY GLACIAL DEFORMATION

John. G. Pawlowicz and Mark M. Fenton

Continental glaciers advanced a number of times over the Plains of Alberta during the Pleistocene epoch. During each advance the weight and motion of the glacier caused local deformation of the underlying material, removal of material by thrusting, and redeposition of the material displaced by thrusting. The products of this deformation are: (1) deformed and/or displaced masses of sediment, including bedrock, older glacial sediment and/or preglacial stratified sediment, and (2) in places, a depression indicating the source from which the displaced material originated. The structure of the deformed material is characterized by any of the following: large-scale folding, faulting, abundant fractures, small-scale crushing with or without compaction, a basal shear zone, shear planes dipping upglacier, and subvertical fractures and shear surfaces below the basal zone. Some glacially thrust hills are as much as 200 m high and extend over an area of several square kilometres.

Glacially deformed bedrock and sediment have been recognized in many of the glaciated regions of North America and Europe (Aber et al., 1989; Moran et al., 1980) including a considerable portion of the Great Plains (Fenton, 1984b). Within the Plains some of the earliest descriptions of glaciotectonism were by Sardeson (1898, 1905, 1906). Later investigations include those of Hopkins (1923), Slater (1926, 1927), Byers (1960), Kupsch (1962), Christiansen and Whitaker (1976), Moran (1971), Fenton and Andriashek (1978), Moran et al. (1980), Bluemle and Clayton (1984), Fenton (1983a, 1983b, 1984a, 1987), Fenton et al. (1985a, 1985b), Aber et al. (1989), and Andriashek and Fenton (1989).

5.1 SIGNIFICANCE TO MINING

Glacial deformation is significant to geotechnical engineering in general, and more specifically to open-pit mining (Sauer 1978; and Fenton et al., 1986 and in press). Observations at various Plains coal mines have shown that the principal effects of glacial deformation are deleterious: the disruption of both the overburden and coal stratigraphy; the removal or repetition of marker beds; and a reduction in the rock strength. Glacial deformation poses similar problems to Alberta's oilsands mines in the design of tailings ponds and foundations, and operational decisions for overburden removal.

Ramifications and/or problems for both exploration and mining include:

- coal recovery: glacially transported blocks of coal may not be economically recoverable;

- coal quality: an increase in the ash content of the coal delivered to the power plant as a result of (a) the fractures, opened by deformation, allowing oxidation and/or the movement of clastic material into the coal, and (b) the inclusion, in the mined coal, of thin partings that can no longer be removed during the mining process because the coal beds and partings are folded rather than flat-lying;

- reserve estimation: glacial removal of the coal masses increases the complexity of the subcrop pattern which can increase the uncertainty in reserve estimates;

- sediment variability: higher sediment variability, both vertically and horizontally, resulting in higher variability in pedogenic and geotechnical soil types;

- highwall stability: deformed bedrock is weaker than undeformed bedrock, and shear planes both at base and within the glacial thrust mass may dip into the pit depending on pit orientation; all these increase the potential for highwall failure;

- drilling operations: drilling targets can be missed in the field if displaced bedrock masses are misinterpreted as the bedrock surface;

- core recovery: glacial deformation involving crushing without compaction can result in material that is comparatively loose and difficult to contain within a core barrel;

- operational problems: for overburden removal in oilsands mines, equipment operators can have difficulty identifying the actual bedrock surface where masses of displaced or deformed bedrock are present;

- drainage: pathways present in the undeformed bedrock may be disrupted and/or sealed during deformation, or glacially induced fractures in the underlying bedrock may result in greater permeability than otherwise would be expected in fine-grained rock;

- access problems: glaciotectonic terrain can be comparatively rugged making

access more difficult.

One advantage of this deformation is the disruption of hard layers in the overburden. This makes excavation by the dragline easier and more efficient, and reduces the need to blast.

5.1.1 Detection Problems

The presence of glacially deformed bedrock and its impact on surface mining are becoming better understood, but there are several obstacles to its detection and evaluation:

- historically, glacially deformed bedrock has been recognized in the subsurface only by examination of core, and usually only by someone who is experienced with this phenomenon;

- the recognition and description of structural and geological features in core is subjective and depends on the experience of the person logging the core;

- the different styles and degrees of deformation (Moell, 1985) add to the difficulty of recognition;

- drilling in deformed bedrock often results in missing data due to poor core recovery;

- core samples primarily taken for geotechnical analysis are often inadvertently biased. Because these samples must be intact for engineering testing, they are often taken preferentially from the more competent beds, thus missing the more critical zones of fractured and weak or crushed rock.

5.1.2 Objective

The main objective of this portion of the research was to determine if conventional log suites and/or dipmeter logs can be used to differentiate between deformed and undeformed bedrock.

The application of borehole geophysical logging to detecting this problematic terrain has the potential to help alleviate some of the above problems. The subjectivity in core description can be reduced by using the geophysical logs as a less subjective way to evaluate the degree of deformation and the physical properties of the strata.

Geophysical log data become very useful in supplementing missing core data. Following standard calibration practices and routine logging procedures as recommended in Sec. 2, the results from logging should be repeatable within the tolerances of the equipment.

The goal and concern in log analysis is to draw inferences that reflect meaningful relationships in the data rather than patterns that appear related by chance. In the analysis for deformation terrain, the log data were analyzed primarily visually through graphic displays and compared to written descriptions of core from field notes. Histograms and scatter plots were used to look for clustering and groupings of data that related to geological observations from the core. Some additional statistical calculations were done to support any noticeable trends. Data from both conventional log suites and the dipmeter logs were analysed.

5.1.3 Geophysical Logs

The logs available for this study from the Highvale Mine and Big Valley areas (Fig. 1-1) were recorded by BPB Wireline Services and are listed below in Table 5-1.

Table 5-1. Geophysical logs available for deformation study.

Geophysical Log	Highvale	Big Valley
• Caliper	√	√
• Gamma	√	√
• Density (Long-Spaced)	√	√
• Density (Short-Spaced)	√	√
• Bulk Density	√	√
• Focussed Resistivity (high-resolution)	√	√
• Sonic (Short-Spaced)	√	√
• Sonic (Medium-Spaced)	√	√
• Sonic (Long-Spaced)	√	√
• Neutron-Neutron	√	√
• Dipmeter (3-Pad)	√	
• Spontaneous Potential		√
• Temperature (absolute and differential)		√

5.2 CONVENTIONAL LOGS: HIGHVALE MINE SITE

Data were selected from six boreholes in the Pit 03 area of the Highvale Mine for deformation terrain analysis. The geophysical logs came from two drilling programs: holes HV7, HV8, HV9 and HV10 were drilled in 1983, and HV404 and HV405 were drilled in 1984. All logs were checked for depth alignment and corrected where necessary. Only the overburden above the coal sequence was studied, and data from the uppermost sections of the holes were not used in order to avoid water table effects.

The general stratigraphic setting of the the overburden in Pit 03 is, from top to bottom: about 3 m of till, a sandstone unit about 20 m thick, and a mudstone bed about 5 m thick that overlies the mineable coal sequence. The cores showed varying amounts and degrees of deformation. For example, in cores from holes HV8 and HV9 the entire overburden sequence consisted of strongly deformed bedrock, as evidenced by the high-angle bedding, high degree of fracturing, and overthickening of the mudstone unit. In other holes, the overburden was mostly undeformed, but in each hole a strongly crushed and/or highly fractured zone was present in the mudstone, which is interpreted to be the basal shear zone.

For this study, the overburden has been subdivided into three types of material, indicated by three different symbols in the scatter plots: 1) deformed sediment, 2) undeformed sediment, and 3) strong, indurated beds. The deformed sediment includes material that clearly displays evidence of post-depositional structural deformation, i.e., fracturing, faulting, crushing, or folding. Such material can form a substantial portion of the overburden, or be restricted to a relatively thin zone below undeformed sediment. Undeformed sediment showed little or no evidence of the above mentioned deformation structures in core. The indurated beds are well-cemented concretionary horizons, ranging in thickness from 10 cm to 3 m, that are generally found in the sandstone. These hard beds were present in both deformed and undeformed bedrock units.

5.2.1 Scatter Plots

The geophysical logs for each hole are presented as scatter plots of data points from each log versus depth using the material type symbols described above. The plots are organized by log type to facilitate comparison of the responses of each type of log. Fig. 5-1 and 5-2 show plots of the caliper log, Fig. 5-3 and 5-4 show the resistivity log, Fig. 5-5 and 5-6 show the natural gamma log, Fig. 5-7 and 5-8 show the sonic log, Fig. 5-9 and 5-10 show the density log and Fig. 5-11 and 5-12 show the dual-spaced neutron log. The clustering of points representing both the deformed zones and the indurated zones

is clearly apparent on the sonic, density and neutron logs (Fig. 5-7, 5-8, 5-9, 5-10, 5-11 and 5-12 respectively) in holes HV7, HV10, HV404 and HV405. In those, the log responses for deformed zones and indurated beds fall on opposite sides of the average distribution of points identified as undeformed sediment. Even though the absolute values vary from hole to hole, the deformed zones show up as relative anomalies within each log. In comparison to the data points identifying undeformed material, the log responses for deformed bedrock show up as longer than normal transit times, lower densities and lower neutron count rates. The sonic, density and neutron log readings in the indurated beds respond in the opposite direction to the deformed bedrock. The reason for this is likely related to changes in porosity due to fracturing or cementing. The use of sonic, density and neutron logs for porosity measurements is well documented in the literature (Keys, 1989a). The resistivity and gamma logs in places show some indication of the deformed and indurated zones, but primarily respond to lithologic changes. For holes HV8 and HV9, where deformed bedrock comprises virtually the entire overburden sequence, none of the scatter plots indicates the severity of the deformation that is present.

Plotting the caliper log at an expanded scale allows closer inspection of hole condition (Fig. 5-1 and 5-2). With the exception of a 10 m section in HV7, all the holes exhibit a scattered hole diameter response which may best be described as hole rugosity due to the poorly consolidated nature of the rock in this formation. Washouts are identified by readings greater than 5.6 inches. This can have an affect on some of the other logs, most notably the density and high resolution logs (Sec. 2 and Keys,1989a). The effect of small-scale changes in hole diameter to the other logs in the suite is uncertain. However, caved zones detected by the caliper are often indicative of weak rock or fracturing. This information used in conjunction with the sonic, density and neutron logs can help isolate zones of weakness.

5.2.2 Histograms

Histograms show the relationship of deformed bedrock to the total distribution of points for each hole and between holes. Histograms of the caliper, resistivity, gamma, sonic, density and neutron logs are illustrated in Fig. 5-13, 5-14, 5-15, 5-16, 5-17 and 5-18 respectively. The sonic, density and neutron histograms for holes HV7, HV10, HV404 and HV405 indicate that the deformed bedrock falls outside the normal distribution of data within each hole. This does not hold true for HV8 and HV9 because the total distribution of data covers only deformed bedrock. The histograms also show that absolute values are not consistent enough for deformed terrain recognition. However, a range of values may be more useful. For example, the sonic readings for deformed rock

in hole HV8 generally fall between 140 and 200 microsec/ft. This contrasts to the undeformed sonic readings in hole HV10 which range from 100 to 160 microsec/ft. It was hoped that the caliper data might show a tendency to increased hole size in deformed rock, but this does not seem to be the case in these holes (Fig. 5-13). The resistivity and gamma plots indicate that the deformed bedrock trends towards low resistivity and higher gamma readings, which suggest a relationship to the finer-grained sediments. The core information confirms that this is indeed the case for the selected holes; most of the deformation is observed in the mudstone. However, this is not to suggest that all deformation is confined to the mudstone. The sandstone in holes HV8 and HV9 is deformed but makes up only a small portion of the overburden data.

5.2.3 Log Comparisons

Logs from each hole were correlated with each other using the Pearson Product-Moment correlation method described in the Data Desk program manual (Velleman, 1989). This is a common method of correlation computed between two variables to measure an association between them. An example of a good correlation from the deformed terrain data set is shown in a crossplot of density and sonic data from hole HV404 (Fig. 5-19). The accompanying table in Fig. 5-19 indicates that the correlation of density and sonic is .680. Fig. 5-20 illustrates an example, using density and natural gamma data from hole HV7, of a poor correlation that has an R = -.106. Correlations for the four remaining holes are presented in Table 5-2. Those examples illustrate how a table of log correlations could be used to select the most useful pairs of logs for crossplotting. The areas identified by the crossplots as deformed or indurated could then be used to check for anomalous log responses from other holes.

5.3 DIPMETER DATA

5.3.1 Basic Assumptions

Deformation of the bedrock causes local changes in the rock properties over short distances. For example, in cores from some test holes in strongly deformed material, sandstone may be present on one side of the core and mudstone on the other. This presents a problem in the interpretation of most logs which measure the average response of all materials within their volume of investigation. In addition, the core samples might not be representative of the major rock type adjacent to the borehole that has caused most of the log response.

Table 5-2. Table of log correlations for deformed terrain, Pit 03, Highvale Mine.

		-Sonic8 ...	NN8	Den8	Gam8	Res8	Cal8
-Sonic	HV8	1.000					
Neutron	HV8	-0.211	1.000				
Density	HV8	0.355	0.545	1.000			
Gamma	HV8	0.293	-0.754	-0.382	1.000		
Resistivity	HV8	-0.589	0.728	0.146	-0.783	1.000	
Caliper	HV8	-0.495	0.411	-0.055	-0.535	0.524	1.000

		-Sonic9	Dens9	Gam9	Res9	Cal9
-Sonic	HV9	1.000				
Density	HV9	0.780	1.000			
Gamma	HV9	-0.306	-0.410	1.000		
Resistivity	HV9	0.446	0.448	-0.734	1.000	
Caliper	HV9	-0.215	0.007	-0.324	0.446	1.000

		-Sonic10	Dens10	NN10	Gam10	Res10	Cal10
-Sonic	HV10	1.000					
Density	HV10	0.498	1.000				
Neutron	HV10	0.658	0.703	1.000			
Gamma	HV10	-0.454	-0.119	-0.721	1.000		
Resistivity	HV10	0.716	0.619	0.905	-0.663	1.000	
Caliper	HV10	0.196	-0.235	0.002	-0.293	0.102	1.000

		-Sonic...	NN405	-LSD405	Gam405	Res405	Cal405
-Sonic	HV405	1.000					
Density	HV405	0.492	1.000				
Neutron	HV405	0.772	0.371	1.000			
Gamma	HV405	0.053	-0.573	0.028	1.000		
Resistivity	HV405	-0.368	0.382	-0.387	-0.542	1.000	
Caliper	HV405	0.553	0.059	0.622	0.250	-0.507	1.000

The dipmeter tool used has three detection pads that are evenly spaced around the tool and contain closely spaced microresistivity electrodes; some tools have four or more pads. Data are recorded from each pad, providing a separate measure of resistivity from three sides of the borehole. The comparison of these three high-resolution logs provides a measure of changes in the rock properties on three sides of the borehole.

Idealy, in an undeformed geological model consisting of flat-lying homogeneous bedrock, the three pad readings at any particular recording depth should be the same. If deformation has changed the rock properties or structure, the pad readings should reflect differences from one side of the hole to the other. In reality though, readings from the three detection pads will likely not be identical to each other in an undeformed homogeneous bedrock unit because of the physical and electrical limitations inherent in the tool and operating conditions. What is hoped for in this analysis is an abnormally large variation between pad readings that corresponds to deformed bedrock.

5.3.2 Site Geology

Data sets from cored holes HV408 and HV409 in the Pit 04 area of the Highvale Mine were used. Core recovery was almost 100%. The stratigraphy in those holes consists mostly of mudstone, interbedded with minor sandstone and bentonite beds, overlying the economic coal seams. The dipmeter logs extended from the surface to below the coal seams, but only the sediment above the uppermost coal seam was studied.

The core from hole HV408 contained deformed sediment from surface to 26 m, which was essentially crushed and/or broken to the base of deformation. The deformed unit in hole HV409 contained predominantly crushed and broken rock to a depth of 35 m, but portions of the core within the deformed unit, particularly the lower third, contained masses of solid rock that appeared undeformed.

5.3.3. Approach

1) Dipmeter data sets from holes HV408 and HV409 were supplied in digital and paper form by TransAlta Utilities. The data were originally recorded by BPB in 1983. Readings on HV408 extended from 2.0 to 55.0 m and in HV409 from 2.9 to 60.9 m Each data set consisted of the depth, caliper, pad 1, pad 2 and pad 3 readings at 10 cm intervals. Data were converted to ASCII format and loaded into Microsoft Excel (v2.2) and Odesta Data Desk (v3.0) programs (Sec. 2.4). Fig. 5-21 shows the flowchart for the data analyses.

2) The caliper log for each hole was plotted and inspected (Fig. 5-22). Caved and washed out zones were identified and dipmeter readings form those depths were eliminated. Next the subset of data for further analyses was selected. This consisted of all the data lying below the water table and above the top of the upper coal seam. Base of deformation was identified from lithologic descriptions.

3) The readings from the three pads were used to calculate, for each depth, the absolute difference between individual pairs of pads (pad 1-pad 2, pad 1-pad 3, pad 3-pad 2), and the sum, average and standard deviation of these differences. These data were inspected to see if there was a difference between the readings from the deformed and undeformed sediment.

4) Multiple regression and correlation techniques (Pearson Product-Moment correlation) were used to compare the variability between the three pad readings at each depth for the deformed and undeformed bedrock groups. The first step was to prepare an artificial data set simulating flat-lying undeformed bedrock in which the three pad readings were the same for an individual depth but varied from depth to depth. The regression and correlation techniques were run on this data set to determine the statistical response to be expected.

5) The lithologically consistent data set was prepared that consisted of readings from only the mudstone, based on the core descriptions. These data were divided into deformed and undeformed groups and the regression and correlation techniques were used to determine if there is a difference between the two groups.

6) A lithologically variable data set was created by taking all the data above the top of Seam 1 and below the till. Again the data were divided into deformed and undeformed groups and regression and correlation techniques used to determine if there is a difference between groups.

7) The deformed and undeformed groups within the lithologically variable data set from hole HV408 were divided into subgroups 2 m thick. Subsequently both holes were divided into subgroups 1 m thick. The regression and correlation techniques were used to determine if the difference between groups is consistent within subgroups.

5.3.4 Results

The caliper logs for both holes (Fig. 5-22) are reasonably consistent, except for the upper

few metres which were deleted from the data analysis. The plots of the pad values against depth (Fig. 5-23 and 5-24) indicate that the pad readings are generally similar to each other, although not identical, for any particular depth and that they vary with depth reflecting changes in the rock properties.

5.3.4.1 Differences Between Pad Readings

Table 5-3 shows the averages, for the deformed and the undeformed rock, of the different variables calculated from the pad readings. Within the deformed group the values for the standard deviation, range, variance and maximum are higher than for the undeformed group. The actual values for any specific measurement vary from hole HV408 to HV409 but relative relationship of the readings for the deformed and undeformed groups remains the same. This suggests a greater variability within the deformed material. The variance values show the greatest contrast.

5.3.4.2 Artificial Data Set

This artificial data set simulated flat-lying undeformed bedrock in which the three pad readings are the same at each particular depth but vary from depth to depth. Comparing Fig. 5-25 to Fig. 5-26 indicates the data distribution within this data set is similar to that of the actual dipmeter data which suggests the results of the analysis should be applicable to the actual dipmeter data set. As can be expected, results from the artificial data set have R^2 and R^2 adjusted values of both 100% and Pearson Product-Moment correlation values of 1.0 for readings between pads 1, 2 and 3.

5.3.4.3 Mudstone Data Set

This data set included only the mudstone readings, thereby eliminating the effects caused by lithologic variation. Table 5-4 shows that both the regression (R^2 and R^2 adjusted) and the correlation analyses (Pearson Product-Moments) can distinguish between the deformed and undeformed groups. The deformed rock has R^2 and R^2 adjusted values of <78 and Pearson values of <0.87; the undeformed group has values of R^2 and R^2 adjusted of >95 and Pearson values of essentially >0.95.

5.3.4.4 Lithologically Variable Data Set

This data set was created by taking all the data above the top of Seam 1 and below the till. Table 5-4 shows that even with the introduction of lithologic variations, the regression and correlation analyses can distinguish between the deformed and undeformed groups.

Table 5-3. Summary of pad difference data for all rock types in analyzed interval.

	DEFORMED							UNDEFORMED						
	N	Mean	Std Dev	Range	Variance	Min	Max	N	Mean	Std Dev	Range	Variance	Min	Max
Pad Differences(Absolute)														
HV408														
P1-P2	219	89	79	397	6191	0	397	116	68	36	221	1279	1	222
P1-P3	219	87	77	500	5886	2	502	116	53	39	180	1500	0	180
P2-P3	219	75	68	352	4630	0	352	116	48	38	257	1479	1	258
HV409														
P1-P2	177	108	59	356	3500	3	359	150	82	39	203	1531	1	204
P1-P3	177	88	44	243	1973	4	247	150	64	32	164	992	0	164
P2-P3	177	54	54	303	2895	1	304	150	37	27	137	733	0	137
Sum of Pad Differences														
HV408	219	250	167	981	27909	23	1004	116	169	73	462	5393	55	517
HV409	177	250	111	696	12325	22	718	150	183	65	347	4206	62	409
Average of Pad Differences														
HV408	219	83	56	327	3099	8	335	116	56	24	154	599	18	172
HV409	177	83	37	323	1366	7	239	150	61	22	115	466	21	136
Standard Deviation of Pad Differences														
HV408	219	50	35	218	1238	5	223	116	32	17	109	291	10	119
HV409	177	49	22	126	496	4	130	150	35	14	74	193	11	85

Table 5-4. Regression and correlation results from analyzed interval of: a) only the mudstone, and b) all the rock types.

	DEFORMED					UNDEFORMED				
		Regression					Regression			
	N	R2 %	R2 Adj%		Correlation*	N	R2 %	R2 Adj%		Correlation*
Mudstone										
Pad 1 vs pads 2 and 3										
HV408	148	76.5	76.2	0.838	0.862	62	95.2	95.1	0.949	0.968
HV409	162	77.8	77.5	0.868	0.817	135	95.4	95.4	0.969	0.972
All lithologies										
Pad 1 vs pads 2 and 3										
HV408	217	65.8	65.5	0.748	0.762	115	97.7	97.7	0.982	0.982
HV409	177	81.9	81.7	0.892	0.848	150	95.2	95.2	0.967	0.971
Pad 2 vs pads 1 and 3										
HV408	217	62.4	62.0	0.734	0.748	115	96.7	96.6	0.973	0.982
HV409	177	83.7	83.6	0.892	0.865	150	95.5	95.5	0.967	0.973
Pad 3 vs pads 1 and 2										
HV408	217	64.2	63.8	0.734	0.762	115	96.6	96.5	0.973	0.982
HV409	177	77.6	77.4	0.865	0.848	150	96.0	96.0	0.973	0.971
Pad differences (p1-p2 vs p1-p3 and p2-p3)										
HV408	217	25.1	24.5	0.468	0.282	115	5.5	3.8	0.232	0.059
HV409	177	21.1	20.7	0.437	0.186	150	36.3	35.3	0.530	0.096

*Pearson Product-Moment correlation

The pad readings from the deformed rock have values of R^2 and R^2 adjusted of <80 and Pearson values of <0.90. However the undeformed group has values of R^2 and R^2 adjusted of >95 and Pearson values of essentially > 0.95. This difference is believed to reflect the greater degree of variability that was produced in the deformed unit by the deformation.

The regression and correlation of the pad differences (pad 1-pad 2 vs pad 1-pad 3 and pad 2-pad 3) do not show a similar result. The pad differences were not used in subsequent analyses.

5.3.4.5 Subgroups

The deformed and undeformed groups within the lithologically variable data set from hole HV408 were divided into subgroups 2 m thick. Table 5-5 shows the results of the analyses of these subgroups. The subgroups within the deformed group are more variable than those within the undeformed group. Generally within the deformed group the R^2 and R^2 adjusted values are <80 and the Pearson values <0.80.

The exceptions are the 12 to 14 m, 20 to 22 m and 24 to 26 m subgroups. These, particularly the first two, have values that suggest the rock is less deformed. An explanation of the higher R^2 values can be found in the core litholog description, which reveals zones of moderate deformation rather than the usual high deformation at depths from 12.7 to 13.5 m, 21.8 to 24.2 m, and 24.8 to 26 m.

The encouraging results from splitting Hole HV408 into 2 m intervals indicated that a 1 m interval might also allow the separation of the deformed subgroups from the undeformed subgroups. Therefore both holes were divided into 1 m thick subunits and multiple regression run on each. The Pearson Product-Moment correlations were not done because: (1) the results from the 1 m subunit test showed regression and correlation results were both equally useful in distinguishing the deformed from the undeformed subgroups, and (2) this approach would decrease the analysis time.

The results in Table 5-6 show that the deformed subunits are characterized by R^2 and R^2 adjusted values generally <85 and the undeformed subunits by values generally >90. The values for the deformed sediment range from -20.9 to 96 and illustrate the variability of the physical properties of this material. Within the deformed unit there are a number of subunits with values >90. This is believed to be caused by masses of comparatively undeformed rock lying within the more highly deformed rock. This was

Table 5-5. Regression and correlation analyses of 2 m thick subunits in the deformed and undeformed groups in hole HV408.

Subunit interval	N	Regression R2 %	R2 Adj%	Correlation*	
		DEFORMED			
4-6m	20	65.9	61.8	0.118	0.809
6-8m	21	45.2	39.1	-0.633	0.235
8-10m	21	41.5	35.0	-0.320	0.586
10-12m	21	63.3	59.3	0.651	0.782
12-14m	21	92.2	91.4	0.960	0.944
14-16m	21	66.6	62.9	0.816	1.673
16-18m	21	52.7	47.4	0.697	0.720
18-20m	21	51.8	46.4	0.641	0.697
20-22m	21	91.8	90.9	0.932	0.913
22-24m	21	41.4	34.9	0.460	0.588
24-26m	21	82.6	80.7	0.805	0.876
		UNDEFORMED			
26.2-28m	19	85.8	84.1	0.866	0.926
28-30m	21	95.6	95.1	0.955	0.973
30-32m	21	95.9	95.4	0.973	0.955
32-34m	20	97.5	97.2	0.987	0.944
34-36m	21	98.5	98.3	0.992	0.981
36-37.6m	17	98.6	98.4	0.981	0.993

* Pearson Product-Moment correlation

Table 5-6. Multiple regression results of 1m thick subunits in holes HV408 and HV409.

HV408					HV409				
Unit	N	R2	R2Adj	Comments	Unit	N	R2	R2Adj	Comments
2\3	10	58.4	46.5	Dmdst	11\12	11	53.4	41.7	Dmdst&Till
3\4	11	89.7	87.1	Till	12\13	11	78.3	72.9	Dmdst
4\5	10	88.6	85.3	Dmdst	13\14	11	92.0	90.0	Dss&Dmdst
5\6	11	34.0	17.5	Dmdst	14\15	11	74.1	67.7	Dmdst
6\7	11	62.5	53.1	Dmdst	15\16	11	48.1	35.2	Dmdst
7\8	11	29.4	11.7	Dmdst	16\17	11	33.5	16.8	Dmdst
8\9	11	51.1	38.8	Dmdst	17\18	11	21.9	2.3	Dmdst
9\10	11	50.4	37.9	Dmdst	18\19	11	80.9	76.1	Dmdst
10\11	11	78.8	73.5	Dmdst	19\20	11	66.3	57.9	Dmdst
11\12	11	91.2	89.0	Dmdst	20\21	11	63.1	53.9	Dmdst
12\13	11	57.9	47.4	Dmdst	21\22	11	52.6	40.8	Dmdst
13\14	11	91.8	89.7	Dmdst&Dcoal	22\23	11	0.9	-23.9	Dmdst
14\15	11	89.2	86.5	Dmdst	23\24	11	65.7	57.1	Dmdst
15\16	11	56.0	45.0	Dmdst	24\25	11	98.1	97.7	Dmdst
16\17	11	79.3	74.1	Dmdst	25\26	11	88.3	85.4	Dmdst
17\18	11	3.3	-20.9	Dmdst	26\27	11	95.6	94.5	Dmdst, Dcoal&Mdst
18\19	11	26.7	8.4	Dmdst	27\28	11	81.1	76.4	Dmdst
19\21	11	80.0	75.0	Dmdst	28\29	11	45.2	31.5	Dmdst
20\21	11	82.6	78.3	Dmdst	29\30	11	58.4	48.0	Ss, minor Dmdst
21\22	11	95.3	94.1	Dmdst	30\31	11	63.5	54.3	Dmdst
22\23	11	49.2	36.5	Dmdst	31\32	11	9.3	13.4	Mdst&Dmdst
23\24	11	30.2	12.7	Dmdst	32\33	11	94.7	93.4	Mdst&Dmdst
24\25	11	90.3	87.9	Dmdst	33\34	11	45.2	31.4	Mdst&Ss
25\26	11	42.9	28.6	Dmdst	34\35	11	33.0	16.3	Mdst&minor Dmdst
26\27	11	68.9	61.2	Dmdst	35\36	11	95.4	94.3	Mdst&Dmdst
«««««««««««««««««« BASE OF DEFORMATION »»»»»»»»»»»»»»»»»»»									
27\28	11	94.4	93.0	Mdst	36\37	11	92.9	91.1	Mdst
28\29	11	95.8	94.7	Mdst&Ss	37\38	11	97.4	96.8	Mdst, minor coal
29\30	11	65.4	56.7	Ss&Mdst	38\39	11	89.0	86.2	Mdst
30\31	11	93.4	91.8	Mdst	39\40	11	99.7	99.6	Mdst
31\32	11	97.8	97.3	Mdst&Ss	40\41	11	99.6	99.5	Mdst&Bentonite
32\33	11	98.4	98.0	Ss&Mdst	41\42	11	57.2	46.5	Mdst& minor coal
33\34	11	97.5	96.9	Mdst&Ss					
34\35	11	98.7	98.4	Ss					
35\36	11	58.3	47.9	Ss					
36\37	11	99.6	99.5	Ss&Mdst					
37\38	11	99.5	99.4	Mdst&Coal					

Abbreviations:

D - deformed
Mdst - mudstone
Ss - sandstone

observed in the core, particularly in hole HV409 where masses of undeformed bedrock over 1 m thick were observed within the highly deformed material.

Within the undeformed rock a few subunits with low R^2 values are present: 65.4 and 58.6 in HV408, and 57.2 in HV409. The reason for this is unknown. The core did not appear fractured at these intervals, but two of these subunits are located where there is a lithologic transition; from sandstone to mudstone in HV409 and mudstone to coal in HV409.

5.4 DISCUSSION

The analyses above show that deformed bedrock can be detected from geophysical logs, but an awareness or understanding of the water table location, local geology and physical properties of the rocks is required to make meaningful interpretations of the logs. There is usually enough contrast between deformed and undeformed material so that sonic, density, neutron and dipmeter log data can be used to detect zones of weakness and induration in the bedrock. Deformation zones are characterized by long transit times on the sonic log, low density values, high neutron count rates and an increased scatter in dipmeter data.

For the first three logs, this is actually a reflection of secondary porosity: increases in fractures and spaces in the rock that have been caused by deformation will normally show up on the tools influenced by porosity. Absolute log values that identify deformation could not be defined because of the variability in local geology and physical properties of the rock. For this reason, the geophysical logs should be calibrated with detailed stratigraphic and geotechnical information for localized areas. With this in hand, anamolous readings on the logs take on more geotechnical significance. The widespread occurrences of deformed bedrock in the Plains strongly suggests that log responses are affected by rock strength as well as lithologic changes.

An approach to delineating deformed bedrock, both vertically and laterally, with the aid of geophysical logs is presented:

1) At the early stages of site investigation, a few holes should be used to obtain detailed stratigraphic information from both core and geophysical logs. Continuous core should be collected from surface and careful attention paid to lithologic, structural and physical characteristics of the core. A comprehensive suite of logs should include caliper, gamma, resistivity, density, sonic, neutron

and possibly dipmeter.

2) Log responses should then be checked against core descriptions to identify lithologic changes, normal responses in undeformed rock for each lithology and the contrasting responses in the deformed rock. The scatter plots, histograms and statistical methods described in this report can be used to help define the log responses that represent deformed zones.

3) From this base of information and interpretation, logs from step-out wells can then be used with more reliability and confidence. This can reduce the need for additional coring, which would be a cost-saving to a mining or exploration program.

Geophysical logs provide a vast amount of data that can be used more effectively today with the aid of a computer. The methods described in this section are just examples of what can be done with very basic software and a desktop computer. The challenge now is to try new and different approaches to analyzing and probing the data for new information.

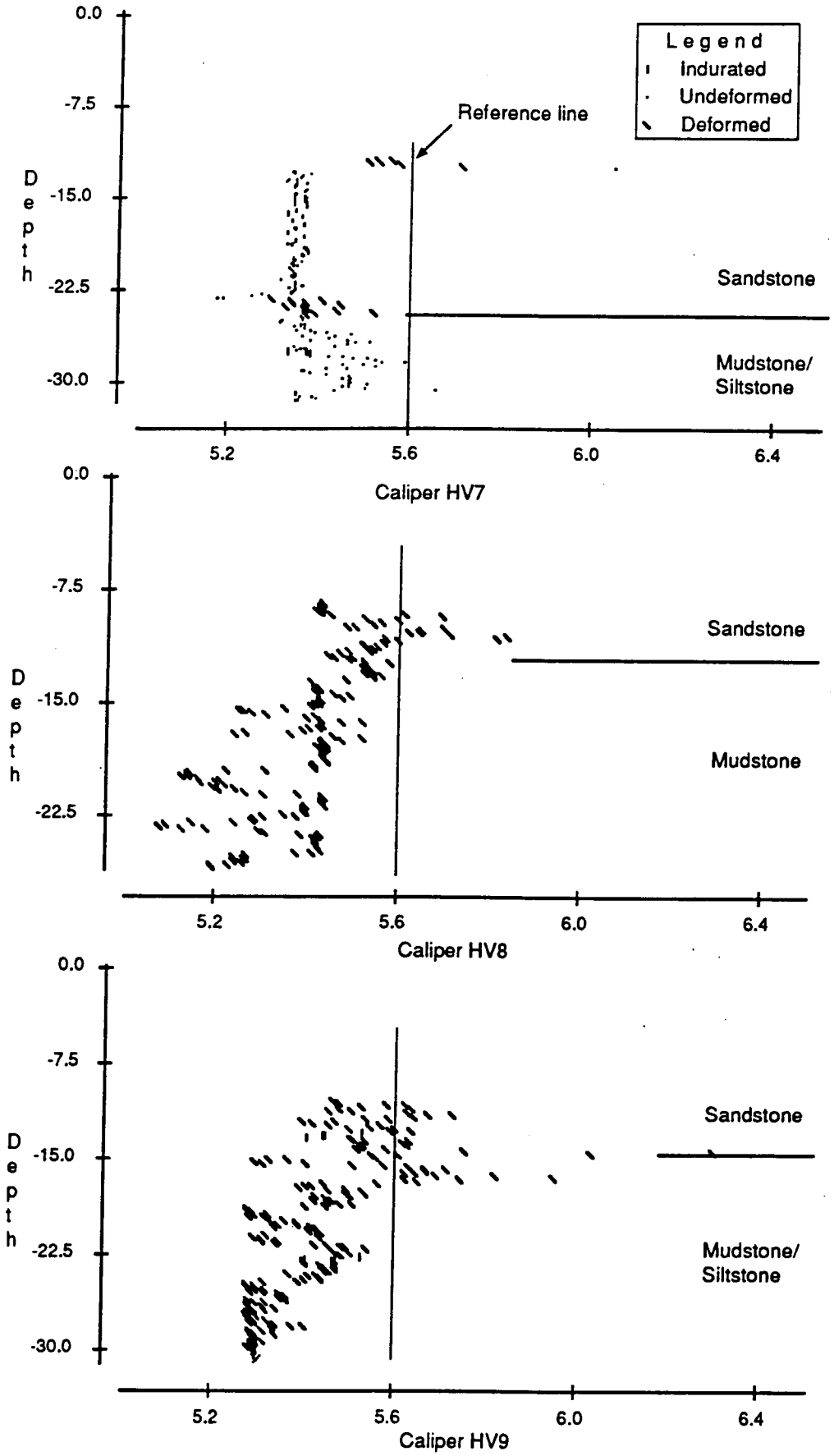

Figure 5-1. Caliper logs in inches of HV7, HV8 and HV9.

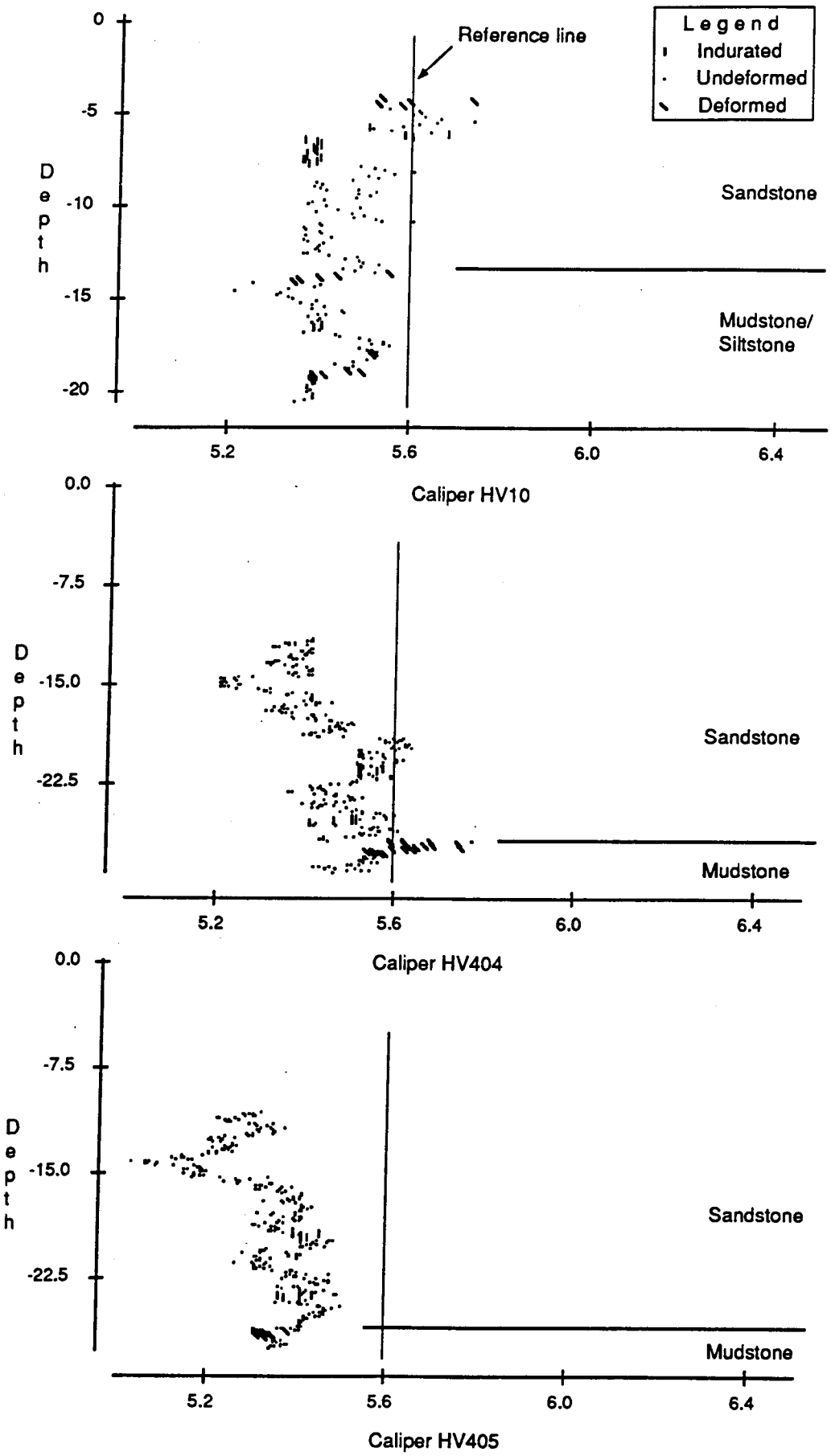

Figure 5-2. Caliper logs in inches of HV10, HV404 and HV405.

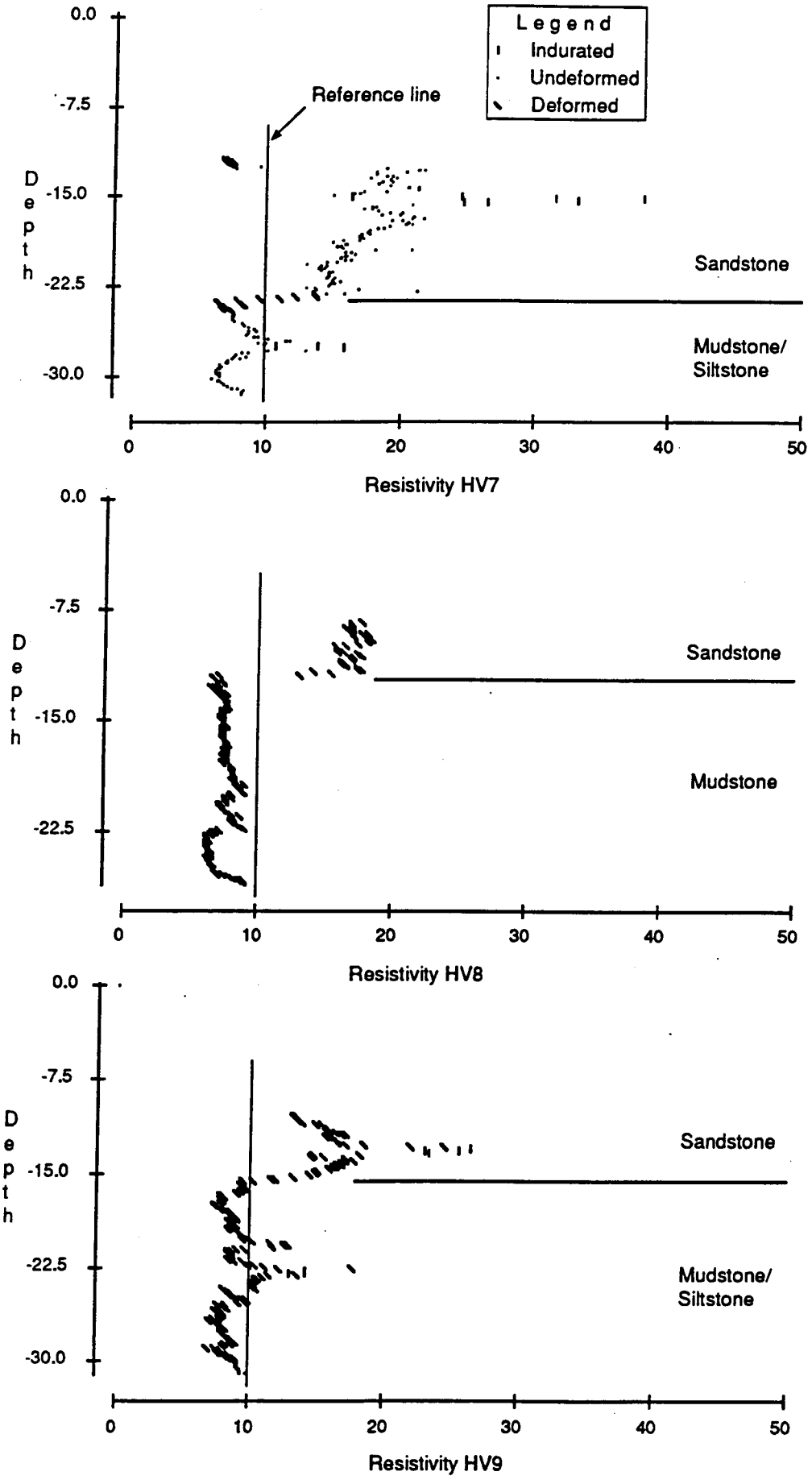

Figure 5-3. Resistivity logs in ohm-meters of HV7, HV8 and HV9.

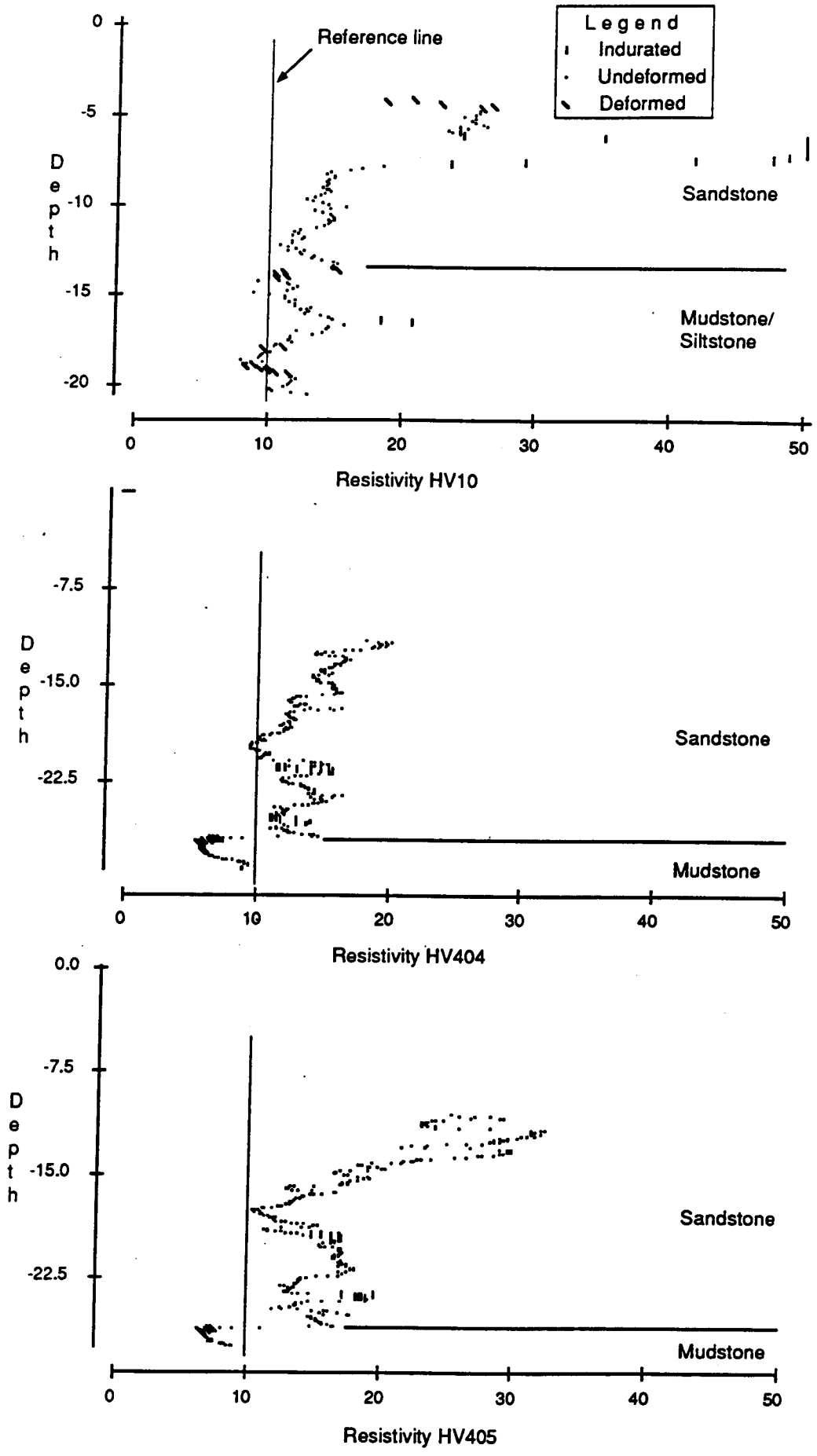

Figure 5-4. Resistivity logs in ohm-meters of HV10, HV404 and HV405.

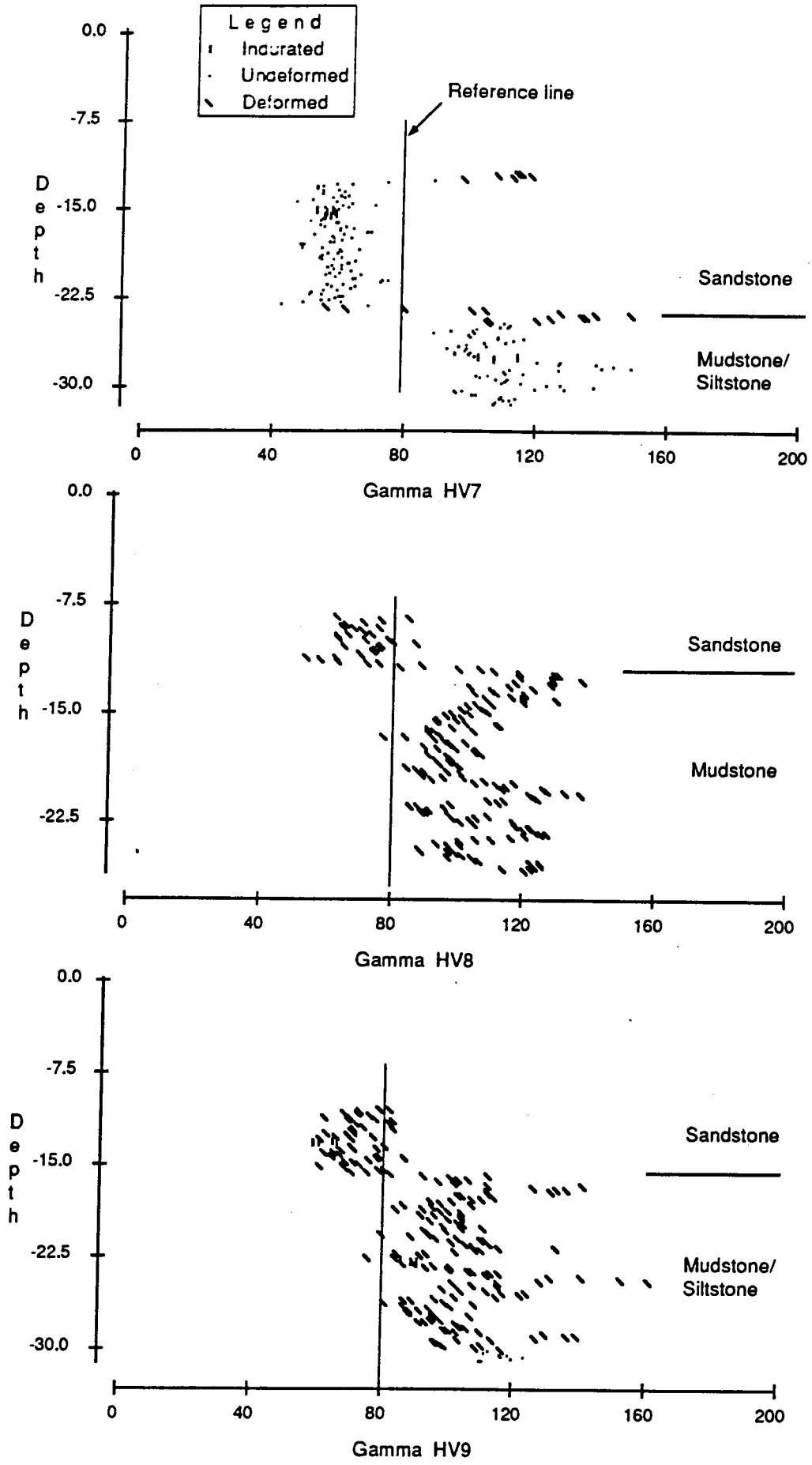

Figure 5-5. Gamma logs in API of HV7, HV8 and HV9.

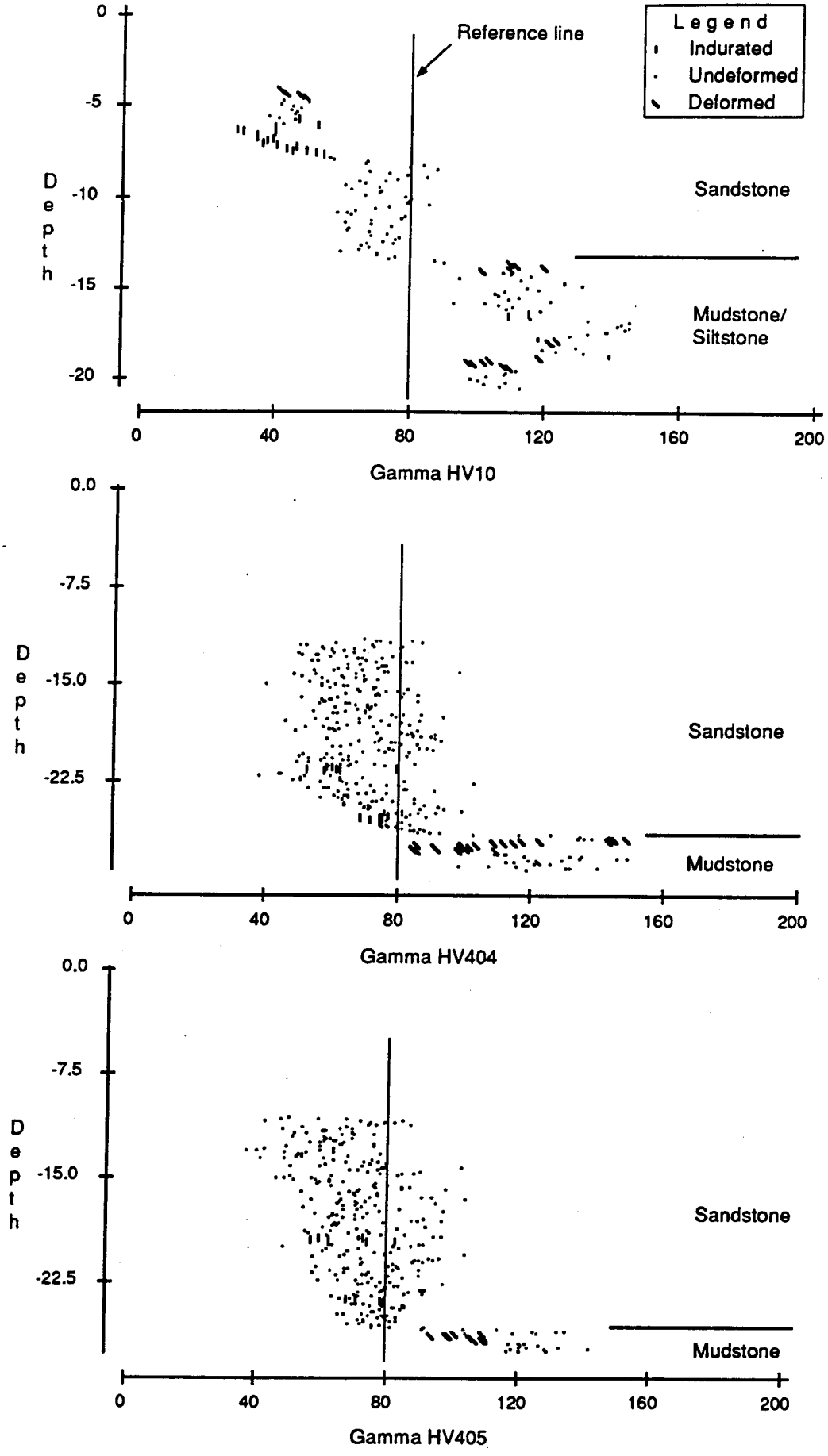

Figure 5-6. Gamma logs in API of HV10, HV404 and HV405.

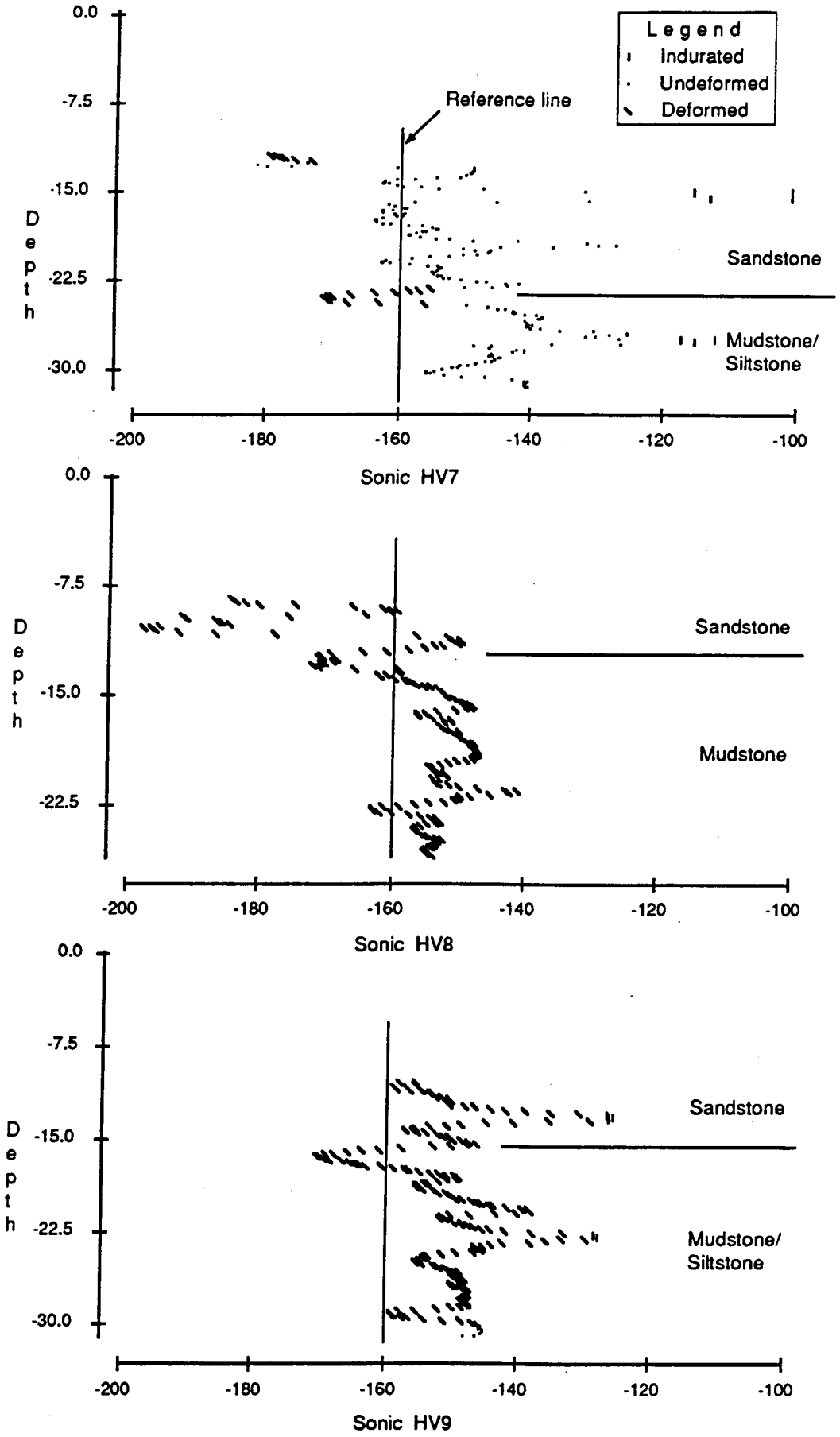

Figure 5-7. Sonic logs in microseconds/foot of HV7, HV8 and HV9.

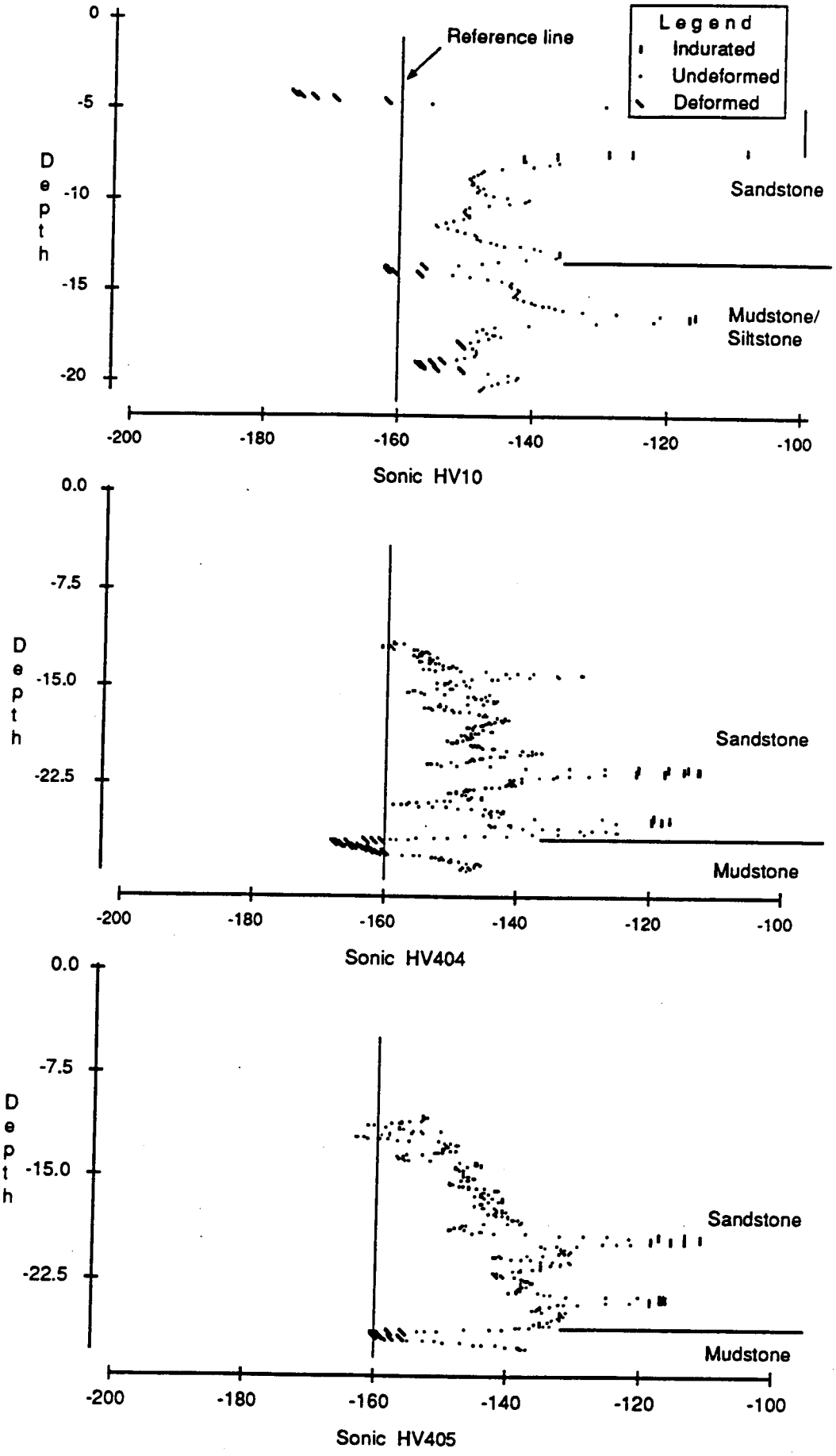

Figure 5-8. Sonic logs in microseconds/foot of HV10, HV404 and HV405.

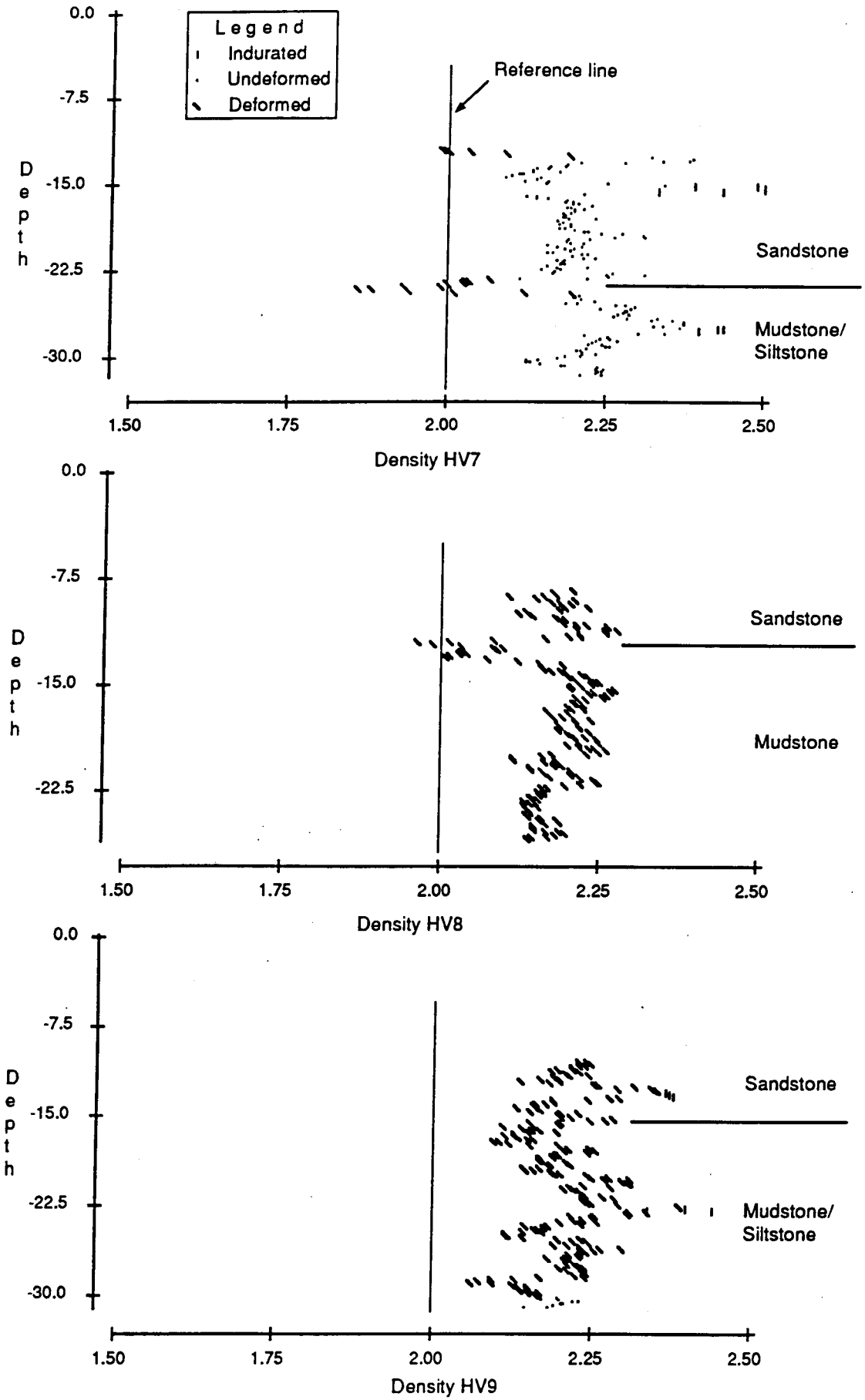

Figure 5-9. Density logs in g/cm3 of HV7, HV8 and HV9.

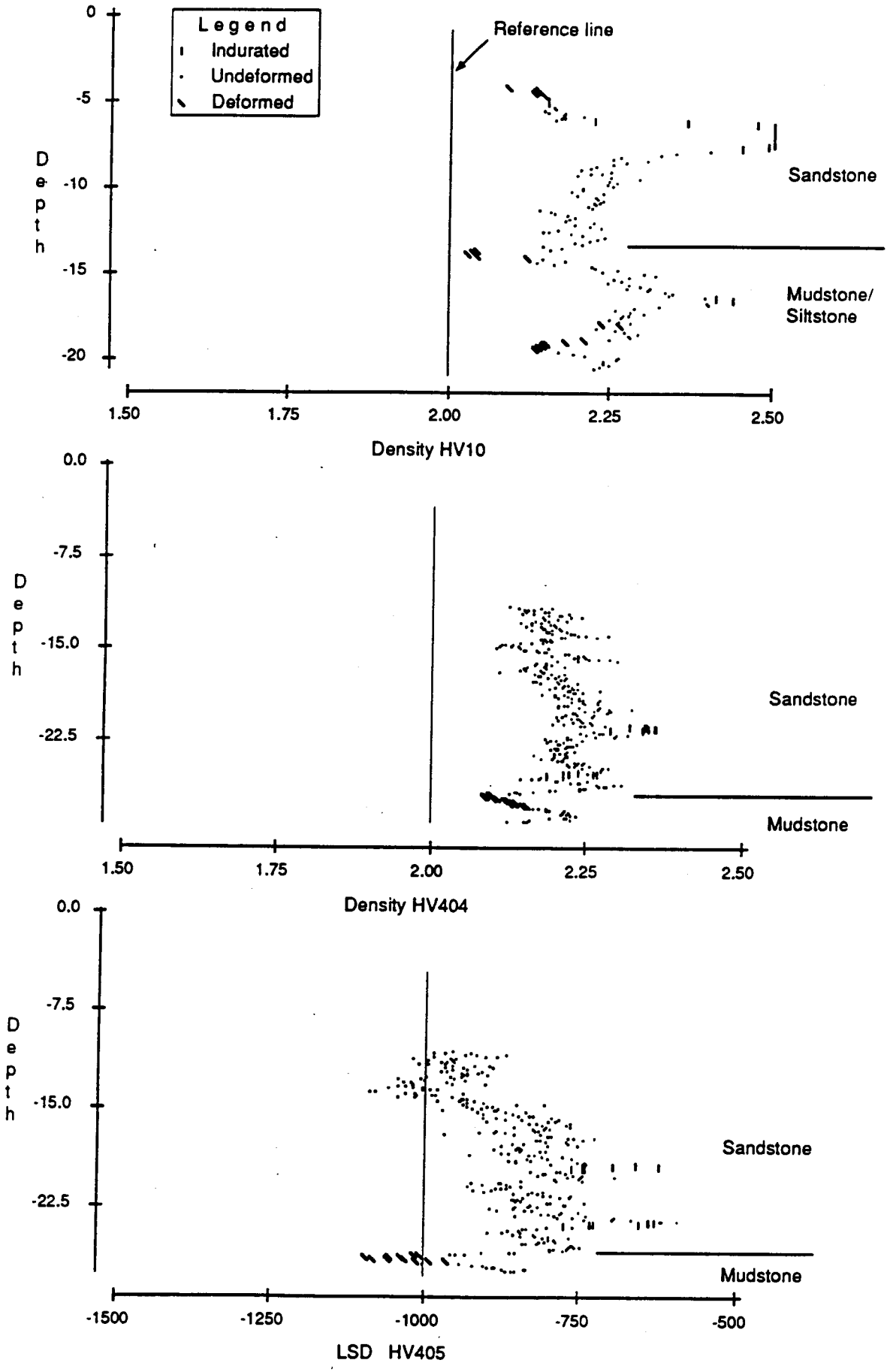

Figure 5-10. Density logs in g/cm3 of HV10 and HV404. HV405 is long-spaced density in counts.

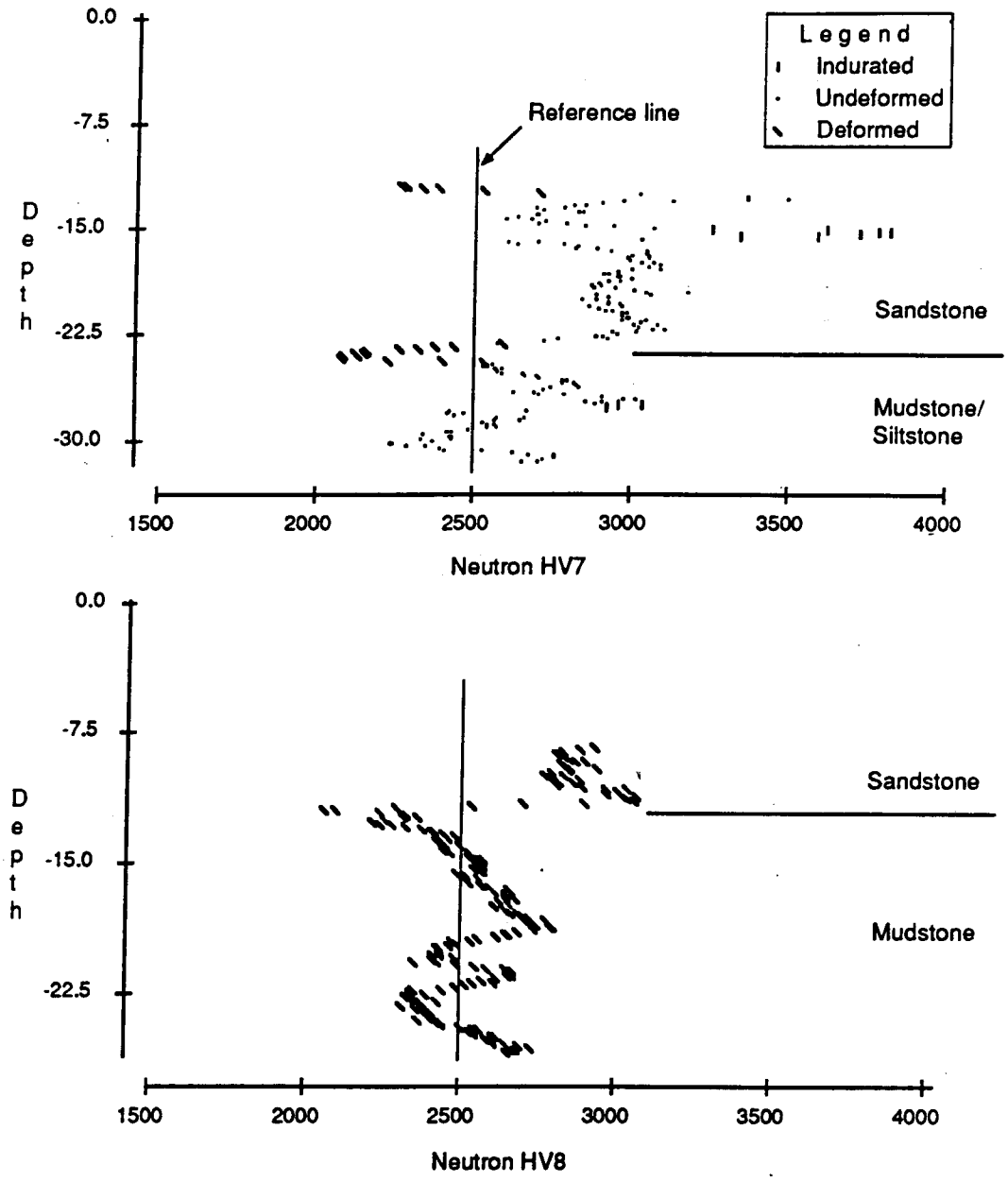

Neutron log of HV9 is missing.

Figure 5-11. Dual spaced neutron logs in counts of HV 7 and HV8.

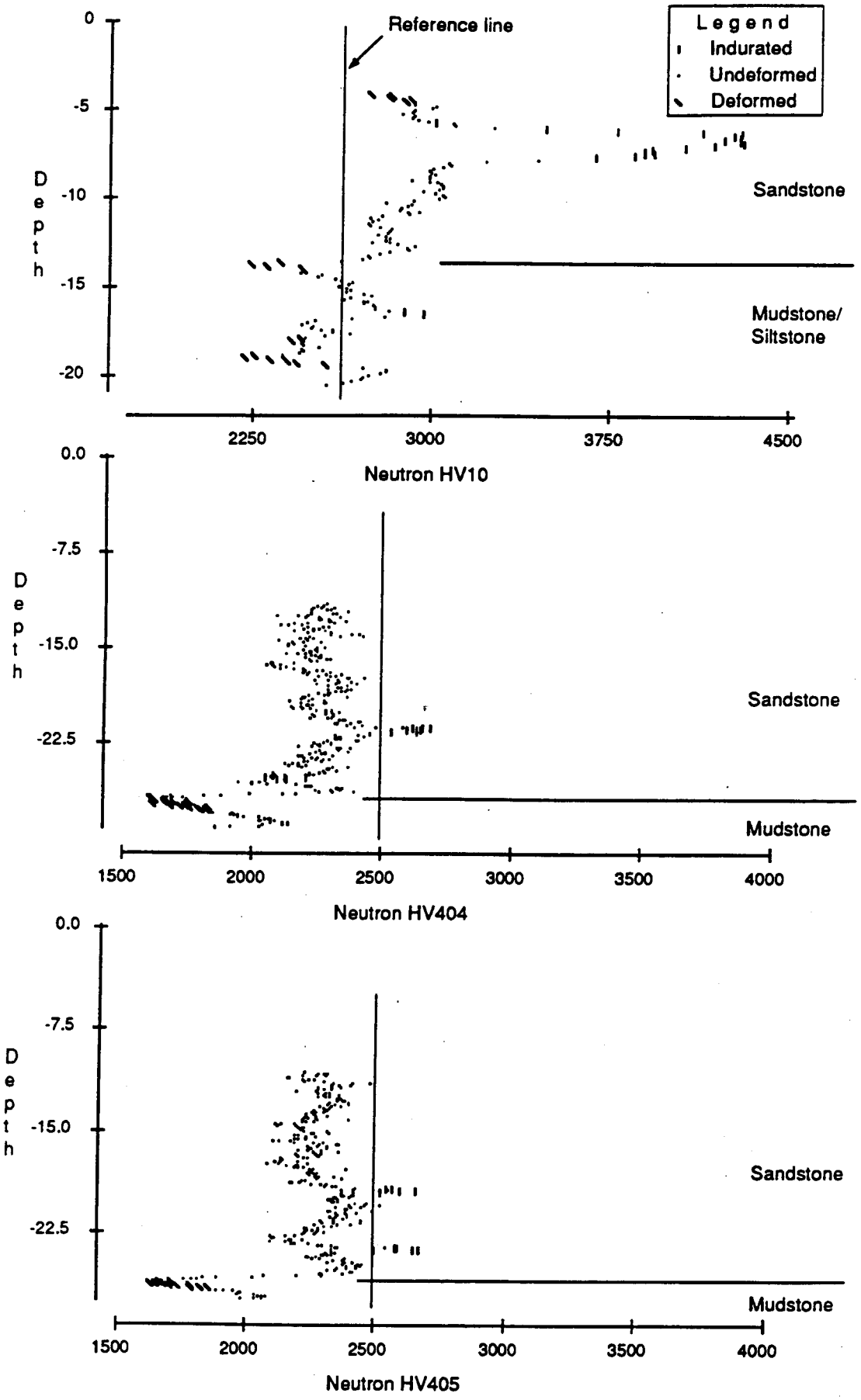

Figure 5-12. Dual spaced neutron logs in counts of HV10, HV404 and HV405.

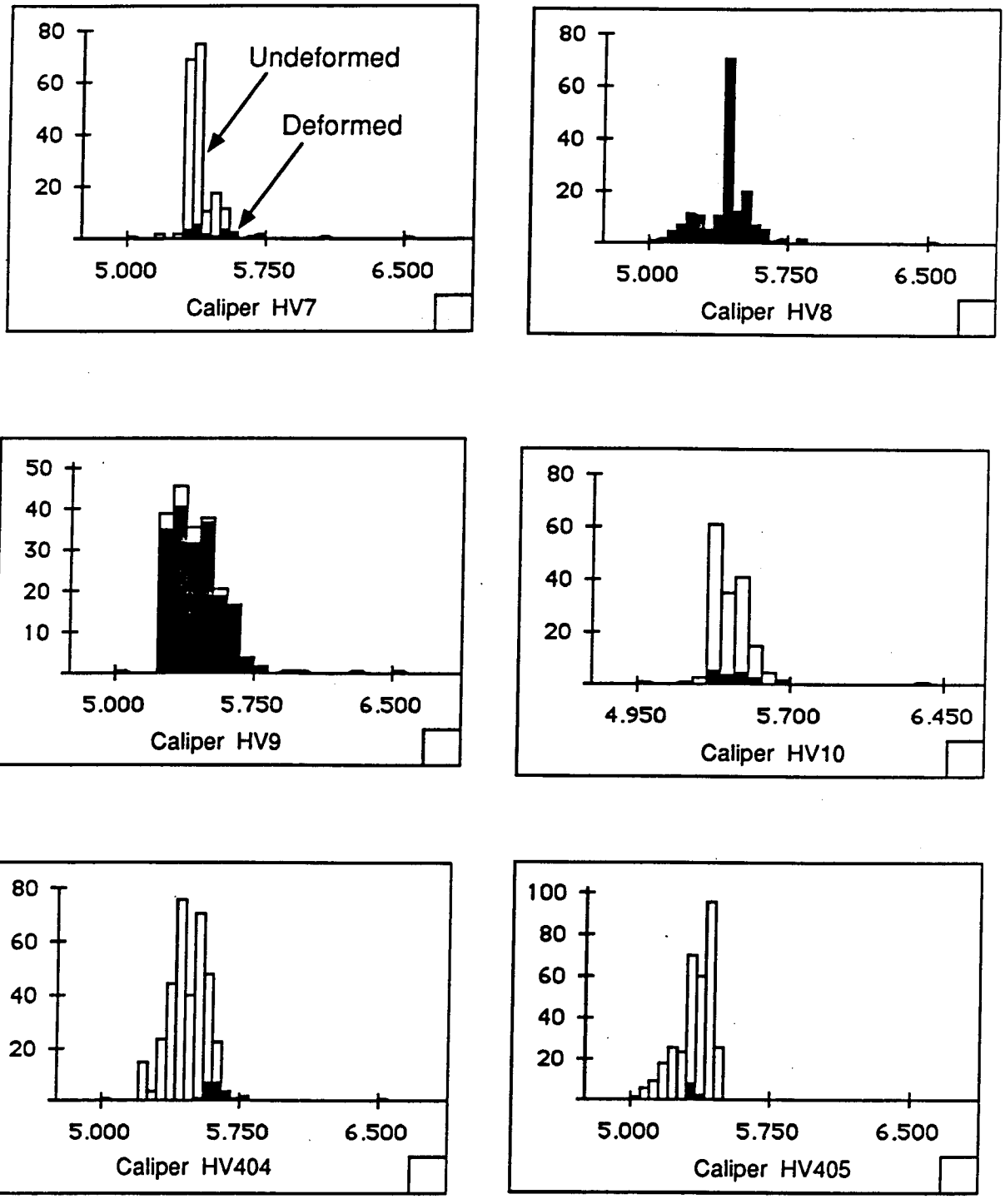

Figure 5-13. Caliper histograms showing deformed and undeformed distribution, Pit 03, Highvale Mine.

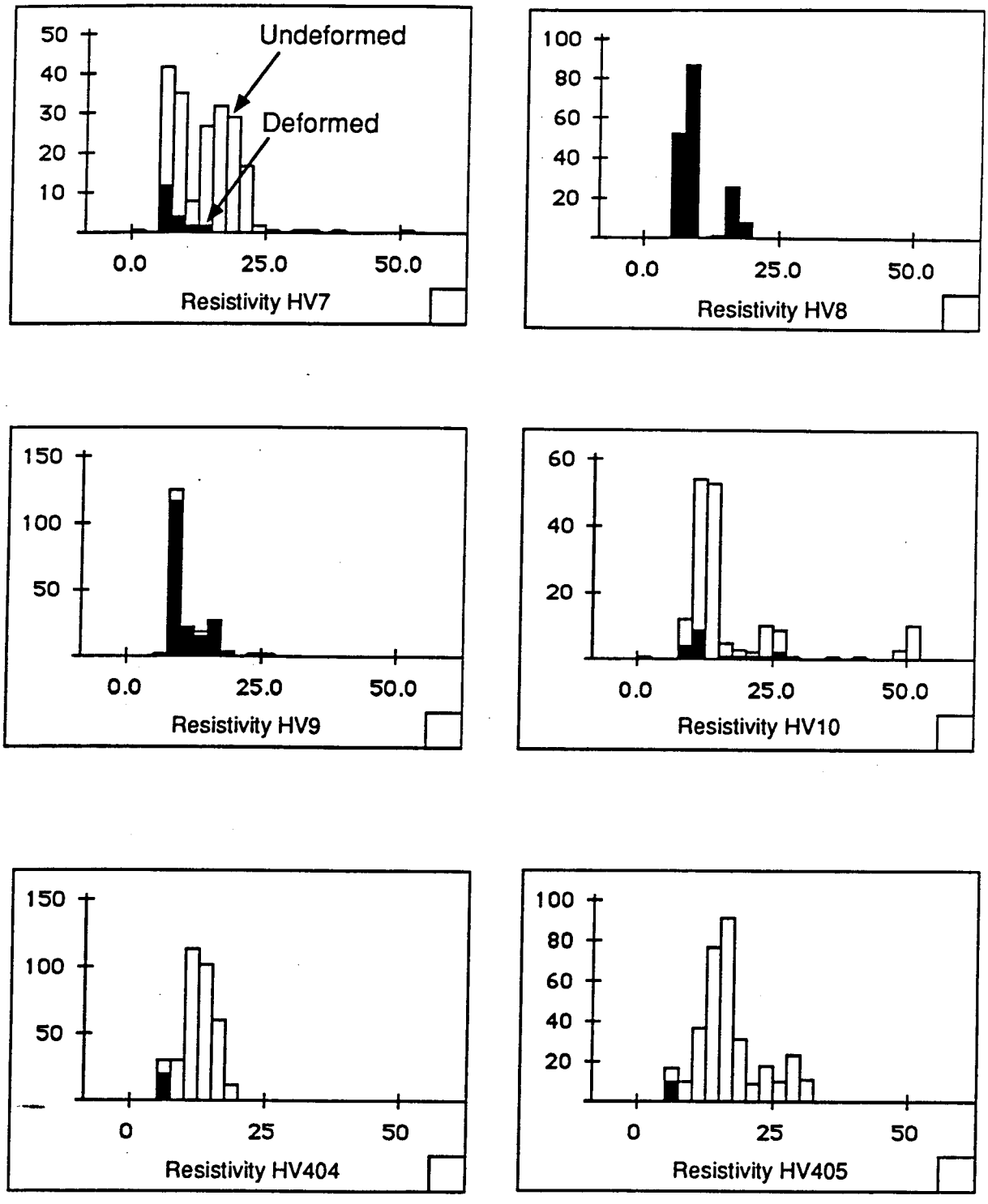

Figure 5-14. Resistivity histograms showing deformed and undeformed distribution, Pit 03 Highvale Mine.

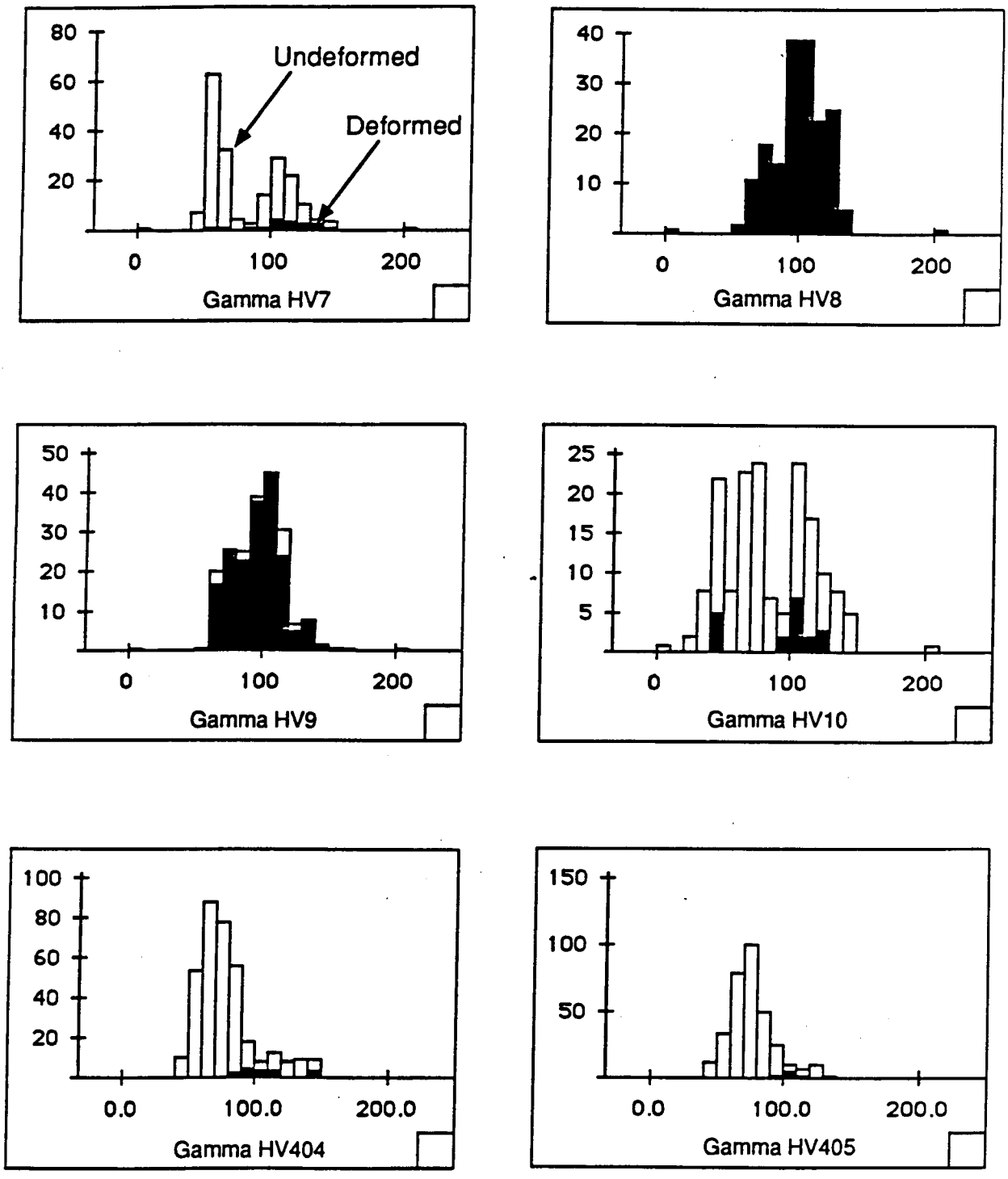

Figure 5-15. Gamma histograms showing deformed and undeformed distribution Pit 03, Highvale Mine.

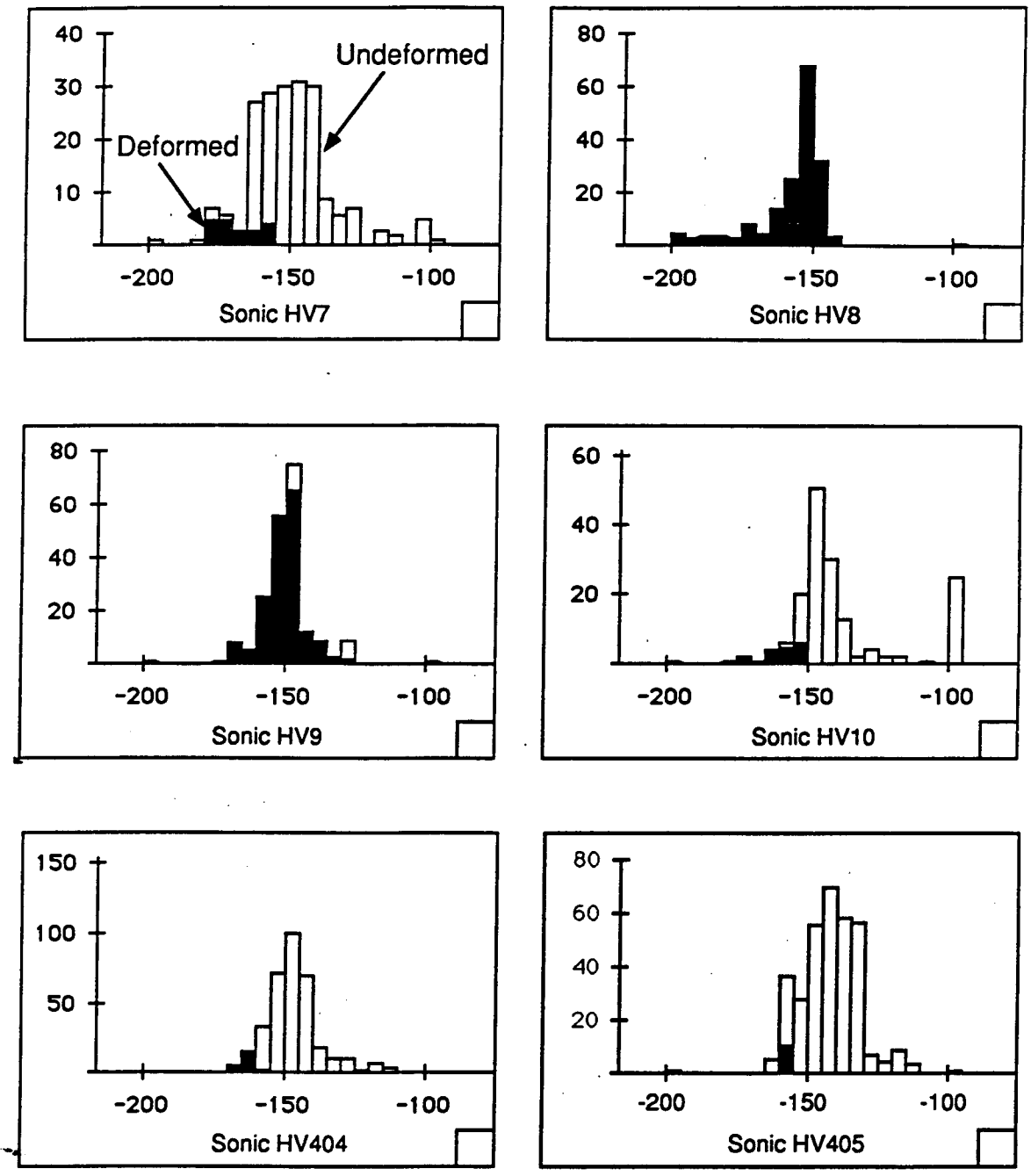

Figure 5-16. Sonic histograms showing deformed and undeformed distribution, Pit 03, Highvale Mine.

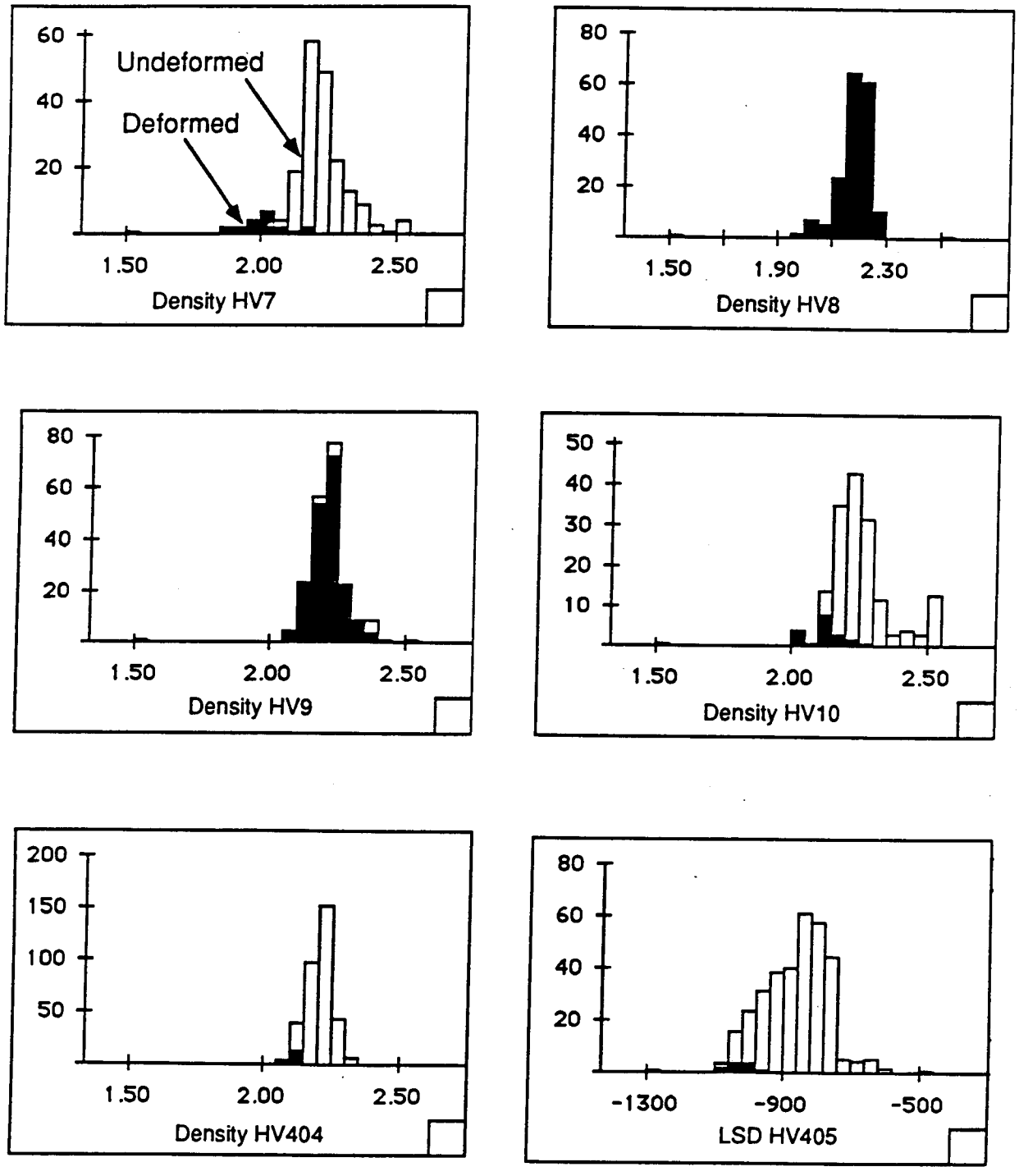

Figure 5-17. Density histograms showing deformed and undeformed distribution Pit 03, Highvale Mine.

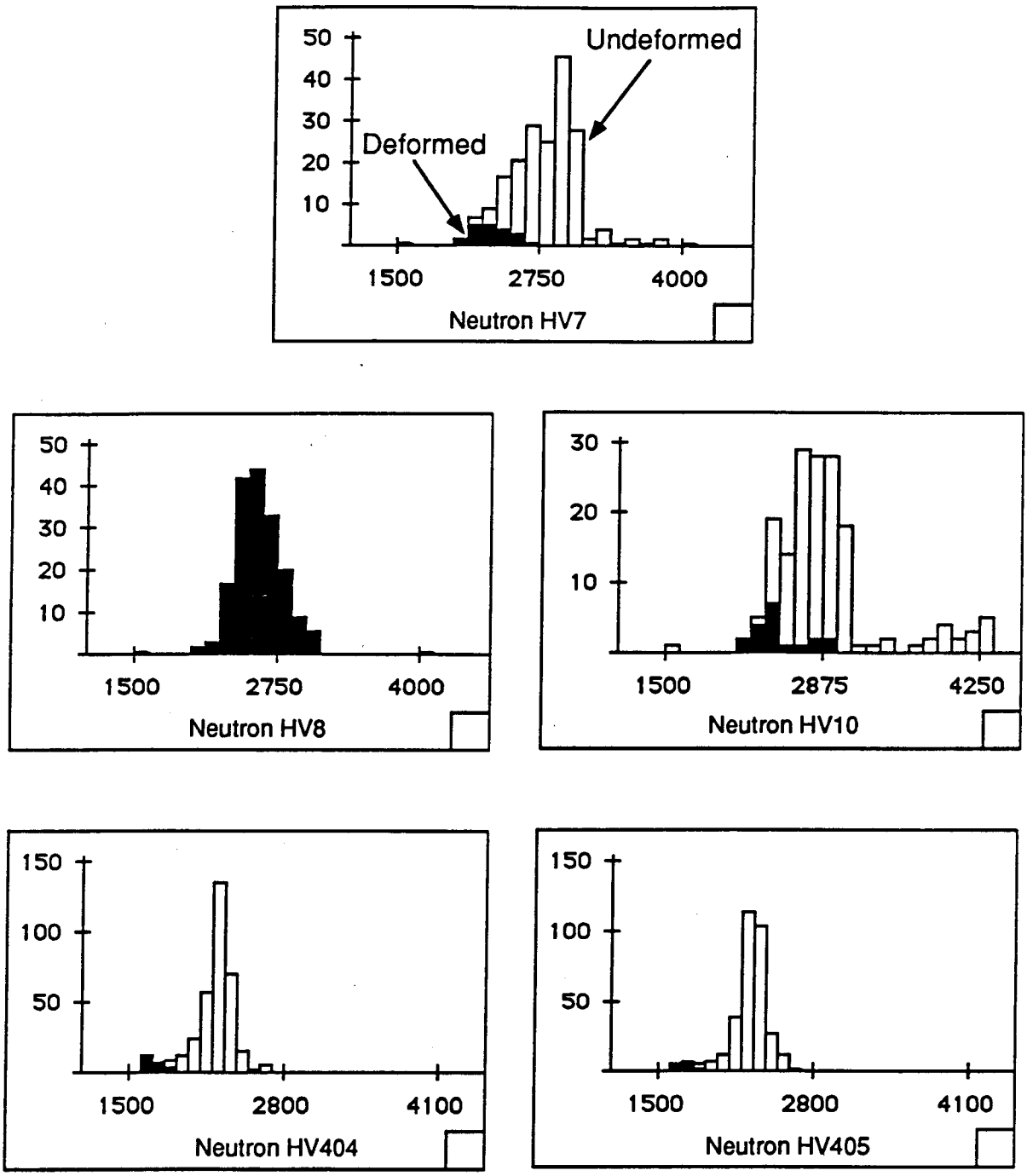

Figure 5-18. Neutron histograms showing deformed and undeformed distribution, Pit 03, Highvale Mine.

HV404, Pit 03, Highvale Mine

Pearson Product-Moment Correlation

641 total cases of which 288 are missing

	-Sonic...	Dens404	NN404	Gam404	Res404	Cal404
-Sonic404	1.000					
Dens404	0.680	1.000				
NN404	0.551	0.636	1.000			
Gam404	-0.250	-0.270	-0.671	1.000		
Res404	0.060	0.057	0.559	-0.579	1.000	
Cal404	0.120	0.266	-0.232	0.345	-0.677	1.000

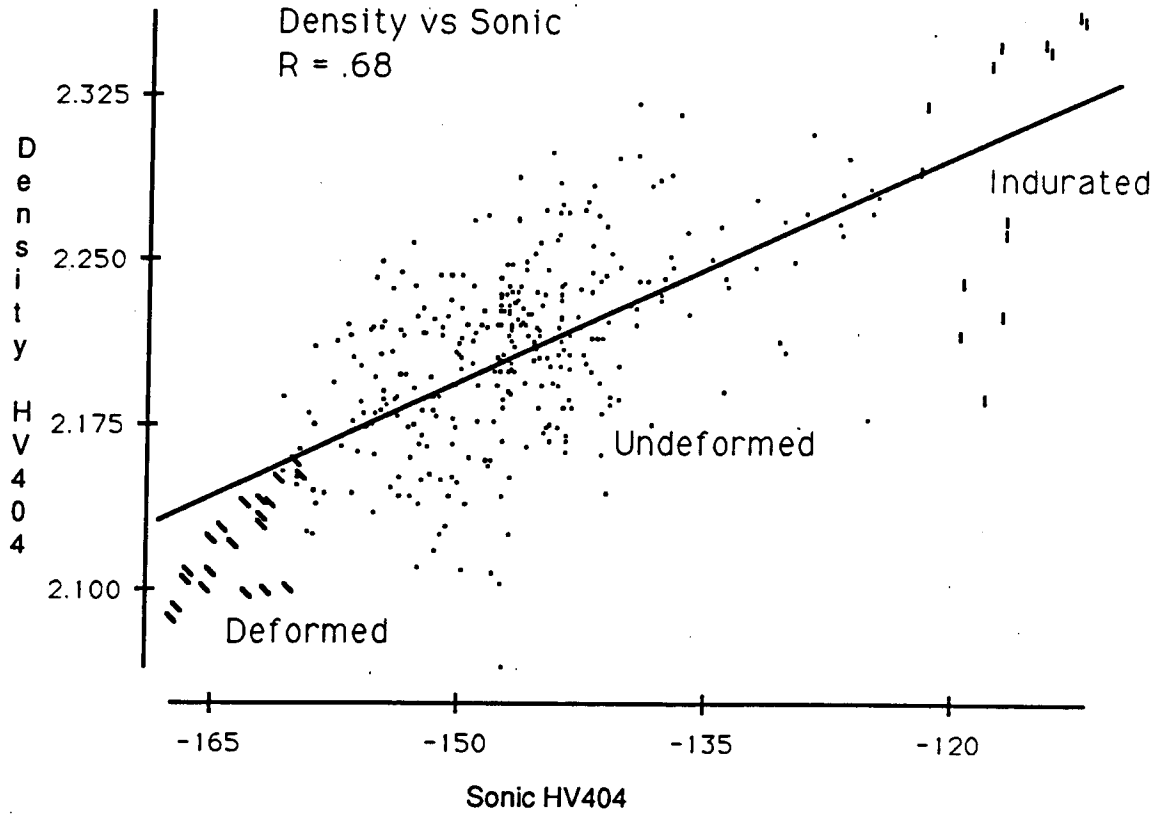

Figure 5-19. Example of good correlation from HV404, density vs sonic.

HV7, Pit 03, Highvale Mine

Pearson Product-Moment Correlation

340 total cases of which 144 are missing

	-Sonic7	DENS7	NN7	GAM7	RES7	CAL7
-Sonic7	1.000					
DENS7	0.753	1.000				
NN7	0.389	0.665	1.000			
GAM7	0.039	-0.106	-0.675	1.000		
RES7	0.151	0.268	0.776	-0.813	1.000	
CAL7	-0.165	0.016	-0.275	0.487	-0.423	1.000

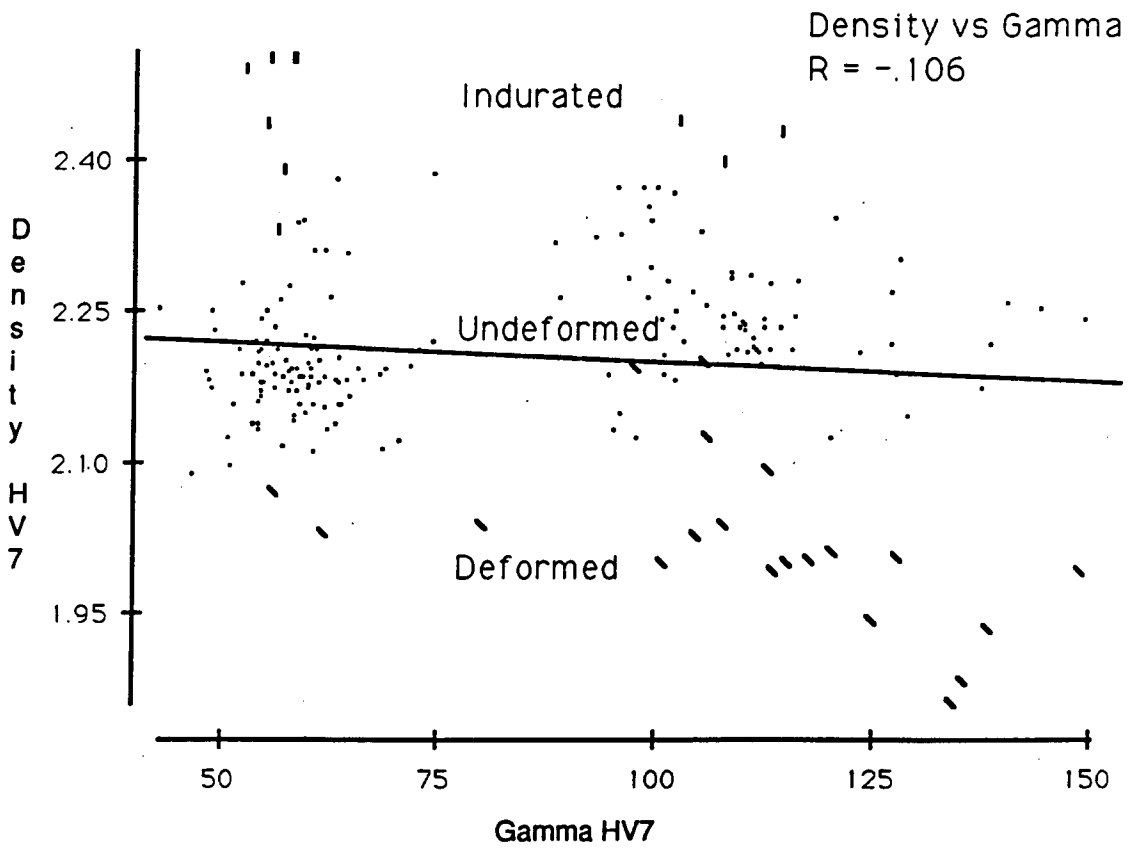

Figure 5-20. Example of poor correlation from HV7, density vs gamma.

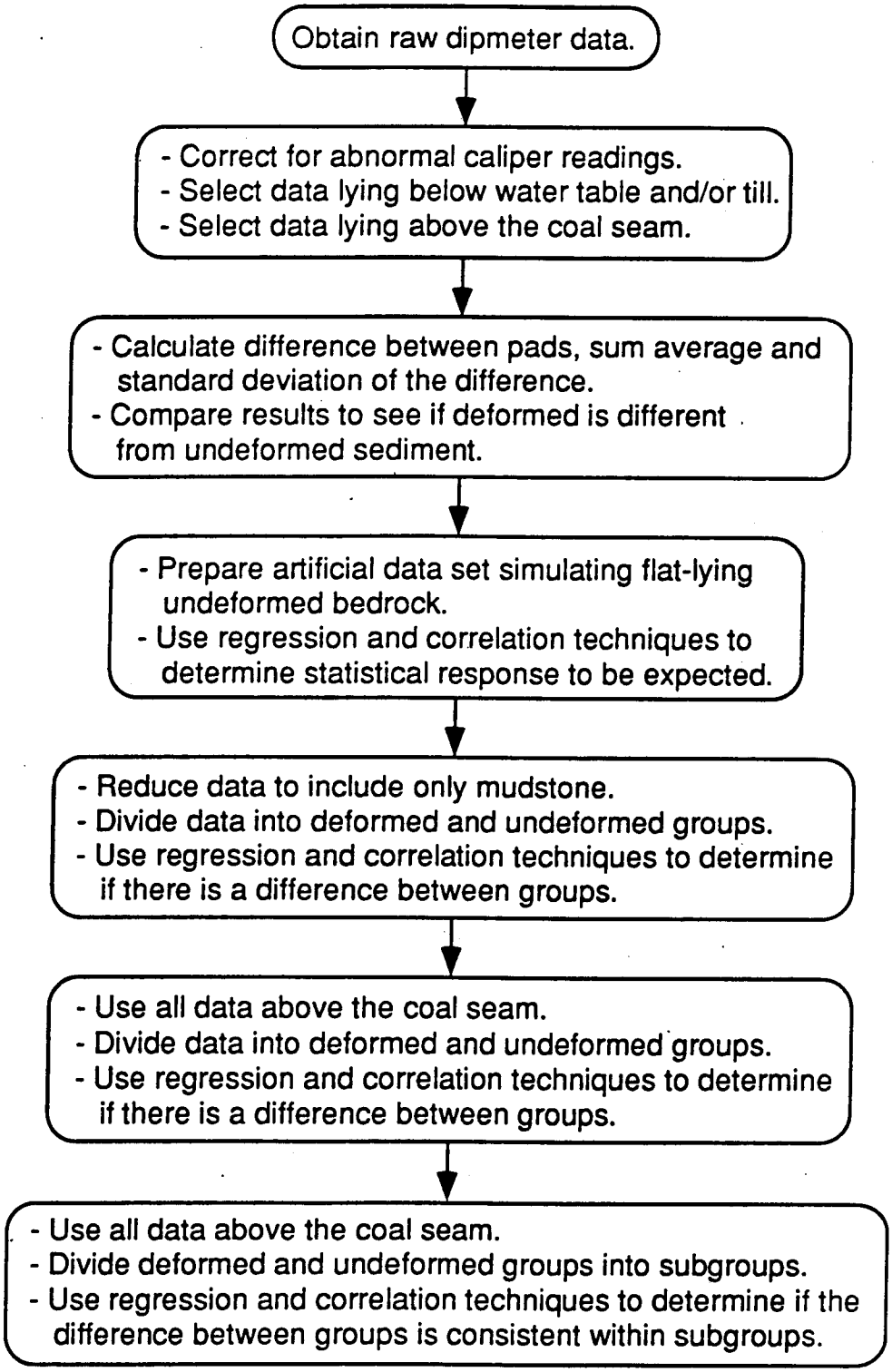

Figure 5-21. Analysis flowsheet for the dipmeter log data.

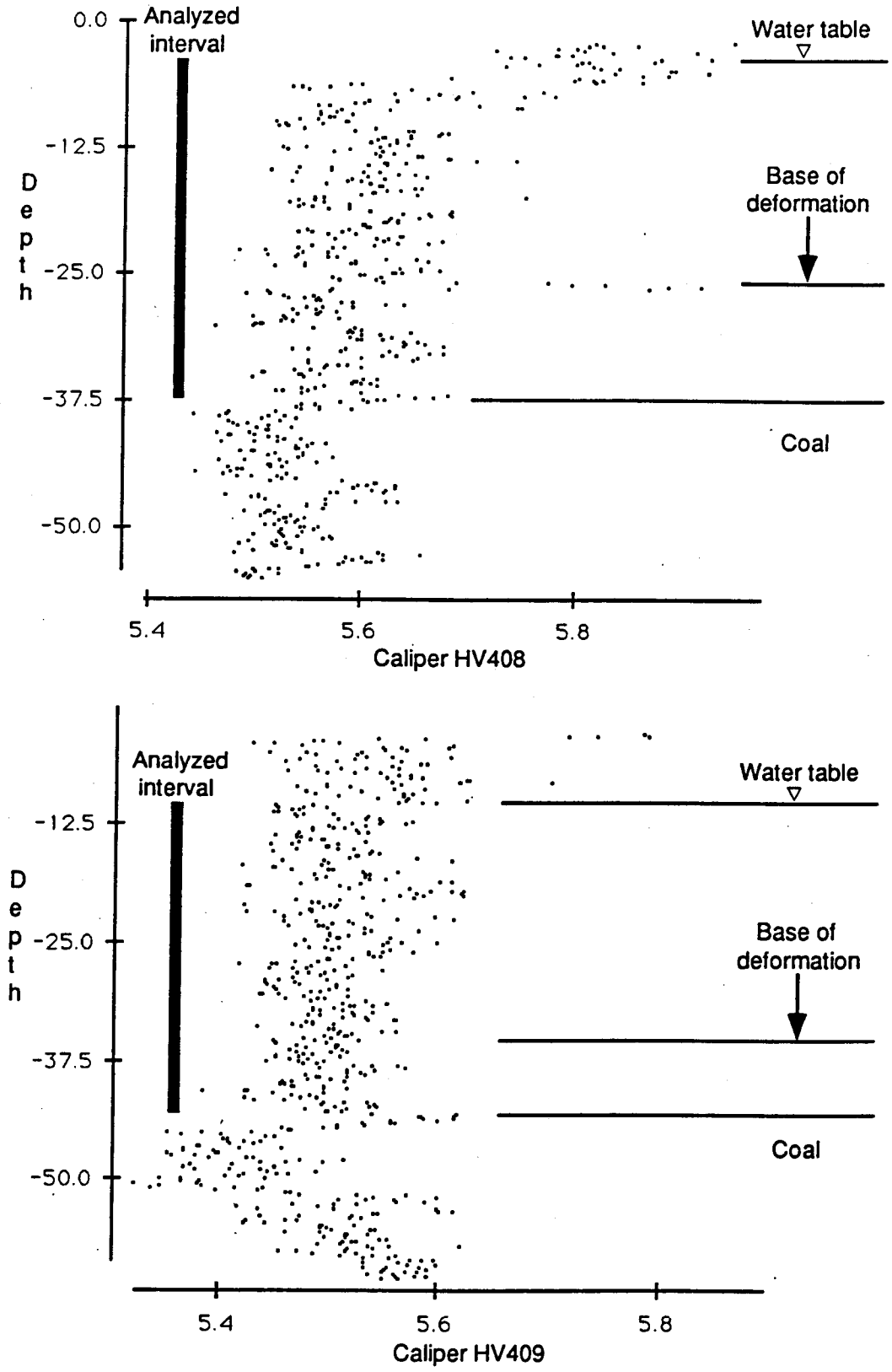

Figure 5-22. Plots of depth vs caliper from holes HV408 and HV409 showing selected intervals used in analysis.

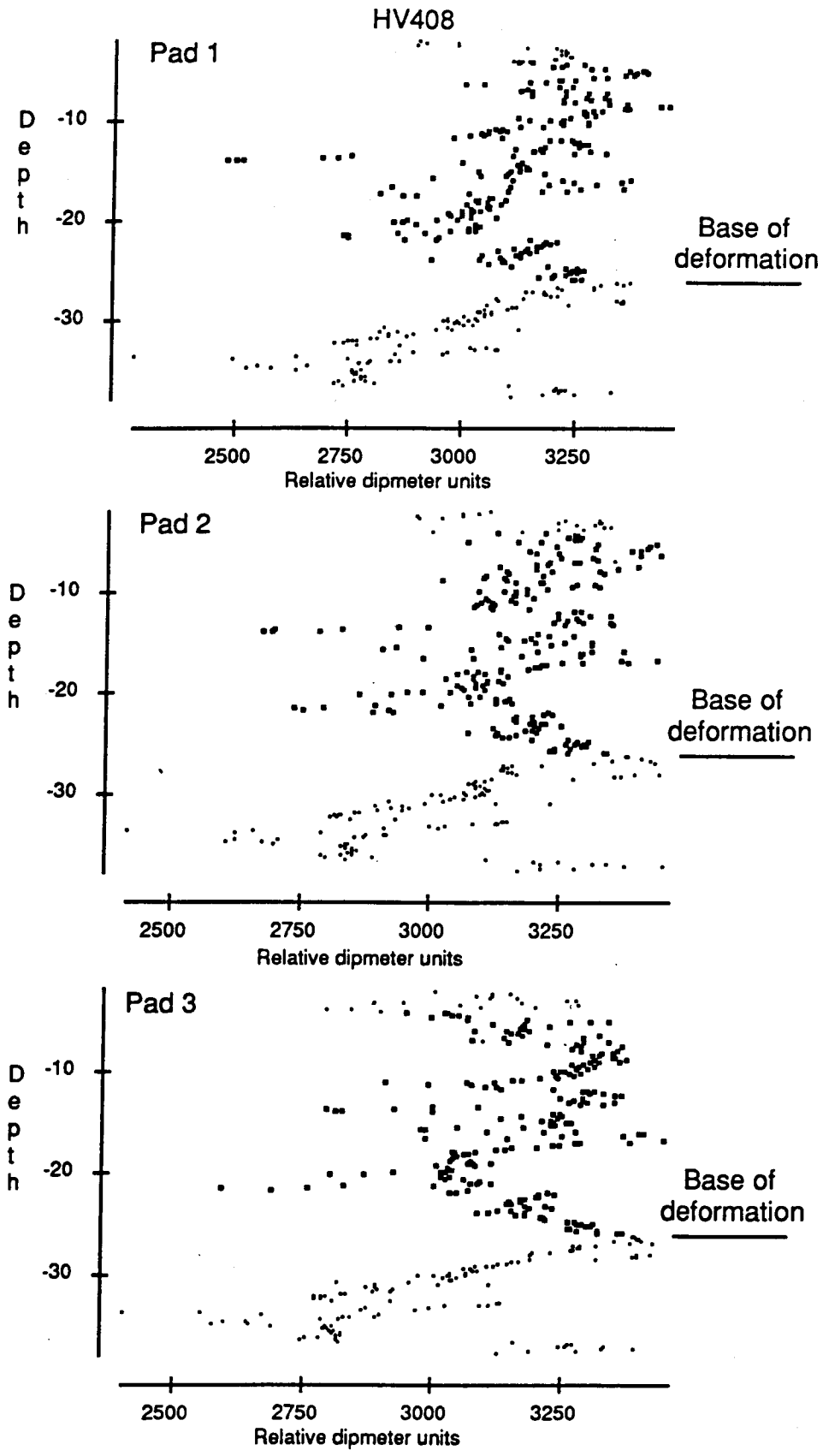

Figure 5-23. Dipmeter pad readings for hole HV408 show all three set of readings are similar although not identical.

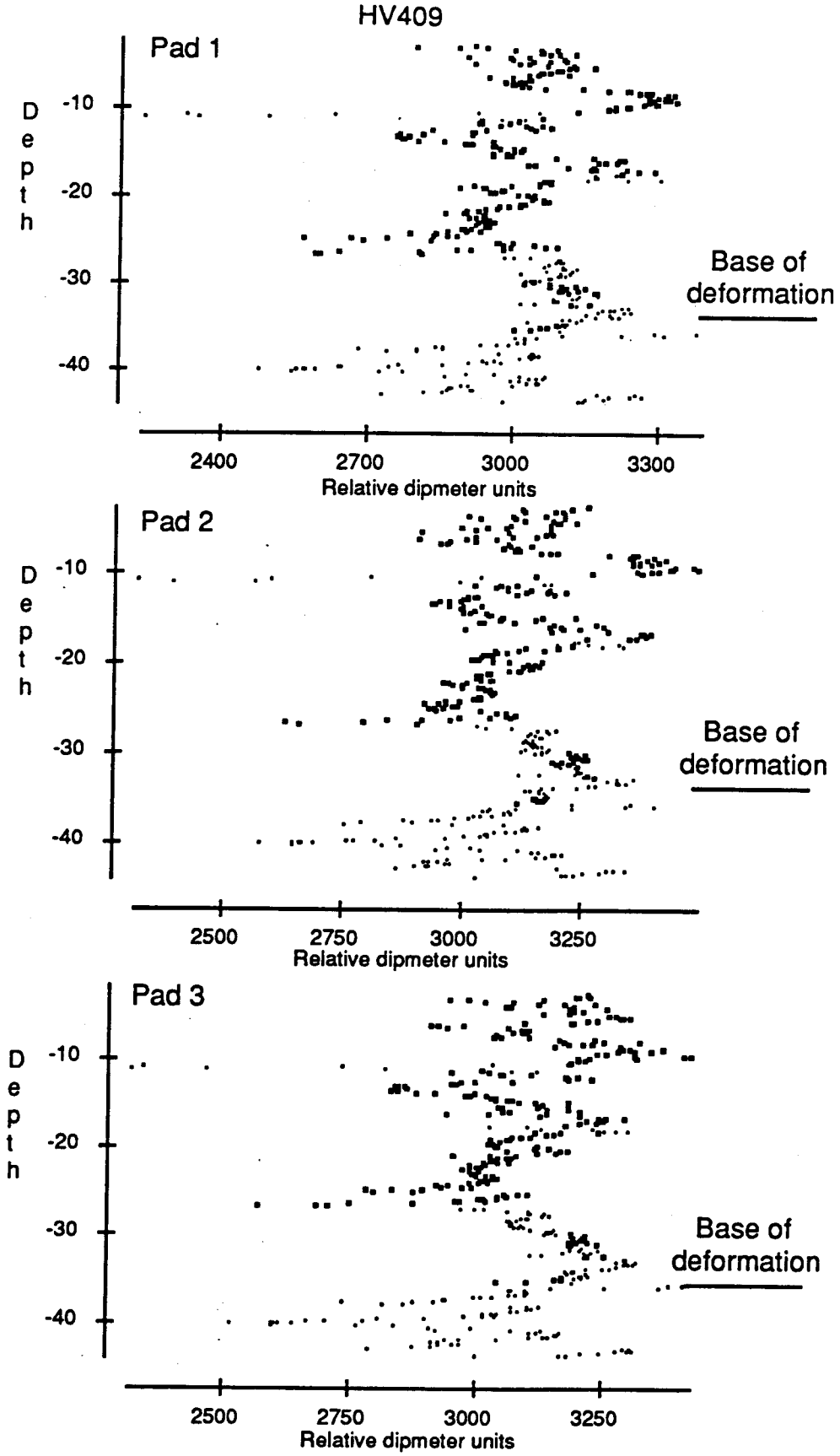

Figure 5-24. Dipmeter pad readings for hole HV409 show all three set of readings are similar although not identical.

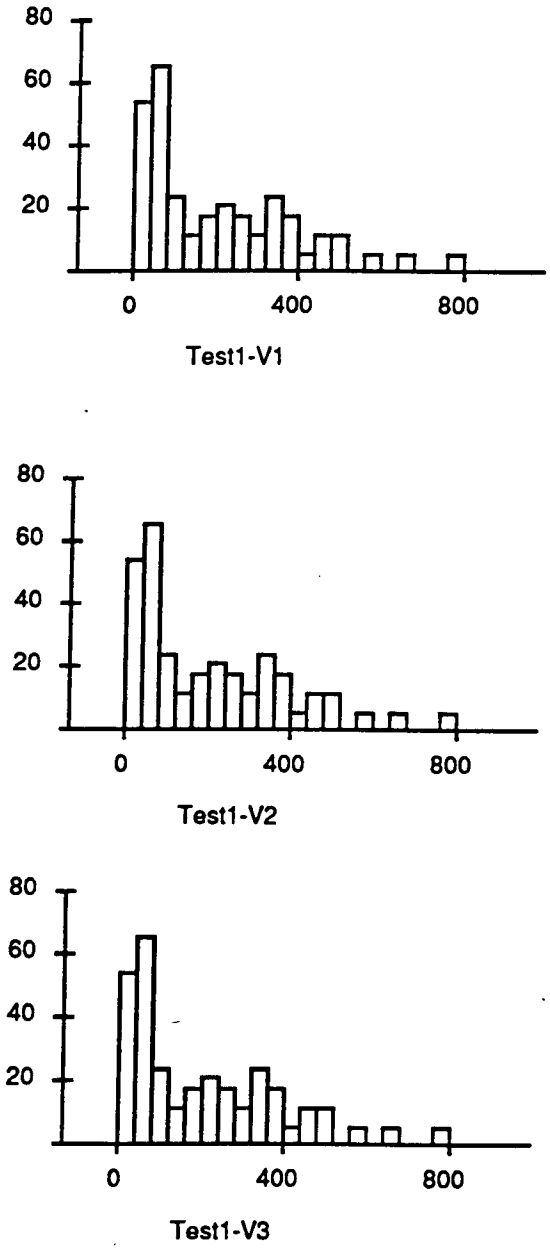

Figure 5-25. Histograms of variables V1, V2 and V3 showing the data distribution within the artificial data set. Data in each of the three variables is identical.

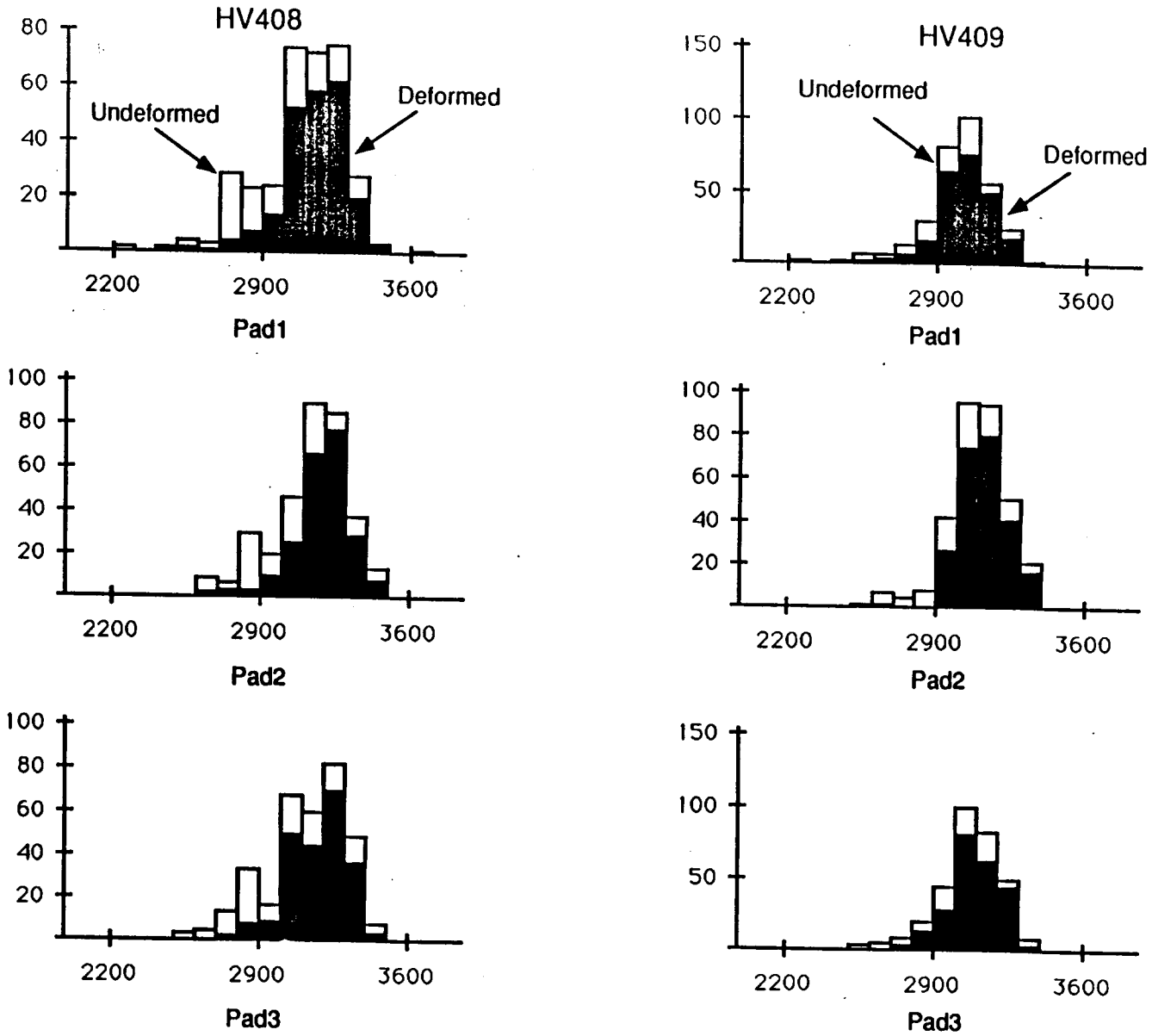

Figure 5-26. Histograms of the three dipmeter pad readings for holes HV408 and HV409 showing deformed and undeformed groups. The pad readings for each group are similar although not identical.

6. USE OF SPECTRAL GAMMA FOR CLAY MINERALOGY

C. Jonathan Mwenifumbo and John G. Pawlowicz

6.1 INTRODUCTION

Gamma ray measurements are used to detect variations in natural radioactivity due to changes in concentrations of trace elements, uranium (U) and thorium (Th), as well as changes in the concentrations of the major element potassium (K). There are a number of commercially available gross-count or total-count gamma ray logging systems. These, however, do not discriminate between the different radioelements which contribute to the overall radioactivity detected. Only spectral gamma ray logging systems are able to provide information on the concentrations of the three naturally occurring radioelements. More information about the nature of the rock formations can therefore be extracted from the spectral gamma ray data than from the total-count gamma ray data. Spectral logs (Total count, K, U and Th) have been used successfully by the petroleum industry for detailed stratigraphic correlation, lithologic identification, determination of type and amount of clay minerals present in the formation (Fertl, 1979, Serra et al., 1980) and for the evaluation of depositional environments of the sediments (Adams and Weaver, 1956).

Natural gamma ray spectral logging measurements were carried out by the Geological Survey of Canada (GSC) at the Highvale Mine in Alberta (Fig. 1-1) during the summer of 1988. The GSC Research and Development (R&D) logging system was used to acquire these data. Several holes in Pits 02 and 05 were logged. These holes intersected a sequence of mudstone, siltstone and sandstone, underlain by the mineable coal seams of the Ardley coal zone (Fig. 1-2). The strata are of Paleocene (lower Tertiary) age (Richardson et al., 1988).

Determinations of potassium, uranium and thorium from laboratory spectral gamma ray measurements were also carried out by the GSC on a number of drill core samples collected in 1988 from the Highvale Mine and the Big Valley area by the Alberta Research Council. The strata at Big Valley are slightly older than those at Highvale (Fig. 1-2), but are lithologically similar. These samples were analyzed for clay mineralogy and their dry density was measured. The laboratory spectral gamma ray measurements are more accurate than those acquired during borehole logging because of the large detectors and longer counting time used. The measurements were carried out on most of the samples with clay mineralogy analyses in order to determine a more accurate relationship between the type of clay minerals and the concentrations of K, U

and Th.

6.2 OBJECTIVE

The objective of this study was to evaluate the application of the spectral gamma ray logging technique in the coal and oil sands mining industries to characterize different lithologies and to determine clay mineralogy. This information is useful during mining operations to predict the geotechnical behaviour of the rock formations.

6.3 BACKGROUND INFORMATION ON NATURAL GAMMA RAY ACTIVITY

There are three common naturally occurring radioactive elements: potassium, uranium and thorium. The principal gamma ray emitter of potassium is the ^{40}K isotope. The relative abundance of this radioactive isotope to natural potassium is a constant and hence the gamma ray emissions from this isotope are used to determine potassium concentration in a given sample or formation. In crustal material, potassium is contained in the K-feldspar orthoclase, muscovite and biotite micas, and clay minerals such as illite.

There are three radioactive isotopes of uranium, ^{238}U, ^{235}U and ^{234}U, the most abundant being ^{238}U (99.3 %). Almost all the gamma rays in the uranium-238 decay series are produced by lead-214 and bismuth-214 which are decay products of radium-226. Lead-214 emits low energy gamma rays while bismuth-214 is a high energy gamma ray emitter. The determinations of uranium concentration are based on the count rates in an energy window positioned around the bismuth- 214 energy peak. There are potential problems of disequilibrium in the uranium decay series when determining the concentrations of the U. The time for the gamma ray activity of radium-226 and its decay products to reach equilibrium is primarily controlled by radon-222 gas with a half-life of 3.82 days. In most crustal materials radon-222 gas is in radioactive equilibrium and hence the gamma rays emitted by lead-214 and bismuth-214 are considered to be in equilibrium with the parent uranium-238. Since the relative proportion of bismuth-214 to total uranium is known, the gamma ray emissions from bismuth-214 are used to determine the equivalent uranium concentration in the material.

The principal gamma ray emitter in the thorium decay series is ^{208}Tl and disequilibrium in this decay series is rarely encountered in nature. Equivalent

concentrations of Th are derived from count rates in an energy window positioned around the ^{208}Tl energy peak. The following is a brief description of the GSC spectral gamma ray logging system and the laboratory gamma ray spectrometry system.

6.4 GSC SPECTRAL GAMMA RAY LOGGING SYSTEM.

Full gamma ray spectra are recorded in 256 channels covering an energy range from approximately 0.1 MeV to 3.0 MeV and gamma ray count rates in 10 preselected windows are accumulated and recorded during data acquisition. The four standard windows used in data analysis include the potassium window (1.36 - 1.56 MeV) positioned around the potassium-40 gamma ray peak at 1.46 MeV, the uranium window (1.61 - 2.30 MeV) positioned around the 1.76 MeV gamma ray emissions of bismuth-214 in the uranium decay series, and the thorium window (2.40 - 3.00 MeV) positioned around the 2.63 MeV gamma ray peak from thallium-208 in the thorium decay series. The fourth window, the total count window, covers a wide energy range from 0.4 to 3.00 MeV and is used to monitor the overall levels of radioactivity. The count rates in the potassium (K), uranium (U) and thorium (Th) windows are converted to percent K, equivalent U in ppm (eU ppm) and equivalent Th in ppm (eTh ppm).

A number of factors determine the logging speeds - size of detector and sample times during the acquisition of gamma ray data. Several sizes of scintillation detectors (sodium iodide and cesium iodide) are available for use in three probe sizes (32, 38 or 50 mm O.D.). Usually the largest detector compatible with the borehole diameter is used to give maximum sensitivity and logging is usually done at 3 m/minute. The large-diameter boreholes at Highvale Mine allowed us to log using the largest probe and detector at a rate of 3 m/minute. Data were accumulated every second, giving a sample every 5 cm. The detector used at Highvale was a 32 mm x 127 mm thallium-activated sodium iodide (NaI(Tl)) scintillation detector.

6.5 LABORATORY GAMMA RAY SPECTROMETRY SYSTEM

The GSC laboratory gamma ray spectrometry system utilizes two, 12.7 x 12.7 cm (5 x 5 inch) thallium-activated sodium iodide detectors (NaI(Tl)) mounted horizontally with their end faces approximately 3.5 cm apart. The detectors are shielded using a rectangular box constructed of 10.2 cm (4 inch) thick lead bricks. Sample cans are rolled automatically into the lead box, between the two detectors using a chute and trap door arrangement. The data recording system and multichannel analyzer is based on a NOVA minicomputer as described by Bristow (1979). This system is similar to the GSC

R&D borehole spectral gamma ray logging system. Data are recorded in 256 channels covering an energy range from 0 to 3.0 MeV. Energy windows positioned around the peak energies of ^{40}K, ^{214}Bi and ^{208}Tl are used for determining gamma ray equivalents of the concentrations of potassium, uranium and thorium. The window settings are similar to those used in the borehole logging system.

The samples were crushed to a fine powder and put into cans of known volume and weight. The weights ranged from 250 to 260 g. The density of the samples were determined and used to correct the data for variations in sample densities (Grasty et al., 1982). The counting time for each sample was 20 minutes in order to obtain good counting statistics, and the spectra were then analyzed to determine the concentrations of the radioelements potassium, uranium and thorium.

Fig. 6-1 shows laboratory gamma ray spectra from some of the samples collected within five different lithologies. Several 20- minute spectra are stacked for each of the five different lithologies. These stacked spectra are offset for clarity. The potassium (^{40}K), uranium (^{214}Bi) and thorium (^{208}Tl) energy peaks are indicated. It should be noted that, even without spectral analysis of the data, the typical mudstone, siltstone and sandstone show prominent, high amplitude potassium peaks indicating that the main contribution of radioactivity within these samples is ^{40}K. There is very little indication of uranium and thorium in these spectra. The spectra from the bentonites and the bentonitic mudstone above coal seam number 1 indicate that all the three radioactive elements are contributing to the overall radioactivity from the samples. The thorium and uranium peaks can be clearly identified.

6.6 CALIBRATION OF THE GAMMA RAY SPECTROMETRY SYSTEMS

The laboratory spectral gamma ray acquisition system is calibrated using reference standards of potassium, uranium and thorium and the borehole logging system is calibrated in model boreholes with known concentrations of K, U and Th. The calibration constants include stripping ratios and window sensitivities. The stripping ratios are those constants used to adjust the count rates in each of the three windows so that the contribution of the gamma rays in each of these windows originate solely from the respective elements (potassium, uranium and thorium). The stripped count rates in the three energy windows are then converted to concentrations of K, U and Th by multiplying with the sensitivities. The sensitivities are usually expressed as counts per second per % K for the potassium window; as counts per second per ppm U for the uranium window; and as counts per second per ppm Th for the thorium window. The

concentrations are stated in % K, eU in ppm, eTh in ppm. Equivalent ('e') is used to emphasize that the method is indirect (i.e., based on measurement of ^{214}Bi and ^{208}Tl) and radioactive equilibrium is assumed.

6.7 DISCUSSION OF FIELD RESULTS

Several holes were logged with the GSC R&D spectral gamma ray logging system. The following is a discussion of the results from two of the holes logged. All the observations from these holes are typical and apply to the spectral data from the other holes.

6.7.1 Gamma Ray Spectral Logs

Fig. 6-2 shows the total count, K, eU, and eTh spectral logs acquired in hole HV427. All the lithologies can be identified from these logs; for example bentonite, sandstone, siltstone and coal. It is interesting to note the relative contribution of the different radioelements to overall radioactivity. The bentonite layer around 30 m and the bentonitic mudstone layers between most of the coal seams exhibit high thorium content and low potassium content. The uranium distribution is quite variable along this hole. There is, however, a slight increase in uranium associated with an increase in thorium. This correlation was confirmed in the analysis of the laboratory samples from both the Highvale Mine and Big Valley, and is presented in Sec. 6.7.3. The low potassium within bentonite and bentonitic layers is a result of the type of clay minerals present. Bentonites are dominantly montmorillonite and these clays are devoid of potassium. The close resemblance of the eTh log to the total-count gamma ray log suggests that Th is the major contributor to the overall observed radioactivity. Another interesting observation is that the radioactivity of the layer between coal seams 2 and 3 is mostly derived from potassium, in contrast to the other in-seam layers, where the radioactivity is due mainly to increases in thorium and uranium. This characteristic layer is observed in all the holes logged at the Highvale Mine, and may, therefore be used as a marker horizon in this stratigraphic sequence.

6.7.2 Frequency Distributions

Fig. 6-3 to 6-14 are histogram plots of % K, eU in ppm and eTh in ppm based on the logs for three lithologies: siltstone, mudstone and bentonite, plus all lithologies combined. The identification of lithologies was based on the geologic log descriptions provided by TransAlta Utilities. The spectral gamma ray log data were acquired in holes HV414 and HV427 at the Highvale Mine. On these distributions, the scale on the right represents

the count or frequency in each bar. The scale on the left represents the proportion of cases falling in each bar divided by the standard deviation. Standardization of the data in this fashion makes it easier to compare histograms based on different scales. The histograms were produced on the SYSTAT/SYGRAPH statistical package. The data on the simple statistics from these distributions are summarized in Table 6-1.

Table 6-1 Simple statistics on the distribution of % K, eU in ppm and eTh in ppm in three different lithological units encountered in holes HV414 and HV427, Highvale Mine.

				%K				
Litho	N	MIN	MAX	Range	Mean	Median	STD	CV
Mdst	193	-0.019	3.334	3.353	2.028	2.449	0.984	0.485
Sltst	145	1.000	3.106	2.106	1.965	2.006	0.392	0.200
Bent.	65	0.076	1.512	1.436	0.753	0.731	0.280	0.372
ALL	403	-0.019	3.334	3.530	1.800	1.800	0.861	0.479

				eU ppm				
Litho	N	MIN	MAX	Range	Mean	Median	STD	CV
Mdst	193	-2.459	8.113	10.572	2.881	2.742	2.263	0.786
Sltst	145	-2.057	5.333	7.390	1.904	1.885	1.689	0.887
Bent.	65	1.494	9.002	7.504	4.620	4.422	1.716	0.371
ALL	403	-2.453	9.002	11.461	2.810	2.695	2.183	0.777

				eTh ppm				
Litho	N	MIN	MAX	Range	Mean	Median	STD	CV
Mdst	193	2.623	19.599	16.976	8.771	8.624	2.762	0.315
Sltst	145	3.902	14.973	11.071	7.440	7.453	2.134	0.287
Bent.	65	8.019	22.141	14.122	15.072	15.335	3.715	0.247
ALL	403	2.623	22.141	19.518	9.518	8.438	3.774	0.405

Mdst	-	mudstone
Sltst	-	siltstone
Bent	-	bentonite
Litho	-	lithology
STD	-	standard deviation
CV	-	coefficient of variation

The distribution of potassium is unimodal within the siltstones and the bentonites, with siltstones having a higher mean value (1.96 %) than the bentonites (0.73 %). The

distribution of potassium within mudstones is bimodal. This may be explained by the fact that some of the mudstones are bentonitic, although this was not always recognized when the drill core was examined and described. The bentonitic mudstones are located in the low % K end of the distribution. The mudstones without bentonite have higher % K. The mean value of potassium is 2.03 %. The histogram for the data from all the lithologies shows quite a spread in % K indicating the variability of potassium concentrations due to changes in lithology.

The distribution of eU is fairly broad within all the three different lithologies (Fig. 6-7 to 6-10) indicating the variability and the inherent mobility of this element within these units. The mean values, however, show some distinction; higher values occur in bentonites, and lower values in mudstones and siltstones. Again the mudstones show a broader range of values of eU due to lithological misclassification; some of the mudstones are in fact bentonitic.

The thorium distribution for siltstone, mudstone and bentonite (Fig. 6-11 to 6-14) have mean values of 7.44, 8.77 and 15.07 eTh ppm, respectively. Thorium is mainly concentrated within bentonite. The higher levels of equivalent thorium in the mudstone compared to siltstone is again attributed to the presence of bentonite in some of these mudstones.

Fig. 6-15 shows a bar graph of the total % clay content in each sample and the distribution of the clay minerals for each sample. This figure indicates that montmorillonite is the dominant clay mineral in the clay size fractions of sandstones, siltstones and mudstones. Fig. 6-16 shows a stacked bar graph of the amount of K, U, and Th in each sample from Highvale and Big Valley. The thorium content is relatively high in all the samples compared to uranium and potassium (note that the units of K are in %, eU and eTh are in ppm). The highest values occur in the mudstones and bentonites. One of the siltstone samples has extremely high contents of thorium and uranium. The high thorium-uranium concentration points to a high percentage of bentonite.

6.7.3 Cross Correlations

Most of the correlation studies were done on the data obtained from the samples. These data include clay mineralogy analyses (% clay, % montmorillonite, % illite, % kaolinite, % chlorite) and spectral gamma ray data (K, U, Th, and U/K, Th/U, Th/K and (U+Th)/K ratios). Thirty five samples were analyzed; 28 from Highvale and 7 samples from Big Valley. The spectral gamma ray data are presented in Table 6-2.

Table 6-2 Laboratory gamma ray spectrometry data from samples collected at Highvale Mine and Big Valley.

SAMPLE Number	K %	U ppm	Th ppm	U/K 10^{-4}	Th/U 10^{-4}	Th/K
HV-02-428	1.23	2.17	5.45	1.764	2.512	4.431
HV-04-428	1.50	1.41	4.10	0.947	2.887	2.733
HV-05-428	0.41	5.22	16.02	12.732	3.069	39.073
HV-07-428	0.40	3.95	21.71	9.875	5.496	54.275
HV-09-424	1.43	3.36	9.52	2.350	2.833	6.657
HV-11-424	1.27	1.77	4.94	1.394	2.791	3.890
HV-13-424	2.04	2.28	5.89	1.118	2.583	2.887
HV-15-427	0.46	4.52	21.37	9.826	4.728	46.456
HV-17-424	1.53	2.73	5.84	1.784	2.139	3.817
HV-19-427	0.70	10.26	28.60	14.657	2.788	40.857
HV-21-429	0.72	8.54	29.81	11.861	3.491	41.403
HV-24-412	1.54	2.63	7.83	1.708	2.977	5.084
HV-26-412	0.40	4.08	8.12	10.200	1.990	20.300
HV-28-412	0.50	11.94	49.37	23.880	4.135	98.740
HV-30-414	2.36	3.70	11.06	1.568	2.989	4.686
HV-34-414	0.28	6.95	22.27	24.821	3.204	79.536
HV-32-414	0.28	5.25	44.37	18.750	8.451	158.464
HV-36-414	0.28	8.64	55.64	30.857	6.440	198.714
JP8804-429	0.77	7.56	25.88	9.818	3.423	33.610
JP8806-429	1.42	5.56	13.21	3.915	2.376	9.303
JP8808-429	2.02	3.27	10.21	1.618	3.122	5.054
JP8809-429	1.56	1.37	4.58	0.878	3.343	2.936
JP8810-429	1.76	3.82	9.96	2.170	2.607	5.659
JP8811-429	1.37	4.04	10.12	2.949	2.505	7.387
JP8812-429	1.55	2.45	8.51	1.581	3.473	5.490
JP8813-427	1.27	3.98	7.53	3.134	1.892	5.929
JP8814-427	2.09	3.27	9.04	1.565	2.764	4.325
JP8815-427	2.85	2.50	11.68	0.877	4.672	4.098
BV-03	2.34	1.89	9.24	0.808	4.889	3.949
BV-11	0.68	3.87	13.09	5.691	3.382	19.250
BV-12	1.64	1.92	7.16	1.171	3.729	4.366
BV-13	1.99	3.25	8.62	1.633	2.652	4.332
BV-15	1.84	2.50	7.20	1.359	2.880	3.913
BV-17	0.83	4.92	15.91	5.928	3.233	19.169
BV-18	1.22	2.92	10.79	2.281	3.695	8.437

Fig. 6-17 shows the total-count gamma ray data obtained from BPB logs, crossplotted against the clay mineralogy data. There seems to be no relationship between the

gamma ray and the different types of clay minerals. There may be some problems in the location of the samples relative to the log data. Another explanation may be that the relative contribution of the three radioelements to the total observed radioactivity in these samples is variable. Fig. 6-18 shows crossplots of Th, U and K versus total count gamma ray. It is evident from these data that thorium and uranium are the main contributing radioelements to the overall observed radioactivity. There appears to be a negative relationship between potassium and gamma ray activity suggesting an antipathetic relationship between potassium and the other two radioelements.

Crossplots of montmorillonite versus Th, U and K, and the ratios Th/K and (U+Th)/K are presented in Fig. 6-19. Thorium, uranium and the ratios Th/K and (U+Th)/K are positively correlated with montmorillonite whereas K is negatively correlated. The correlation coefficients are much higher for the ratios than for the radioelements. The ratios Th/K and (U+Th)/K are therefore better indicators of % montmorillonite.

Fig. 6-20 shows crossplots of % illite versus Th, U, K and kaolinite plus chlorite. A crossplot of kaolinite plus chlorite versus K is also presented in this figure. There is a fairly good positive correlation between % K and the clay minerals kaolinite and chlorite even though these minerals do not contain potassium in their chemical structure. This apparent correlation is due to illite (a potassium clay mineral) associated with these two clay minerals (Fig. 6-21). Illite is poorly correlated with either U or Th but shows a reasonably good correlation with % K.

The correlation coefficients determined using the Pearson Product-Moment Correlation method for pairs of a number of variables are summarized in Table 6-3. The correlation between gamma ray and percent clay is poor, suggesting that the total-count gamma ray log may not be a useful log for determining the clay content or shaliness of the formations in this area. A good positive correlation, however, exists between % clay and montmorillonite whereas % clay and the clay minerals illite, kaolinite and chlorite are poorly correlated. This indicates that montmorillonite is the dominant clay mineral. It is interesting to note that montmorillonite is negatively correlated with % K. This is not surprising since montmorillonite is not a potassium clay mineral $((Ca,Na)(Al,Mg,Fe)[(Si,Al)O]\ (OH).nH_2O)$. Uranium and thorium, however, seem to be associated with montmorillonite. Although these two radioelements are usually associated with heavy accessory minerals such as zircon, sphene, monazite, allanite and apatite (Adams and Weaver, 1958, Serra, et al., 1980), none of those minerals were present in these samples. This suggests that uranium and thorium are adsorbed within the structure of the montmorillonite clay mineral. This mode of occurrence has been discussed in literature (Adams and Weaver, 1958;

Table 6-3. Pearson product-moment Correlation

	%Clay	%Mont	%Ill.	%Kaol	%Chlo	Gamma	K	U	Th	U/K	Th/U	Th/K	(U+Th)/K
%Clay	1.000												
%Mont	0.842	1.000											
%Ill.	0.068	-0.464	1.000										
%Kaol	-0.027	-0.494	0.774	1.000									
%Chlo	-0.096	-0.483	0.748	0.415	1.000								
Gamma	0.199	-0.000	0.338	0.454	-0.011	1.000							
K	-0.489	-0.707	0.536	0.316	0.680	-0.508	1.000						
U	0.393	0.391	-0.101	0.111	-0.315	0.901	-0.586	1.000					
Th	0.529	0.328	0.219	0.455	-0.181	0.951	-0.604	0.911	1.000				
U/K	0.558	0.525	-0.091	0.185	-0.429	0.878	-0.797	0.871	0.903	1.000			
Th/U	0.323	-0.211	0.752	0.667	0.446	0.137	0.061	-0.160	0.234	0.087	1.000		
Th/K	0.589	0.495	0.007	0.298	-0.390	0.830	-0.790	0.735	0.885	0.945	0.327	1.000	
(U+Th)/K	0.584	0.504	-0.015	0.273	-0.400	0.848	-0.799	0.771	0.897	0.966	0.278	0.997	1.000

Serra et al., 1980). Because of the antipathetic relationship between thorium and potassium, the ratios Th/K and (U+Th)/K, tend to improve the correlation with montmorillonite. These ratios may be used to identify relative proportions of montmorillonite to the total percent clay within a given sample.

6.7.4 Ternary Plots

The crossplots presented in the above section show the relationship between two parameters. To present three parameter relationships in two dimensions, ternary or triangular plots are generated. The laboratory spectral data and the borehole spectral logs; K, U, and Th are presented as ternary diagrams in the following figures. The borehole data were obtained in holes HV414 and HV427 for the three different lithologies (siltstone, mudstone and bentonite). These ternary diagrams were generated with the following coordinate transformations (Doveton, 1986).

$$X = \frac{P_2 - P_1}{SQRT(2)} \qquad Y = \frac{2 \times P_3 - P_1 - P_2}{SQRT(6)}$$

where P_1, P_2, P_3 are the values of the three parameters (K, U and Th, respectively) and X, Y are the transformed two-dimensional coordinates.

In following figures, each of the three data sets (K, U, Th) were normalized by their respective means before the coordinate transformation was undertaken. Fig. 6-21 and 6-22 are K-U-Th ternary plots for the siltstones and bentonites, respectively. The siltstones cluster in the region with greater than 50 percent of potassium and the bentonites cluster mainly within the high thorium region. Fig. 6-23 shows a ternary plot of the spectral data from the siltstones and bentonites. There is a very clear distinction between the two clusters of the two data sets. This distinction makes it easy to identify bentonites and siltstones. The ternary plot for mudstones is shown in Fig. 6-24. The mudstones seem to form two clusters, one within the siltstone region and the other in the bentonite region. The mudstone within the bentonite region are actually bentonitic. The ternary diagram in Fig. 6-25 shows the logging data from all three lithologies. There are two clusters; one along the thorium-uranium plane which constitutes the bentonite cluster and the other in the potassium region which is the siltstone-mudstone cluster. The siltstones and mudstones cannot be clearly distinguished from each other because the relative proportions of the radioactive elements are fairly similar. In general, most of the mudstones have a higher potassium content than the average siltstone.

Fig. 6-26 shows the K-U-Th ternary diagram for laboratory gamma ray spectral data derived from sandstone, siltstone, mudstone and bentonite samples. Again two distinct clusters are observed; the "bentonite" cluster along the thorium-uranium side of the triangle, and the other high % K, low thorium and uranium cluster. This distribution is identical to that observed in the borehole logging spectral gamma ray data. Mudstones and siltstones in the "bentonite" cluster actually contain an appreciable amount of bentonite. A closer examination of the core log and sample lithology description indicate that these samples were taken from the carbonaceous, bentonitic mudstone layer above coal seam number 1 and the carbonaceous, coaly and bentonitic mudstone layer between coal seams 3 and 4.

6.8 CONCLUSIONS

The bentonites at the Highvale Mine and Big Valley are believed to have been formed from volcanic ash deposits. The original compositions of the western Alberta bentonites ranged from dacites to rhyolite (Lerbekmo, 1968) and montmorillonite is a major clay mineral of these bentonites. The chemistry of these benonites is very distinctive: the thorium content is extremely high, greater than 20 ppm (laboratory sample data); uranium is quite low, from 4 to 12 ppm; and the potassium content is far lower compared to all other lithologies, even sandstones. It is the high thorium content that causes the high gamma ray activity that bentonites exhibit in this area. Montmorillonite is a major clay mineral of bentonites and of the good correlation between montmorillonite and thorium, the spectral logs provide the best indication of bentonite.

Spectral gamma ray logs show good promise for identifying the bentonites and bentonitic mudstones that can create problems during open-pit mining operations. During this study spectral gamma data proved capable of distinguishing between bentonitic and nonbentonitic mudstones, a difference that was not apparent from any of the other types of geophysical logs or, in many cases, from visual examination of the drill core. The stability of pit walls is dependent on the shear strengths and on the compressibility of the underlying strata, parameters that are highly dependent on the mineral constituents of the rocks, especially the amount and type of clay minerals present. Proper classification and identification of the problematic minerals through spectral gamma ray logging may identify areas that require more detailed attention as the mining advances.

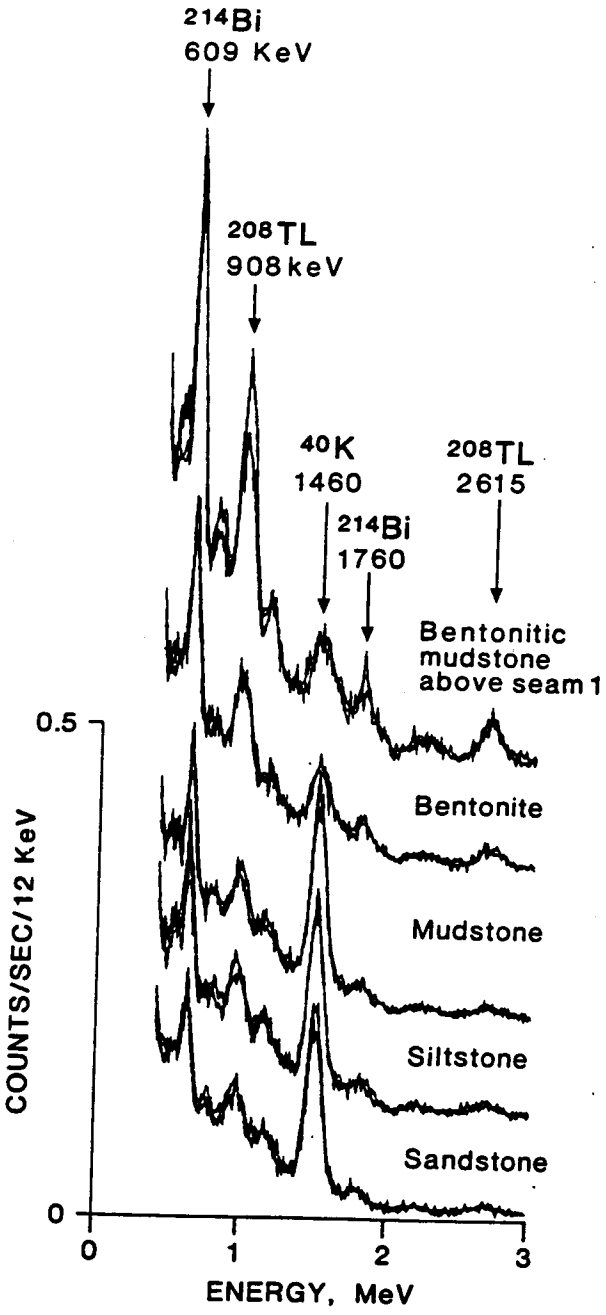

Figure 6-1. Laboratory gamma ray spectra from sandstone, siltstone, mudstone and bentonite samples showing the ^{40}K, ^{214}Bi and ^{208}Tl peaks. 20 - minute spectra from 3 to 4 samples are stacked for each of the five lithologies. The spectra are offset for clarity.

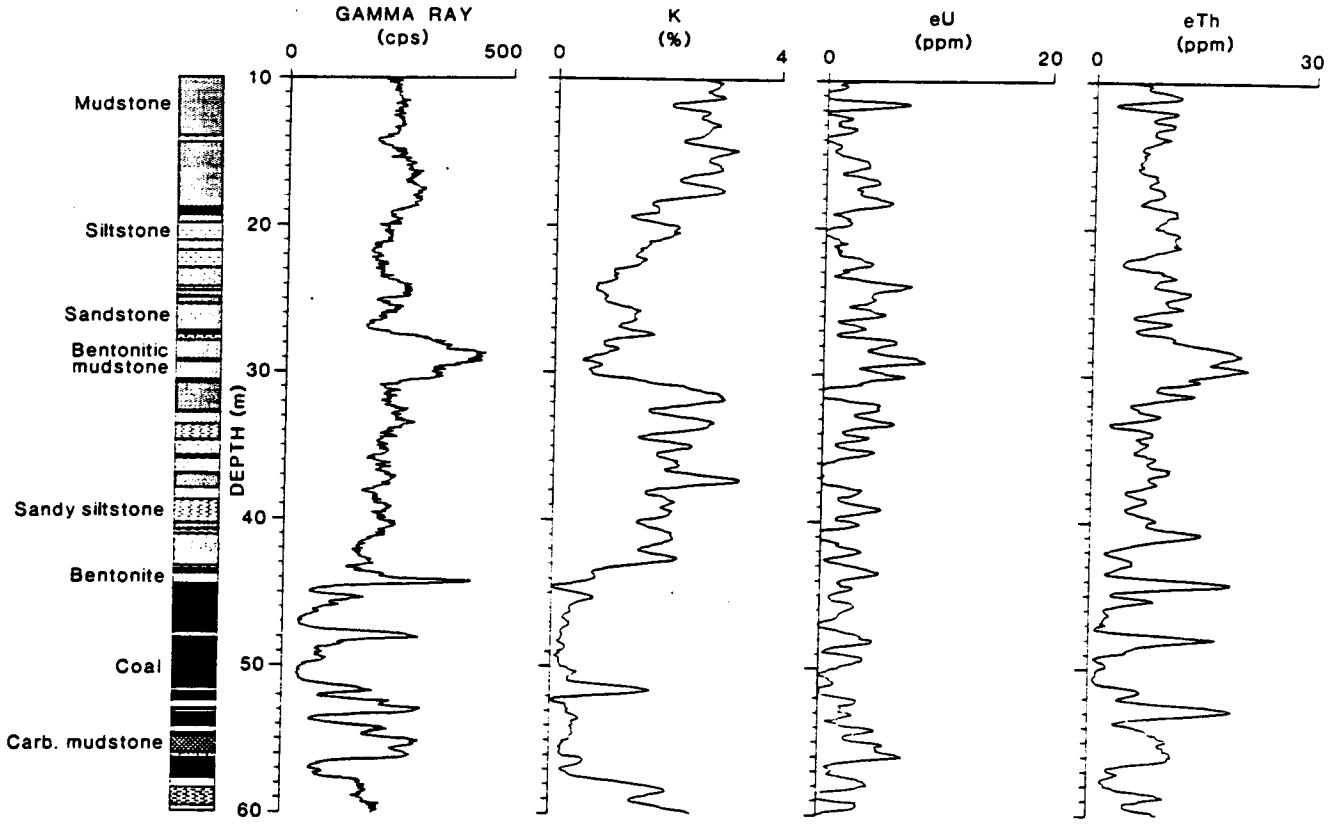

Figure 6-2. Gamma ray spectral logs; total count, K, eU and eTh, from GSC logging of hole HV427 at the Highvale Mine. Note extremely high thorium associated with marked depletion of K within bentonites or bentonitic mudstones.

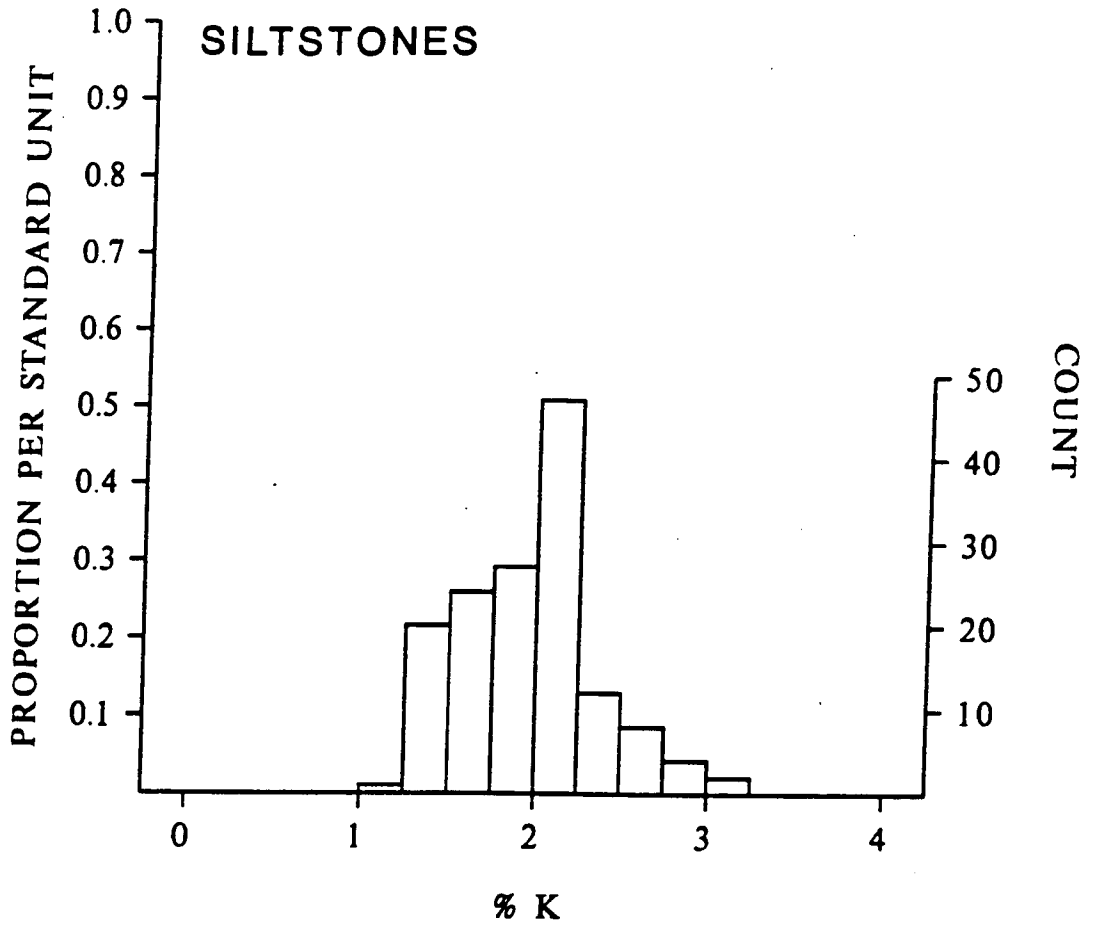

Figure 6-3. Histogram of % K from GSC borehole logging data in siltstones at Highvale. The scale on the left represents the count or frequency in each bar and the scale on the left represents the proportion of samples falling in each bar divided by the standard deviation.

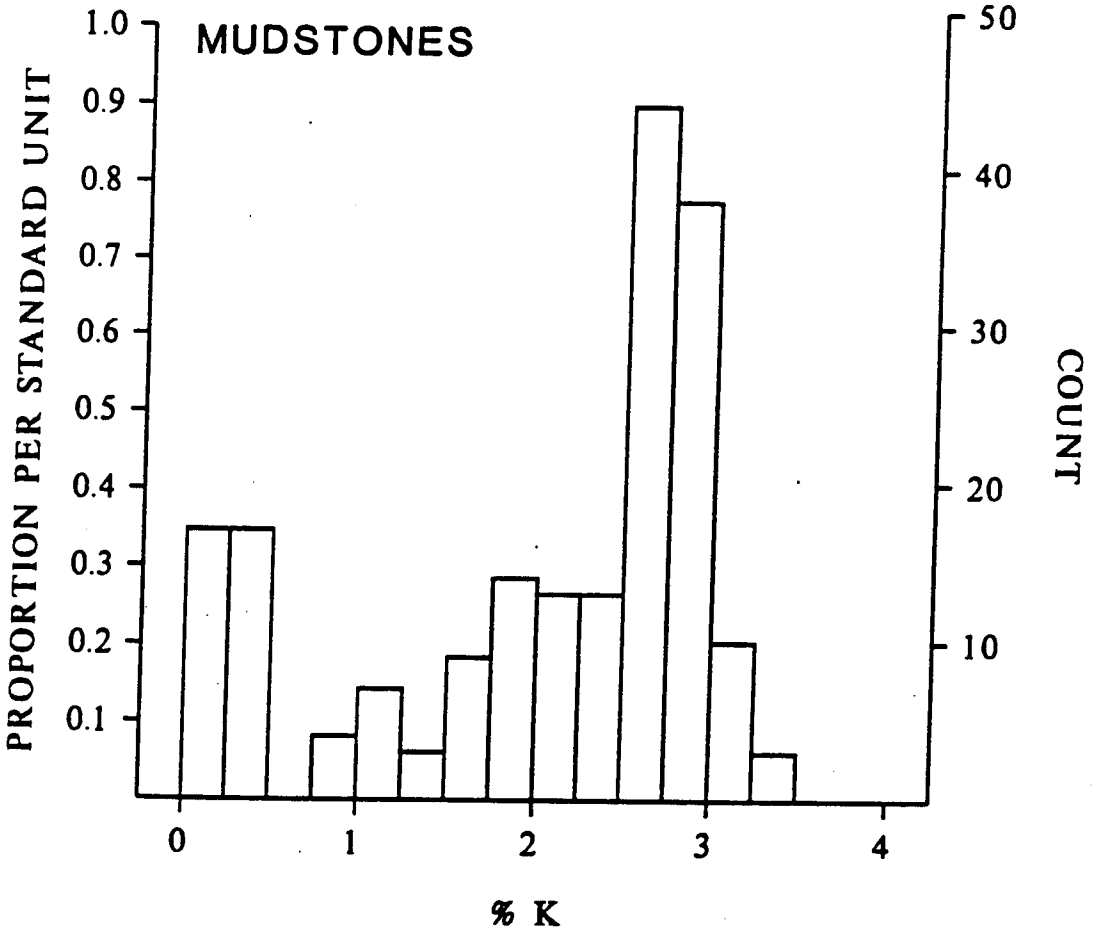

Figure 6-4. Histogram of % K from GSC borehole logging data in mudstones at Highvale.

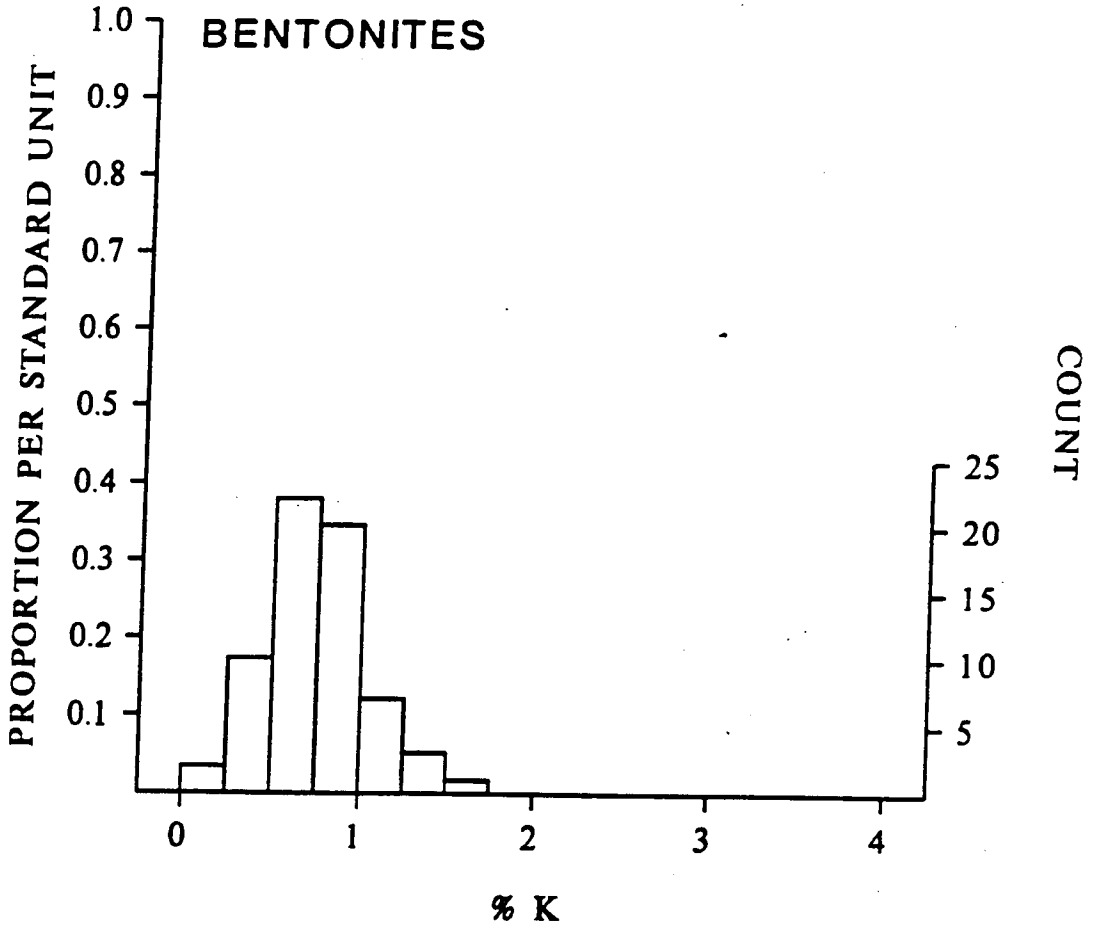

Figure 6-5. Histogram of % K from GSC borehole logging data in bentonites at Highvale.

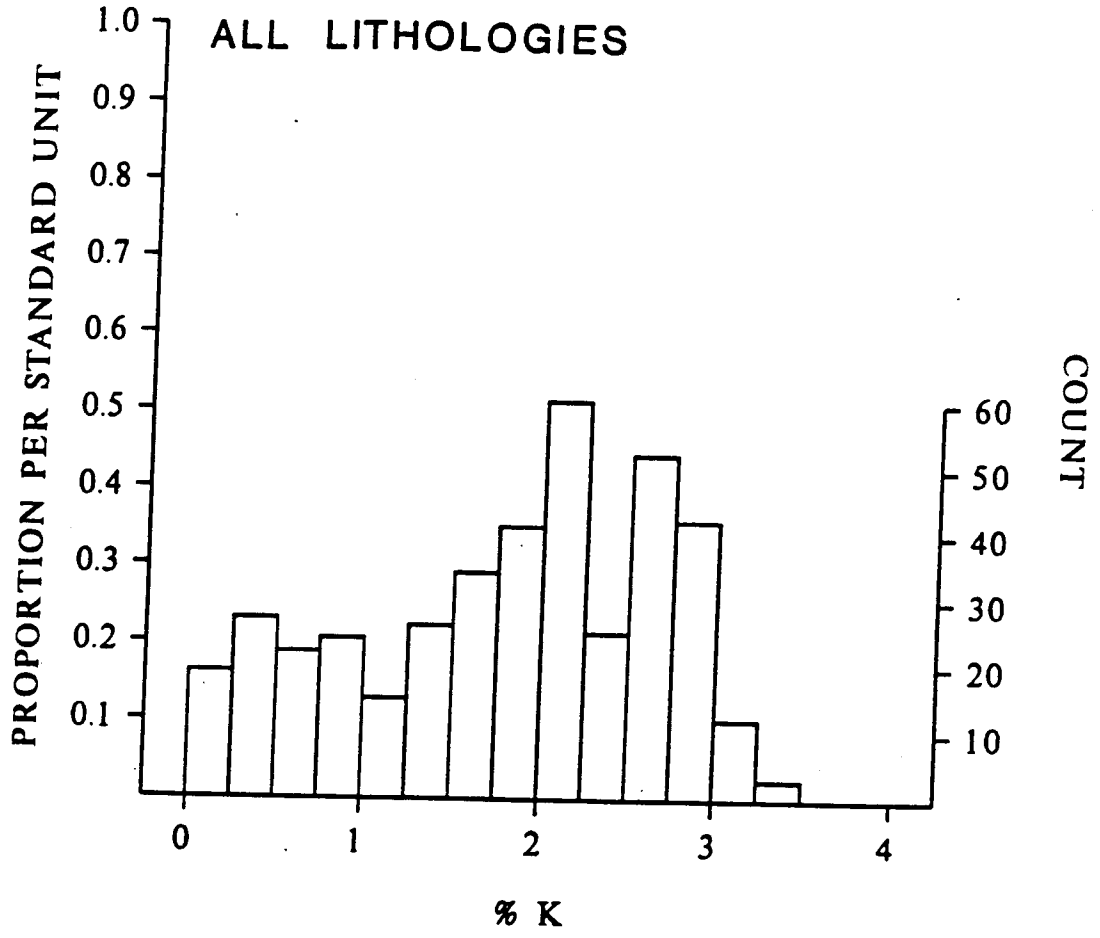

Figure 6-6. Histogram of % K from GSC borehole logging data in the three lithologies at Highvale; siltstones, mudstones and bentonites.

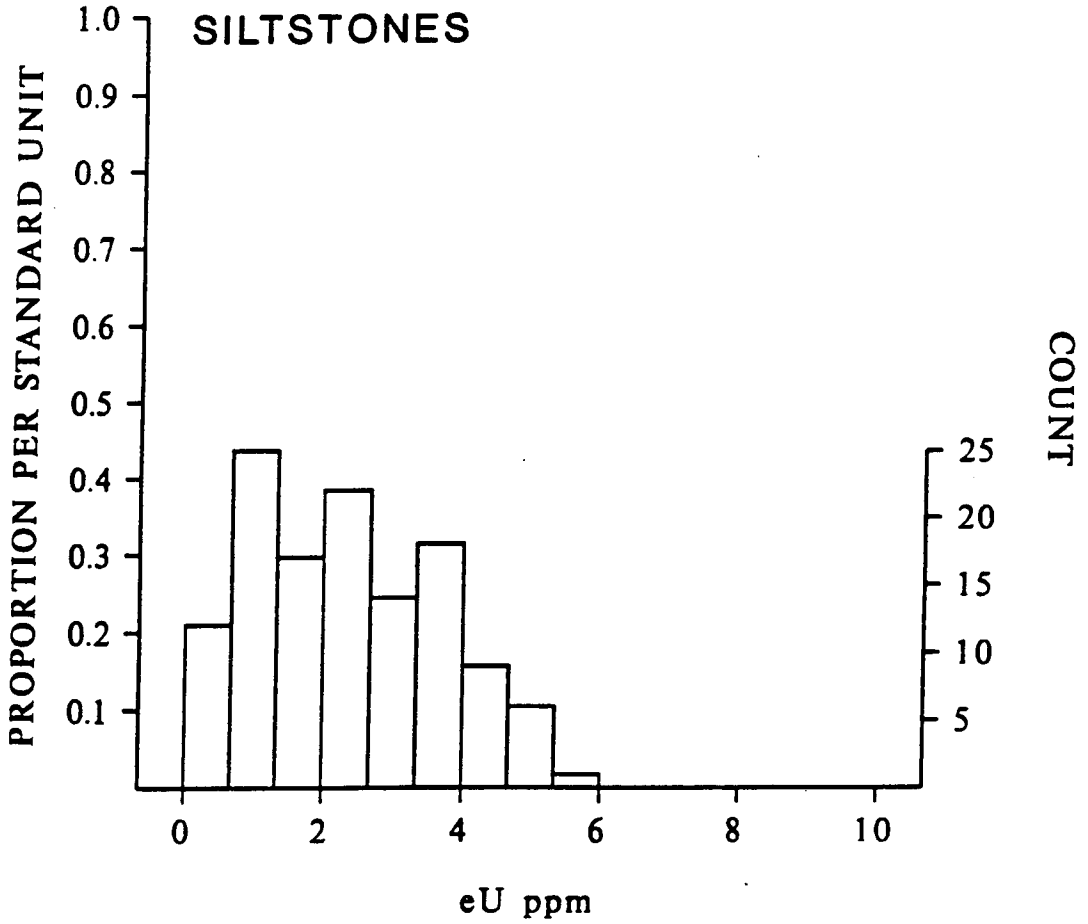

Figure 6-7. Histogram of eU in ppm from GSC borehole logging data in siltstones at Highvale.

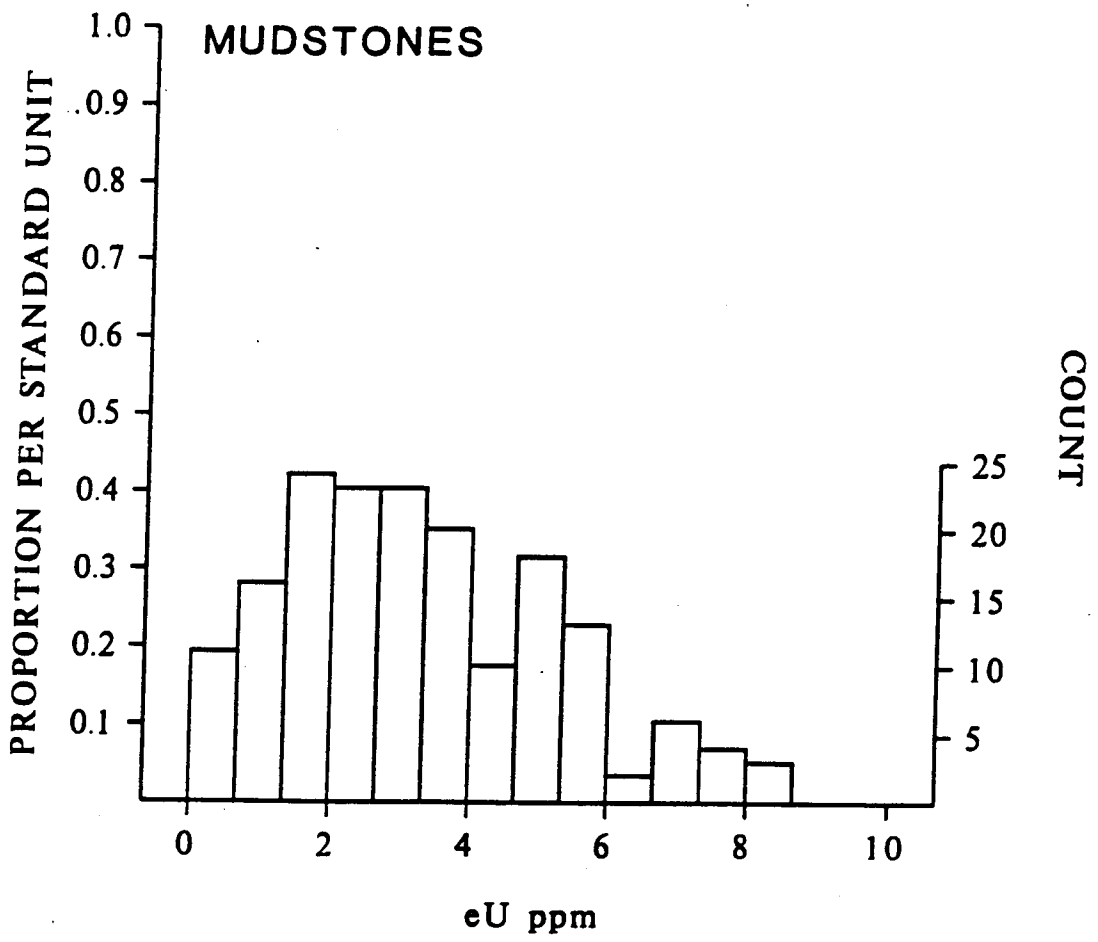

Figure 6-8. Histogram of eU in ppm GSC from borehole logging data in mudstones at Highvale.

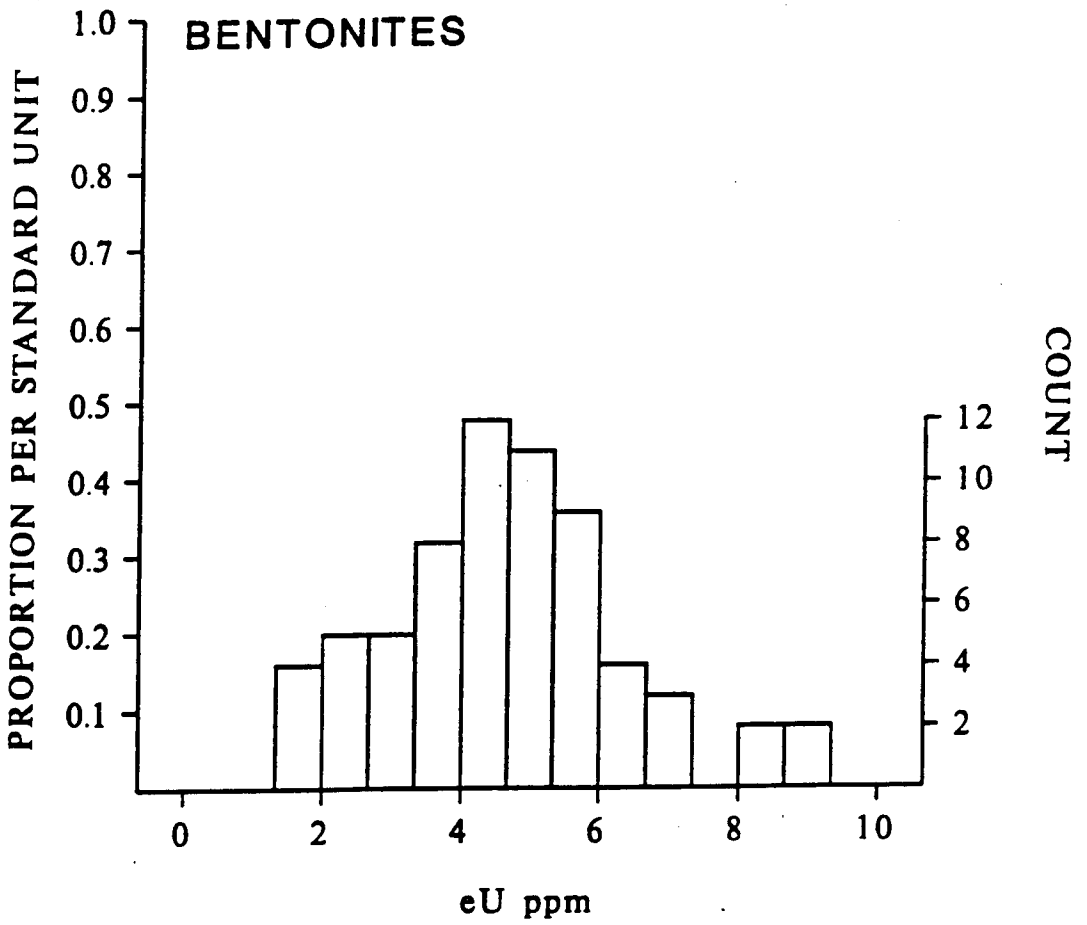

Figure 6-9. Histogram of eU in ppm from GSC borehole logging data in bentonites at Highvale.

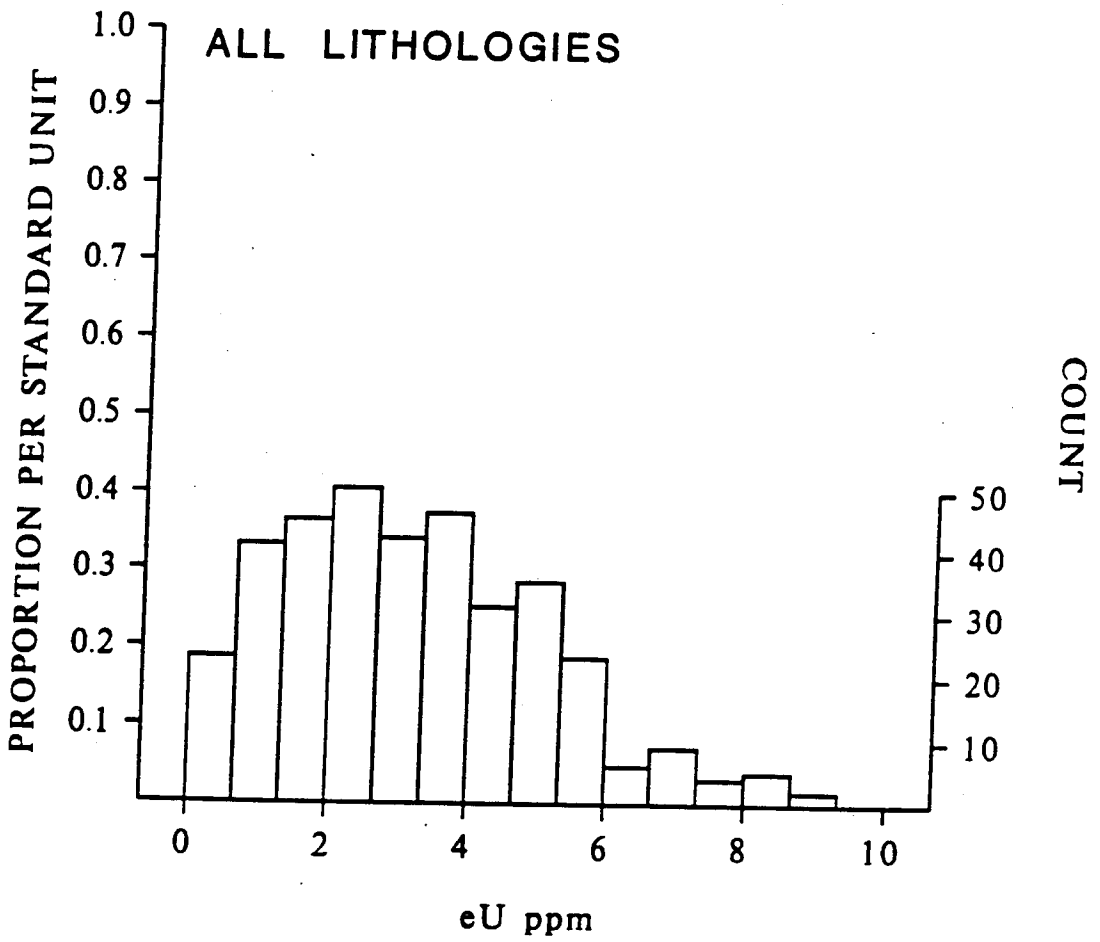

Figure 6-10. Histogram of eU from GSC borehole logging data in the three lithologies at Highvale; siltstones, mudstones and bentonites.

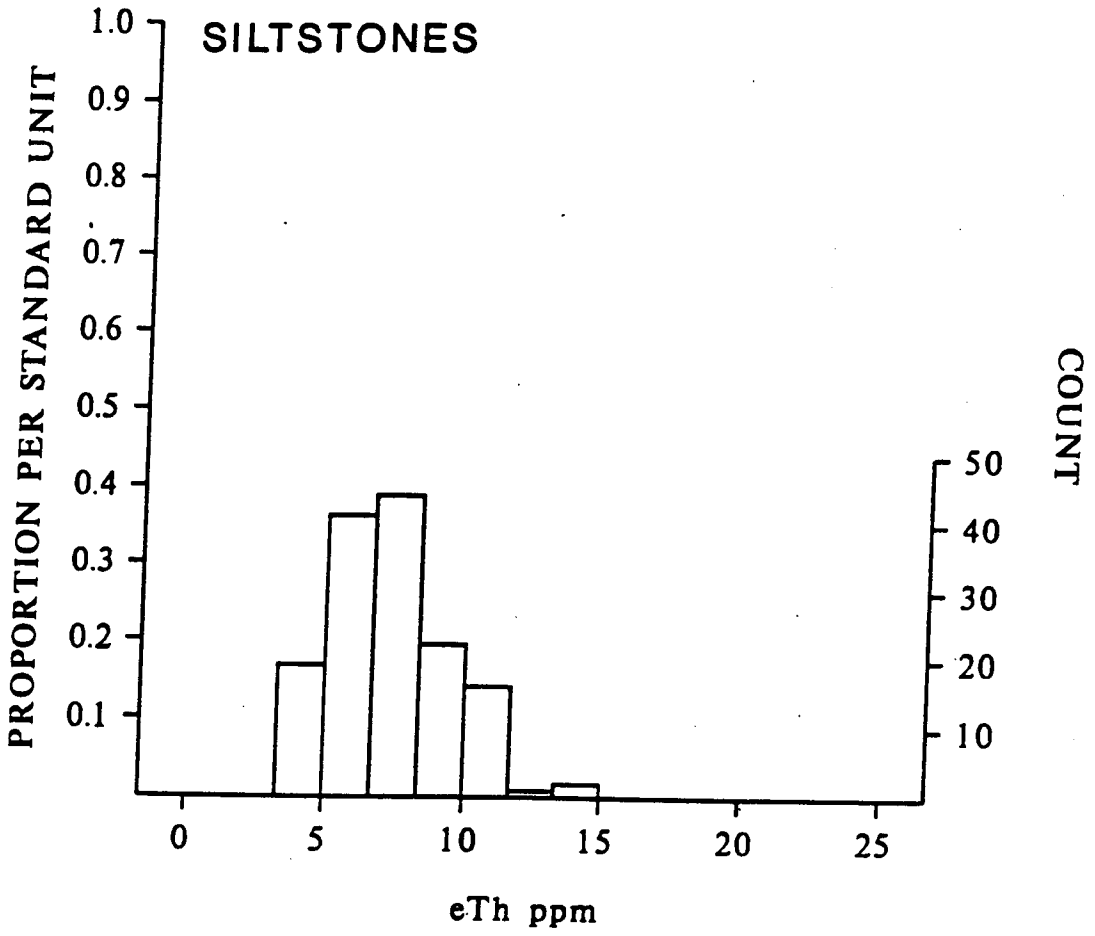

Figure 6-11. Histogram of eTh in ppm from GSC borehole logging data in siltstones at Highvale.

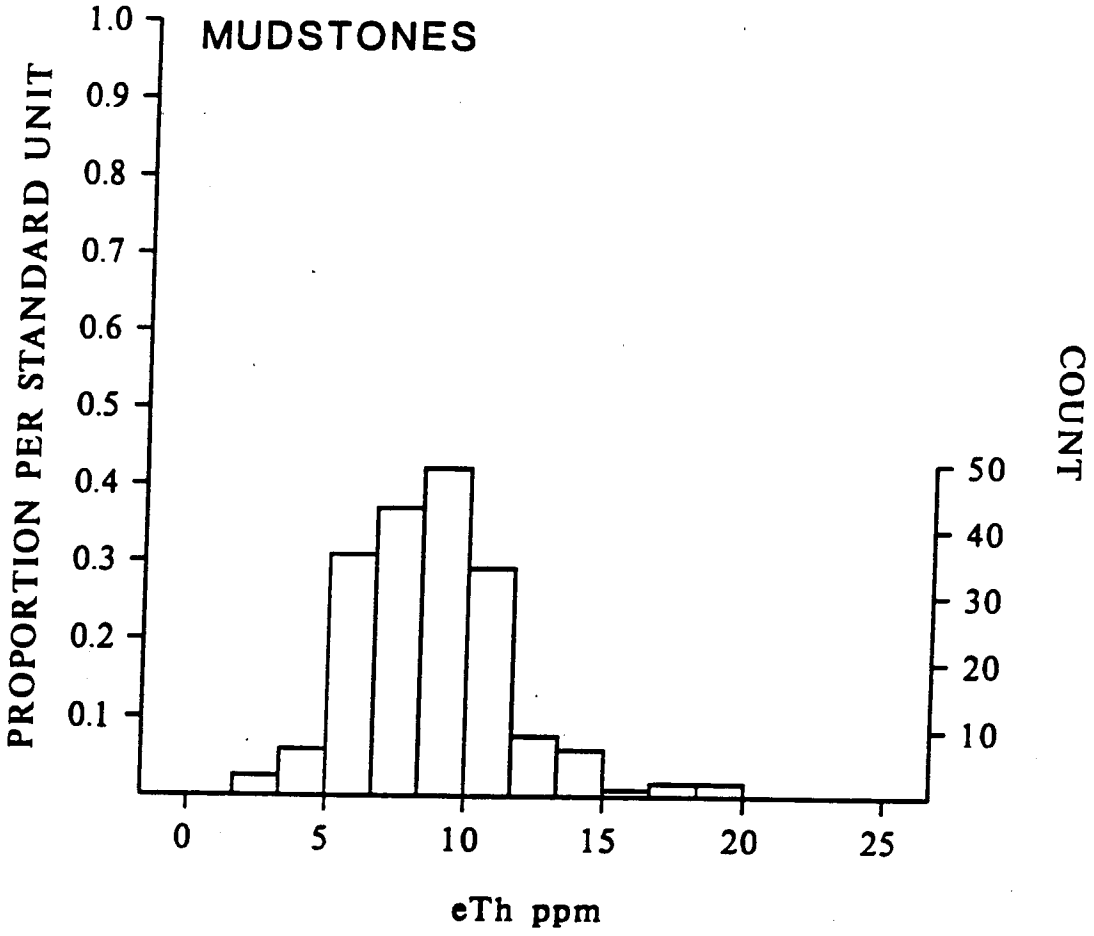

Figure 6-12. Histogram of eTh in ppm from GSC borehole logging data in mudstones at Highvale.

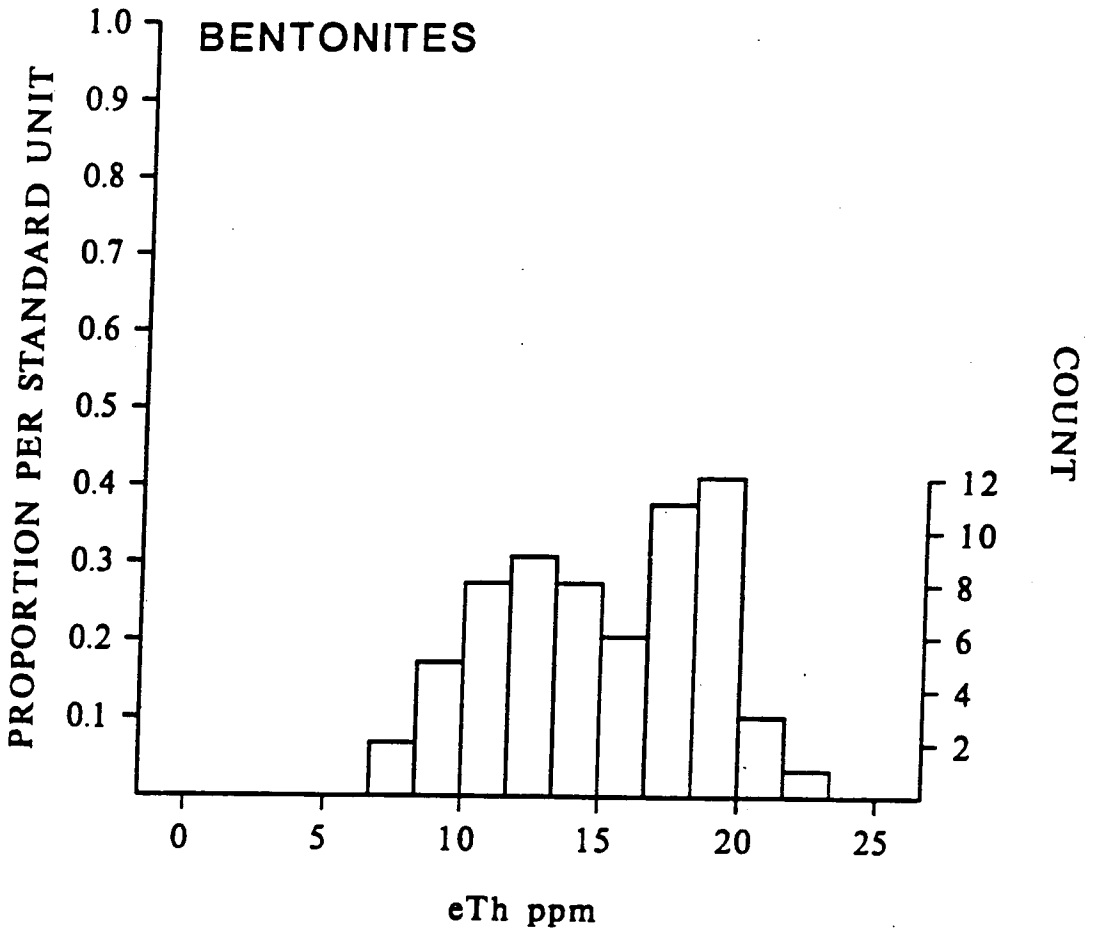

Figure 6-13. Histogram of eTh in ppm from GSC borehole logging data in bentonites at Highvale.

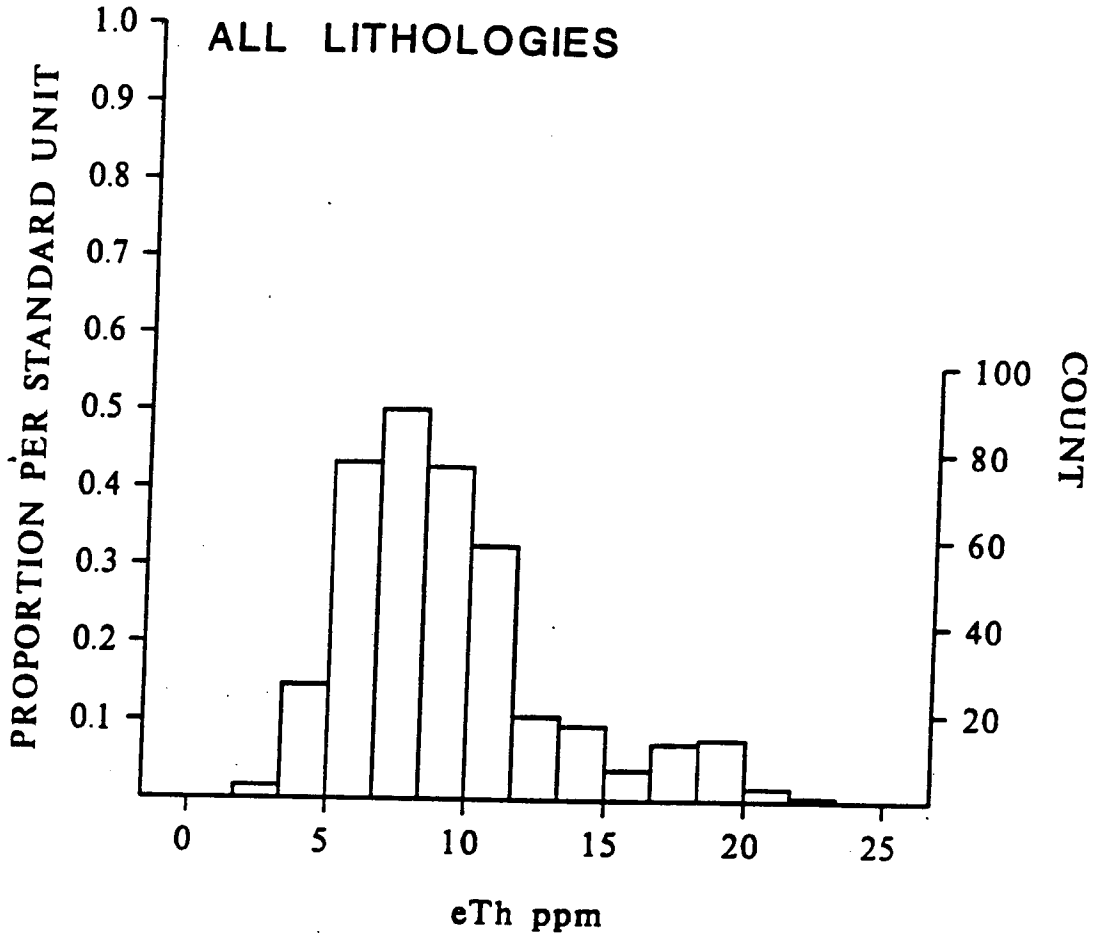

Figure 6-14. Histogram of eTh from GSC borehole logging data in the three lithologies at Highvale; siltstones, mudstones and bentonites.

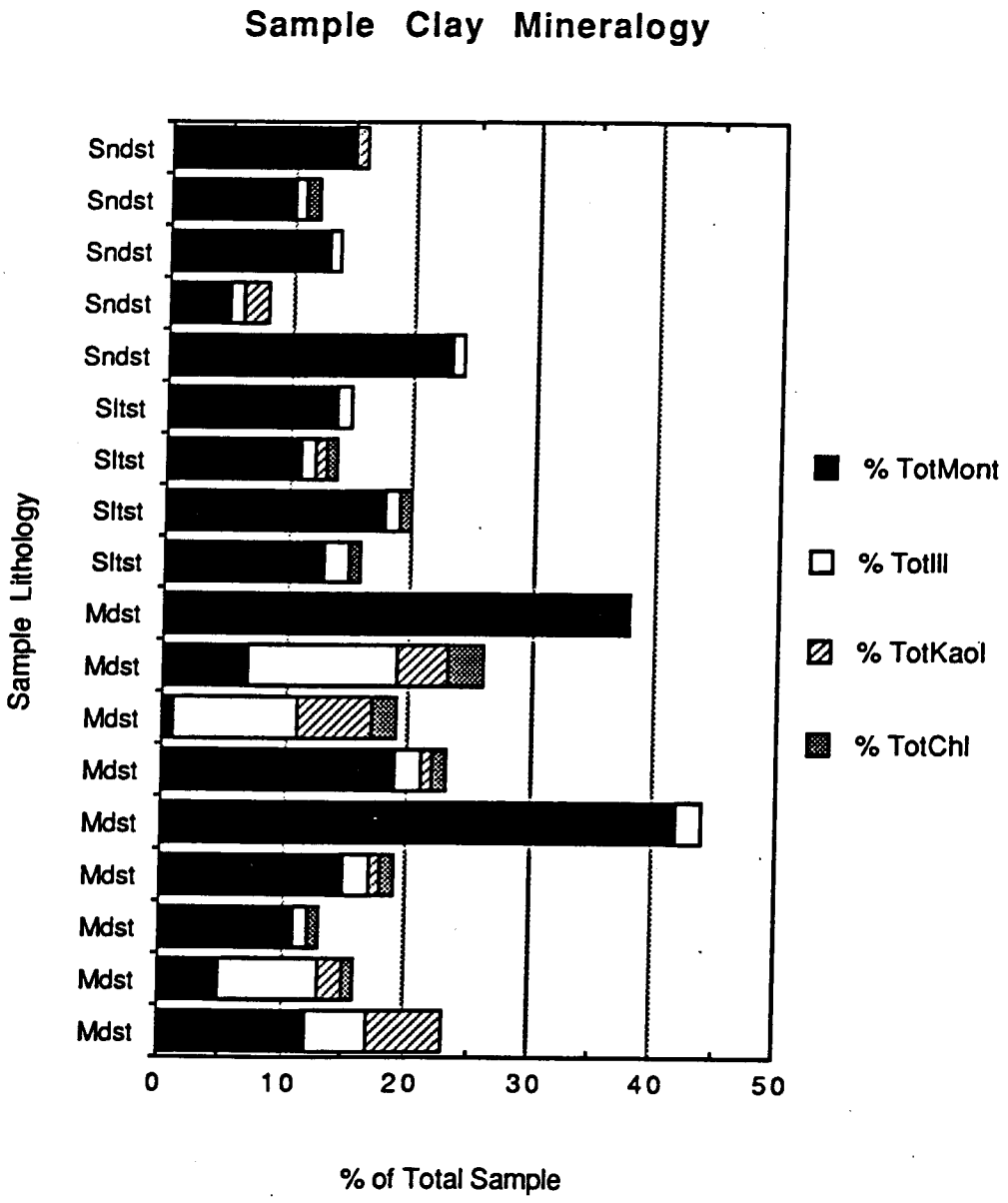

Figure 6-15. Stacked bar graph of total % clay minerals in each sample, determined by X-ray diffraction analysis; samples from Highvale and Big Valley.

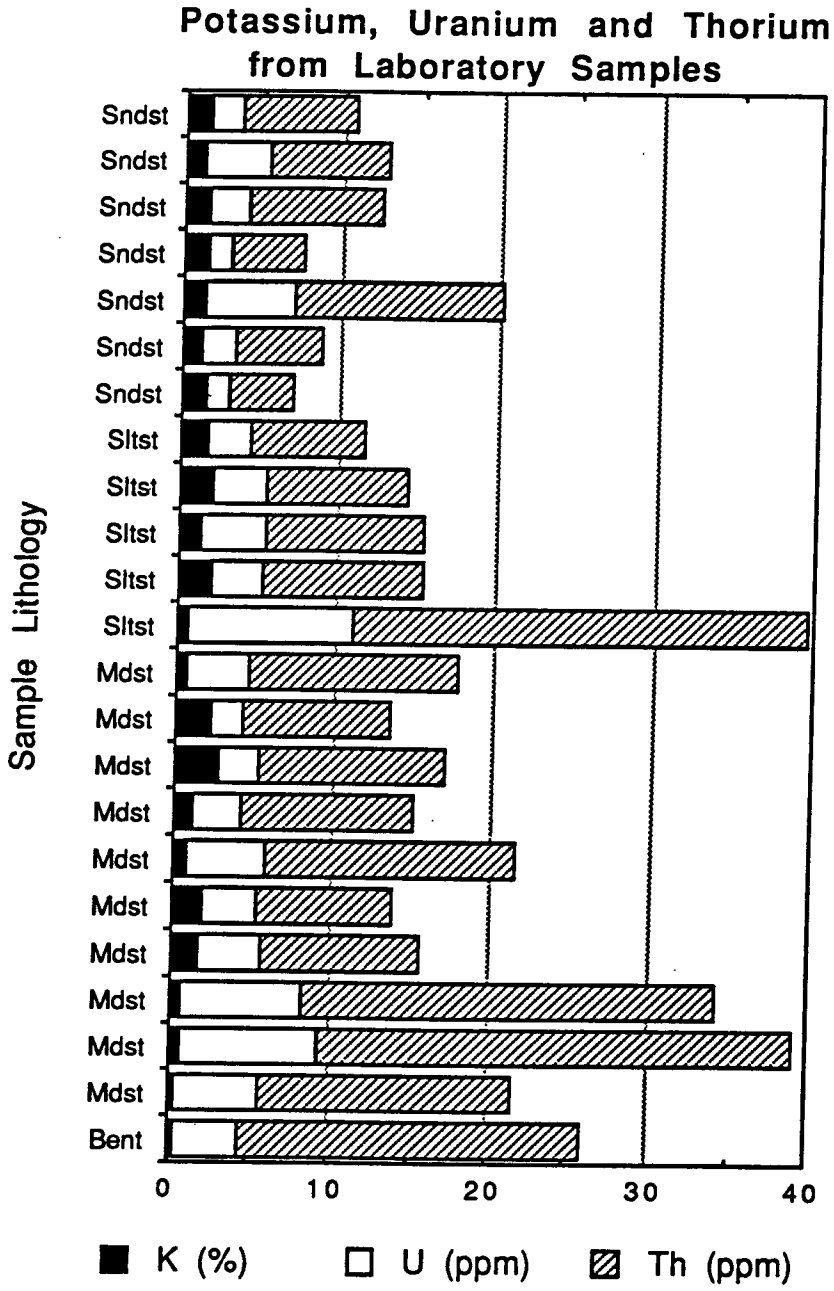

Figure 6-16. Stacked bar graph of % K, eU in ppm, and eTh in ppm from laboratory spectral data; samples from Highvale and Big Valley.

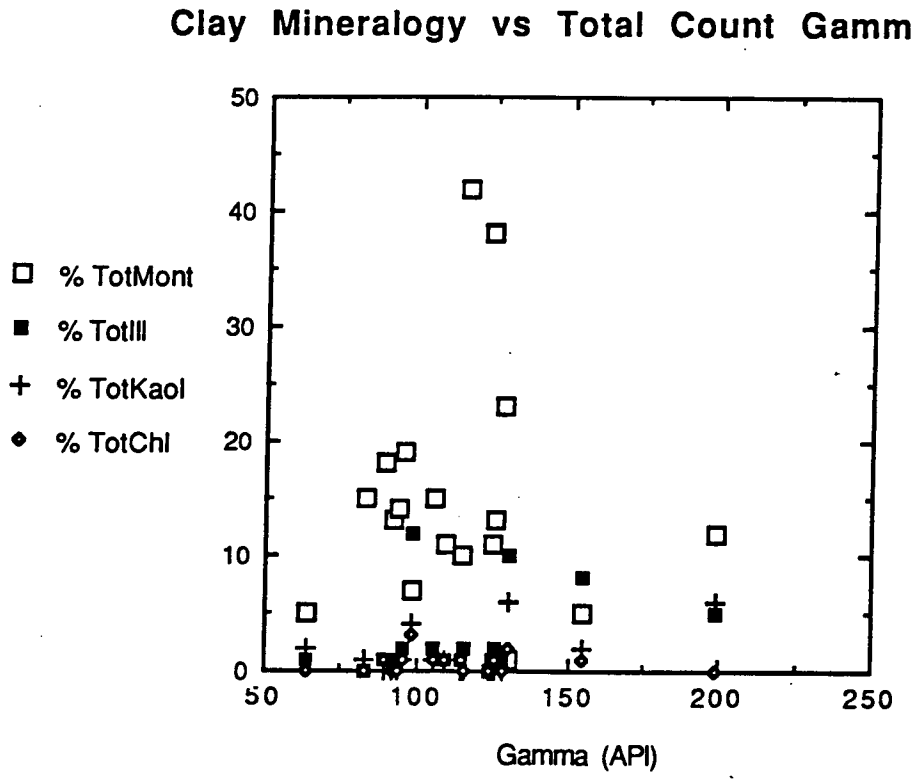

Figure 6-17. Crossplot of total-count gamma ray (API) versus clay mineralogy in each sample; samples from Big Valley and Highvale.

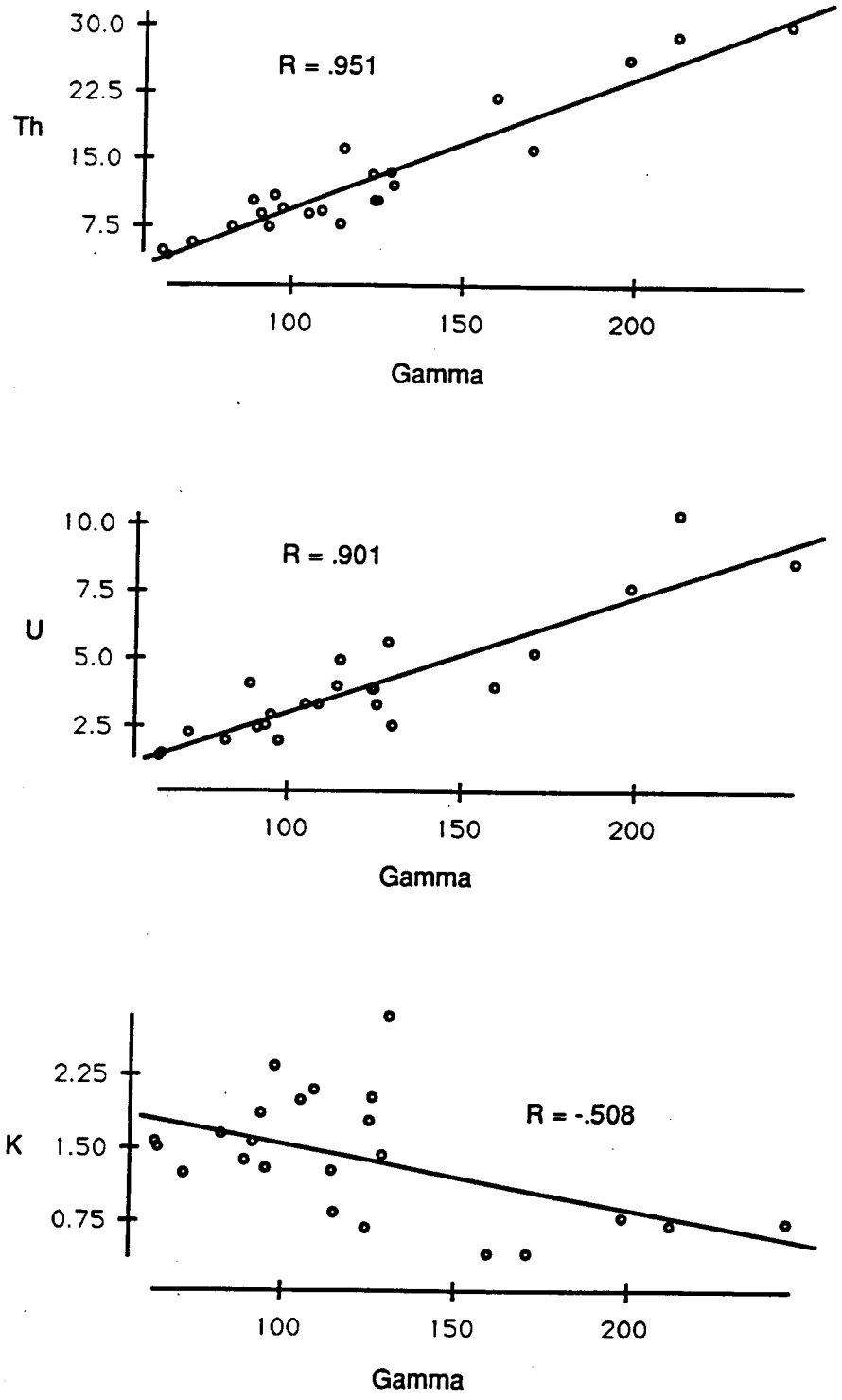

Figure 6-18. Crossplots of eTh, eU and % K from samples versus total-count gamma ray log (API); Highvale and Big Valley data.

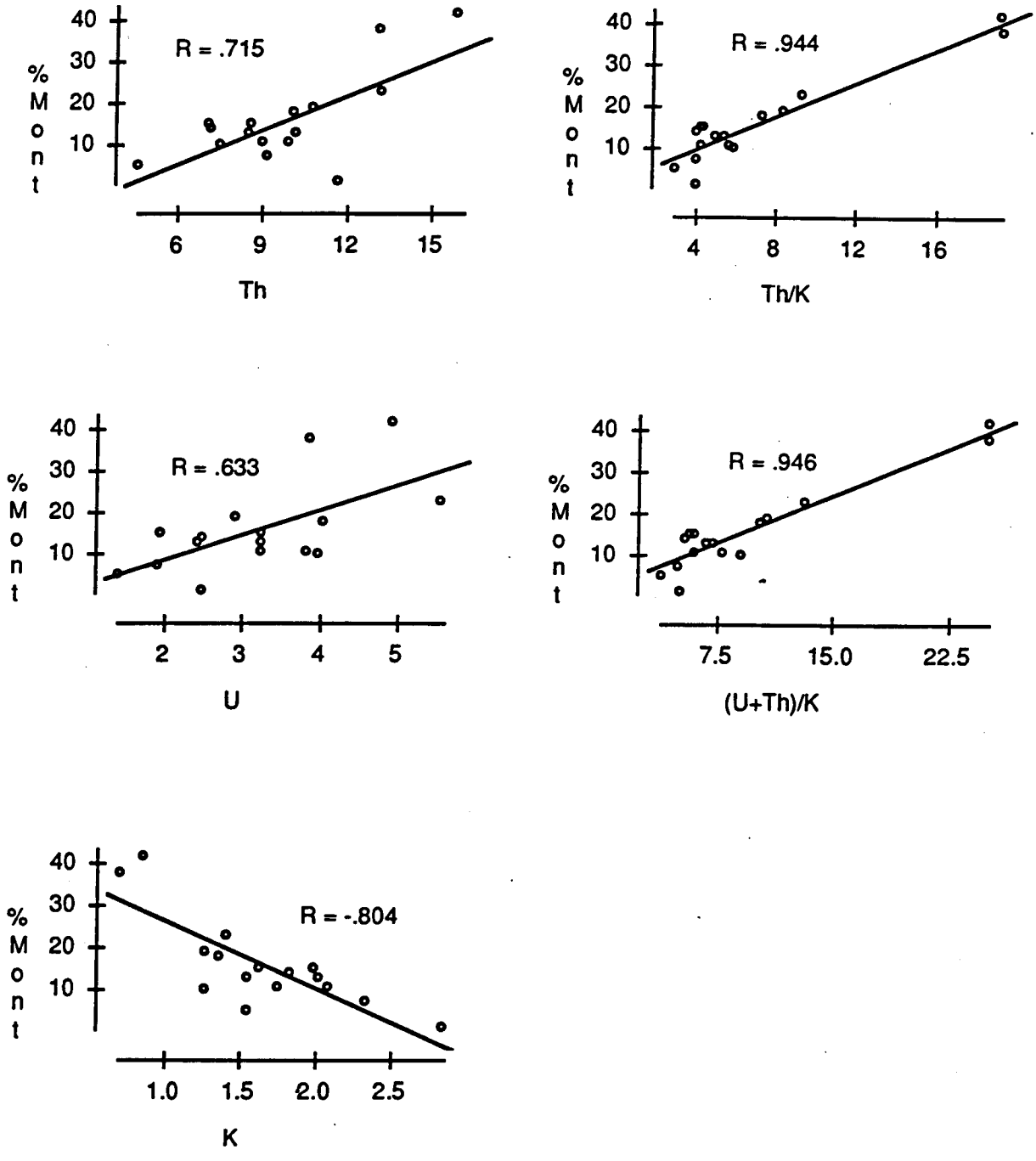

Figure 6-19. Crossplots of montmorillonite versus eTh, eU, % K, and the ratios Th/K adn (U+Th)/K, from Highvale and Big Valley sample data.

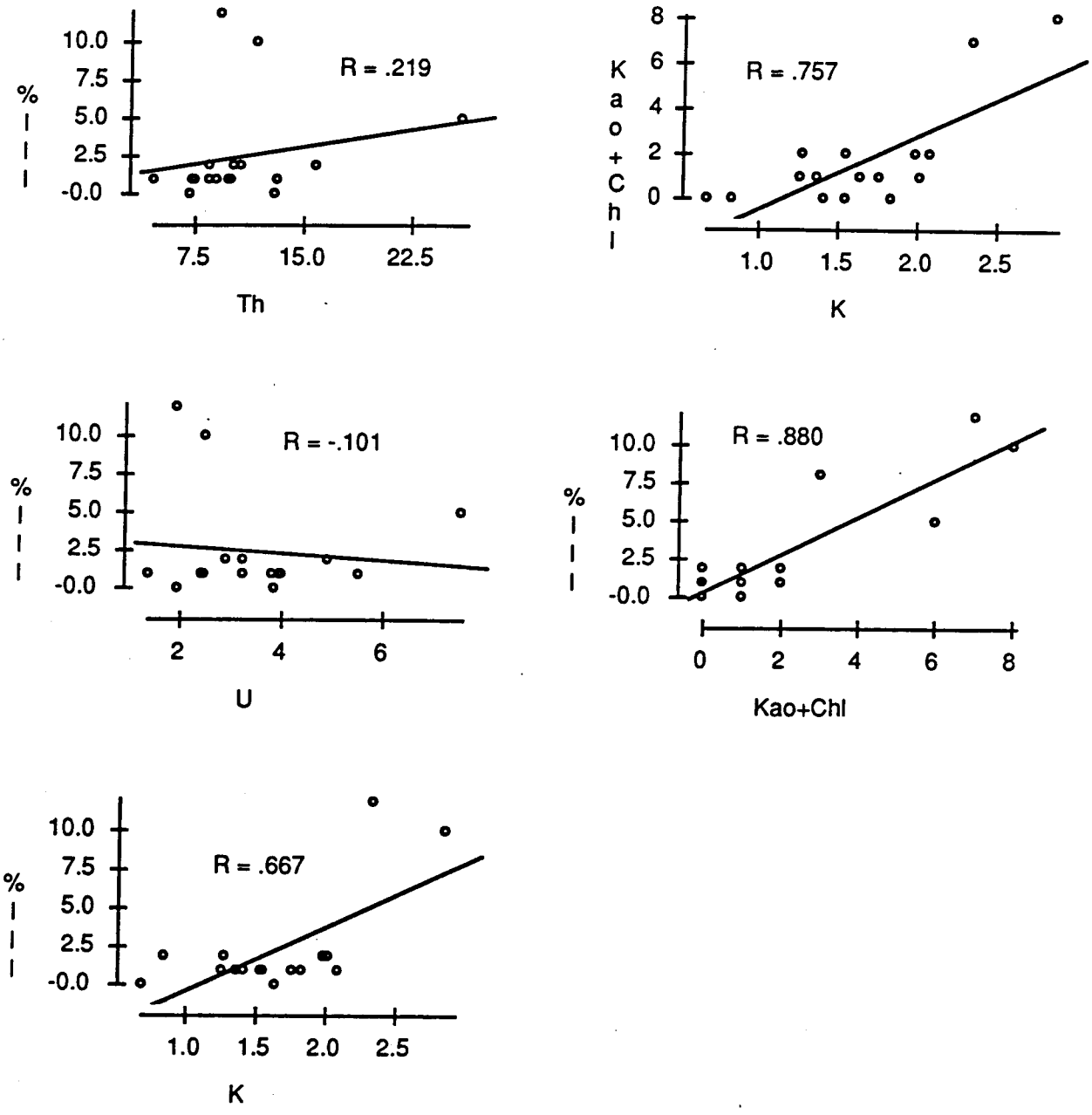

Figure 6-20. Crossplots of % illite versus eTh, eU, % K, and kaolinite plus chlorite; and a crossplot of kaolinite plus chlorite versus K. Data from Highvale and Big Valley samples.

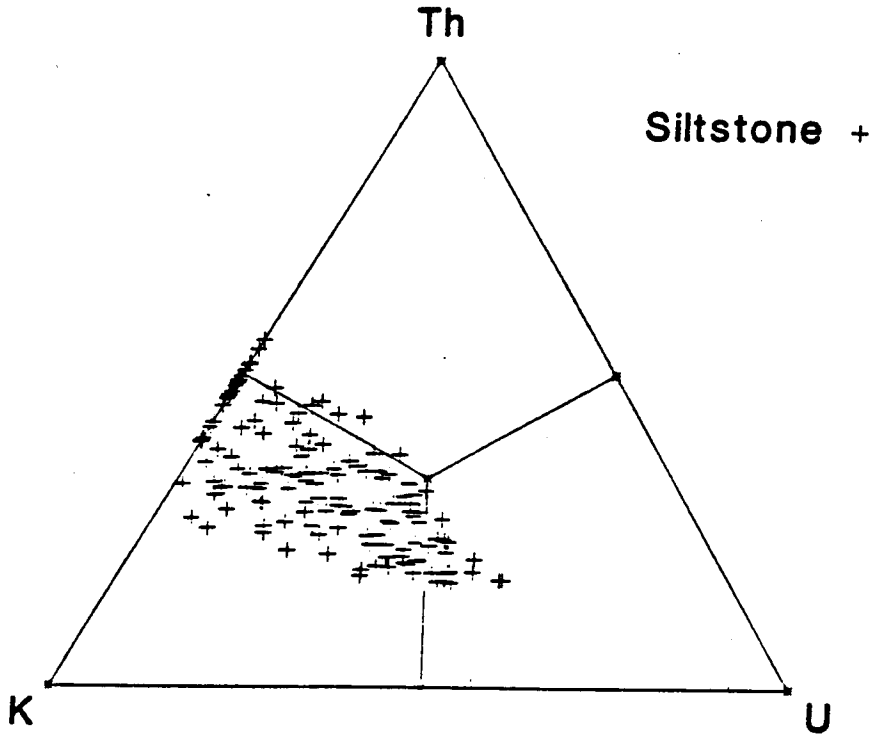

Figure 6-21. K-U-Th ternary plot of the GSC borehole logging spectral gamma data from the siltstones in holes HV414 and HV427.

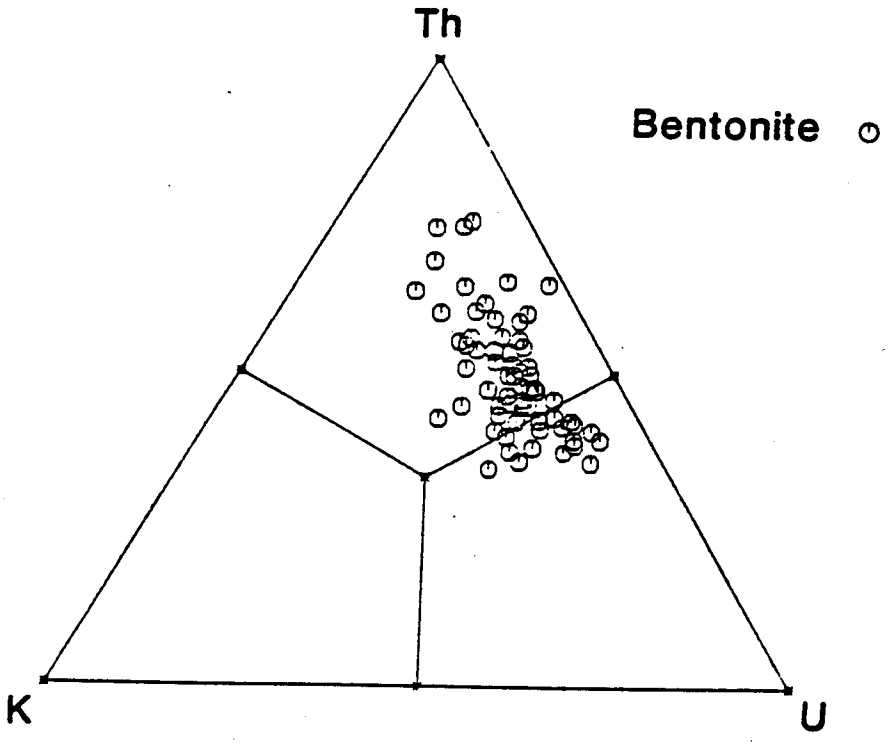

Figure 6-22. K-U-Th ternary plot of the GSC borehole logging spectral gamma data from the bentonites in holes HV414 and HV427.

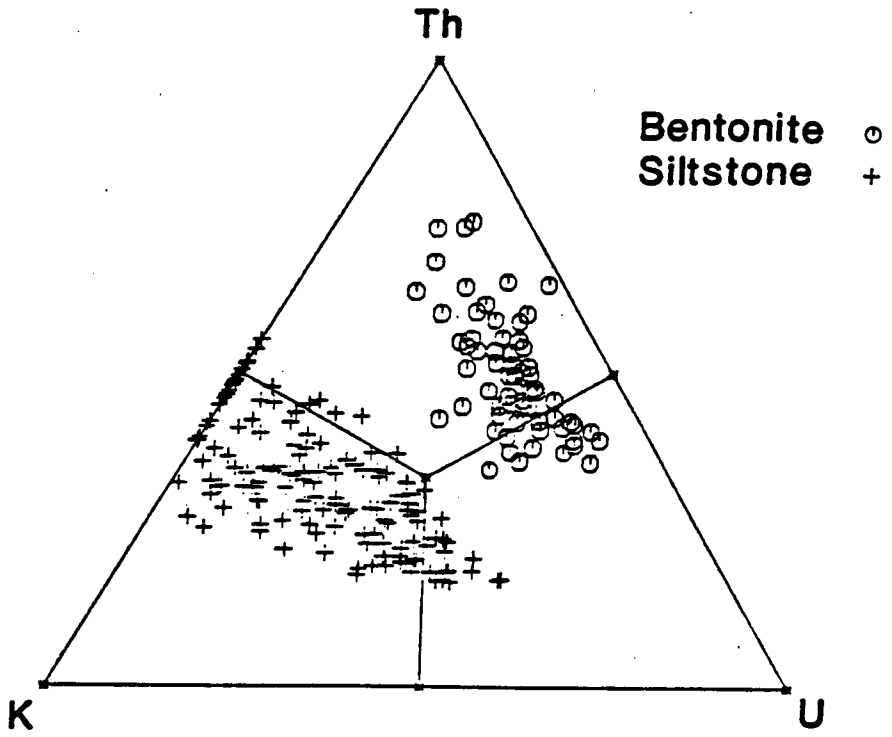

Figure 6-23. K-U-Th ternary plot of the GSC borehole logging spectral gamma data from the siltstones plus bentonites in holes HV414 and HV427.

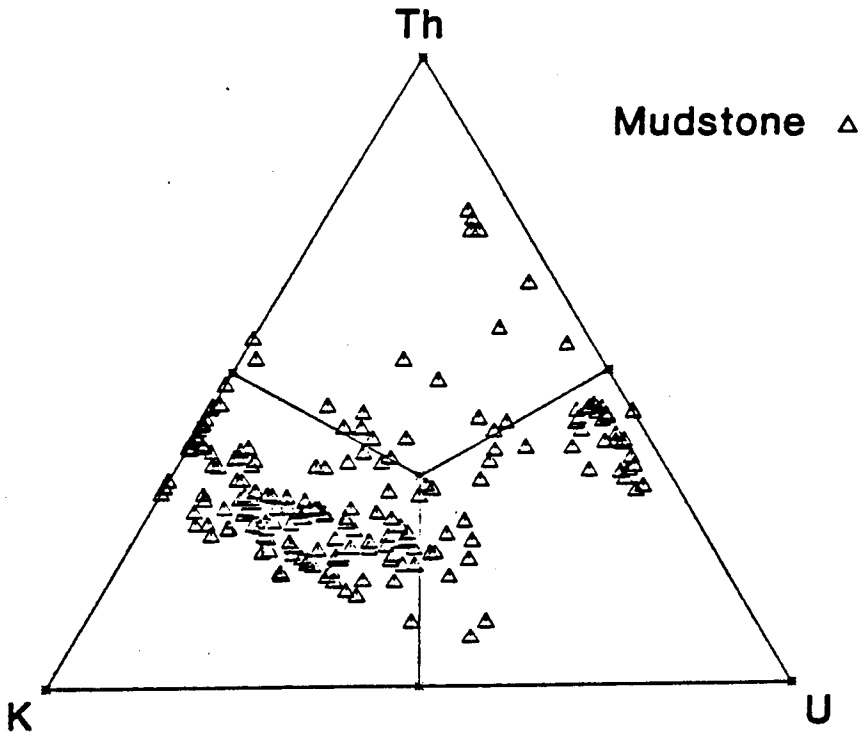

Figure 6-24. K-U-Th ternary plot of the GSC borehole logging spectral gamma data from the mudstones in holes HV414 and HV427.

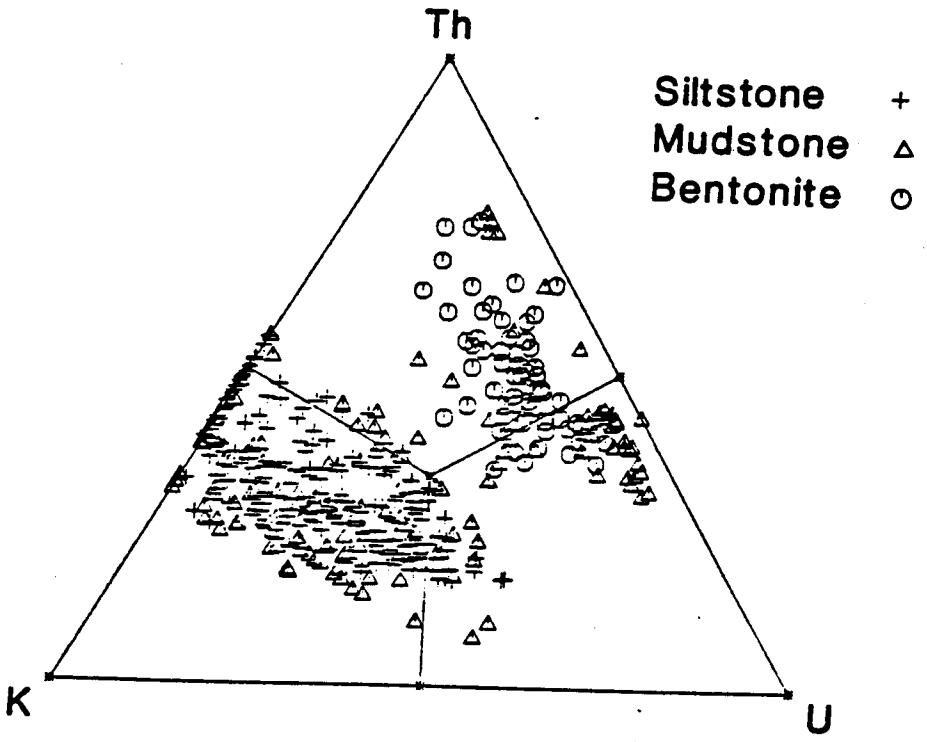

Figure 6-25. K-U-Th ternary plot of the GSC borehole logging spectral gamma data from all three lithologies in holes HV414 and HV427.

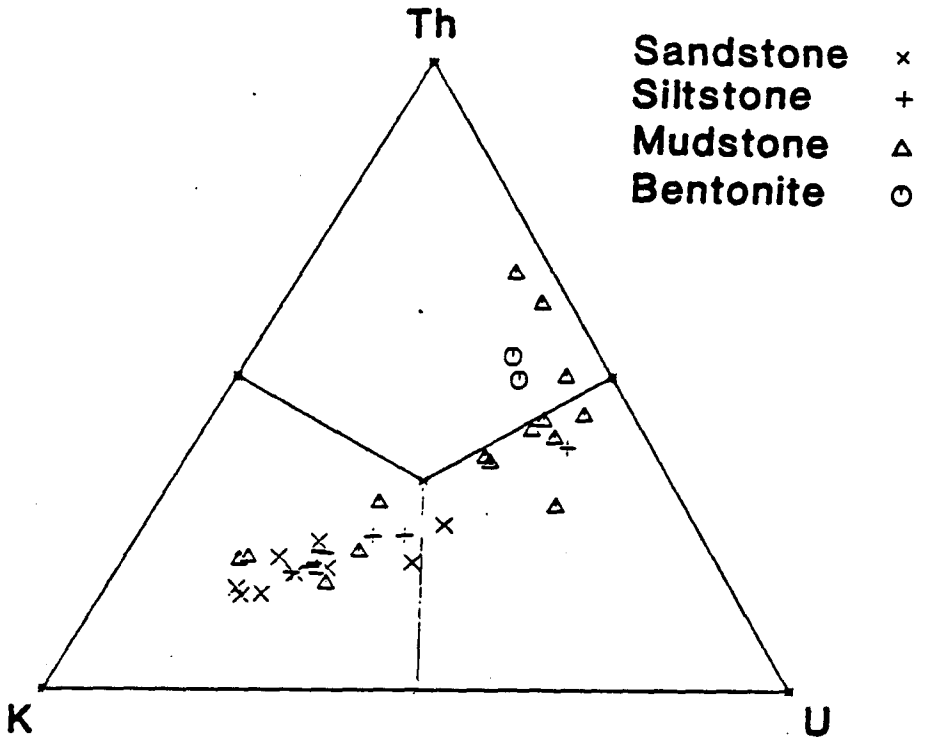

Figure 6-26. K-U-Th ternary plot of the laboratory spectral data from sandstones, siltstones, mudstones and bentonites samples collected in several holes at the Highvale Mine.

7. POTENTIALLY APPLICABLE NEW TOOLS

W. Scott Keys, C. Jonathan Mwenifumbo and Edgar W. Hulatt

7.1 FULL-WAVE SONIC

Considerable information related to lithology and rock structure is available through analyses of the various components of the waveform from a sonic or acoustic velocity probe. The main components of the received signal include the compressional wave (P-wave), which arrives first, the shear wave (S-wave), and the slower but much higher amplitude tube wave or fluid wave (Fig. 7-1). Analyses of the waves may include amplitude changes, ratios of the velocities of various components of the wave train, and frequency-dependent effects. Acoustic-wave forms can be recorded digitally, pictures can be made of the display on an oscilloscope, or a variable-density log can be made. The variable-density log or 3-dimensional velocity log (3-D) is recorded photographically, so that variations in darkness of the record are related to changes in amplitude of cycles in the waveform. Troughs in the waveform produce dark bands on the log; peaks produce light bands. A digitized waveform log is the most useful type, because the data can be analyzed quantitatively. Velocities and amplitudes of all parts of the recorded waveform can be measured from a digital record. Acoustic waveform logs have not been used widely in groundwater hydrology or mining; however, the potential for obtaining useful information is significant, and the equipment to record the data is available commercially.

Fully digitized, continuous waveform sonic logs have been available with oilfield equipment for a number of years, but have not been commonly used in shallow, small-diameter drillholes. A small-diameter sidewall sonic sonde has been developed by BPB Wireline Services which allows stationary waveform measurement to be taken in the borehole. This device was demonstrated at the Highvale Mine during this research project, and its specifications are provided in Appendix J.

The elastic properties of rocks can be calculated from the velocities of compressional and shear waves and from corrected bulk density derived from a calibrated gamma-gamma log. The elastic properties or constants that can be determined are Poisson's ratio, Young's modulus, shear modulus, and bulk modulus. Guyod and Shane (1969) discuss the relation of these constants; Helander (1983) discusses the equations to be used to calculate the constants from log data. These properties have their greatest application in mining and civil engineering.

Paillet (1980 and 1981), and Davison and others (1982) describe the characterization of fractures by various acoustic techniques. A significant finding was that a semiquantitative correlation exists between the attenuation of tube-wave amplitude in small-diameter drillholes in crystalline rocks in Canada and the permeability of fractures determined by packer isolation tests. Thus, tube-wave amplitude logging has potential for predicting the relative flow through fractures in hard rocks. The tube wave is part of the fluid wave propagated along the borehole under certain conditions; it apparently is attenuated where water in the borehole is free to move in and out of fractures. It is not yet known if tube wave amplitude would provide useful information in the rocks associated with Alberta coal and oilsand deposits.

7.2 ACOUSTIC-TELEVIEWER LOGGING

The acoustic televiewer is a logging device that can provide high-resolution information on the location and character of secondary porosity, such as fractures and solution openings. It also can provide the strike and dip of planar features, such as fractures and bedding planes. The acoustic televiewer also is called the borehole televiewer; this term occasionally causes it to be confused with borehole television. Unlike television the acoustic televiewer does not require light and can be operated with mud in the drillhole or mudcake on the borehole wall. The televiewer requires considerable expertise to operate the equipment properly in order to optimize results, particularly when the borehole conditions and rock types are new to the operator.

The acoustic televiewer employs a rotating 1.3 MHz transducer that functions as both transmitter and receiver (Zemanek and others, 1969). The piezoelectric transducer is rotated at 3 r/s and is pulsed approximately 1,200 times per second. The high-frequency acoustic energy is reflected from, but does not penetrate, the borehole wall. A trigger pulse is transmitted to the surface equipment from a fluxgate magnetometer each time the transducer rotates past magnetic north. This pulse triggers the sweep on an oscilloscope, so that each sweep represents a 360 degree scan of the borehole wall. The brightness of the oscilloscope trace is proportional to the amplitude of the reflected acoustic signal, somewhat analogous to a depth-finder in a boat. The probe must be centralized accurately with bow springs, so the signal path will be the same length in all directions. As the probe moves up the hole, a signal is generated that moves the sweeps across the oscilloscope or other type of graphic recorder. The log must be run at speeds less than 2 m/min., depending on vertical scale, or the sweeps will be too far apart to produce a continuous image.

A camera or graphic recorder, employing continuous light-sensitive paper, is used to make a record of the intensity of the sweeps that produces a continuous image. If a Polaroid camera is used to record the acoustic image, the pictures are taped together to form a continuous log. The equipment can be run on any logger that has 4- or 7-conductor cable and is available for purchase, rental or through service logging companies in both Canada and the United States.

The acoustic televiewer provides very high-resolution data related to variations in acoustic reflectivity of the borehole wall. Although it has been used primarily for locating and determining the orientation of fractures, it is an excellent tool for determining the thickness and strike and dip of beds. For this reason it may be useful for locating and characterizing glacially deformed bedrock (Sec. 5). The only requirements are that the borehole contain either mud or water and that the beds to be defined have differences in acoustic reflectivity. Acoustic reflectivity, which can be recorded continuously, is related to rock hardness and borehole surface characteristics so the measurement of reflectivity may provide data on geotechnical parameters (Keys and Sullivan, 1979). Under the proper conditions the televiewer may define features as small as one millimetre. Thus it might show slip planes in glacially deformed bedrock and it will define beds too thin to be accurately resolved by other logging techniques.

7.3 GEOLOGICAL SURVEY OF CANADA LOGGING TOOLS

A number of new logging tools to the coal industry were tested by the Geological Survey of Canada (GSC) at the Highvale Mine in 1988. The (GSC) Research and Development (R&D) logging system has five logging probes which measure thirteen different parameters:

1. Spectral gamma ray (SGR) probe: total count, K, eU, and eTh (Sec. 6.6);
2. Spectral gamma-gamma (SGG) probe: density and SGG ratio;
3. Induced polarization (IP) probe: IP, resistivity and self-potential (SP) with a variety of electrode arrays;
4. Temperature probe: temperature and temperature gradient;
5. Magnetic susceptibility (MS) probe: MS and conductivity.

Probably the most commonly used logs in the coal industry are the natural gamma ray (total count), gamma-gamma density and resistivity logs. These three logging techniques have evolved into a new generation of techniques; natural spectral gamma ray, spectral gamma-gamma and induced polarization. The new logging tools are currently routinely carried out with the GSC's R&D logging system and provide much more information than the old tools. Temperature logging has been in existence for a

number of years but has not been widely used in either the coal or mining industry. A high-sensitivity temperature probe has been developed at the GSC and makes temperature logs more attractive because they can be used to compute detailed temperature gradient logs for use in stratigraphic mapping and for detection of water flow in fracture zones. Magnetic susceptibility measurements are virtually unknown in the coal logging industry.

All the five logging probes were used in the surveys carried out at the Highvale Mine. A few examples of these will be given in later sections to illustrate the type of information that can be obtained using these logs. First, however, is a brief review of the GSC logging system and the principles of operation of the five logging probes.

7.3.1 The GSC Logging System

The GSC logging system is a digital data acquisition system built around a Data General NOVA microcomputer. As an R&D system, specialized software has been written to acquire data in greater detail than might be required for a production logging system. Data are recorded on 9-track magnetic tapes. A digital CRT displays data, spectra or waveforms as required by the operator to run the system. Data input is via modules specific to the parameters being measured and communication with the system is by a standard keyboard terminal. A software-controlled, electrostatic chart recorder provides a customized hardcopy of the logs with alphanumerics for field quality control. Some field processing is done in 'replay' mode but detailed processing and interpretation are carried out at the headquarters in Ottawa. The characteristics of the logging tools and their measurements are briefly described below.

7.3.1.1 Spectral Gamma Ray (SGR) Logging Tool: Total Count, K, eU and eTh

The GSC spectral gamma ray system and the results of its use oat the Highvale Mine are described in Sec. 6. Although the GSC logging system is not always available to industry, spectral-gamma logging is becoming widely available from logging service companies. It is being used more frequently in the petroleum industry, but its potential in mining and groundwater studies has not yet been fully recognized. An example of a commercial spectral-gamma log is shown in Fig. 7-2.

7.3.1.2 Spectral Gamma-Gamma (SGG) Logging Tool: Density and SGG Ratio

This is essentially a spectral gamma ray logging tool in the gamma-gamma density configuration. The tool consists of a 10 millicurie gamma ray source (^{60}Co, ^{137}Cs or

^{192}Ir) and a sodium iodide or cesium iodide scintillation detector. Gamma rays emitted by the source collide with electrons and lose energy by Compton scattering and by photoelectric absorption. The scattered gamma rays are then counted at the detector at a fixed distance from the source. A number of source-detector (SD) spacings are available (7.5, 12.5, 17.5 and 22.5 cm); the choice being dependent on the spatial resolution requirements and on the need to reduce the borehole effects. The SD spacing used in the acquisition of the Highvale data was 17.5 cm. Experiments were also carried out to determine the optimum SD spacing for the large-diameter holes that were drilled in this area. The probe diameter comes in three sizes: 32, 38 and 50 mm O.D.

The data acquisition system is the same as that used for the spectral gamma ray logging. Backscattered gamma ray spectra are recorded on a 9-track magnetic tape in 1024 channels covering an energy range from 0.1 to 1.0 MeV. A number of windows may be selected across the spectrum to analyze the data. Density information is determined from the count rate in a high energy window from about 180 keV to 500 keV. This window relates mainly to Compton scattering which is a function of electron density in the surrounding material. The electron density is then related to the bulk density of the material. Information about the mineralogic composition of the rock can be obtained from the ratio of two energy windows; ratio of a high-energy window (Compton scattering) to a low-energy window called the spectral gamma gamma ratio (SGG ratio). Count rates in the low-energy window (50 - 120 keV) are mainly influenced by photoelectric absorption plus Compton scattering. Thus, the ratio emphasizes the response from photoelectric absorption. This ratio increases through zones containing high-Z material. The SGG ratio is similar to the Pe parameter in the lithodensity tools. The density log responses are highly variable and not particularly diagnostic of specific lithologic changes with the exception of coal. The SGG ratio, however, is less influenced by porosity changes and should, therefore, provide diagnostic information on mineralogic changes.

All data at the Highvale Mine were acquired at a logging speed of 3 m/minute with a sample time of 1 second giving a measurement every 5 cm.

7.3.1.3 Induced Polarization (IP/R/SP) Logging Tool

The IP/R/SP logging tool consists of a time domain current transmitter, probe electronics and a variety of electrode arrays. The diameter of the probe is 40 mm O.D. The transmitter is a constant-current source capable of supplying up 250 mA. There are 4 selectable pulse times for the current waveform; 0.25, 0.5, 1 and 2 second (i.e., full waveforms of 1 to 8 second durations). The long pulse time would mean logging at very low speeds in order to avoid errors that may be introduced in sampling over large depth

intervals. Experiments carried out at the GSC, however, indicate that IP response from data acquired with short pulse times are virtually identical to those acquired with long pulse times. With the short pulse times (0.25 s) logging can be done at 6 m/minute with a sample depth interval of 10 cm or at 9 m/minute with a sample depth interval of 15 cm. The choice of the logging speed depends on the required depth (spatial) resolution. Unlike most of the IP logging equipment in the mineral logging industry, the GSC system has a downhole receiver in the probe. Data from the receiver are transmitted digitally uphole. This eliminates coupling problems that are inherent in the systems with uphole receivers where data is transmitted in an analog fashion. A complete waveform (digitized at 4 ms intervals) is recorded on a 9-track tape. This provides an option to select any appropriate windows for computing the IP parameters at a later date. There are from 256 to 1024 data points on each complete waveform depending on the period of the full waveform (1 to 8 seconds). This high density of data points would make it relatively easy to determine spectral IP parameters from the data. Currently 10 semi-logarithmical spaced time-windows are determined from the decay waveform.

IP, resistivity and self potential can be measured with three types of electrode arrays: 40-cm normal, lateral (pole-dipole) and 10-cm micronormal arrays. The downhole current and potential electrodes are gold-plated brass cylinders, 40 mm in diameter. The standard IP parameter is chargeability determined during the middle part of the 'off' time of the decaying waveform between 0.45 to 1.1 s or equivalent for pulse times other than 2 s. The resistivity measurements are computed from the voltages determined during the constant current 'on' time of the square wave IP waveform, after the initial IP charging effects are over. Self-potential (SP) is determined during the late 'off' time on the IP decay waveform. SP measurements are carried out either in the gradient mode with the same arrays as are used in the IP/resistivity measurements, or in the potential mode with a single Pb or $Cu/CuSO_4$ electrode downhole and a reference electrode on the surface. In the gradient mode SP is measured simultaneously with the IP/resistivity measurements or in a separate logging run with the current off. The latter is the preferred approach. In the potential mode an analog SP signal is transmitted uphole.

Induced polarization measurements primarily respond to the presence of polarizable and conductive minerals. Some clay minerals are also polarizable and the IP log can, therefore, be useful in detecting clay-rich zones in sedimentary rock formations.

7.3.1.4 Temperature Logging Tool

The temperature profile in a borehole is affected by a number of factors to varying

degrees and these include (a) drilling fluid circulation; (b) changes in lithology with different thermal properties (thermal conductivity and thermal capacity); (c) ground water flow; (d) presence of massive conductive sulphides; and (e) seasonal and climatic temperature variations. The most prominent temperature anomalies are those caused by groundwater flow, water having a heat capacity 3 to 5 times that of the rock. If logging is carried out immediately after drilling then the effects of the drilling fluids on the temperature distribution seem to dominate.

The objectives of temperature logging at the Highvale Mine were to demonstrate the utility of temperature logs in (a) locating the water table and groundwater flow in the borehole, and (b) lithostratigraphic and coal seam mapping. The latter requires that there be a reasonable thermal conductivity contrast between the different sediments intersected by the drillhole and that the influence of other factors affecting the temperature distribution in the hole be minimal.

The GSC temperature probe has a diameter of 25 mm O.D. The sensor consists of a 10 cm long tip of thermistor beads with a sensitivity of 0.0001 °C. Changes in the borehole fluid temperatures are recorded continuously as changes in the thermistor resistance and then converted into true temperatures. The processing of temperature data involves applying an inverse operator with an appropriate time-constant to remove the effects of the probe time constant from the measurements. Temperature gradients are derived from the temperature data with the application of a gradient operator.

All the temperature logs were acquired continuously during a downhole run at a logging speed of 3 m/minute with data sampled every 200 milliseconds giving a measurement approximately every 1 cm. This high spatial resolution of data is necessary for the determination of accurate temperature gradients with the use of gradient operators. Probe depths are measured with a resolution of 1 mm by an optical shaft encoder mounted on a well-head pulley assembly.

7.3.1.5 Magnetic Susceptibility Logging Tool

The magnetic susceptibility of a volume of rock is a ratio of the intensity of magnetization produced in the rock to the strength of an external magnetic field. It is primarily dependent on the amount of ferromagnetic minerals (magnetite, ilmenite and pyrrhotite) present within a formation. Magnetic susceptibility measurements can, therefore, provide a rapid estimate of the magnetic minerals present. The variations in the content of these minerals are interpreted to reflect lithological changes, degree of homogeneity and the presence of alteration zones within a rock mass. Susceptibility measurements have been successfully applied in stratigraphic

mapping in igneous and volcanic rocks. Logging at the Highvale coal mine was carried out to illustrate the feasibility of using susceptibility logs in lithologic mapping in a sedimentary environment.

The MS tool measures magnetic susceptibility and electrical conductivity. Since the measurements are made inductively, the tool can be used inside plastic casing. The electrical conductivity measurements are limited to a high conductivity range, (virtually massive sulphides or equivalent conductors) as a result of optimizing the tool parameters for the magnetic susceptibility measurements. The data are acquired with a Geo-Instruments Ky of Finland Model TH-3C probe that has a diameter of 42 mm O.D. The coil dimensions are 42 mm in diameter by 0.5 m in length. The coil is in an electrical bridge circuit energized at a frequency of 1400 Hz. A digital signal processing unit developed at the GSC is used with the Geo-Instrument probe. There are 4 sensitivity ranges on this system: 20, 80, 320 and 1280 x 10^{-3} SI units with the highest setting giving a measurement resolution of approximately 0.005 x 10^{-3} SI units. Susceptibility data are acquired continuously at a sample rate of approximately 5 samples per second. Usual logging speed is 6 m/minute which provides samples every 2 cm along the borehole. The holes at Highvale were, however, logged at 3 m/minute providing a measurement every 1 cm along the hole length.

7.3.2 Field Examples: Highvale Mine

Table 7-1 lists the holes and parameters logged at the Highvale Mine. Twelve holes, ranging in depths from 50 to 100 m, were logged in Pit 02 and Pit 05 areas. These holes were cored during the drilling program conducted in May and June, 1988, by TransAlta Utilities. Whenever possible each hole was logged through the entire depth. However, as logging usually occurred several days after drilling, a few holes caved in, preventing logging to the bottom of the holes.

7.3.2.1 Spectral Gamma Ray Logs

Examples of spectral gamma ray logs are discussed in Sec. 6.

7.3.2.2 Spectral Gamma-Gamma Logs

Fig. 7-3 shows typical spectra recorded with the spectral gamma-gamma tool. These spectra were obtained in coal and mudstone layers. The positions of a low-energy window (W1) and a high-energy window (W5) are indicated in the figure. The density information is derived from window W5 and the SGG ratio is defined as W5/W1.

Fig. 7-4 shows the total-count gamma ray, normal resistivity, density (in arbitrary units) and the SGG ratio logs. The information from the SGG ratio within the coal seams is similar to that depicted on the density log. There are, however, some differences in the response characteristics within the upper sedimentary sequence. High SGG ratios are observed around 26 m and 30 m implying that the effective Z values at these location is higher suggesting the presence of high Z-value minerals. The lower density values between 27 and 29 m may be interpreted to reflect porosity and not

Table 7-1. Summary of GSC logging at the Highvale Mine.

HOLE	LOGGING PARAMETERS								
HV401	T	SGR	SGG	SP	SPR	IP	R10		RS	
HV405	T	SGR	SGG	SP	SPR	IP	R10	R40	RS	MS
HV412	T	SGR	SGG	SP	SPR	IP	R10	R40	RS	
HV414	T	SGR	SGG	SP	SPR	IP	R10		RS	
HV417	T			SP						
HV422	T	SGR	SGG	SP	SPR	IP	R10	R40	RS	MS
HV424	T	SGR	SGG	SP	SPR	IP	R10	R40	RS	MS
HV425	T			SP	SPR					
HV426	T	SGR	SGG	SP	SPR	IP	R10		RS	
HV427	T	SGR	SGG	SP	SPR	IP	R10		RS	MS
HV428	T	SGR	SGG	SP	SPR	IP	R10		RS	
HV429	T	SGR	SGG	SP	SPR	IP	R10		RS	

T	-	temperature
SGR	-	spectral gamma ray
SGG	-	spectral gamma-gamma
SP	-	self-potential
SPR	-	single-point resistance
IP	-	Induced polarization
R10	-	10-cm micronormal resistivity
R40	-	40-cm normal resistivity
RS	-	symmetrical lateral resistivity
MS	-	magnetic susceptibility

mineralogic changes because the SGG ratio is fairly uniform in this region. On the average the sandstone layer between 20 and 27 m seems to have lower SGG ratios. The siltstones and mudstones contain an appreciable amount of mafic minerals which have elements with high Z values and hence, one should expect higher SGG ratios in those layers.

7.3.2.3 IP/R/SP Logs

Electrical logging with a variety of electrode arrays (Fig. 7-5) was carried out in 15 cm diameter holes to evaluate their response characteristics and their performances. Fig. 7-6 shows a comparison between self-potential, single-point resistance, 10-cm micronormal and symmetrical lateral resistivity responses in the coal seams. Corrections for the effects of borehole fluid, invasion zone and borehole diameter on the response characteristics of the resistivity have not been applied to any of these data. The objective here was to compare the resistivity data in their raw form and evaluate their characteristics with regard to coal seam recognition, bed-boundary resolution and the effect of finite bed thickness on the magnitude of the apparent resistivities. All logs clearly indicate the resistive coal seams and resolve the coal bed-boundaries fairly well. The single-point resistance and normal resistivity logs show smooth variations in resistivities within the coal seams, especially in seams number 1 and 2 with increasing resistivities towards the lower contact. The resistivity response of the symmetrical lateral array is, however, sharper at the contacts and hence provides better bed-boundary definition. The fine details in the resistivity variations within the coal seams are also better defined on the symmetrical lateral log. It is interesting to note that both the single-point resistance and the normal resistivity logs show lower resistivity values in seams 3, 4 and 6. This does not necessarily imply that the resistivities of these seams are lower than those of seam numbers 1 and 2 but rather this is a characteristic response of these logs to thin beds in these large diameter holes. The symmetrical lateral resistivity log, in contrast indicates that the resistivities of seams 3, 4 and 6 are equivalent to those of the thicker seams 1, and 2.

The IP logs from all the holes showed very low chargeabilities that were not characteristic of any formations. The values were virtually within the noise level of the detection capabilities of the system.

7.3.2.4 Temperature Logs

Fig. 7-7 shows the electrical resistivity, self-potential and transient temperature logs acquired in hole HV422. The resistivity log indicates a resistive sandstone layer between 29 and 36 m. Variations in resistivity within this layer may reflect changes in porosity. Calcareous cementation is prevalent in a number of sections in sandstone layers in this region. Cementation reduces porosity and consequently increases the electrical resistivity. A high transient temperature anomaly observed around 31.5 m correlates well with a self-potential anomaly and coincides with a slightly lower resistivity zone. It is interpreted as resulting from the infiltration of warmer drilling

fluids into a more permeable zone within the sandstone creating, a transient heat source that decays with time. The self-potential anomaly is thus probably due to filtration of water from the formation pores into the borehole. This is in keeping with fact that SP data have at times been used to detect porous and permeable zones of a formation surrounding the borehole. These measurements indicate that temperature logging immediately after drilling can be used to locate more permeable and porous zones. Fig. 7-8 shows natural gamma ray, electrical resistivity and temperature gradients logs acquired in hole HV412. Two temperature gradients logs run 11 and 15 days after completion of drilling are superimposed to show reproducibility of the data, which is excellent. The general increasing trend in gradients from 10 to 20 metres is due to the fact that this section of the data is close to the zero-gradient region and is increasing towards the equilibrium value at depth. The logs delineate all the coal seams and correlate well with resistivity data. The gamma ray and temperature gradient logs in the upper stratigraphic section of the hole, where there are no coal seams, show a good positive correlation. The higher radioactivity zones correlate with the mudstone whereas the lower radioactivity zones correspond to the sandy siltstone layers. Mudstone has higher thermal resistivity than the sandstone; hence exhibits higher thermal gradients. The resistivity is negatively correlated with the temperature gradient. The temperature gradients, in conjunction with the electrical resistivity and natural gamma ray logs can, therefore, be used to distinguish sandy layers from clay layers and resistive sandstone layers from resistive coal seams.

7.3.2.5 Magnetic Susceptibility

Only a few holes were logged with the magnetic susceptibility tool because the signal levels were too low and measurements were discontinued in other holes. Fig. 7-9 shows the natural gamma ray, MS and normal resistivity logs acquired in hole HV424. The susceptibilities are, in general, fairly low. Higher susceptibilities are observed within the siltstone layer between 20 and 30 m than in the sandstone layer below. This suggests that magnetic minerals may have a tendency to concentrate in the finer sediments.

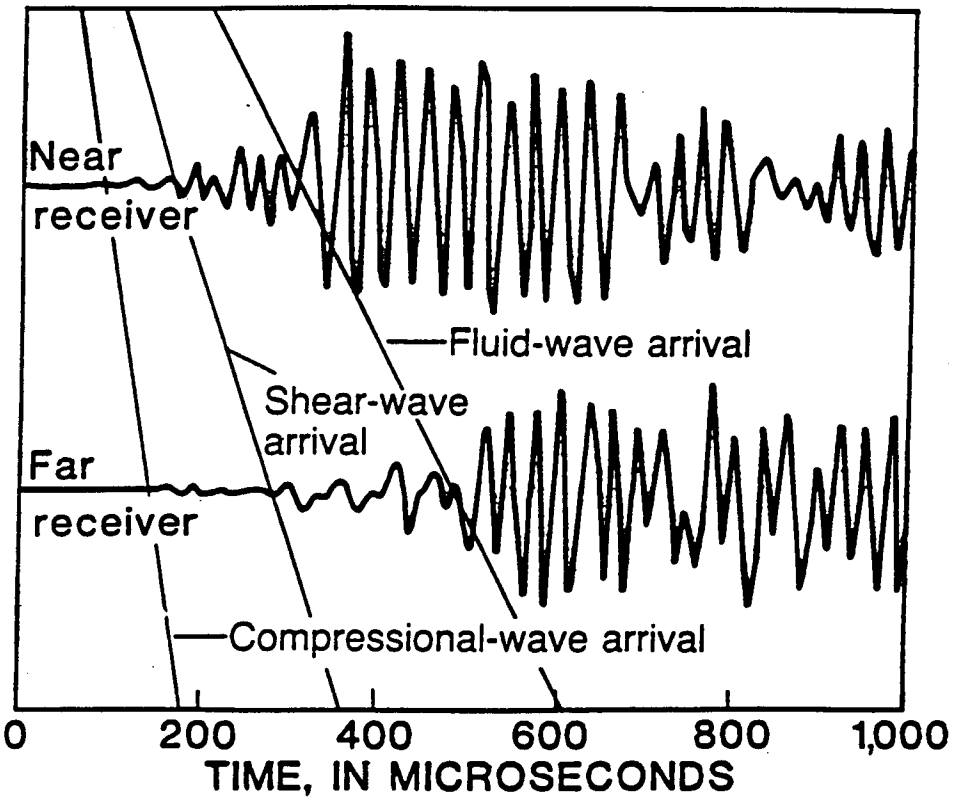

Figure 7-1. Sonic full-wave forms for a two-receiver system and arrival times of compression, shear and fluid or tube waves (modified from Paillet and White, 1982).

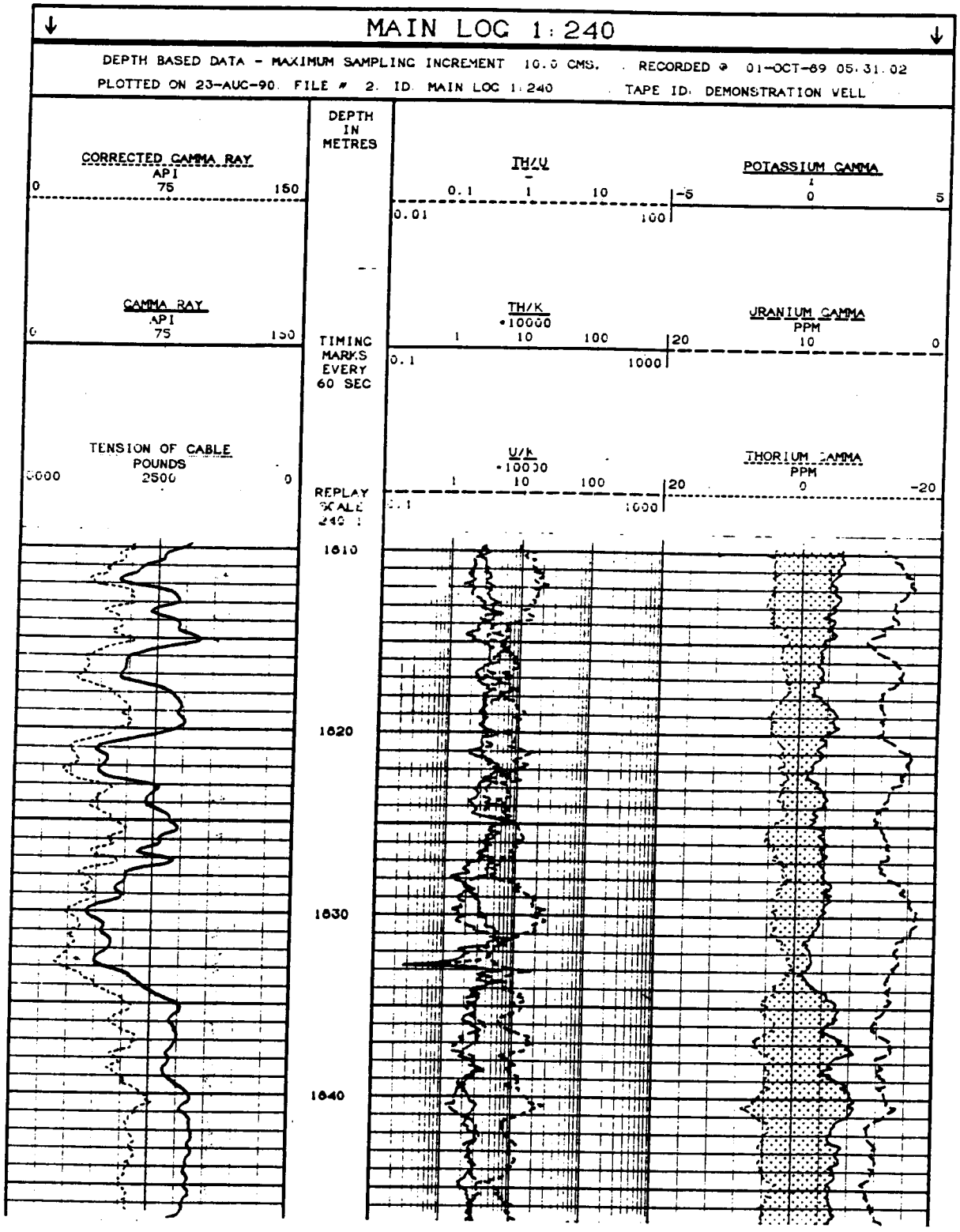

Figure 7-2. Example of spectral gamma log showing plots of total-count gamma, potassium, uranium, thorium, and Th/U, Th/K and U/K ratios.

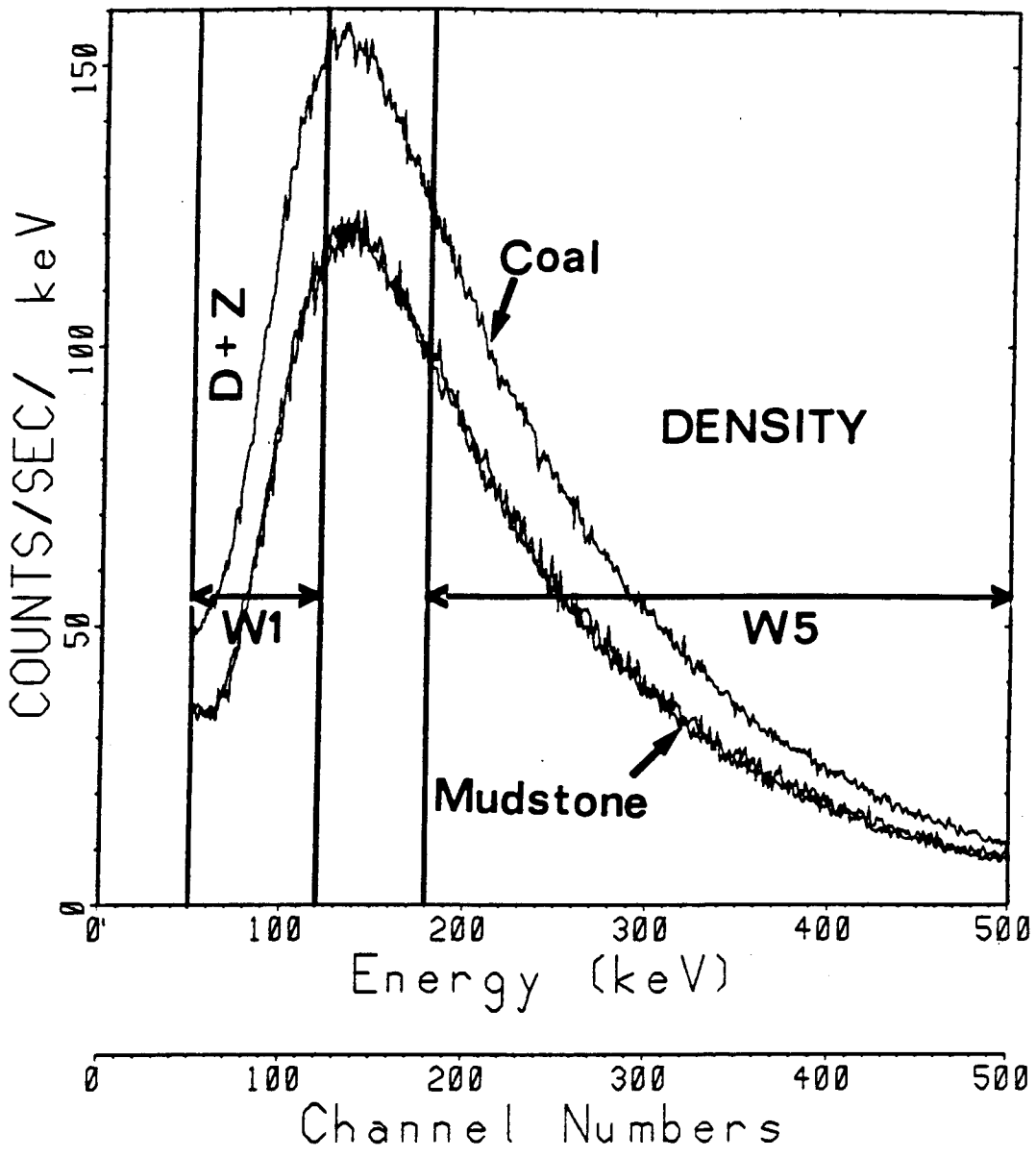

Figure 7-3. Spectra acquired in coal and mudstone layers with the spectral gamma-gamma tool. Two energy windows are set to count gamma rays in the low energy region (W1) and the high-energy region (W5). The SGG log is a plot of the spectral ratio W5/W1.

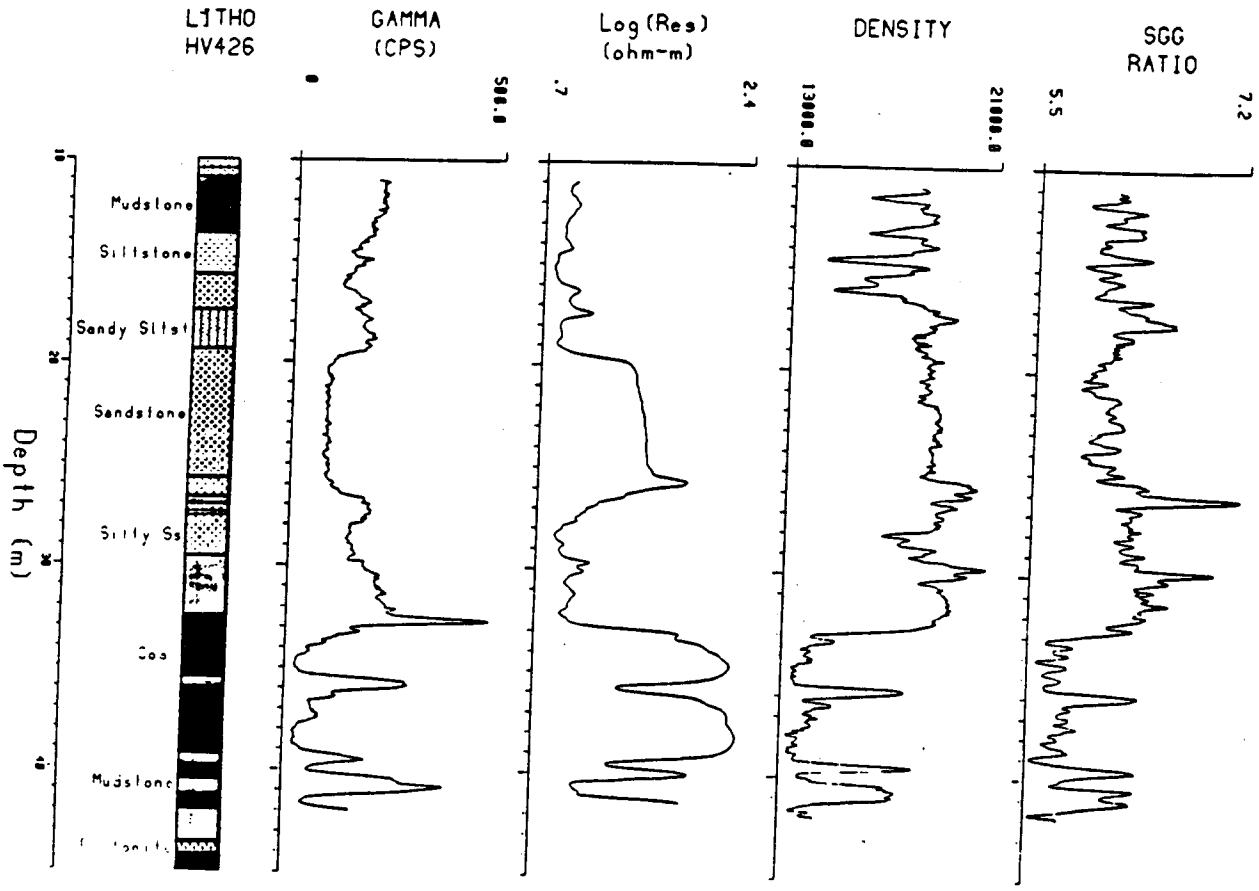

Figure 7-4. Gamma ray, normal resistivity, density and SGG ratio; GSC logging hole HV426.

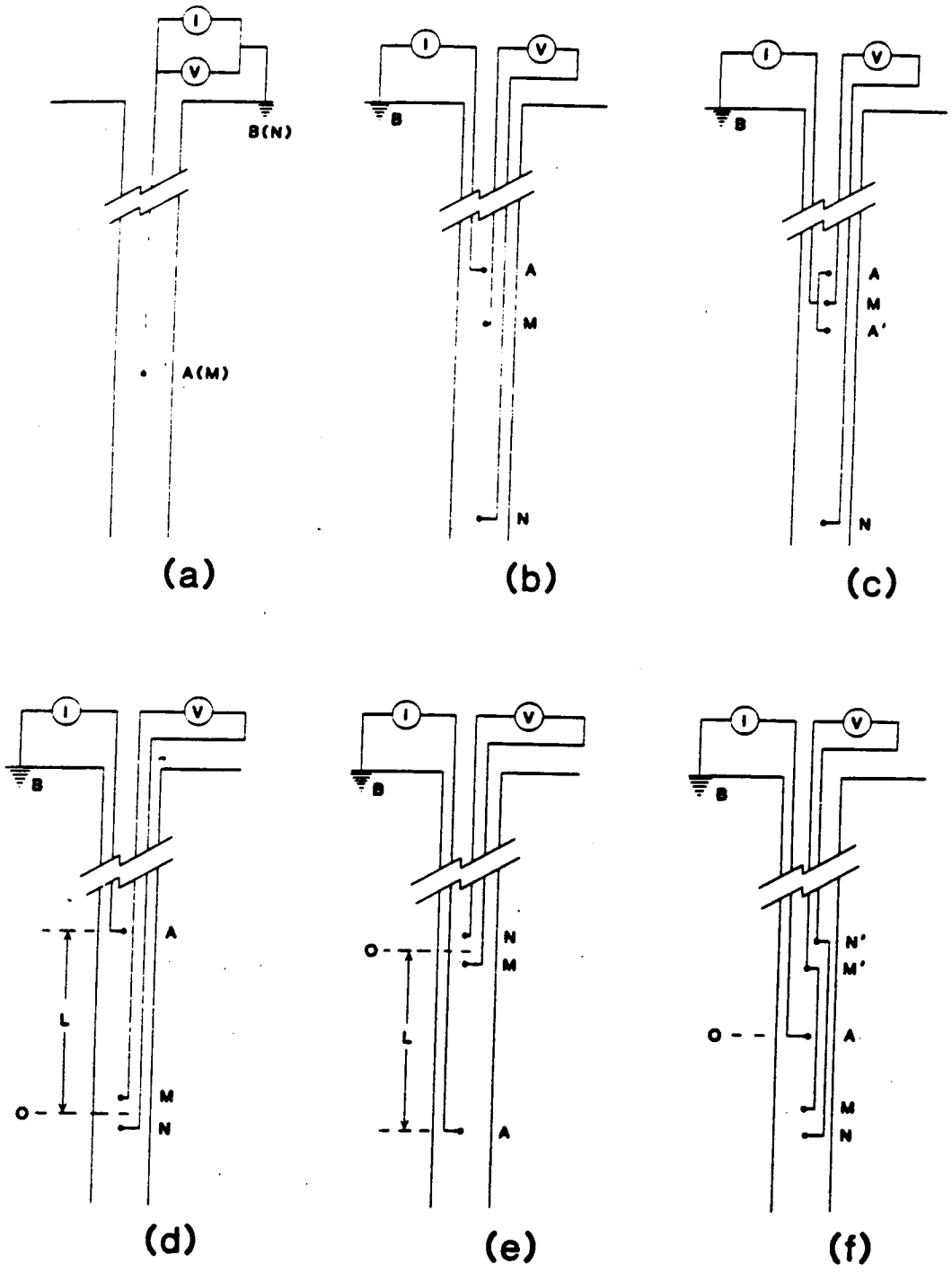

Figure 7-5. Electrode arrays. 1(a) single point resistance, 1(b) inverted normal, 1(c) Darknov micronormal, 1(d) lateral, 1(e) inverted lateral and 1(f) symmetrical lateral. The downhole and surface current electrodes are labelled A and B, respectively, and the potential electrodes, M and N.

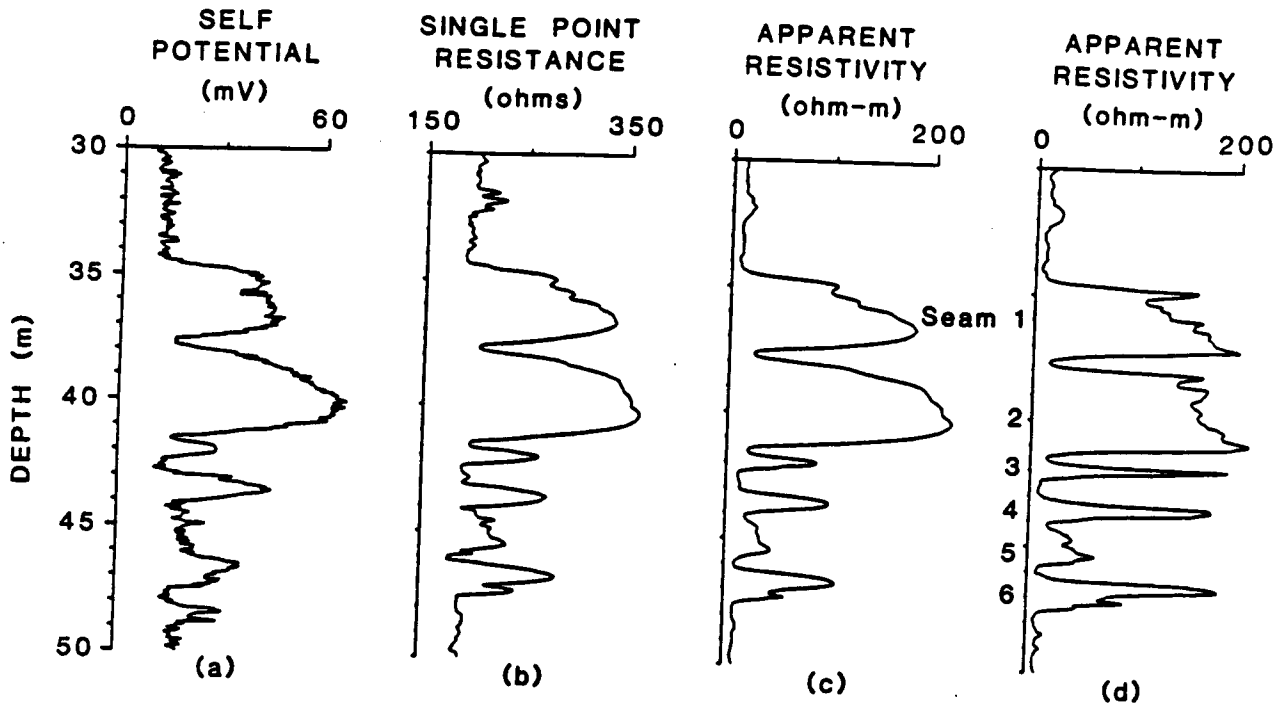

Figure 7-6. Symmetrical lateral resistivity (d) log compared with standard electrical logs: self-potential (a), single-point resistance (b), and 10-cm normal resistivity (c).

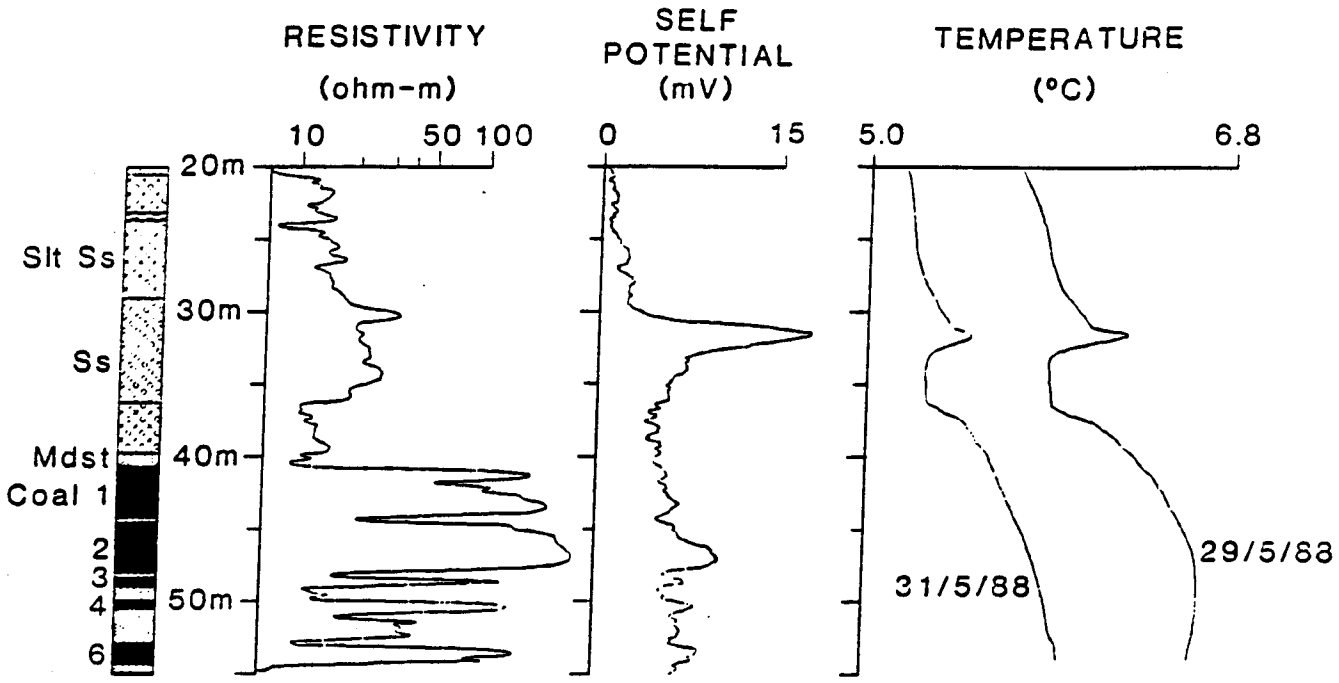

Figure 7-7. Electrical resistivity, self-potential and transient temperature gradient logs; GSC logging hole HV422. The prominent peak on the temperature gradient profile indicates a permeable zone within the sandstone and is confirmed by a corresponding high SP anomaly and lower resistivity. Temperature measurements were recorded 1 and 3 days after drilling. Mdst - mudstone, Slt Ss - silty sandstone, Ss - sandstone.

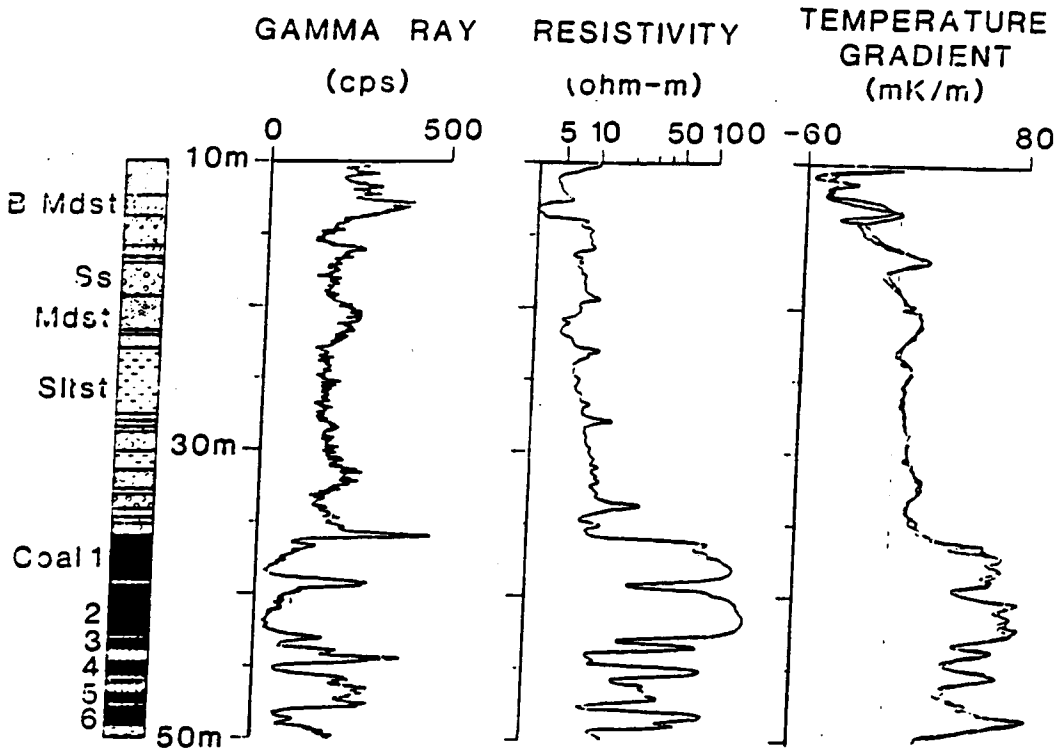

Figure 7-8. Gamma ray, electrical resistivity and temperature gradient profiles; GSC logging hole HV412. The two temperature gradient logs recorded 11 and 15 days after drilling, respectively, show excellent repeatability. BMdst - bentonitic mudstone, Mdst - mudstone, sltst - siltstone, Ss - sandstone.

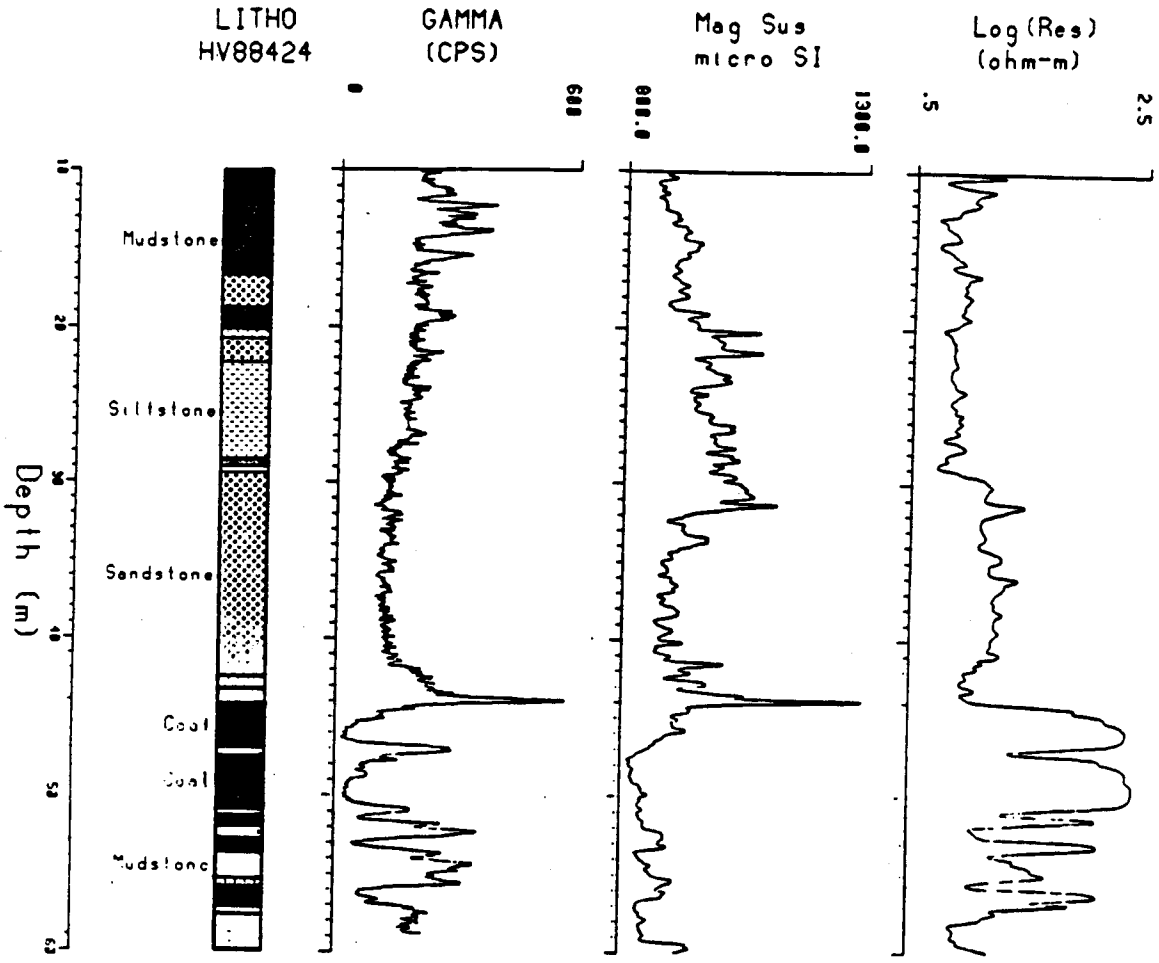

Figure 7-9. Gamma ray, magnetic susceptibility and normal resistivity logs; GSC logging hole HV424.

8. CONCLUSIONS

8.1 PROJECT ORGANIZATION

• A multi-party research project such as this can be developed and completed for the benefit of all participants. Over the four years of this project the participants exchanged expertise and gained a much more detailed understanding of the variety of information that can be derived from the geophysical logs that are in routine use in western Canada.

• From a management perspective, the changes in personnel and sources of funds require flexibility in the contracts between participants and funders, the assignment of portions of the work to various researchers, and the management structure itself. For consistency of reporting, one group or person should be charged with the final writing of all reports throughout the project. This party must have a clear concept of project requirements and technical matters, provide the guidance to the various working groups as to the work and substance of the reporting. This guidance also keeps the various groups working towards the same goal.

• Communications between the various participants, funders and researchers is of critical importance to keeping such a large project on track. In addition to regular progress reports, the Downhole Geophysics Project made good use of electronic mail, working seminars with various experts, full and partial project meetings, telephone conference calls, and conversion of digital data into standardized files for distribution.

8.2 DATA ACQUISITION, ANALYSIS AND INTERPRETATION

• Data related to geotechnical and groundwater parameters can be derived from geophysical logs, and used to supplement data obtained by more expensive conventional means such as core testing.

• The relationships between geophysical log response and geotechnical and hydrologic parameters are site-specific and have to be substantiated at each new site by comparison with data from core samples.

• One of the most important techniques available for log analysis today is the use of computers to obtain information that is not available from standard visual inspection

of paper log charts. Computers can efficiently: (1) correct log suites for depth and other variables; (2) crossplot data obtained from logs against data from other logs, core analyses, or tests; and (3) analyze these data both graphically and statistically. Hardware and software are available that can perform these tasks efficiently.

- The recommendations concerning data quality described in Sec. 9.1 and Sec. 2 must be followed if quantitative analysis is to be effective.

- A marked increase in the variability of most types of logging data occurs in the uppermost portions of drillholes from surface to a depth of about 10 m. This is probably caused by a combination of factors related to borehole size, less consolidated rocks, and unsaturated materials. These depths are often critical for water table and many civil engineering applications.

8.3 GEOTECHNICAL DATA

- By depth-aligning geotechnical samples with the corresponding geophysical log intervals (where this is possible), a number of different geotechnical parameters were successfully correlated with individual logs. Some enhancement of the correlation was generally possible when groups of logs were used.

- Most of the satisfactory correlations ($R>0.70$) between geotechnical parameters and geophysical logs appear to be site-specific or at least specific to either the Highvale coal or Syncrude oilsands geological environments, because combining the data sets from the two areas generally produced poorer correlations.

- Although correlation coefficients are sometimes enhanced by using logarithmic functions of the parameters, the procedure may actually desensitize the resulting relationship thereby diminishing its effectiveness as a predictive expression. This is particularly true in the 3-parameter plots where the desensitizing effects of logarithmic functions are compounded by the normalizing procedures used to transform from three variables to two.

8.4 GROUNDWATER

- Generally the water table could be more readily detected in coarse-grained (sandy) sediment than in fine-grained (clayey) sediments.

• The sonic log gave the best indication of the water table in both clay-rich and sandy material, at the Big Valley and Highvale sites. The resistivity, neutron and density logs could also detect the water table under some conditions, and should be used to support the response of the sonic log.

• A suite of logs from a drillhole interpreted together as an assemblage of data gave more accurate results than the same logs analyzed individually.

• Crossplotting of log data emphasized the difference in response above and below the water table.

• Changes in log response produced by the water table must be distinguished from changes produced by other factors such as lithologic changes, borehole conditions and fluid level in the hole.

8.5 GLACIALLY DEFORMED BEDROCK

• Data from the sonic, density, and neutron logs were most useful in detecting glacially deformed bedrock at the Highvale Mine. The caliper logs indicated the deformed material in some but not all of the holes.

• Histograms and crossplots of the log data showed that deformed bedrock was characterized by long sonic interval times, low density and lower neutron count rates.

• Multiple regression and correlation analyses of the raw dipmeter data were used to distinguish between deformed and undeformed bedrock.

8.6 SPECTRAL GAMMA RAY AND CLAY MINERALOGY

• The spectral gamma log proved to be capable of identifying bentonitic and montmorillonitic c lays that cause problems for pit wall stability. It was more effective than ordinary total-count gamma logs for this purpose.

• More information about mineralogy can be extracted from spectral gamma data than from total-count gamma data. The correlation between total-count gamma ray and percent clay is poor, suggesting that the total-count log may not be a useful log for determining the clay content or shaliness in this region.

• Thorium and uranium are the main contributing elements to the overall observed radioactivity shown on a gamma log in this region, whereas there appears to be a negative relationship to potassium.

• The major clay mineral in the bentonites and other lithologies from the lower Tertiary and Upper Cretaceous formations of the Highvale and Big Valley regions is montmorillonite. The spectral data indicates that the bentonites are characterized by very high thorium concentrations, with low uranium and potassium content.

• For illite, there appears to be some correlation with the potassium detected by the spectral gamma tool. This correlation needs to be further tested in formations where illite content is greater than at Highvale.

• Ratios of the radioelements (such as Th/K) should provide better indicators of the amounts and types clay than single-element logs.

8.7 NEW TOOLS

• The full-wave sonic log can provide data to calculate elastic properties or constants that are important to mining and geotechnical engineering, including: Poisson's ratio, Young's modulus, shear modulus, and bulk modulus. Under some conditions information on the permeability of fractures may also be obtained.

• The acoustic-televiewer can provide high-resolution information on the strike and dip of beds, and the location, character and orientation of secondary porosity such as fractures and solution openings. Under the proper conditions the televiewer may define features as small as one millimetre, thus it may show slip planes in glacially deformed bedrock, and it may define the thickness and orientation of beds that are too thin to be accurately resolved by other logging techniques.

• Advances in slimline logging techniques such those demonstrated by the GSC at the Highvale Mine will provide more and better information than the older tools commonly used in the coal industry. Service companies, now using digital surface equipment with improved software and new small-diameter logging tools, will be able to provide the quality of data similar to that of more expensive oilfield tools. This should improve the use and reliability of the log data in making quantitative correlations with parameters of interest to mining companies.

9. RECOMMENDATIONS

9.1 DATA ACQUISITION, ANALYSIS AND INTERPRETATION

• Quantitative log analysis by computer can provide information that is not available from standard visual inspection of paper log charts, but to be practical and effective, appropriate software is needed.

• Log interpretations and correlations should be made by someone who is well trained. It is necessary to have detailed knowledge of the algorithms used and be familiar with the local geology and hydrology in order to to avoid misleading conclusions.

• A number of steps must be taken to ensure reasonable accuracy of the data if geophysical logs are to be interpreted quantitatively: (1) the equipment must be properly calibrated and standardized to ensure that log response is reproducible and can be related to environmental units such as density or percent porosity; (2) logs should be checked for extraneous effects such as hole diameter changes and partial resolution of thin beds; and (3) corroborating core samples should be taken carefully after examination of the geophysical logs, so that their depth correlation with thicker, uniform beds shown by the logs is known with certainty.

• Before quantitative log analysis can start: (1) depths must be corrected so that corresponding points on each log and core sample are at consistent depths; (2) effects produced by drilling fluids, changes in borehole diameter, and well construction techniques must be corrected; and (3) beds that are thinner than the limits of resolution, which are a product of tool design and logging speed, must be eliminated from consideration or corrected. Log data that cannot be corrected for the above factors are unsuitable for quantitative analysis.

• A suite of logs from a drillhole should be interpreted together as an assemblage of data, not separately. This increases the accuracy of analysis by allowing more equations to be constructed and solved simultaneously.

• All logs should be provided by the logging contractor both as a paper print and in digital form. A paper print of each log must be provided in the field. The digital data may be provided later and should be an ASCII file on a 3-1/2 inch floppy disk, with a space-delimited columnar format, and the depth values and each corresponding set of log values in separate labelled columns.

9.2 GEOTECHNICAL DATA

- All correlations for the Highvale and Syncrude mines should be confirmed by incorporating more observations from a wider range of lithologies. For all of the satisfactory correlations obtained at Highvale and Syncrude, the level of confidence will be increased if it can be shown that, by increasing the number of data points, the generated R values are not materially reduced.

- The effect on geophysical log response of carbonaceous or bituminous strata in overburden formations should be assessed.

- The correlations should be extended to include other geotechnical parameters such as grain size, strengths from triaxial tests, and consolidation test parameters.

- Additional data from full-wave sonic logs should be obtained to correlate with various geotechnical parameters including Young's modulus and Poisson's ratio.

9.3 GROUNDWATER

- The sonic log should be included with the suite of resistivity, neutron and density logs for detection of the water table.

- All logs from the suite should be plotted and interpreted side by side so that apparent water table effects can be correlated across the logs.

- Crossplotting of log data or the ratios between two logs may show clustering of data points that may emphasize and support water table effects.

- The portable neutron moisture probe should be considered for long-term monitoring of moisture changes where the water table is shallow (less than 10 m deep).

9.4 GLACIALLY DEFORMED BEDROCK

- A suite of logs including sonic, density, neutron, and caliper logs should be run and interpreted together for the detection and evaluation of glacially deformed bedrock. If possible, dipmeter and acoustic-televiewer logs should also be run.

• To improve resolution, dipmeter data should be provided in digital form with values every 1 cm, as well as in paper chart form. Use of a four-arm dipmeter would also improve resolution.

9.5 SPECTRAL GAMMA RAY AND CLAY MINERALOGY

• The spectral gamma ray logging tool should be used: (1) for better lithologic correlations between holes, and (2) where more detailed understanding of mineralogy and clay content is required.

• Different formations in the Plains should be logged with the spectral gamma tool to test the correlations with the additional clay minerals. For example, the relationship between illite and potassium needs to be further studied to see if the correlation can be improved.

• Continuous spectral-gamma logging tools of the type provided by service companies should be tested to determine their correlations between natural radioisotope content and clay content, clay mineralogy and/or geotechnical index properties.

9.6 APPLICATION AT COAL AND OILSAND MINES

• Mines should use quantitative log analysis to derive supplementary data from geophysical logs, because this offers a cost-effective way to enlarge their geotechnical and hydrologic databases, and maximize the information obtained from their drilling, testing and logging programs.

• To implement a program of quantitative log interpretation, a mine should begin building a database that can be used to establish the relationships between log response and geotechnical or hydrological parameters for their site(s), by: (1) obtaining their geophysical log data in digital form; (2) ensuring that log quality is suitable for quantitative analysis as described in Sec. 2; and (3) ensuring that core samples (or hydrological tests) are taken with reference to the geophysical logs, so that the correspondence between them is known with certainty.

• To identify and apply the relationships between log response and the parameters of interest, a mine should obtain appropriate computing hardware and software. This task is rapidly becoming easier and less expensive because of the rapid advances in both hardware and software capabilities.

9.7 FUTURE RESEARCH

- Research on the relationship between geophysical log response and parameters of interest to mining should continue. The research should be extended to include new geotechnical and hydrological parameters, and possibly other factors such as coal quality or oilsands grade.

- Additional data from full-wave sonic logs should be obtained to correlate with the various geotechnical parameters including Poisson's ratio, Young's modulus, shear modulus, and bulk modulus.

- The acoustic-televiewer should be applied to the evaluation of fractures and glacially deformed bedrock.

- Geophysical logging data from the uppermost 10 m of a drillhole are usually characterized by increased variability, and research on improving log interpretation in this zone is warranted because these depths are often critical for the water table and many civil engineering applications.

- For future research on glacially deformed bedrock, two test sites should be chosen: one underlain by at least 20 m of glacially disturbed bedrock, and one in the same stratigraphic sequence with undisturbed bedrock extending to the surface. Caliper, density, sonic, resistivity, neutron, gamma, dipmeter (1 cm data spacing), self-potential, and acoustic-televiewer logs should be run. Tests should be conducted to determine: (1) if deformed bedrock can be detected within intervals less than 1 m in thickness; (2) if the material within individual thrust masses can be subdivided based on the degree of deformation ; and (3) if near the surface, the variations in geophysical properties in undeformed bedrock the resemble those in the deformed.

- For any future studies, geophysical logs, core samples and/or hydrological tests should be taken at a site that has: (1) well-documented geology; and (2) good drilling characteristics so that core recovery can be maximized and hole caving can be minimized. The drillers should be instructed that both core recovery and hole condition have high priorities. The holes should be continuously cored, there should be sufficient logging time available to test variations in logging speed and related factors, and there should be provision for complete laboratory analysis of core samples. Log response must be used to select the core samples, because the the correspondence between the two must be known with certainty. If the water table is of interest, the water table should be known from piezometer data to be stable at a depth greater than 4

m. The research should be conducted at an active mine, so that when mining eventually proceeds into the study area, production rates and problems can be compared with those anticipated from the study results; project funding and timing must be sufficient to allow for this task.

10. REFERENCES

Aber, J.S., D.G. Croot, and M.M. Fenton, 1989. *Glaciotectonic Landforms and Structures*. Kluwer Academic Publishers, Dordrecht, the Netherlands, 157 p.

Adams, J.A.S. and C.E. Weaver, 1956. Thorium-to-uranium ratios as indicators of sedimentary processes; example of concept of geochemical facies. Bulletin of the American Association of Petroleum Geologists, v. 42, no. 2, p. 387-430.

Alger, R.P., 1966. Interpretation of electric logs in fresh water wells in unconsolidated formations. 7th Annual Logging Symposium, Society of Professional Well Log Analysts, Paper CC, 25 p.

Andriashek, L.D. and M.M. Fenton, 1989. Quaternary stratigraphy and surficial geology of the Sand River area 73L, Alberta. Alberta Research Council, Bulletin No. 57, 154 p.

Babcock, E.A., 1978. Measurement of subsurface fractures from dipmeter logs. American Society of Petroleum Geologists ,Bulletin, v. 62, no. 7, p. 111.

Bass, J.D., D. Schmitt and T.J. Ahrens, 1986. Holographic in-situ stress measurements. Geophysical Journal of the Royal Astronomical Society, v. 85, no. 1, p. 13-41.

Bernius, G.R., 1981. Boreholes near Ottawa for the development and testing of borehole logging equipment - a preliminary report. *In:* Current Research, Part C; Geological Survey of Canada Paper 81-1C, p. 51-53.

Black, J.D.F. and P.D. Mitchell, 1986. Near-surface soil moisture measurements with a neutron probe. Journal Australian Institute of Agriculture, v. 34, p. 181-182.

Bluemle, J.P. and L. Clayton, 1984. Large-scale glacial thrusting and related processes in North Dakota. Boreas, v. 13, p. 279-299.

Bond, L.O., R.P. Alger and A.W. Schmidt, 1971. Well log applications in coal mining and rock mechanics. Transactions, Society of Mining Engineers, v. 250, p. 355-362.

BPB Instruments Ltd., 1981. Coal Interpretation Manual. BPB Instruments Ltd., East Leake, Loughborough, LE126JQ England; 100 p.

BPB Wireline Services Ltd., 1989. Evaluation of the full-wave sonic tool. Unpublished technical memorandum to TransAlta Utilities Corporation, March 1989.

Bristow, Q., 1979. NOVA-based airborne and vehicle mounted systems for real-time acquisition, display and recording of geophysical data. Proceedings of the 1979 Annual Meeting of the Data General Users Group.

Byers, A.R., 1960. Deformation of the Whitemud and Eastend Formations near Claybank, Saskatchewan. Royal Society of Canada, Transactions, v. 53, ser. 3, sec. 4, p. 1-11.

Carroll, R.D., 1966. Rock properties interpreted from sonic velocity logs. J. SMF Div., ASCE; 92.

Carroll, R.D. and D.C. Muller, 1973. Techniques for the quantitative determination of alluvial physical properties from geophysical logs, Southern Yucca Flat, Nevada Test Site. U.S. Geological Survey, Report 74-175, 108 p.

Caterpillar, 1989. Caterpillar Performance Handbook, 20th ed. Caterpillar Inc., Preoria, Illinois.

Cato, K.D., 1985. Variation in physical rock properties determined from sonic logs at a south Texas lignite mine. M.Sc. Thesis, Texas A & M University, College Station, Texas; 113 p.

Chanasyk, D.S. and R.H. McKenzie 1986. Field calibration of a neutron probe. Canadian Journal of Soil Sciences, v. 66, p. 173-176.

Chanasyk, D.S. and M.A. Naeth, 1988. Measurement of near-surface soil moisture with a hydrogenously shielded neutron probe. Canadian Journal of Soil Sciences, v. 68, p. 171-176.

Christiansen, E.A. and S.H. Whitaker, 1976. Glacial thrusting of drift and bedrock. *In:* R.F. Legget, ed., Glacial till, an interdisciplinary study; Royal Society of Canada in cooperation with the National Research Council of Canada. Royal Society of Canada Special Publication 12, p. 121-130.

Conaway, J.G., 1977a. Deconvolution of temperature gradient logs. Geophysics, v. 42, no. 4, p. 823-837.

Conaway, J.G., 1977b. Fine scale correlation between temperature gradient logs and lithology. Geophysics, v. 42, no. 7, p. 1401-1410.

CPN Corp., 1984. Operator's maual, 501DR Depthprobe moisture depth gauge. CPN Corp., Pacheco, California.

Croft, M.G., 1971. A method of calculating permeability from electric logs. U.S. Geological Survey Professional Paper 750-B, p. 265-269.

Davis, J.C., 1986. *Statistics and Data Analysis in Geology*. John Wylie & Sons, 636 p.

Davison, C.C., W.S. Keys and F.L. Paillet, 1982. Use of borehole-geophysical logs and hydrologic tests to characterize crystalline rock for nuclear-waste storage. Whiteshell Nuclear Research Establishment, Manitoba and Chalk River Nuclear Laboratory, Ontario, Canada; Columbus, Ohio, Battelle Project Management Division Office of Nuclear Waste Isolation Technical Report 418, 103 p.

Doveton, J. H., 1986. *Log Analysis of Subsurface Geology*. John Wiley and Sons, 273 p.

Drury, M.J., 1984. Borehole temperature logging for the detection of water flow. Geoexploration, v. 22, p. 231-244.

Dyck, A.V. and R.P. Young, 1985. Physical characterization of rock masses using borehole methods. Geophysics, v. 50, no. 12, p. 2530-2541.

Dyck, J.H., W.S. Keys and A.W. Meneley, 1972. Application of geophysical logging to groundwater studies in southeastern Saskatchewan. Canadian Journal of Earth Sciences, v. 9, no. 1, p. 78-94.

Elkington, P.A.S., J.R. Samworth and M.C. Enstone, 1989. High- resolution logging for thin beds. BPB Instruments Ltd., East Leake, Loughborough, LE126JQ, England.

Elkington, P.A.S., P. Stouthamer, and R.J. Brown, 1982. Rock strength prediction from wireline logs. International Journal of Rock Mechanics, Mineral Science and Geomechanical Abstracts, v. 19, p. 91-97.

Emerson, D.W. and B. M. Hanes, 1974. The interpretation of geophysical well logs in water bores in unconsolidated sediments. Bulletin, Australian Society of Exploration Geophysics, v. 5, no. 3, p. 89-117.

Fenton, M.M., 1983a. Composition of deformation terrain (glacial thrust terrain): a clue to glacial entrainment and transport. Geological Association of Canada, Program with Abstracts, v. 8, p. A22.

Fenton, M.M., 1983b. Deformation terrain mid-continent region: properties, subdivision, recognition. Geological Society of America, North-Central Section, Program with Abstracts, v. 15, p. 250.

Fenton, M.M., 1984a. Deformation terrain Canadian prairies: morphology and sediment facies. INQUA Commission on Genesis and Lithology of Quaternary Deposits, Symposium on the Relationship Between Glacial Terrain and Glacial Sediment Facies, abstracts and program, Alberta Research Council publication, p. 7-8.

Fenton, M.M., 1984b. Quaternary stratigraphy, Canadian Prairies. *In:* International Geological Correlation Program Project 73/1/24; Quaternary Glaciations in Northern Hemisphere, Canadian Summary Volume. Geological Survey of Canada Paper, p. 57-68.

Fenton, M.M., 1987. Deformation terrain on the northern Great Plains. *In:* W.L. Graf, ed., Geomorphic Systems of North America. Geological Society of America Centennial Special Volume No. 2, Chapter 6 Great Plains, p. 176-182.

Fenton, M.M., and L.D. Andriashek, 1987. Glaciotectonic features in the Sand River area northeastern Alberta, Canada. Abstracts 5th Biennial Meeting American Quaternary Association, Edmonton, Alberta, p. 199.

Fenton, M.M., C.W. Langenberg., C.E. Jones; M.R. Trudell, J.G. Pawlowicz, J.A. Tapics, and D.J. Nikols, 1985a. Tour of the Highvale open pit coal mine. Guidebook for the Petroleum Society of CIM and Canadian Society of Petroleum Geologists joint conference, Edmonton, Alberta. Alberta Research Council Open File Report 1985-7, 55 p.

Fenton, M.M., C.E. Moell, J.G. Pawlowicz and C.W. Langenberg, 1985b. Deformation terrain Canadian Prairies: landforms, lithofacies and processes. Geological Society of America, Program with Abstracts, North Central Section annual meeting, Dekalb, Illinois, v. 17, p. 287.

Fenton, M.M. and J.G. Pawlowicz, 1989. Glacially thrust bedrock: styles and ramifications for coal mining. *In:* Advances in Western Canadian Coal Geoscience - Forum Proceedings; Alberta Research Council, Information Series No. 103, p. 365.

Fenton, M.M. and J.G. Pawlowicz, in press. Glacially deformed bedrock: implications for coal exploration and highwall stability. AAPG/EMD Volume on Geology in Coal Resource Utilization.

Fenton, M.M., M.R. Trudell, J.G. Pawlowicz, C.E. Jones, S.R. Moran and D.J. Nikols, 1986. Glaciotectonic deformation and geotechnical stability in open pit coal mining. *In:* R.K. Singhal, ed., *Geotechnical Stability in Surface Mining*, A.A. Balkema, Rotterdam, p. 225-234.

Fertl, W.H., 1979. Gamma ray spectral data assists in complex formation evaluation. The Log Analyst, v. XX, no. 5, Sept.-Oct., p. 3-37.

Flach, P.D., 1984. Oil sands geology - Athabasca deposit north. Alberta Research Council, Bulletin No. 36, 31 p.

Gaur, R.S. and I. Singh, 1965. Relationship between permeability and gamma ray intensity for the Oligocene sand of an Indian field. Oil and Natural Gas Commission of India, Bulletin v. 2, no. 1, p. 74-77.

Grasty, R.L., Q. Bristow, G.W. Cameron, W. Dyck, J.A. Grant and P.G. Killeen, 1982. Preliminary calibration of a laboratory gamma ray spectrometer for the measurement of potassium, uranium and thorium. Uranium Exploration Methods (Symposium Proceedings), OECD/NEA, Paris, 1982, p. 699-712.

Guyod, H., and L.E. Shane, 1969. Introduction to geophysical well logging - acoustical logging. *Geophysical Well Logging*, v. 1. Hubert Guyod, publisher, Houston, Texas; 256 p.

Halker, A., N.J. Kuzuiv, W.D. Mellor, and R.K. Whitworth, 1982. The synthesis of fracture/strength logs using borehole geophysics: a new geotechnical service. Quarterly Journal of Engineering Geology, Geological Society of London, v. 15, p. 15-18.

Hearst, J.R., 1979. Calibration of a neutron log in partially saturated media. 20th Annual Meeting, Society of Professional Well Log Analysts, Paper B.

Hearst, J.R. and P.H. Nelson, 1985. *Well Logging for Physical Properties*. McGraw-Hill, New York; 571 p.

Hebblewhite, B.K., R.L. Blackwood, G.E. Holt, P.A. Mokula, A. Richmond, G. O'Regan, C. Mallett and J. Enever, 1986. Rock mechanics and stability of excavations. Australasian Coal Mining Practice, Monograph 12; AIMM, Victoria, Australia.

Helander, D.P., 1983. *Fundamentals of Formation Evaluation*. Tulsa Oil & Gas Consultants International, Inc., 332 p.

Heslop, A., 1974. Gamma ray log response of shaley sandstones. 15th Annual Logging Symposium, Society of Professional Well Log Analysts, Paper M.

Hess, A.E., 1982. A heat pulse flowmeter for measuring low velocities in boreholes. U.S. Geological Survey Open-file Report 82-699.

Hess, A.E., 1984. Use of a low velocity borehole flowmeter in the study of hydraulic conductivity in fractured rock. Proceedings, Surface and Borehole Geophysical Methods in Groundwater Investigations, February 6-9, San Antonio, Texas.

Hess, A.E., 1986. Identifying hydraulically conductive fractures with a slow-velocity borehole flowmeter. Canadian Geotechnical Journal, v. 23, p. 69-78.

Hoffman, G.L., G.R. Jordan and G.R. Wallis 1982. *A Geophysical Borehole Logging Handbook for Coal Exploration.* Coal Mining Research Company, Devon, Alberta; 270 p.

Holmes, J.W., 1966. Influence of bulk density of soil on neutron moisture meter calibration. Soil Science, v. 102, p. 35-36.

Holtz, R.D. and W.D. Kovacs, 1981. An Introduction to Geotechnical Engineering. Prentice-Hall Inc., Englewood Cliffs, New Jersey; 733 p.

Hopkins, O.B., 1923, Some structural features of the Plains area of Alberta caused by Pleistocene glaciation. Geological Society of America, Bulletin, v. 34, p. 419-430.

Huang, C.F. and J.A. Hunter, 1984. The tube wave methods of estimating in-situ rock fracture permeability in fluid-filled boreholes. Geoexploration, v. 22, p. 245-260.

Irish, E.J.W., 1970. The Edmonton Group of south-central Alberta. Bullertin of Canadian Petroleum Geology, v. 18, p. 125-155.

Jeffries, F.S., 1966. Computer correlation of wireline log parameters and core analysis parameters. The Log Analyst, v. 7, no. 3, p. 6-14.

Kenny, T.C., 1967. The influence of mineral composition on the residual strength of natural soils. Proc. Geot. Conf., Oslo, Norway; v.1.

Keys, W.S., 1979. Borehole geophysics in igneous and metamorphic rocks. 20th Annual Logging Symposium, Society of Professional Well Log Analysts, Paper OO.

Keys, W.S., 1986. Analysis of geophysical logs of water wells with a microcomputer. Groundwater v. 24, no. 6, p. 750-760.

Keys, W.S., 1989a. *Borehole Geophysics Applied to Ground-Water Investigations.* U. S. Geological Survey, Open-File Report OFR 87-539; also published by National Water Well Association, Dublin, Ohio; 313 p.

Keys, W.S, 1989b. Methods for analyzing geophysical logs and core analyses, Highvale Mine, Alberta, Canada. Unpublished technical memorandum to TransAlta Utilities Corp., Feb. 1989.

Keys, W.S. and L.M. MacCary, 1971. *Application of Borehole Geophysics to Water-Resources Investigations.* U.S. Geological Survey, Techniques of Water-Resources Investigations, Book 2, chap. E1, 126 p.

Keys, W.S., and J.K. Sullivan, 1979. Role of borehole geophysics in defining the physical characteristics of the Raft River geothermal reservoir, Idaho. Geophysics, v. 44, no. 6, p. 1116-1141.

Killeen, P.G., 1982. Gamma-ray logging and interpretation. *In:* A.A. Fitch, ed., *Developments in Geophysical Exploration Methods*, Book 3, Chapter 7, p. 95-150; Applied Science Publishers, Barking, Essex, England.

Killeen, P.G. (ed.), 1986. Borehole Geophysics for Mining and Geotechnical Applications. Geological Survey of Canada, Paper 85-27, 400 p.

Killeen, P.G. and J.G. Conaway, 1978. New facilities for calibrating gamma ray spectrometric logging and surface exploration equipment; Canadian Mining and Metallurgy Bulletin. v. 71, no. 793, p. 84-87.

Killeen, P.G. and C.J. Mwenifumbo, 1989. Interpretation of new generation geophysical logs in Canadian mineral exploration. *In:* Proceedings of the Second International Symposium on Borehole Geophysics for Minerals, Geotechnical and Groundwater Applications; Mineral and Geotechnical Logging Society, Society of Professional Well Log Analysts, p. 167-178.

Kupsch, W.O., 1962. Ice-thrust ridges in western Canada. Journal of Geology, v. 70, no. 5, p. 582-594.

Kwader, T., 1982. Interpretation of borehole geophysical logs in shallow carbonate environments and their application to groundwater resource investigations. Ph.D. Thesis, Florida State University; 201 p.

Kwader, T., 1984. Estimating aquifer permeability from formation resistivity factors. Proceedings, Surface and Borehole Geophysical Methods in Groundwater Investigations, February 6-9, San Antonio, Texas; p. 713-721.

Kwader, T., 1985. The use of geophysical logs for determining formation water quality. Groundwater, v. 24, no. 1, p. 11-15.

Lau, J.S.O., 1980. Borehole television survey. *In:* Canadian Institute of Mining and Metallurgy, Special Volume 22.

Lerbekmo, J.F., 1968. Chemical and modal analyses of some Upper Cretaceous and Paleocene bentonites from Western Alberta. Canadian Journal of Earth Sciences, v. 5, p. 1505-1511.

Locker, J.G., 1973. Petrographic and engineering properties of fine-grained rock of central Alberta. Alberta Research Council Bulletin 30.

Manabe, H., S. Ueno and M. Morino, 1983. Use of the microflowmeter in investigation of underground water. Report TN-42, OYO Corporation, Urawa Research Institute, Urawa Saitama, Japan. 18 p.

Mathewson, C.C. and K.D. Cato, 1986. "Pre and post" mine geotechnical conditions for surface mines, developed from the comprehensive exploration program. Proceedings, International Symposium on Geotechnical Stability in Surface Mining; Calgary, Alberta, November 6-7, 1986, p. 3-10.

McKeague, J.A., 1978. *Manual on Soil Sampling and Methods of Analysis;* 2nd edition. Canadian Society of Soil Science; 212 p.

McNalley, G.H., 1987. Geotechnical applications and interpretations of downhole geophysical logs. Unpublished ACIRL End-of-Grant Report to the Australian Coal Association, Project A21.

Melville, J.G., F.J. Malz and O. Guren, 1985. Laboratory investigation and analysis of a groundwater flowmeter. Groundwater, v. 23, no. 4, p. 486-495.

Moell, C.E., J.G. Pawlowicz, M.R. Trudell, M.M. Fenton, C.W. Langenberg, G.J. Sterenberg, and C.E. Jones, 1985. Highwall stability project, Highvale Mine, report of 1984 activities. Unpublished report prepared for TransAlta Utilities Corporation by Terrain Sciences Department, Alberta Research Council, 256 p.

Monenco, 1981. Investigation of St. Mary's Compensating Works, Great Lakes Power Limited, Sault Ste. Marie, Ontario. Report for Great Lakes Power Limited by Monenco Consultants Ltd., Calgary.

Monenco, 1988. Highvale Mine material diggability for the ultimate mine - preliminary application of criteria. Report for TransAlta Utilities Corporation by Monenco Consultants Ltd., Calgary.

Monenco, 1989. Highvale Mine geotechnical assessment of the 1991-1995 contract area. Report for TransAlta Utilities Corporation by Monenco Limited, Calgary.

Monenco, 1990. Highvale Mine material diggability for the ultimate mine - blasting/diggability mapping. Report for TransAlta Utilities Corporation by Monenco Consultants Ltd., Calgary; 2 vols.

Moran, S.R., 1971. Glaciotectonic structures in drift. *In:* R.P. Goldthwait, ed., *Till: A Symposium.* Ohio State University Press, Columbus, Ohio, p. 127-148.

Moran, S.R., L. Clayton, R. Hooke, LeB., M.M. Fenton, and L.D. Andriashek, 1980. Glacier-bed landforms of the prairie region of North America. Journal of Glaciology, v. 25, no. 93, p. 457-476.

Morgenstern, N.R. and J.S. Tchalenko, 1967. Microscopic structures in kaolin subjected to direct shear. Geotechnique, v. 17.

Mwenifumbo, C.J., 1989. The use of temperature logs in coal seam mapping. *In:* Advances in Western Canadian Coal Geoscience - Forum Proceedings; Alberta Research Council, Information Series No. 103, p. 365.

Mwenifumbo, C.J., P.G. Killeen and B. Elliott, 1989. Application of state-of-the-art borehole geophysical techniques to coal mining problems, Highvale Mine. *In:* Advances in Western Canadian Coal Geoscience - Forum Proceedings; Alberta Research Council, Information Series No. 103, p. 366.

NAVFAC, 1971. *Soil Mechanics, Foundations and Earth Structures.* U.S. Dept. of the Navy, Design Manual DM-7.

Nelson, P.H., 1982. Advances in borehole geophysics for hydrology. Geological Society of America, Special Paper 189, p. 207-219.

New, B.M., 1986. A seismic transmission tomography technique for rock quality evaluation in borehole geophysics for mining and geotechnical applications. Geological Survey of Canada, Paper 85-27, p. 173-180.

Nieuwenhuis, J.D. and P.A. Ruijgrok, 1978. Measurement of in-situ density of thick fill layers by radiometric methods. Engineering Geology 3, sec. 4, v. 2, p. 44-45.

O'Regan, G., A.L. Davies and B.I. Ellery, 1987. Correlation of bucketwheel performance with geotechnical properties of overburden at Goonyella Mine, Australia. Proceedings, International Symposium on Surface Mining, Edmonton, Alberta. Surface Mining, v. 1, no. 1-3, p. 381-396.

Olsson, O., O. Forslund, E. Sandberg, and L. Falk, 1986. Borehole radar; a new technique for investigation of large rock volumes. *In:* Expanded Abstracts, Society of Exploration Geophysicists.

Paillet, F.L., 1980. Acoustic propagation in the vicinity of fractures which intersect a fluid-filled borehole. *In:* Society of Professional Well Log Analysts, 21st Annual Logging Symposium, LaFayette, Louisiana; Transactions, Society of Professional Well Log Analysts, Houston, Paper DD, p. DD1-DD33.

Paillet, F.L., 1981. A comparison of fracture characterization techniques applied to near-vertical fractures in a limestone reservoir. *In:* Society of Professional Well Log Analysts, 22nd Annual Logging Symposium, Mexico City, 1981; Transactions, Society of Professional Well Log Analysts, Houston, Paper XX, p. XX1-XX29.

Paillet, F.L., 1985. Applications of borehole-acoustic methods in rock mechanics. Proceedings, 26th U.S. Symposium on Rock Mechanics, Rapid City, South Dakota, 26-28 June 1985; E. Ashworth, ed.; p. 207-220.

Paillet, F.L. and A.E. Hess, 1986. Geophysical well-log analysis of fractured crystalline rocks at East Bull Lake, Ontario, Canada. U.S. Geological Survey, Water-Resources Investigations Report 86-4052.

Paillet, F.L. and J.E. White, 1982. Acoustic modes of propagation in the borehole and their relationship to rock properties. Geophysics, v. 47, no. 8, p. 1215-1228.

Patten, E.P. and G.D. Bennett, 1963. Application of electrical and radioactive well logging to groundwater hydrology. U.S. Geological Survey, Water Supply Paper 1544-D, 59 p.

Pauls, D.R. and G. Lobb, 1986. Geotechnical and hydrogeological bibliographic citations from computerized databases. Unpublished technical memorandum to TransAlta Utilities Corporation.

Pawlowicz, J.G., M.M. Fenton, J.D. Henderson and A.N. Sartorelli, 1989. Geophysics for Plains Coal Mining. *In:* Advances in Western Canadian Coal Geoscience - Forum Proceedings; Alberta Research Council, Information Series No. 103, p. 341-353.

Plumb, R.A., Brie, A. and Hsu, K., 1985. Fracture detection and evaluations using new wireline methods. 26th U.S. Symposium on Rock Mechanics, Rapid City, S.D., June 26-28.

Poole, D., 1984. Acoustic evaluation of rock quality. Tunnels and Tunnelling, v. 16, no. 11, p. 41-42.

Quirein, J.A., J.S. Gardner and J.T. Watson, 1982. Combined natural gamma ray spectral/lith-density measurements applied to complex lithologies. Society of Petroleum Engineers of the American Institute of Mining, Metallurgical, and Petroleum Engineers, Paper SPE 11143, 14 p.

Rabe, C.L., 1957. A relation between gamma radiation and permeability, Denver-Julesberg Basin. Transactions American Institute of Mining Metallurgical and Petroleum Engineers, v. 210, p. 358-360.

Richardson, R.J.H., R.S. Strobl, D.E. Macdonald, J.R. Nurkowski, P.J. McCabe and A. Bosman, 1988. An evaluation of the coal resources of the Ardley coal zone, to a depth of 400 m in the Alberta plains area. Alberta Reseach Council, open file report 1988-02, 96 p.

Sardeson, F.W., 1898. The so-called Cretaceous deposits in southeastern Minnesota. Journal of Geology, v. 6, p. 679-691.

Sardeson, F.W., 1905. A peculiar case of glacial erosion. Journal of Geology, v. 13, p. 351-357.

Sardeson, F.W., 1906. The folding of subjacent strata by glacial action. Journal of Geology, v.14, p. 226-232.

Schimschal, U., 1981a. Flowmeter analysis at Raft River, Idaho. Groundwater v. 19, no. 1, p. 93-97.

Schimschal, U., 1981b. The relationship of geophysical measurements to hydraulic conductivity at the Brantley Damsite, New Mexico. Geoexploration, v. 19, p. 115-125.

Seed, H.B. and I.M. Idriss, 1971. Simplified procedure for evaluation soil liquefaction potential. Journal Soil Mechanics and Foundations Division of American Society of Civil Engineering, v. 97, no. SM9, Paper 8371, p. 1249-1273.

Serra, O., J. Baldwin and J. Quirein, 1980. Theory, interpretation and practical applications of natural gamma ray spectroscopy. 21st Annual Logging Symposium, Society of Professional Well Log Analysts, Houston, Texas.

Singh, R.N., F.P. Hassani and P.A.S. Elkington, 1983. The application of strength and deformation index testing to the stability assessment of coal measures excavations. Proceedings, 24th U.S. Symposium on Rock Mechanics, College Station, Texas, June 1983, p. 599-607.

Skempton, A.W., 1964. Long term stability of clay slopes. 4th Rankine Lecture, Geotechnique, ICE, London, U.K.

Soonawala, N.M., 1983. Geophysical logging in granites. Geoexploration, v. 21, p. 221-230.

Sterenberg, C.J., 1988. Big Valley drilling program - report of results and procedures. Unpublished report for TransAlta Utilities Corporation by Alberta Geological Survey, Alberta Research Council.

Syms, M.C., 1980. Interpretation of flowmeter and temperature logs from geothermal wells. Report 168, Department of Scientific and Industrial Research, New Zealand, 63 p.

Syms, M.C., 1982. Downhole flowmeter analysis using an associated caliper log. Groundwater v. 20, no. 5, p. 606-610.

Tate, T.K., A.S. Robertson and D.A. Gray, 1970. The hydrogeological investigation of fissure flow by borehole logging techniques. Quarterly Journal of Engineering Geology, v. 2, p. 195-215.

Timofeev, O.V., E.P. Popov, I.G. Shelekhov and E.R. Vishnyakov, 1972. Use of gamma-gamma density logging to study the deformation of rock support by bolts. Soviet Mining Science 8/5, p. 593-596.

TransAlta Utilities Corporation, 1989. Downhole Geophysics Project, Phase 3A Progress Report. Unpublished report on behalf of the joint venture research group, 22p.

TransAlta Utilities Corporation, 1988. Determining geotechnical and hydrogeological parameters using downhole geophysics in the Canadian plains. Phase 2 Report, Correlations of Existing Data. Unpublished report on behalf of the joint venture research group, 57 p.

TransAlta Utilities Corporation, 1987. Determining geotechnical and hydrogeological parameters using downhole geophysics in the Canadian plains. Phase 1 Report, A Review of Potential Applications. Unpublished report on behalf of the joint venture research group, 56 p.

Underwood, L.B. and N.A. Dixon, 1976. Dams on rock foundations. Proceedings, Specialty Conference on Rock Engineering for Foundations and Slopes; University of Colorado, Boulder, Colorado. American Society of Civil Engineers, publishers, 1977.

Velleman, P.F., 1989. Data Desk Handbook, Volume 1. Odesta Corporation, Northbrook, Illinois.

Wade, N.H., 1989. Overburden diggability for surface coal mines. *In:* Advances in Western Canadian Coal Geoscience - Forum Proceedings; Alberta Research Council, Information Series No. 103, p. 315-329.

Wade, N.H., D.J. Nikols and F. Naderi, 1988. Role of the computer in managing and applying geotechnical data to surface mine design. Proceedings, 1st Canadian Conference on Computer Applications in the Mineral Industry; Quebec City; p.339-352, A.A. Balkema, Rotterdam.

Wade, N.H., G.M. Olgilvie and R.M. Krzanowski, 1987. Assessment of BWE diggability from geotechnical, geological and geophysical parameters. Proceedings, International Symposium on Surface Mining; Edmonton, Alberta. Surface Mining, v. 1, no. 1-3, p. 375-380.

Wenk, G.J. and B.L. Dickson, 1981. The gamma logging calibration facility at the Australian Mineral Development Laboratories. Bulletin Australian Society of Exploration Geophysicists, v. 12, no. 3, p. 37-39.

Wheatcraft, S.W., K.C. Taylor, J.W. Hess and T.M. Morris, 1986. Borehole sensing methods for groundwater investigations at hazardous waste sites. Desert Research Institute, University of Nevada System, Publication #41099, 69 p.

Wilder, D.G. and L. Chung Hsing, 1983. Liquefaction potential assessment based on borehole geophysical logging concept and case history. 24th Annual Logging Symposium, Society of Professional Well Log Analysts, Houston, Texas.

Wilson, R.A. and R.G. Chopiuk, 1987. Current research in Alberta into the use of geophysics for geotechnical and hydrogeological data collection. *In:* Proceedings of the Second International Symposium of Borehole Geophysics for Minerals, Geotechnical and Groundwater Applications, Minerals and Geotechnical Logging Society, Society of Professional Well Log Analysts, Houston, Texas, p. 45-50.

Wong, J., N. Bregman, G. West and P. Hurley, 1987. Cross-hole seismic scanning and tomography. Leading Edge, v. 6, no. 1, p. 36-40.

Worthington, P.F., 1975. Quantitative geophysical investigations of granular aquifers. Geophysical Surveys, v. 2, p. 313-366.

Zemanek, J., R.L. Caldwell, E.E. Glenn, Jr., S.V. Holcomb, L.J. Norton and A.J.D. Straus, 1969. The borehole televiewer - a new logging concept for fracture location and other types of borehole inspection. Journal of Petroleum Technology, v. 21, no. 6, p. 762-774.

Zeevart, L., 1983. *Foundation Engineering for Difficult Subsoil Conditions;* 2nd ed. Van Nostrand Reinhold, New York; 552 p.

11. APPENDICES

A. LAS: A SIMPLE FLOPPY DISK STANDARD FOR LOG DATA
B. LIST OF HIGHVALE LOGS & GEOPHYSICAL SONDES (GEOTECHNICAL)
C. DEVELOPMENT OF A 3-DIMENSIONAL GRAPH USING CARTESIAN CO-ORDINATES
D. GOOD SYNCRUDE CORRELATIONS (GEOTECHNICAL)
E. GOOD CORRELATIONS FOR HIGHVALE & BIG VALLEY (GEOTECHNICAL)
F. 3-PARAMETER CORRELATIONS (GEOTECHNICAL)
G. EXAMPLES OF POOR CORRELATIONS (GEOTECHNICAL)
H. DIGGABILITY PROGRAM
I. NEUTRON MOISTURE PROBE
J. FULL-WAVE SONIC SONDE - BPB SPECIFICATIONS

APPENDIX A

LAS:

A SIMPLE FLOPPY DISK STANDARD FOR LOG DATA

LAS;

A SIMPLE FLOPPY DISK

STANDARD FOR LOG DATA

BY

CWLS Foppy Disk Committee

Case Struyk	- Gulf Canada Resources Ltd. (Chairman)
Richard Bishop	- BPB Wireline Services
Eric Foster	- Q.C. Data Collectors Ltd.
Doug Fortune	- Riley's Datashare International Ltd.
Don Gordon	- Atlas Wireline Services
Ted d'Haene	- Halliburton Logging Services
Dave Joyce	- Schlumberger of Canada
Steven Kenny	- Digitech Information Services Ltd.
Harold Kowalchuk	- Computalog Ltd.
Mike Stadnyk	- Great Guns Logging Canada Ltd.

ABSTRACT

The Canadian Well Logging Society's Floppy Disk Committee has designed a standard for log data on floppy disks. It is known as the LAS format (Log ASCII Standard). LAS consists of files written in ASCII containing minimal header information and is intended for optical curves only. Details of the LAS format are described in this paper.

The purpose of the LAS format is to supply basic digital log data to users of personal computers in a format that is quick and easy to use.

Log analysts who use personal computers in log analysis have in the past been entering log data into their machines mainly through a hand digitizing procedure because this was found to be the most efficient method. Most personal computers are unable to handle data from magnetic tapes. The industry was beginning to address this problem by making log data available on floppy disks in a variety of formats. It was at this point that the Canadian Well Logging Society set up the Floppy Disk Committee to design a standard for log data on floppy disks that would meet the requirements of the users of personal computers.

Various standards for digital well log data already exist, the LIS format (Log Information Standard) is one of the more popular standards. A more complete standard is presently being prepared by the American Petroleum Institute which will be known as the DLIS format (Digital Log Interchange Standard). Both of these standards are very useful but because of their completeness, they have become complex and therefore do not address the needs of the personal computer users who have serious space limitations on their machines.

Personal computer users are normally only interested in the optically presented curves and need to get these curves into their machines quickly and easily. The LAS format addresses these needs and can be compared to a "Readers' Digest" version of the LIS or DLIS formats. It should address the needs of 80% of the personal computer users. If more detailed log information is needed then the LIS or DLIS format should be used. The LAS format is intended to complement the LIS or DLIS formats as each has its own specific purpose.

GENERAL DESCRIPTION

The LAS format was so designed that it can be easily understood by the user and at the same time contains enough flags to assist the programmer. The LAS format must always be written in ASCII. If it is written using a compression routine, in binary or in any other form, an executable program must exist on the floppy disk that will convert the file back to LAS format.

The LAS format consists of files that are independent units. For example, a repeat section would make up one file and the main pass another. Each of the file names will end in ".LAS" so that they may be easily identified. Each floppy disk must not contain partial files that continue onto a second floppy disk. Large file that do not fit on one floppy must be split into two or more files.

Each file consists of up to six sections. These sections are not order specific except for the last section which must always be the data section. The first section is usually the "VERSIONS" section which contains the version number of the LAS format and whether the data is in wrap mode or not. The "WELL INFORMATION" section contains information on the well name, location, and the start and stop depths of the data in this file. The "CURVE INFORMATION" section contains the curve mnemonics, units used and definition of mnemonics in the order that they appear in the data section. The "PARAMETER" section contains information on parameters and constants and is optional. The "OTHER" section is also optional and contains any other information or comments. The last section is always the "ASCII LOG DATA" section. Each column of data must be separated by a space and depth values should appear in the first column. The exact LAS format specifications can be found in the appendix.

REFORMAT PROGRAM

To assist users of LAS formatted data, a program was written to modify LAS files into a form which may be more compatible to the user's needs. The program is called REFORMAT and can perform the following tasks:

1)Reverse depth direction

2)Change sampling interval

3)Extract specific curves

4)Extract a specific depth interval

5)Convert wrap mode to unwrap mode

The REFORMAT program was written by Robin Winsor of Gulf Canada Resources Ltd. in ANSI standard "C" and has been compiled with a Microsoft C 5.1 compiler. The author of this program does not reserve any rights and does not warrant the program for any specific purpose. The actual source code will be made available after March 30,1990. The time delay is to ensure that most of the bugs in the program have been eliminated. An executable form of the program can be obtained from various sources including the CWLS.

CONCLUSIONS

Testing of the LAS format and the REFORMAT program has taken place and suggestions received were used to create this version 1.2 . The CWLS Floppy Disk Committee will be monitoring the LAS format, address problems and make modifications to the standard as required. Feedback concerning the user's likes or dislikes would be greatly appreciated and should be sent to the CWLS to the attention of the Floppy Disk Committee.

It is hoped that by creating the LAS format, more widespread use will be made of digital log data.

APPENDIX

LAS FORMAT SPECIFICATIONS FOR VERSION 1.20

PART 1 GENERAL DESCRIPTION

The CWLS LAS Format was designed to store log data on floppy disks. This standard is intended to simplify the exchange of digital log data between users. The general specifications of this format are as follows:

1) The floppy disk size, type, or density is not specified because conversion between them is straight forward.

2) It is the intent of this standard to store optically presented log curves although other curves may also be stored. Raw count rates, wave form data, etc. is much more efficiently stored on magnetic tape using LIS or DLIS format.

3) Floppy disks in the LAS format must be MS/DOS or PC/DOS compatible

4) The file will be written in ASCII. If the file is written using a compression method, in binary or any other form an executable program must exist on the floppy to convert it back to LAS format.

5) Each floppy disk must not contain partial files that continue onto a second floppy. Large files that do not fit onto one floppy must be split into two or more separate files.

6) All files in LAS format must end in ".LAS" so that they may be easily recognized.

7) The LAS format is a minimum standard. It is expected that most users and suppliers will exceed this minimum standard.

PART 2 MAJOR COMPONENTS OF A LOG FILE

Each log file contains up to six sections and each section begins with a tilde (~) mark. The last section in a file will always be the log data section.

The sections that make up a log file are as follows:

- **~V** - contains version and wrap mode information
- **~W** - contains well identification
- **~C** - contains curve information
- **~P** - contains parameters or constants
- **~O** - contains other information such as comments
- **~A** - contains ASCII log data

Each of these sections are described in more detail in part four of this paper.

PART 3 FLAGS

Flags are used to assist computers in identifying specific lines in a file. The following flags are used in the LAS format:

a) "~" (tilde): The ASCII equivalent of this flag is decimal 126 or hexadecimal 7E. This flag when used will be the first non-space and non-quotation character on a line. It is used to mark the beginning of a section in a file. The first letter directly after the tilde identifies the section. (See part two.) All upper case letters in the space following a tilde mark are reserved for use by the committee. The remainder of the line will be treated as comments.

b) "#" (pound); The ASCII equivalent of this flag is decimal 35 or hexadecimal 23. This flag when used will be the first non-space and non-quotation character on a line. The Pound sign is used to indicate that the line is a comment line. Comment lines can appear anywhere above the data section.

c) "." and ":" : In sections other than the data section, dots and colons are used to delimit information within the line . They are usually aligned with ones on the lines below for ease of reading. Information to the right of the colon is a detailed definition of the mnemonics that are located to the left of the colon. The dot is used to separate two mnemonics. Spaces may occur to the right or left of a dot or colon.

PART 4 DETAILS

The actual format for each of the sections discussed in this part of the paper is best understood by looking at the examples in the boxed areas. The exact spacing is not critical because computer programs will use the dots, colons and spaces to decipher each line.

(I) ~V (Version Information)

-This section is mandatory and must always appear at the very beginning of the file.

-It identifies which version of CWLS standard is being used and whether wrap mode is used.

-This section must contain the following lines:

"VERS. 1.20: CWLS LOG ASCII STANDARD - VERSION 1.2"
Refers to which version of LAS was used.

"WRAP. YES: Multiple lines per depth step"
OR
"WRAP. NO: One line per depth step"
Refers to whether a wrap-around mode for the data trailing the depth increment was used or not. If no wrap mode is used the line will have a maximum length of 256 characters (this includes the carriage return and line feed). If wrap mode is used the depth value will be on its own line and all lines of data will be no longer than 80 characters (this includes carriage return and line feed).

-Additional lines are optional.

```
~Version Information
 VERS.                  1.20:   CWLS log ASCII Standard -VERSION 1.20
 WRAP.                    NO:   One line per depth step
```

(II) ~W (Well Information)

-This section is mandatory.

-It identifies the well, its location and indicates the start and stop depth of the file.

-This section must contain the following lines with the mnemonics as indicated:

"STRT.M nnn.nn:"
Refers to the first depth in the file. The "nnn.nn" refers to the depth value. The number of decimals used is not restricted, The ".M" refers to meters and can be replaced when other units are used. The start depth can either be greater or less than the stop depth.

"STOP.M nnn.nn:"
Refers to the last depth in the file. The "nnn.nn" refers to the depth value. The number of decimals used is not restricted. The ".M" refers to meters and can be replaced when other units are used.

"STEP.M nnn.nn:"
Refers to the depth increment used. A minus sign must precede the step value if the start depth is greater than the stop depth (ie, from TD to casing has a minus step value). A step value of zero indicates a variable step.

"NULL. -nnn.nn:"
Refers to null values. Two common ones in use are -9999 and -999.25 .

"COMP. COMPANY : "
Refers to company name.

"WELL. WELL:"
Refers to the well name.

"FLD. FIELD:"
Refers to the field name.

"LOC. LOCATION:"
Refers to the well location.

"PROV. PROVINCE:"
Refers to the province. For areas outside Canada this line may be replaced by:
"CNTY. COUNTY:"
"STAT. STATE:"
"CTRY. COUNTRY:"

"SRVC. SERVICE COMPANY:"
Refers to logging company.

"DATE. DATE:"
Refers to date logged.

"UWI . UNIQUE WELL ID:"
Refers to unique well identifier. (See References.) For areas outside of Canada this may be replaced by:

"API . API NUMBER:"

-Additional lines are optional. There is no limit set on the number of additional lines.

```
~Well Information Block
#MNEM.UNIT       Data Type    Information
#---------    -------------   ------------------------------
 STRT.M                635:
 STOP.M                400:
 STEP.M             -0.125:
 NULL.              -999.25:
 COMP.              COMPANY:   ANY OIL COMPANY INC.
 WELL.                 WELL:   ANY ET AL A9-16-49-20
 FLD .               FIELD:    EDAM
 LOC .            LOCATION:    A9-16-49-20W3M
 PROV.            PROVINCE:    SASKATCHEWAN
 SRVC.     SERVICE COMPANY:    ANY LOGGING COMPANY INC.
 DATE.           LOG DATE:     13-DEC-86
 UWI .     UNIQUE WELL ID:     100091604920W300
```

(III) ~C (Curve Information)

-This section is mandatory.

-It describes the curve and its units in the order that they appear in the data section of the file.

-The mnemonics used are not restricted but must be defined on the line on which they appear.

-API codes are optional. (See References.)

-The curves described in this section must be present in the data set.

-The first curve normally described should be depth.

-The following is an example of the curve section without API codes.

"SP .MV :SPONTANEOUS POTENTIAL"

-The following is an example of the curve section with API codes.

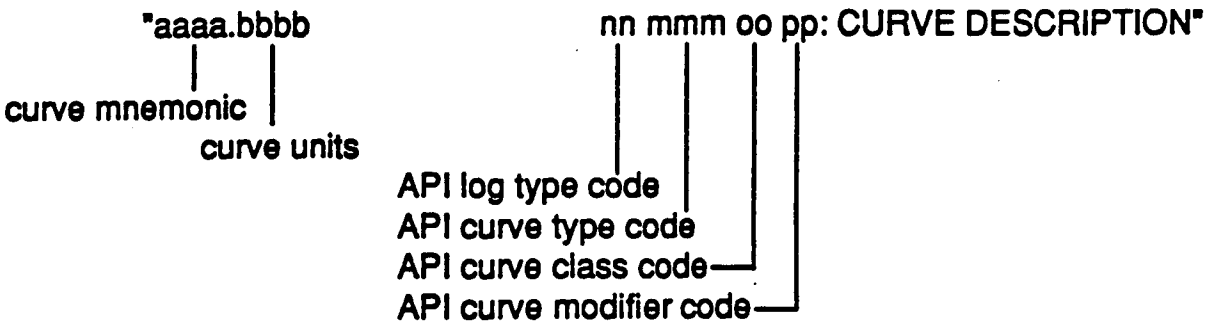


```
~Curve Information Block
#MNEM.UNIT      API CODE      Curve Description
#---------    ------------    ------------------------------
 DEPT.M                         1  DEPTH
 RHOB.K/M3     7 350 02 00:     2  BULK DENSITY
 NPHI.V/V      7 890 00 00:     3  NEUTRON POROSITY -SANDSTONE
 SFLU.OHMM     7 220 01 00:     4  Rxo RESISTIVITY
 SFLA.OHMM     7 222 01 00:     5  SHALLOW RESISTIVITY
 ILM .OHMM     7 120 44 00:     6  MEDIUM RESISTIVITY
 ILD .OHMM     7 120 46 00:     7  DEEP RESISTIVITY
 SP  .MV       7 010 01 00:     8  SPONTANEOUS POTENTIAL
 GR  .GAPI     7 310 01 00:     9  GAMMA RAY
 CALI.MM       7 280 01 00:    10  CALIPER
 DRHO.K/M3     7 356 01 00:    11  DENSITY CORRECTION
 PEF .         7 358 01 00:    12  LDT PHOTOELECTRIC
```

(IV) ~P (Parameter Information)

-This section is optional. It describes parameters or constants and their values.

-The mnemonics used are not restricted but must be defined on the line on which they appear.

-There is no limit on the number of lines that can be used.

-An example of a parameter line is as follows:

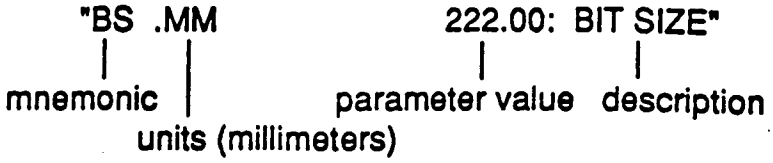


```
~Parameter Information Block
#MNEM.UNIT        Value        Description
#---------    -------------    ------------------------------
 BHT .DEGC         24.0000:    Bottom Hole Temperature
 BS  .MM          222.0000:    Bit Size
 FD  .K/M3        999.9999:    Fluid Density
 MDEN.K/M3       2650.0000:    Logging Matrix Density
 MATR.              1.0000:    Neutron Matrix(0=LIME,1=SAND,2=DOLO)
 FNUM.              1.0000:    Tortuosity  Constant Archie's (a)
 FEXP.              2.0000:    Cementation Exponent Archie's (m)
 DFD .K/M3       1200.0000:    Mud Weight
 DFV .S            50.0000:    Mud Viscosity
 DFL .C3            8.0000:    Mud Fluid Loss
 DFPH.             10.0000:    Mud pH
 RMFS.OHMM          2.8200:    Mud Filtrate Resistivity
 EKB .M           566.9700:    Elevation Kelly Bushing
 EGL .M           563.6799:    Elevation Ground Level
```

(V) ~O (Other Information)

-This section is optional; it is intended to be read as comments.

(VI) ~A (ASCII LOG DATA)

-The data section will always be the last section in a file.

-The depths should always appear in the first column

-Each column of data must be separated by at least one space.

-A line of less than 256 characters long will normally not be wrapped. This includes a carriage return and a line feed. Wrap mode will be used if the data is longer than 256 characters.

-In wrap mode, depth will be on its own line.

-In wrap mode a line of data will be no longer than 80 characters. This includes a carriage return and line feed.

-If wrap mode is used, the decimal points must be aligned for ease of reading.

-Exponents are not permitted. The curve section can be used to overcome this limitation by changing the units.

References

UWI codes : Formation Water Resistivities of Canada, CWLS, 1987.

API codes : API - Bul. D-9, 3rd edition, 1981.

Example #1

Illustrating Log ASCII Standard

(LAS)

```
~Version Information
 VERS.                  1.20:   CWLS log ASCII Standard -VERSION 1.20
 WRAP.                    NO:   One line per depth step
~Well Information Block
#MNEM.UNIT       Data Type    Information
#---------    -------------   ------------------------------
 STRT.M                635:
 STOP.M                400:
 STEP.M             -0.1250:
 NULL.              -999.25:
 COMP.              COMPANY:   ANY OIL COMPANY INC.
 WELL.                 WELL:   ANY ET AL A9-16-49-20
 FLD .                FIELD:   EDAM
 LOC .             LOCATION:   A9-16-49-20W3M
 PROV.             PROVINCE:   SASKATCHEWAN
 SRVC.     SERVICE COMPANY:   ANY LOGGING COMPANY INC.
 DATE.            LOG DATE:   13-DEC-86
 UWI .      UNIQUE WELL ID:   100091604920W300
~Curve Information Block
#MNEM.UNIT      API CODE      Curve Description
#---------    -------------   ------------------------------
 DEPT.M                        1  DEPTH
 RHOB.K/M3     7 350 02 00:    2  BULK DENSITY
 NPHI.V/V      7 890 00 00:    3  NEUTRON POROSITY -SANDSTONE
 SFLU.OHMM     7 220 01 00:    4  Rxo RESISTIVITY
 SFLA.OHMM     7 222 01 00:    5  SHALLOW RESISTIVITY
 ILM .OHMM     7 120 44 00:    6  MEDIUM RESISTIVITY
 ILD .OHMM     7 120 46 00:    7  DEEP RESISTIVITY
 SP  .MV       7 010 01 00:    8  SPONTANEOUS POTENTIAL
 GR  .GAPI     7 310 01 00:    9  GAMMA RAY
 CALI.MM       7 280 01 00:   10  CALIPER
 DRHO.K/M3     7 356 01 00:   11  DENSITY CORRECTION
 PEF .         7 358 01 00:   12  LDT PHOTOELECTRIC
~Parameter Information Block
#MNEM.UNIT        Value       Description
#---------    -------------   ------------------------------
 BHT .DEGC         24.0000:   Bottom Hole Temperature
 BS  .MM          222.0000:   Bit Size
 FD  .K/M3        999.9999:   Fluid Density
 MDEN.K/M3       2650.0000:   Logging Matrix Density
 MATR.              1.0000:   Neutron Matrix(0=LIME,1=SAND,2=DOLO)
 FNUM.              1.0000:   Tortuosity  Constant Archie's (a)
 FEXP.              2.0000:   Cementation Exponent Archie's (m)
 DFD .K/M3       1200.0000:   Mud Weight
 DFV .S            50.0000:   Mud Viscosity
 DFL .C3            8.0000:   Mud Fluid Loss
 DFPH.             10.0000:   Mud pH
 RMFS.OHMM          2.8200:   Mud Filtrate Resistivity
 EKB .M           566.9700:   Elevation Kelly Bushing
 EGL .M           563.6799:   Elevation Ground Level
~A  Depth       RHOB        NPHI       SFLU       SFLA       ILM        ILD
  635.0000  2256.0000      0.4033    22.0781    22.0781    20.3438    3.6660
  634.8750  2256.0000      0.4033    22.0781    22.0781    20.3438    3.6660
```

Example #2

Illustrating The Minimum Requirements

Of The Log ASCII Standard

(LAS)

```
~Version Information
 VERS.                 1.20:   CWLS log ASCII Standard -VERSION 1.20
 WRAP.                   NO:   One line per depth step
~W
 STRT.M                 635:
 STOP.M                 400:
 STEP.M              -0.1250:
 NULL.               -999.25:
 COMP.               COMPANY:   ANY OIL COMPANY INC.
 WELL.                  WELL:   ANY ET AL A9-16-49-20
 FLD .                 FIELD:   EDAM
 LOC .              LOCATION:   A9-16-49-20W3M
 PROV.              PROVINCE:   SASKATCHEWAN
 SRVC.      SERVICE COMPANY:   ANY LOGGING COMPANY INC.
 DATE.             LOG DATE:   13-DEC-86
 UWI .       UNIQUE WELL ID:   100091604920W300
~C
 DEPT.M                     :        DEPTH
 RHOB.K/M3                  :        BULK DENSITY
 NPHI.                      :        NEUTRON POROSITY - SANDSTONE
 SFLU.OHMM                  :        Rxo RESISTIVITY
 SFLA.OHMM                  :        SHALLOW RESISTIVITY
 ILM .OHMM                  :        MEDIUM RESISTIVITY
 ILD .OHMM                  :        DEEP RESISTIVITY
 SP  .MV                    :        SPONTANEOUS POTENTIAL
 GR  .GAPI                  :        GAMMA RAY
 CALI.MM                    :        CALIPER
 DRHO.K/M3                  :        DENSITY CORRECTION
 PEF .                      :        LDT PHOTOELECTRIC
~A
  635.0000  2256.0000     0.4033     22.0781     22.0781     20.3438     3.6660
  634.8750  2256.0000     0.4033     22.0781     22.0781     20.3438     3.6660
```

APPENDIX B

LIST OF HIGHVALE LOGS & GEOPHYSICAL SONDES USED

IN SECTION 3

DOWNHOLE GEOPHYSICS

GEOPHYSICAL LOGS

SUMMARY OF SONDE NUMBER

TESTHOLE NUMBER	FOCUSSED ELECTRIC	COAL COMBINATION	DUAL SPACED NEUTRON	MULTI-CHANNEL SONIC
HV-87-428	222	118	514	331
HV-87-430	222	118	514	331
HV-87-439	222	118	514	331
HV-87-441	222	118	514	331
HV-87-442	222	118	514	331
HV-87-443	222	118	514	331
HV-87-445	222	118	514	331
HV-87-447	222	118	514	331

DOWNHOLE GEOPHYSICS

GEOPHYSICAL LOGS

SUMMARY OF SONDE NUMBER

TESTHOLE NUMBER	FOCUSSED ELECTRIC	COAL COMBINATION	DUAL SPACED NEUTRON	MULTI-CHANNEL SONIC
HV-88-402	220	101	501	336
HV-88-403	220	101	501	336
HV-88-404	220	101	501	336
HV-88-405	220	101	501	336
HV-88-406	220	101	501	336
HV-88-407	220	101	501	336
HV-88-408	N/A	N/A	N/A	N/A
HV-88-409	220	160	501	336
HV-88-410	220	160	501	336
HV-88-411	220	160	501	336
HV-88-412	220	160	501	336
HV-88-413	232	101	501	336
HV-88-414	220	101	501	336
HV-88-415	232	101	501	336
HV-88-416	232	101	501	336
HV-88-417	232	101	501	336
HV-88-418	232	101	501	336
HV-88-419	232	101	501	336
HV-88-420	220	N/A	501	336
HV-88-421	232	101	501	336
HV-88-422	232	101	501	336
HV-88-423	232	101	501	336
HV-88-424	232	101	501	336
HV-88-425	232	101	501	336
HV-88-426	232	101	501	336
HV-88-427	232	101	501	336
HV-88-428	232	101	501	336
HV-88-429	232	101	501	336
HV-88-430	232	101	501	336
HV-88-431	232	101	501	336

DOWNHOLE GEOPHYSICS

GEOPHYSICAL LOGS

SUMMARY OF SONDE NUMBER

TESTHOLE NUMBER	FOCUSSED ELECTRIC	COAL COMBINATION	DUAL SPACED NEUTRON	MULTI-CHANNEL SONIC
HV-89-400	232	160	N/A	N/A
HV-89-401	232	160	514	331
HV-89-402	232	160	514	331
HV-89-403	232	160	514	331
HV-89-404	232	160	514	331
HV-89-405	N/A	N/A	N/A	N/A
HV-89-406	N/A	N/A	N/A	N/A
HV-89-407	221	129	N/A	N/A
HV-89-408	221	129	N/A	N/A
HV-89-409	221	129	501	N/A
HV-89-410	N/A	N/A	N/A	N/A
HV-89-411	221	129	N/A	N/A
HV-89-412	221	129	N/A	N/A
HV-89-413	221	129	501	331
HV-89-414	221	129	N/A	331

APPENDIX C

DEVELOPMENT OF A 3-DIMENSIONAL GRAPH

USING CARTESIAN CO-ORDINATES

Development of a 3-dimensional Graph using Cartesian Co-ordinates

Procedure

1. Establish three axes by plotting on an x-y plane an equilateral triangle with each side 100 units long. The corners of the triangle are arbitrarily chosen with the following co-ordinates:

Point	X	Y
A	0	0
B	50	86.6
C	100	0

2. Express the numerical value of each parameter of the observed data as a percentage of the sum of the values of the three parameters forming a set, e.g.,

Values of Observed Parameters			Values of Parameters in %			Sum of %
a	b	c	a'	b'	c'	
10	20	25	18.18	36.36	45.45	100
5	30	15	10	60	30	100
0	50	30	0	62.5	37.5	100
etc.						

3. Relate a', b' & c' to x & y co-ordinates from geometry of Fig.1:

Parameter	X	Y
a'	100-a'	0
b'	b'(cos60)	b'(sin60)
c'	c'	0

4. Determine x & y co-ordinates for each data point in terms of parameters a', b', c'. From Fig.1, the equation for line 1 which extends along a gridline of constant c' through point P is:

$$y = m_c x + b_c \qquad \ldots\ldots\ldots (1)$$

Similarly, the equations for lines 2 and 3, which are colinear with gridlines for b' and a', respectively, are:

$$y = m_b x + b_b \quad \ldots\ldots\ldots (2)$$

$$y = m_a x \quad b_a \quad \ldots\ldots\ldots (3)$$

Since at the intersection of any two lines, the values of x and y are the same. Hence for lines 1 and 2, an expression for x in terms of b' and c' can be obtained by equating Equations (1) and (2) and simplifying. Thus,

$$x = \{b_b - b_c\}/\{m_c - m_b\} \quad \ldots\ldots (4)$$

From Fig.1, the slope and y-intercept values can be obtained for the three lines in terms of the variable parameters a', b', c' as follows:

$$m_a = - \tan 60$$
$$m_b = 0$$
$$m_c = + \tan 60$$

$$b_a = (100-a')(\tan 60)$$
$$b_b = + b'\sin 60$$
$$b_c = - c'\tan 60$$

Substituting the above values in Equations (4) and (1) and simplifying, we get:

$$x = 0.5b' + c' \quad \ldots\ldots\ldots\ldots (5)$$

and

$$y = 0.866b' \quad \ldots\ldots\ldots\ldots (6)$$

But

$$b' = 100b/(a+b+c) \quad \ldots\ldots\ldots\ldots (7)$$

and

$$c' = 100c/(a+b+c) \quad \ldots\ldots\ldots\ldots (8)$$

Hence, in terms of the observed variables:

$$x = 50(b+2c)/(a+b+c) \quad \ldots\ldots\ldots (9)$$

and

$$y = 86.6b/(a+b+c) \quad \ldots\ldots\ldots (10)$$

3–D Plot Using x–y Co–ordinates

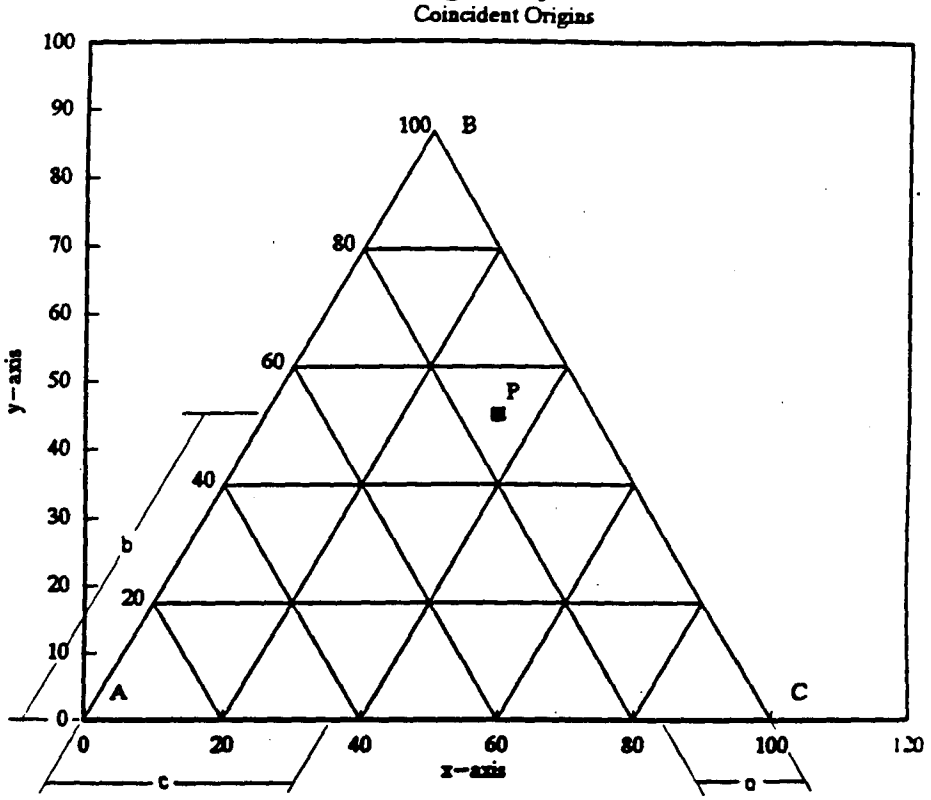

APPENDIX D

GOOD CORRELATIONS, SYNCRUDE DATA

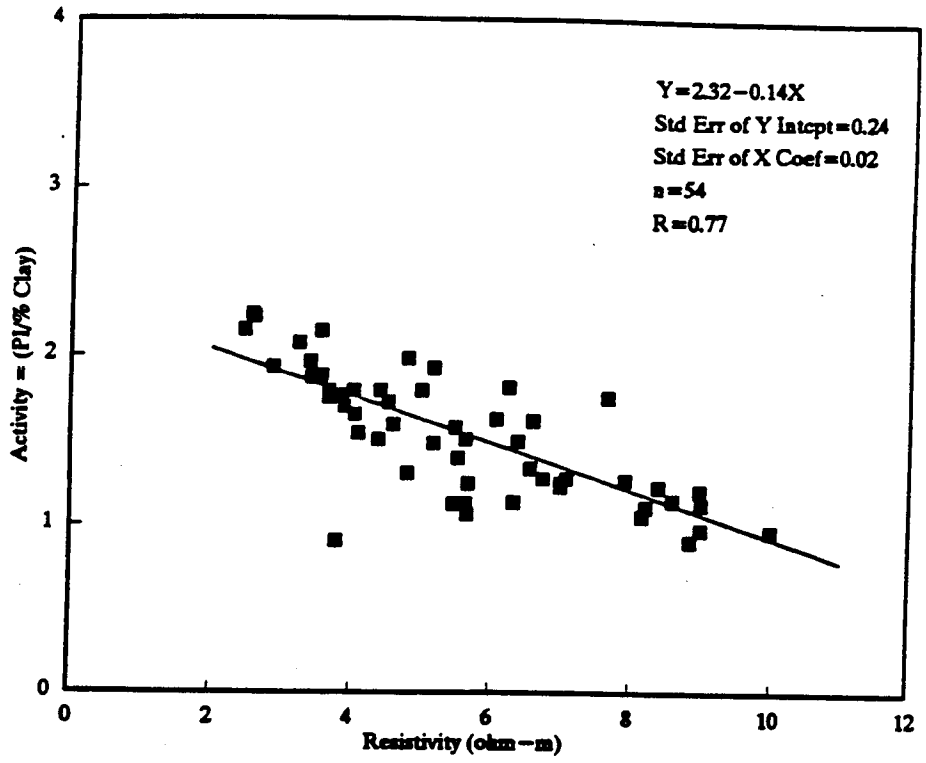

Figure D-1. Activity vs resistivity - Syncrude hole 01.

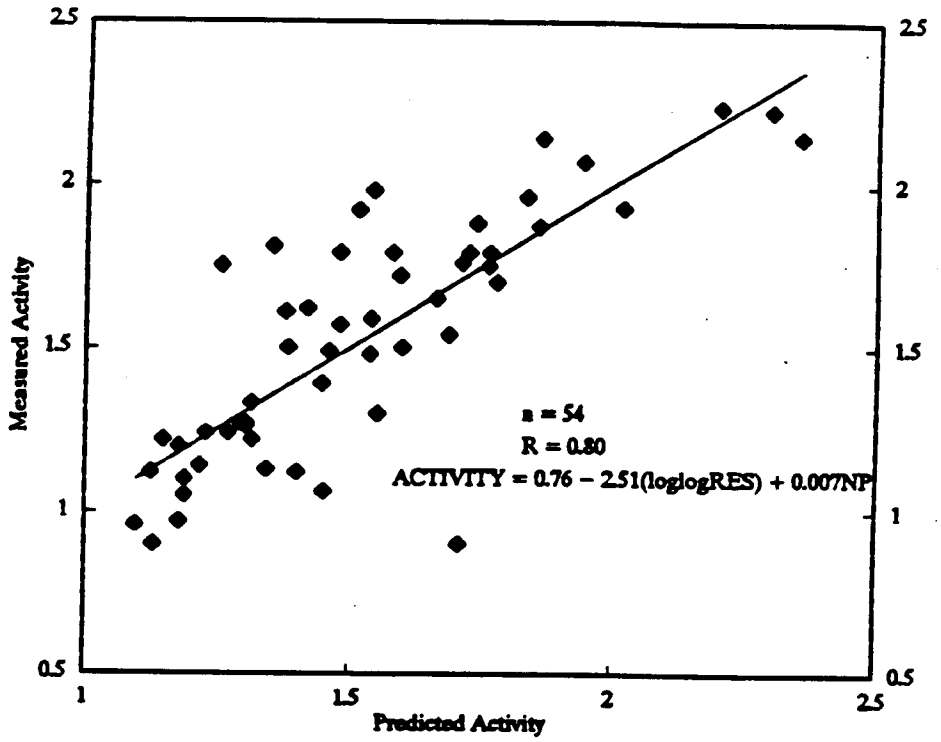

Figure D-2. Activity - predicted vs measured.

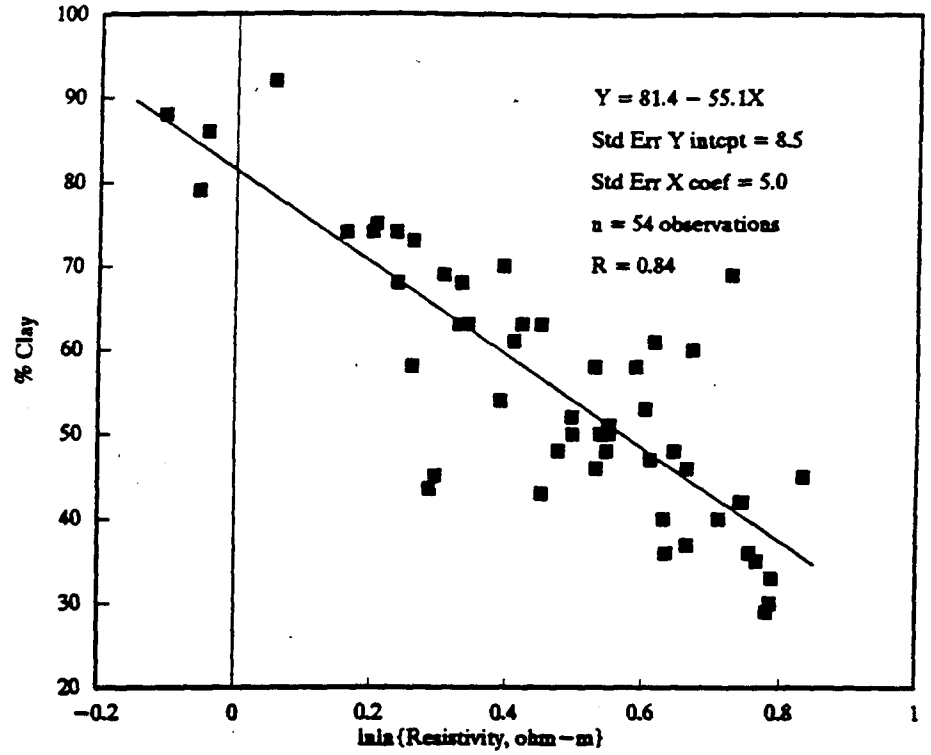

Figure D-3. % Clay vs resistivity - Syncrude hole 01.

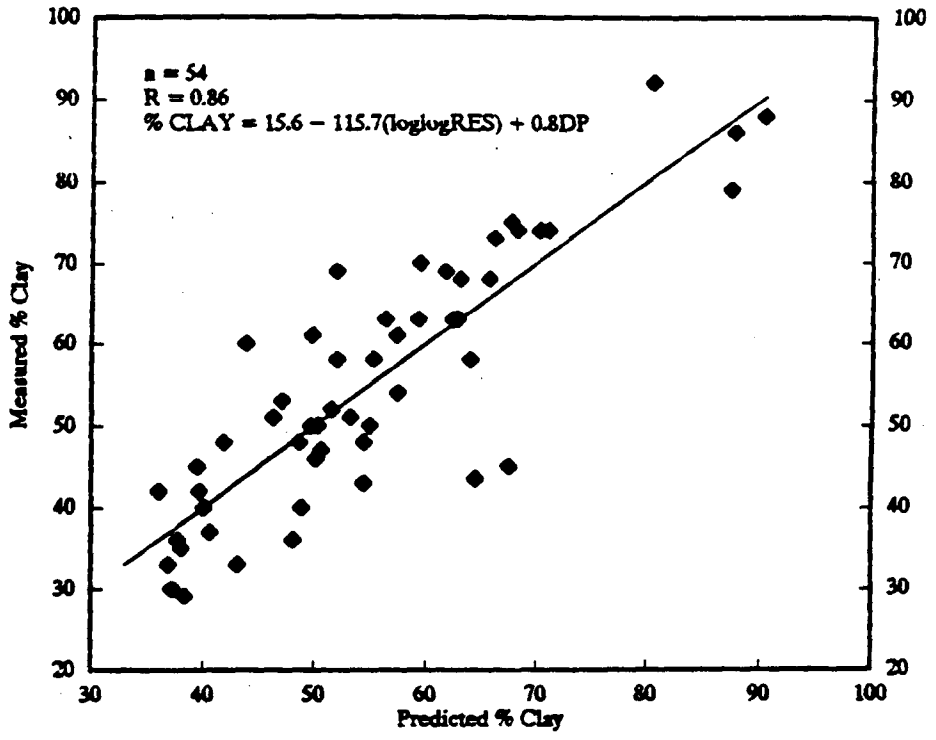

Figure D-4. % Clay - predicted vs measured.

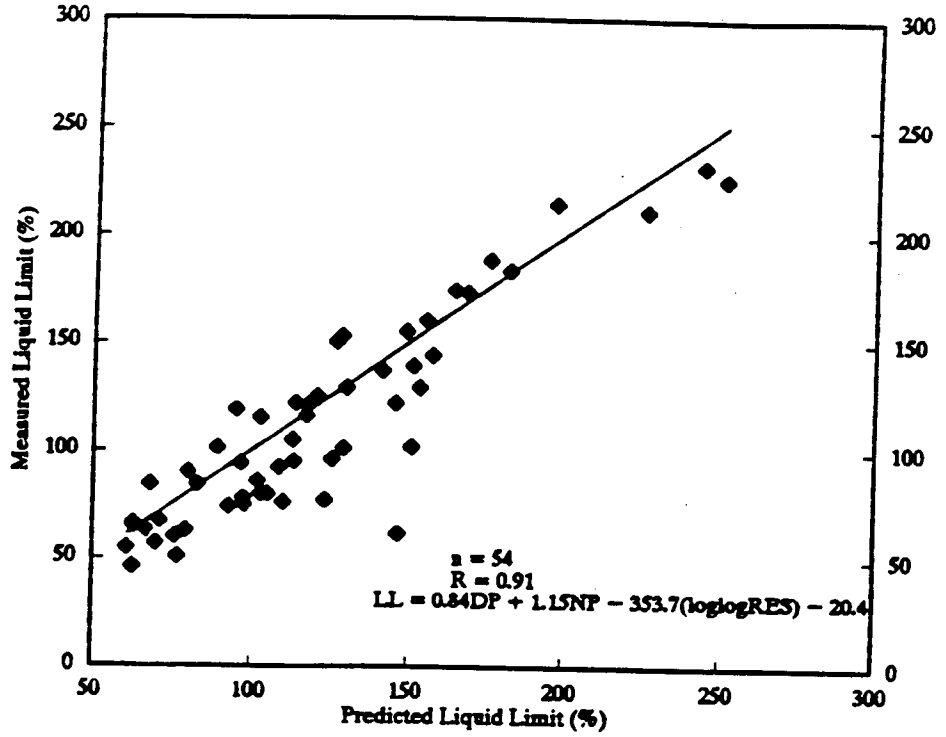

Figure D-5. Liquid Limit - predicted vs measured.

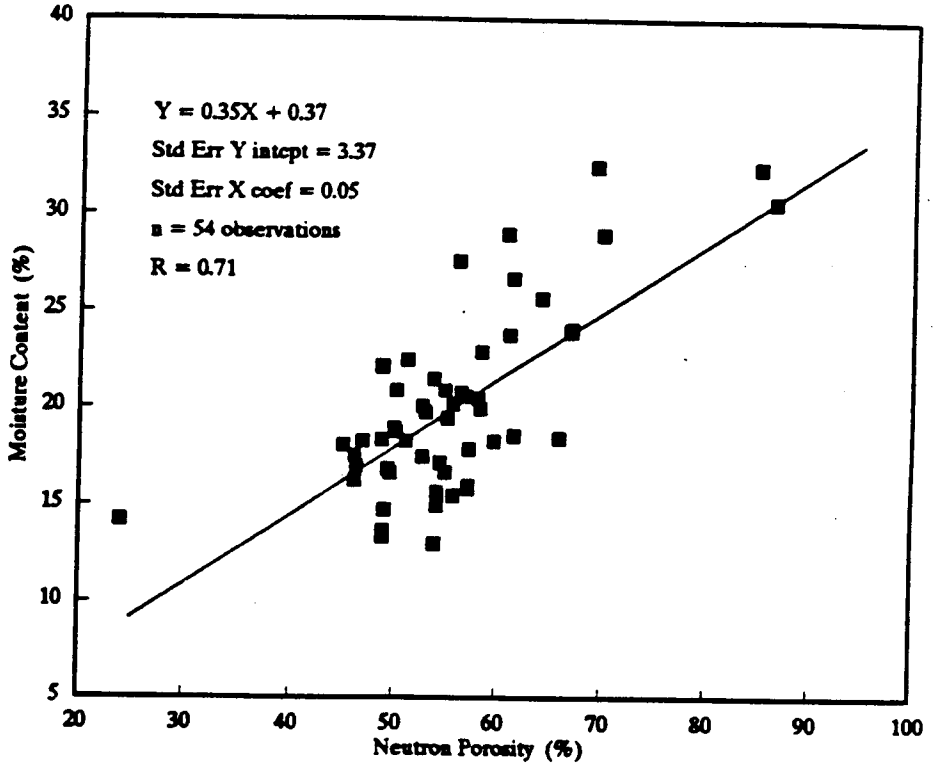

Figure D-6. Moisture content vs neutron porosity log - Syncrude hole 01.

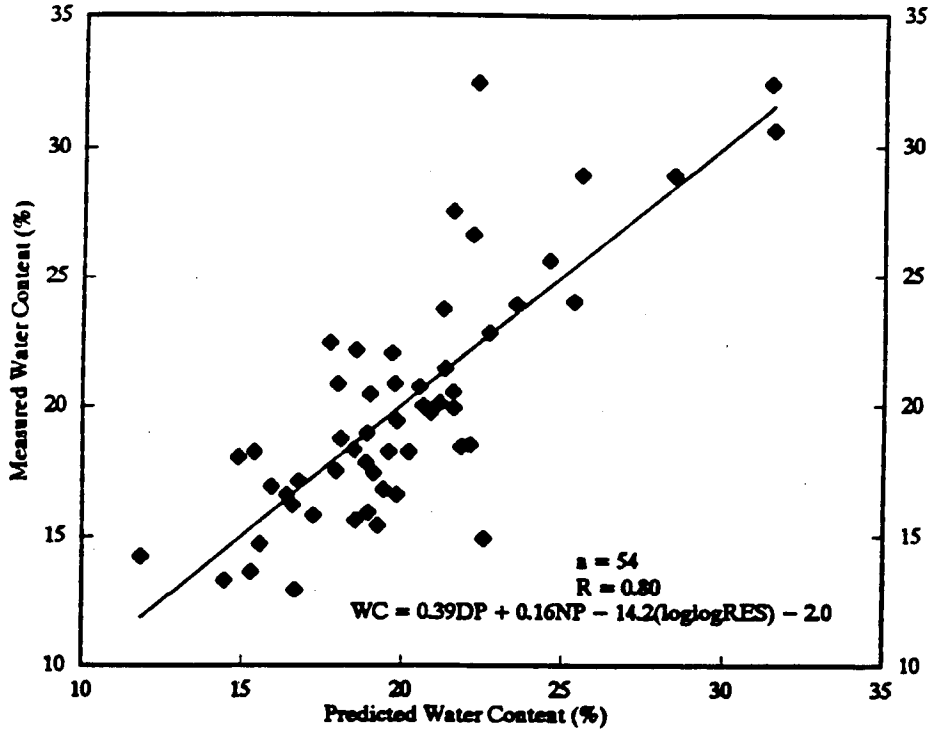

Figure D-7. Moisture content vs - predicted vs measured.

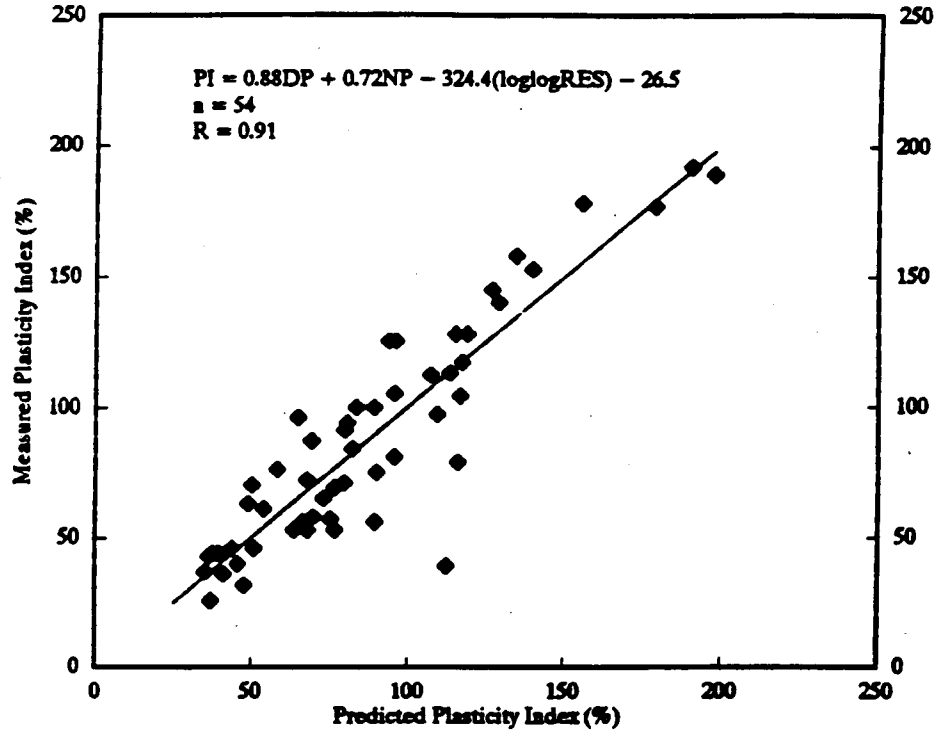

Figure D-8. Plasticity Index - predicted vs measured.

APPENDIX E

GOOD CORRELATIONS FOR HIGHVALE & BIG VALLEY

Geotechnical/Geophysical Correlations

Geophysical Crossplots

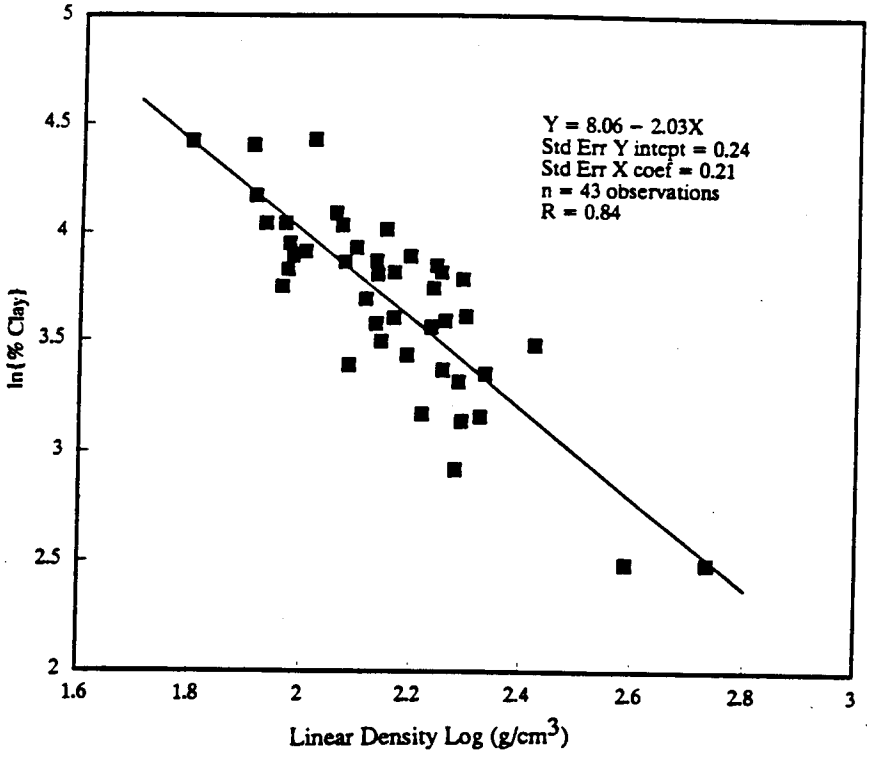

Figure E-1. % Clay vs linear density log - Highvale 1988-89 data.

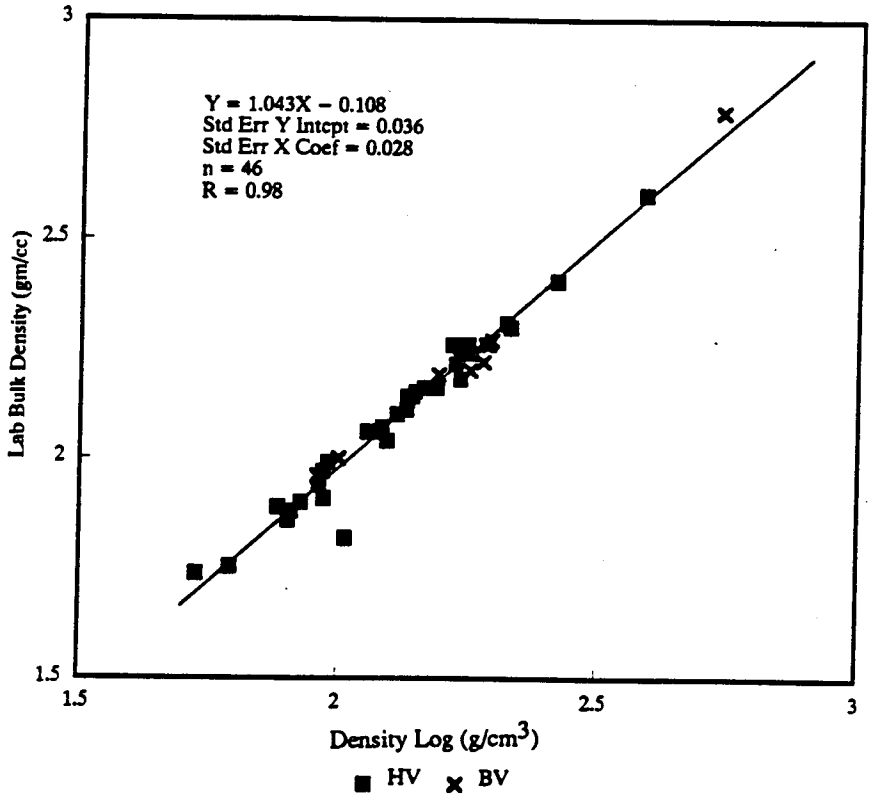

Figure E-2. Lab bulk density vs density log - Highvale & Big Valley data.

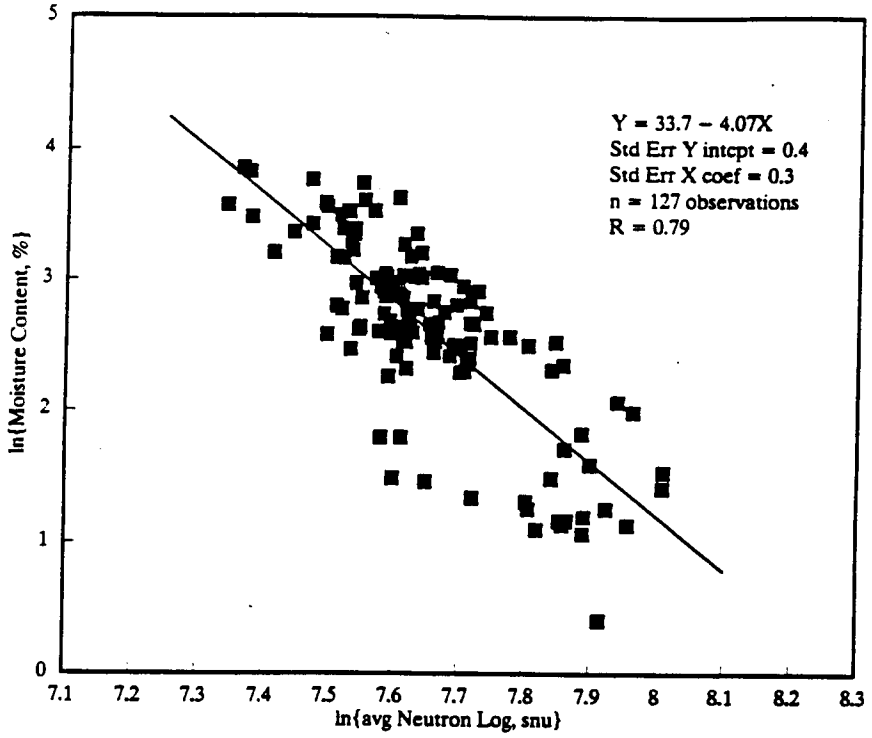

Figure E-3. Moisture content vs neutron log - Highvale & Big Valley data.

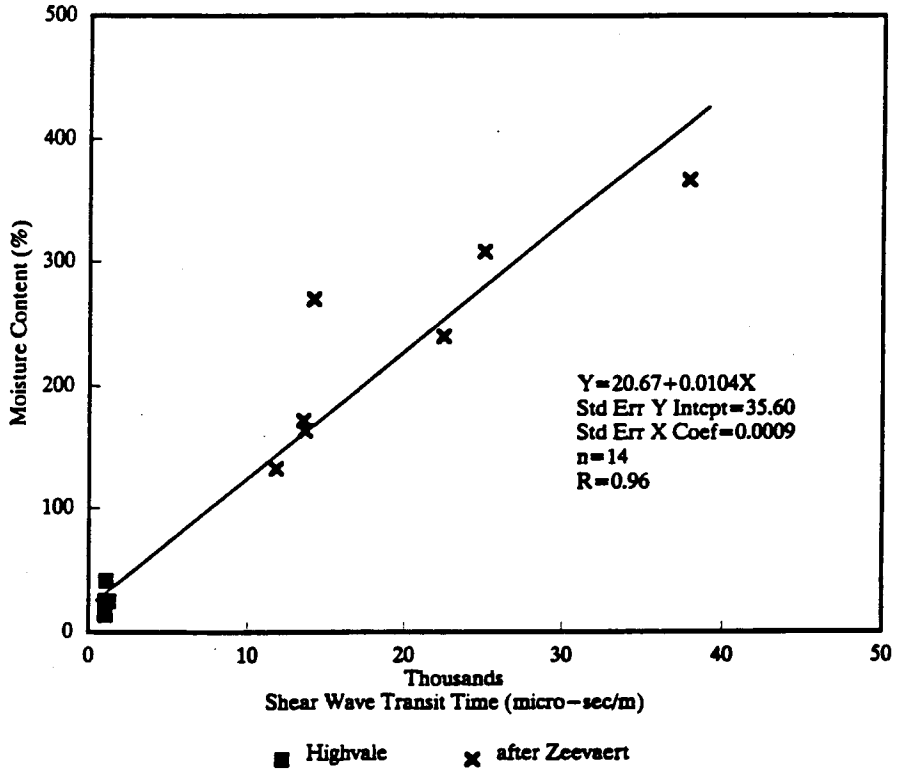

Figure E-4. Moisture content vs shear wave travel time - bentonitic materials.

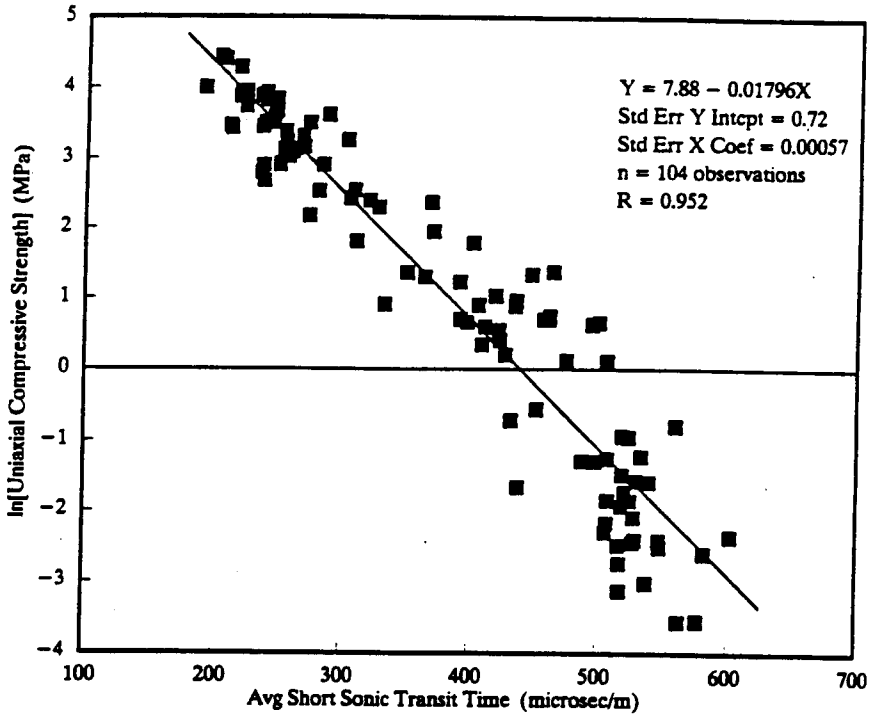

Figure E-5. ln(Qu) vs short-spaced sonic - Highvale 1987-89 data.

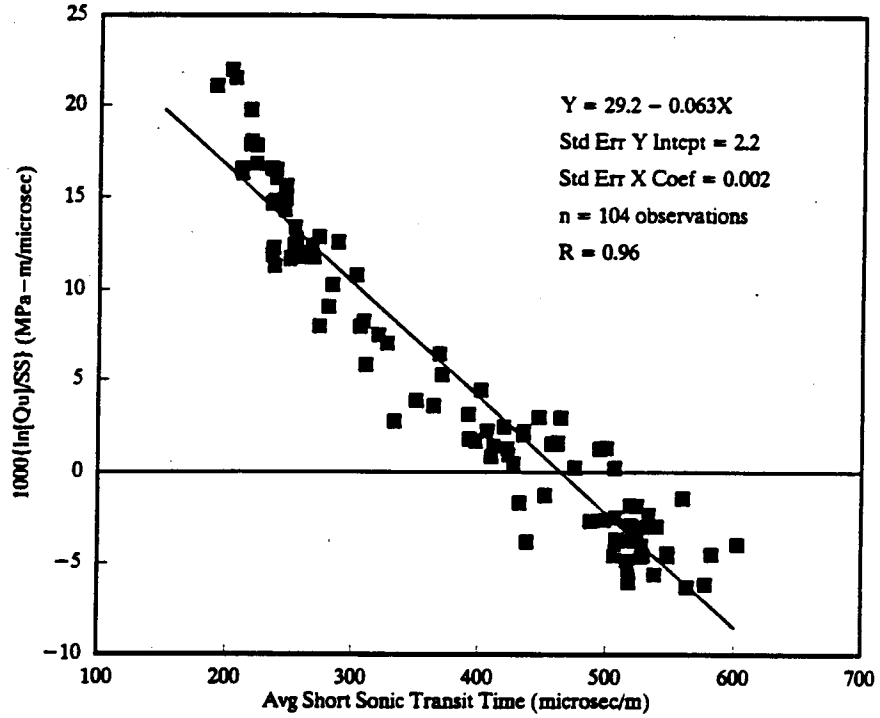

Figure E-6. f (Qu, short spaced sonic) vs short-spaced sonic - Highvale 1987-89 data.

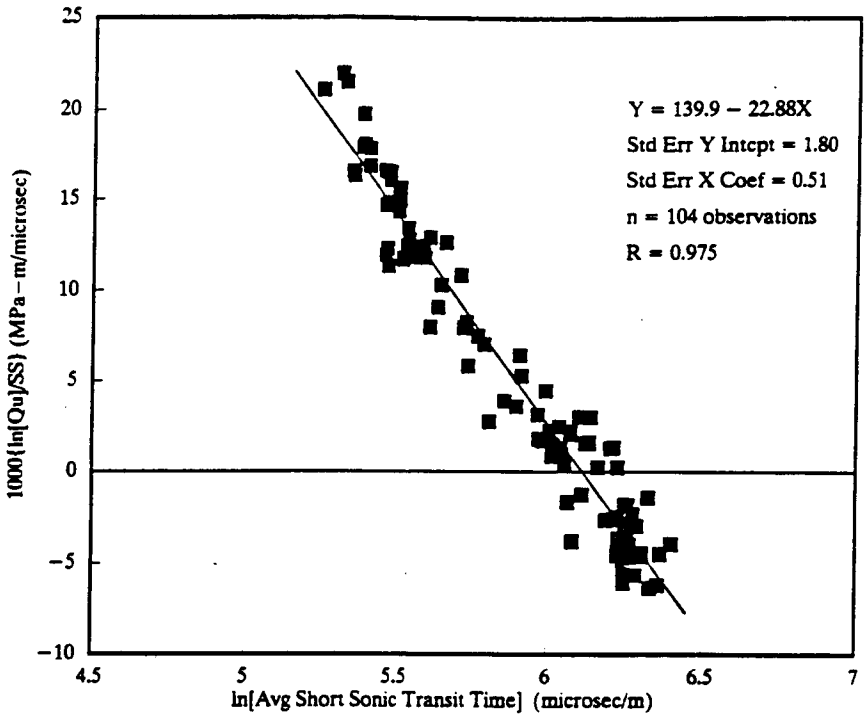

Figure E-7. f (Qu, short-spaced sonic) vs f '(short-spaced sonic) - Highvale 1987-89 data.

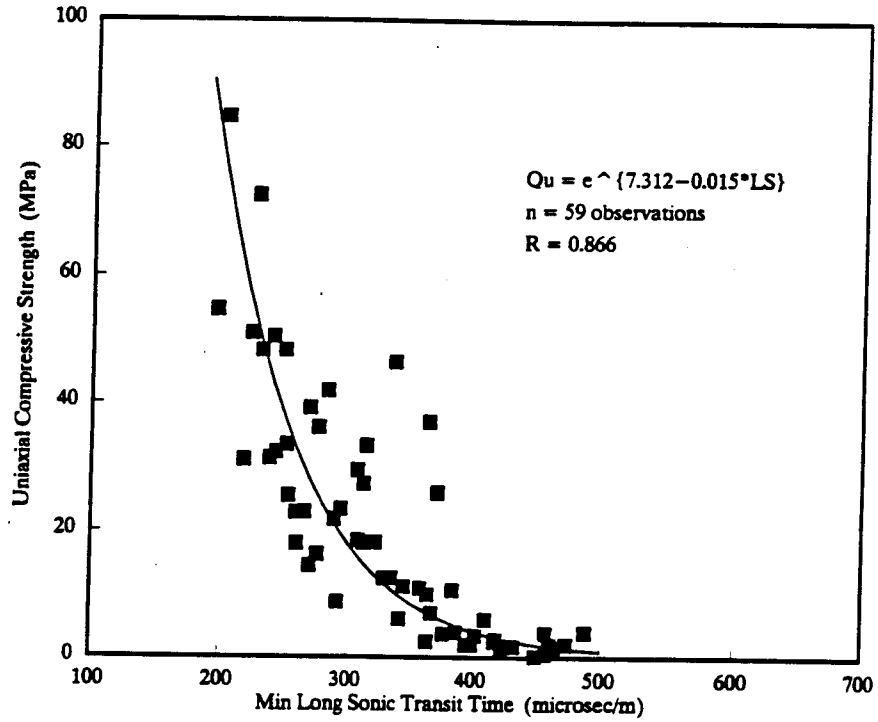

Figure E-8. Qu vs minimum long-spaced sonic - Highvale 1987-89 data.

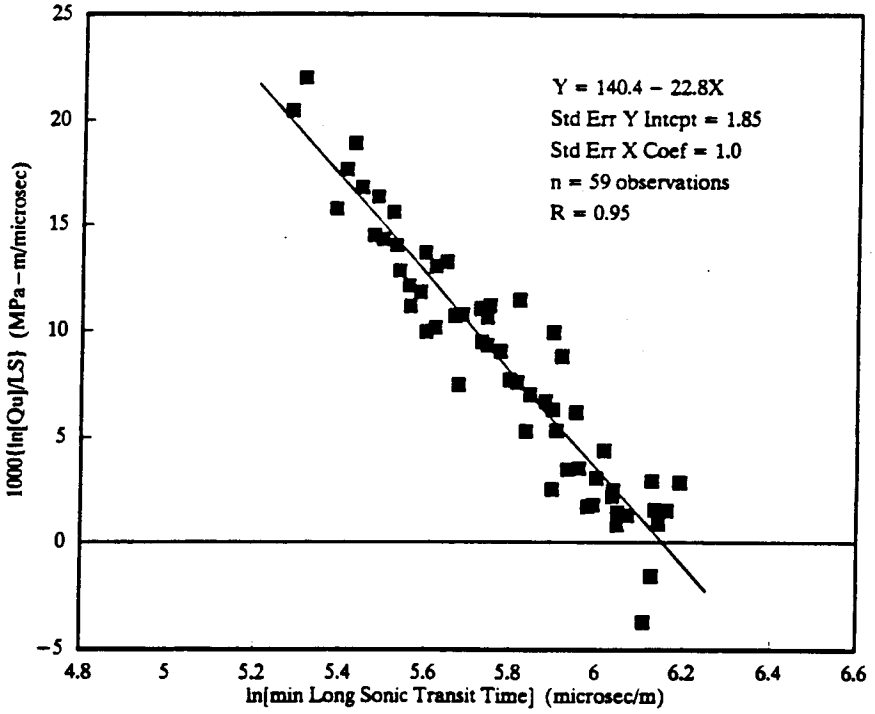

Figure E-9. f (Qu, long-spaced sonic) vs f '(long-spaced sonic) - Highvale 1987-89 data.

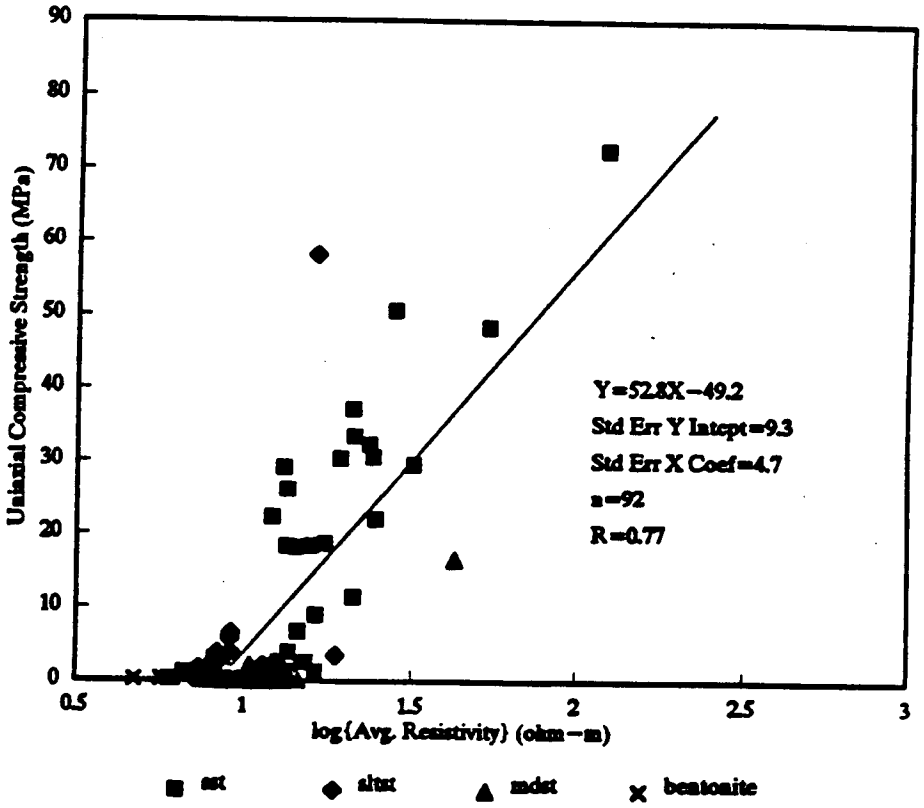

Figure E-10. Qu vs log (average resistivity) - Highvale 1987-89 data.

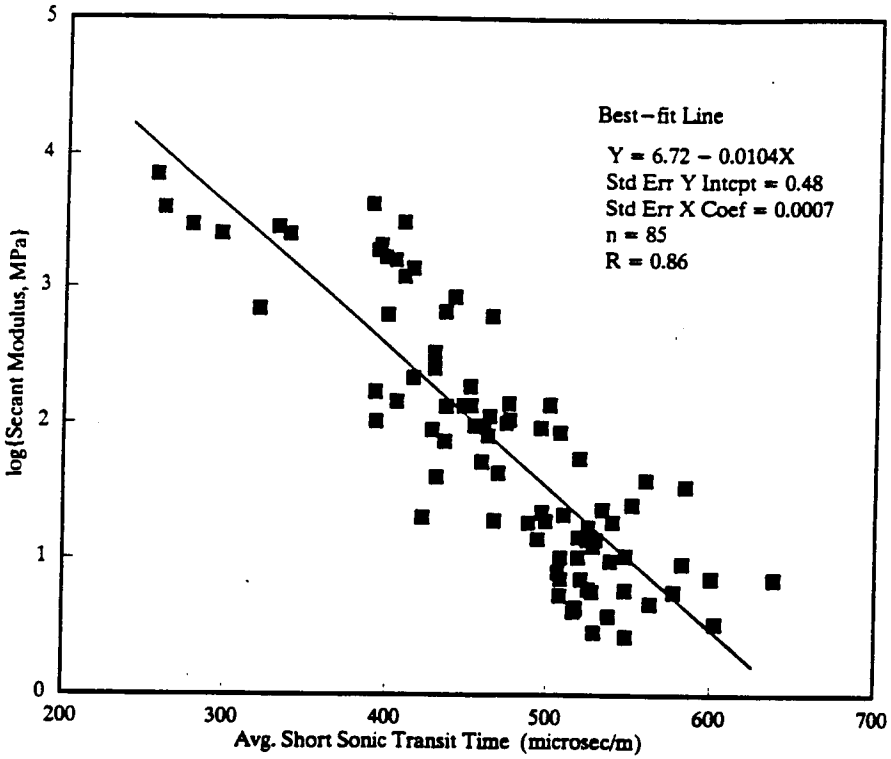

Figure E-11. Secant modulus vs short-spaced sonic - Highvale 1988-89 data.

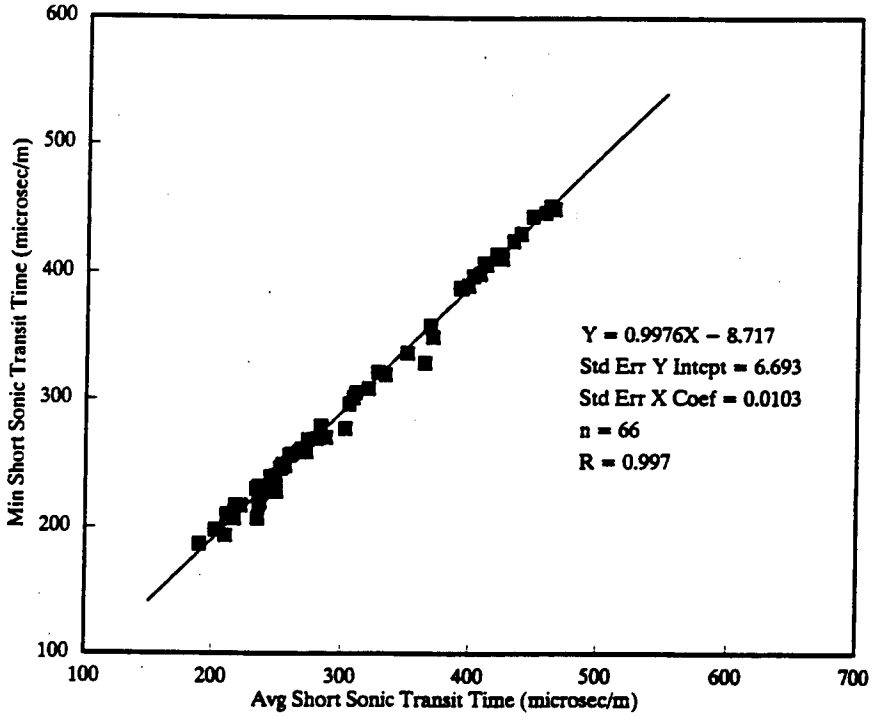

Figure E-12. Minimum vs average short-spaced sonic - Highvale 1987-89 data.

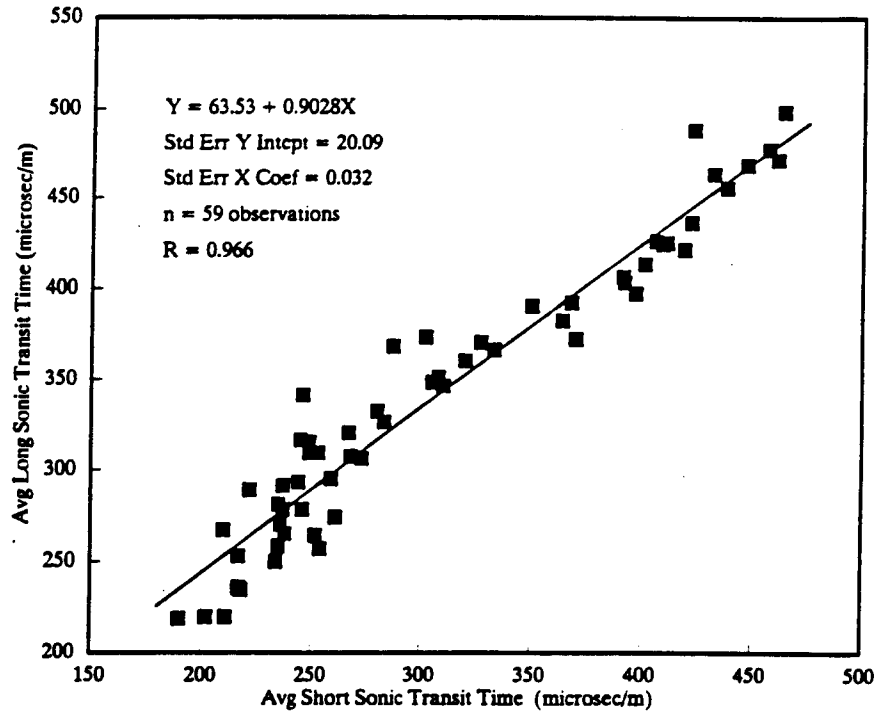

Figure E-13. Long-spaced sonic vs short-spaced sonic - Highvale 1987-89 data.

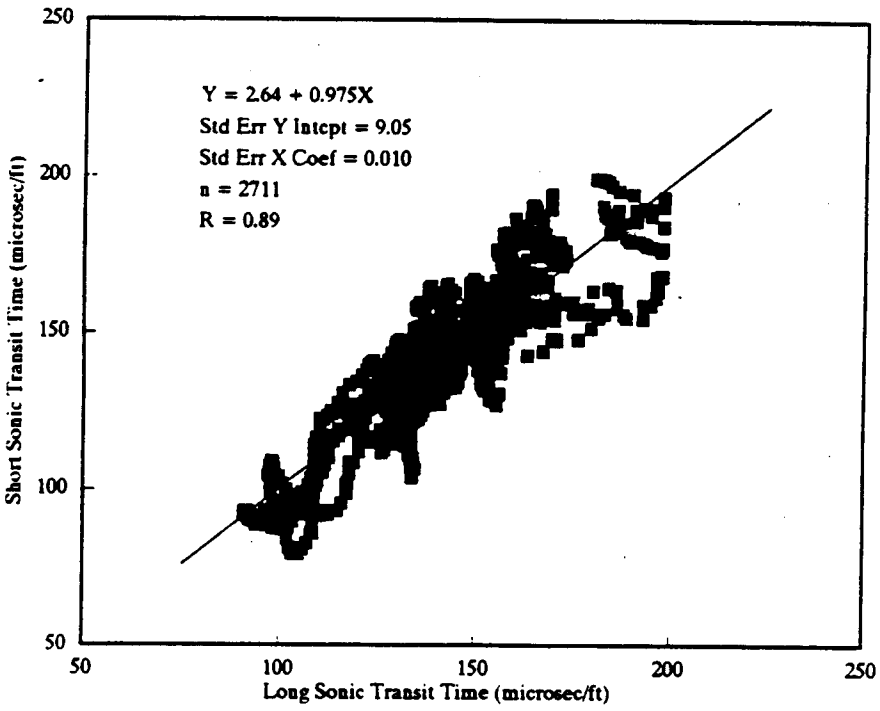

Figure E-14. Short-spaced sonic vs long-spaced sonic - Highvale hole 89-402.

APPENDIX F

3-PARAMETER CORRELATIONS

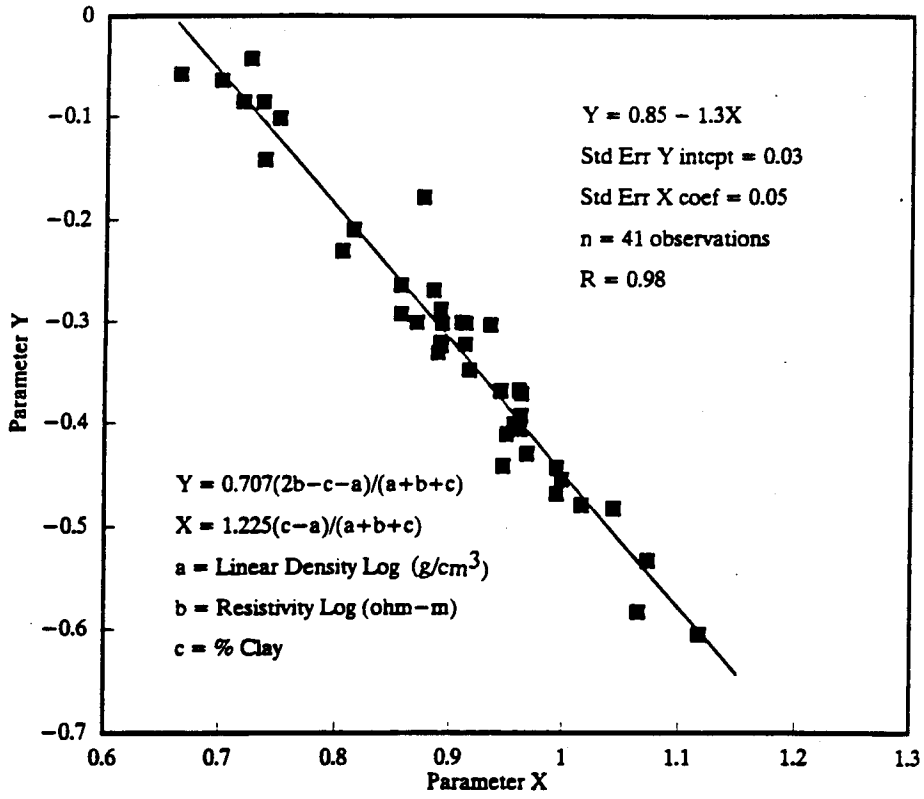

Figure F-1. Relationship between density log, resistivity log and % Clay - Highvale & Big Valley data - sheet 1.

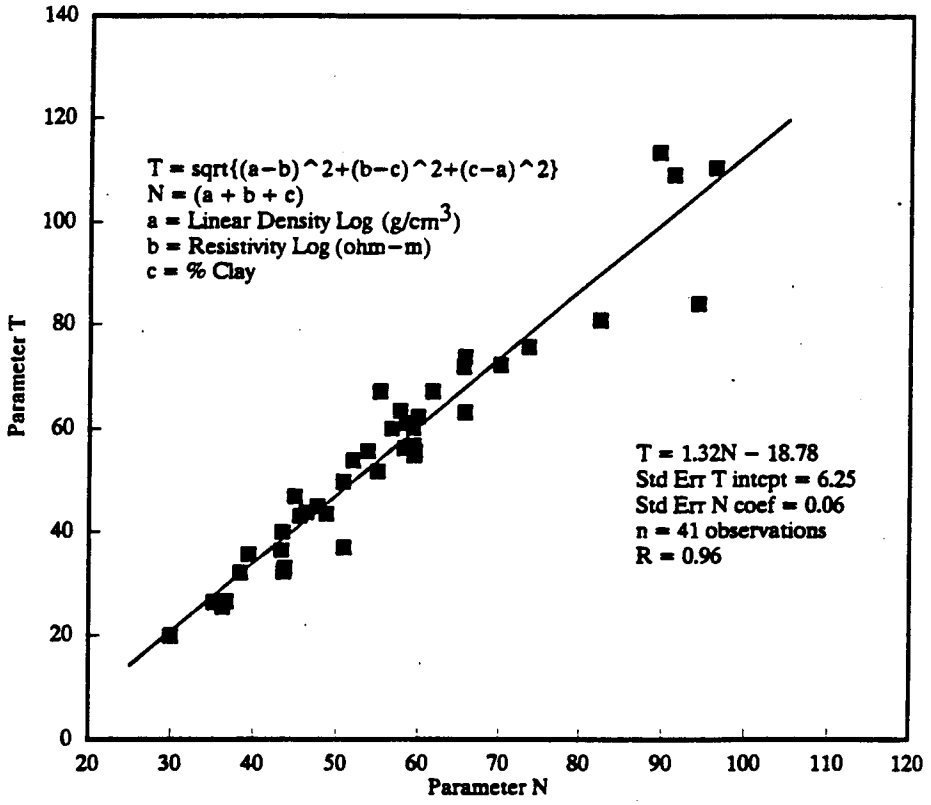

Figure F-2. Relationship between density log, resistivity log and % Clay - Highvale & Big Valley data - sheet 2.

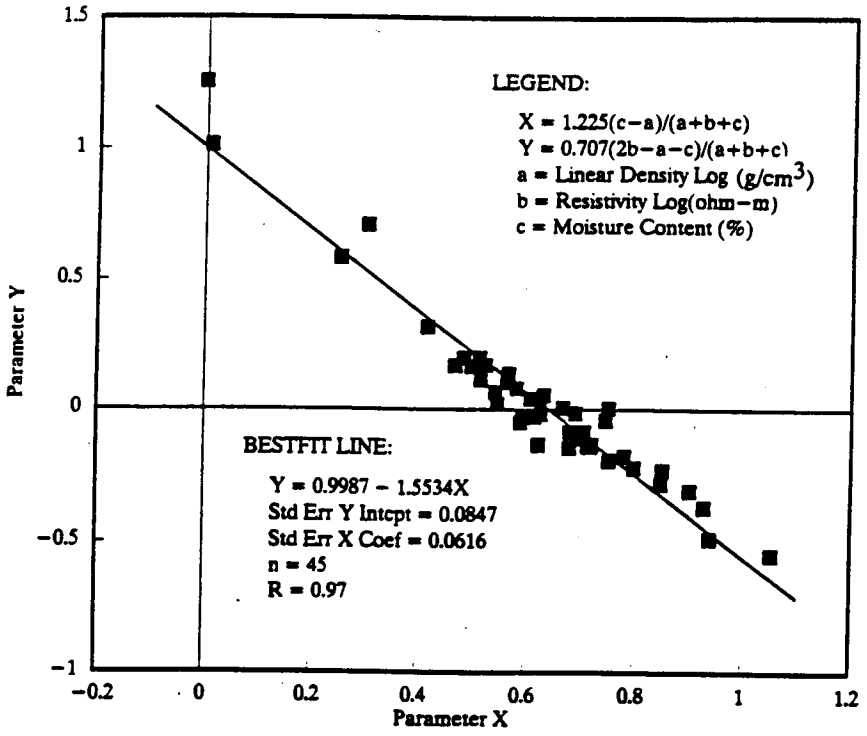

Figure F-3. Relationship between density log, resistivity log and moisture content - Highvale & Big Valley data - sheet 1.

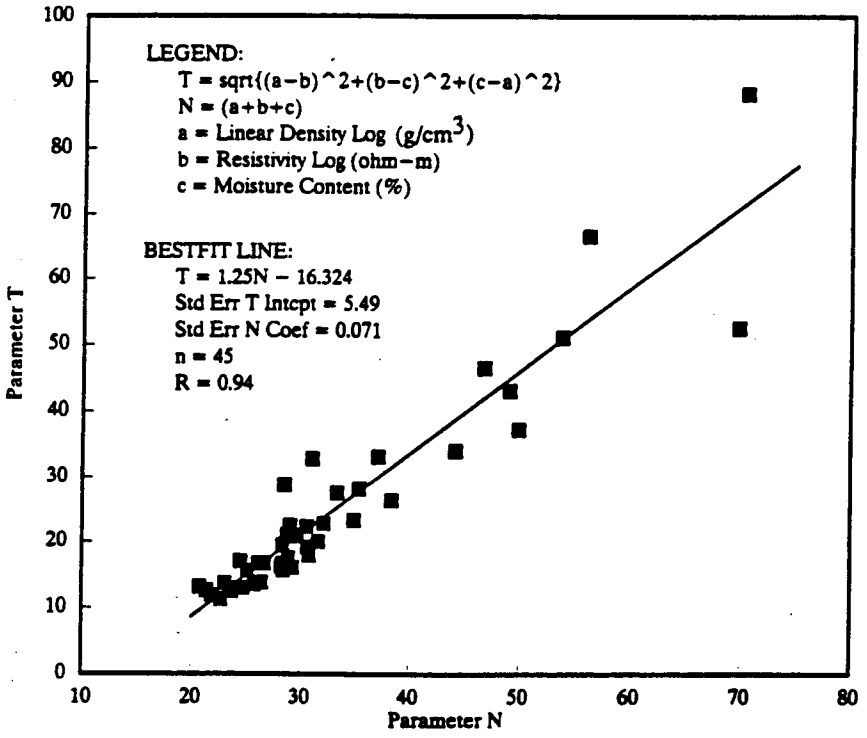

Figure F-4. Relationship between density log, resistivity log and moisture content - Highvale & Big Valley data- sheet 2.

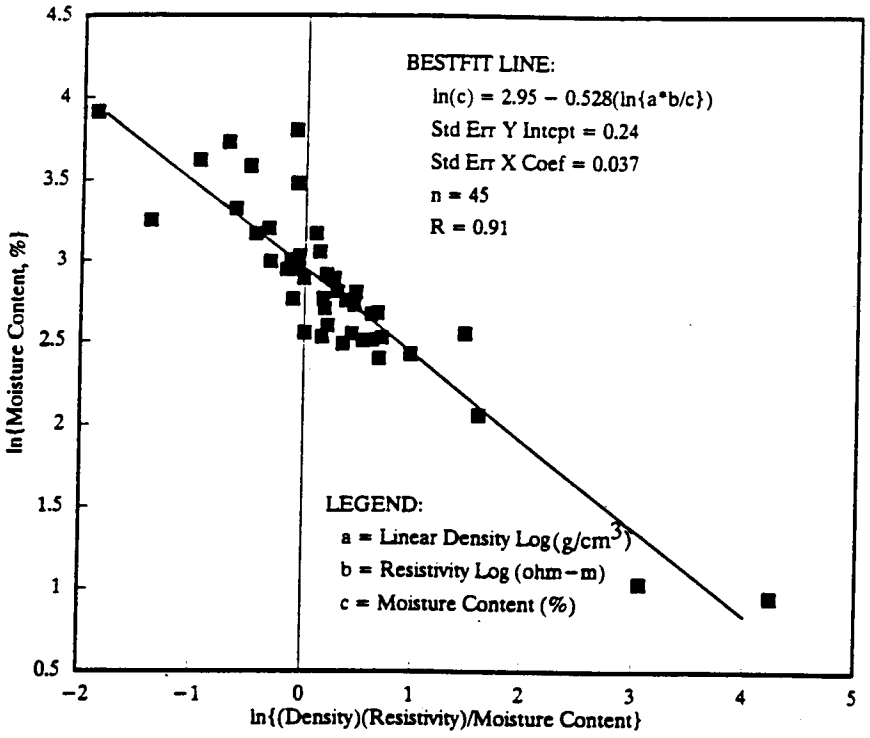

Figure F-5. Relationship between density log, resistivity log and moisture content - Highvale & Big Valley data - sheet 3.

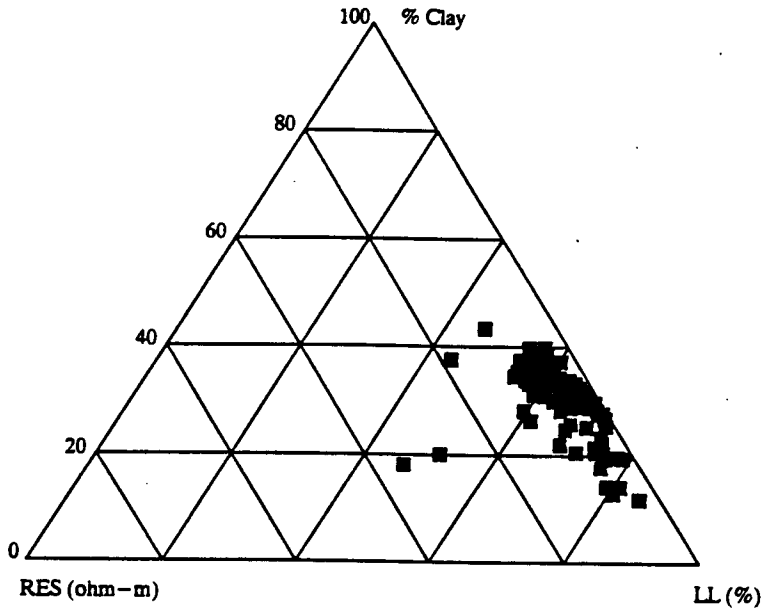

Figure F-6. Relationship between resistivity log, % clay and Liquid Limits - Highvale, Big Valley & Syncrude data - sheet 1.

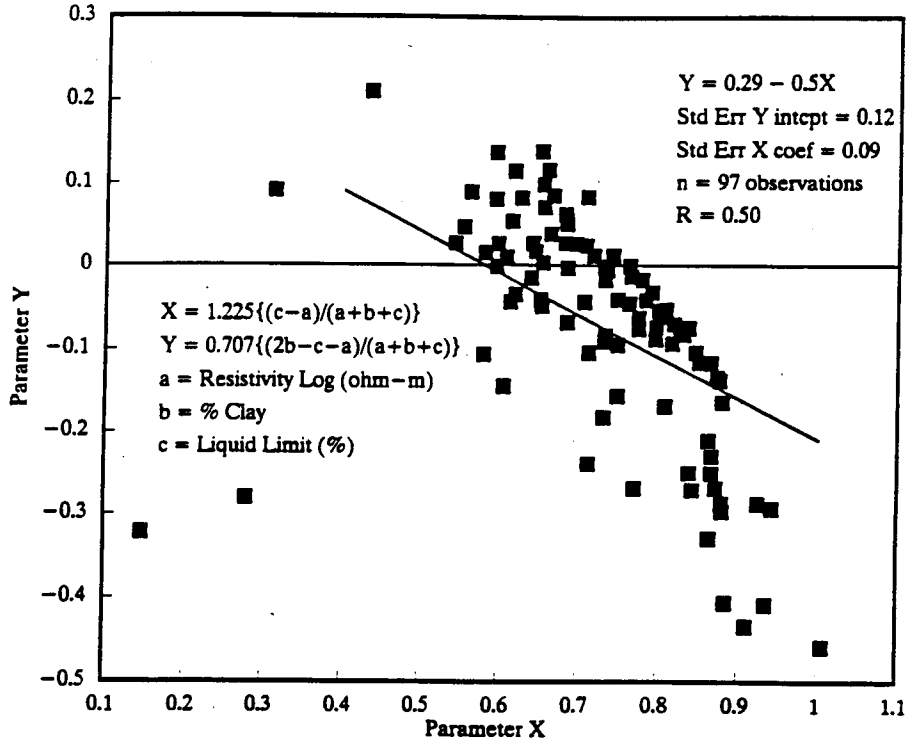

Figure F-7. Relationship between resistivity log, % clay and Liquid Limits - Highvale, Big Valley & Syncrude data - sheet 2.

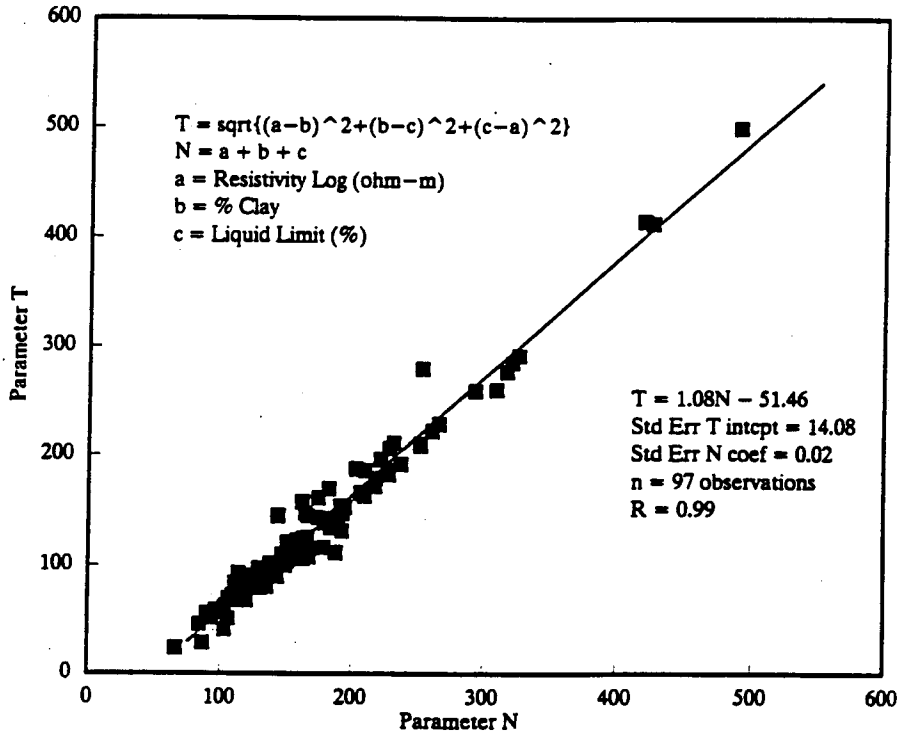

Figure F-8. Relationship between resistivity log, % clay and Liquid Limits - Highvale, Big Valley & Syncrude data - sheet 3.

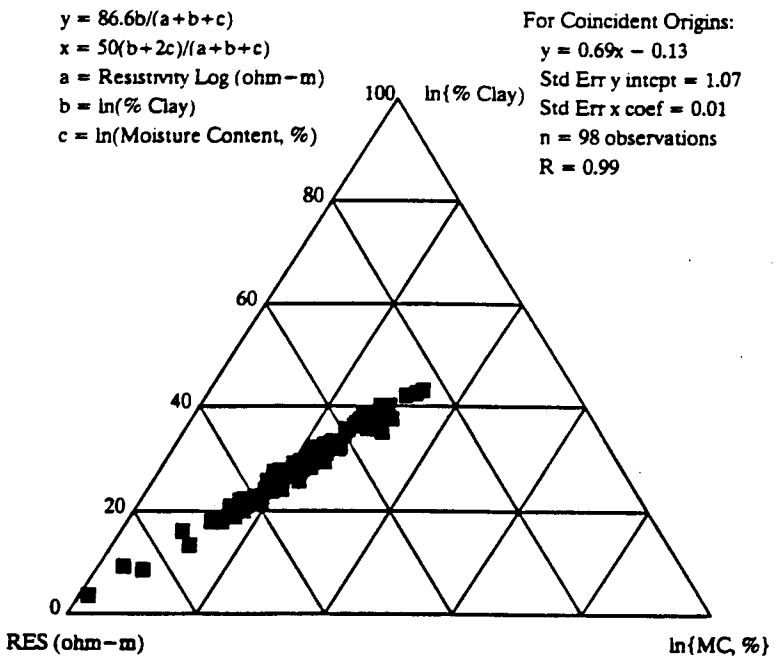

Figure F-9. Relationship between resistivity log, % clay and moisture content - Highvale, Big Valley & Syncrude data - sheet 1.

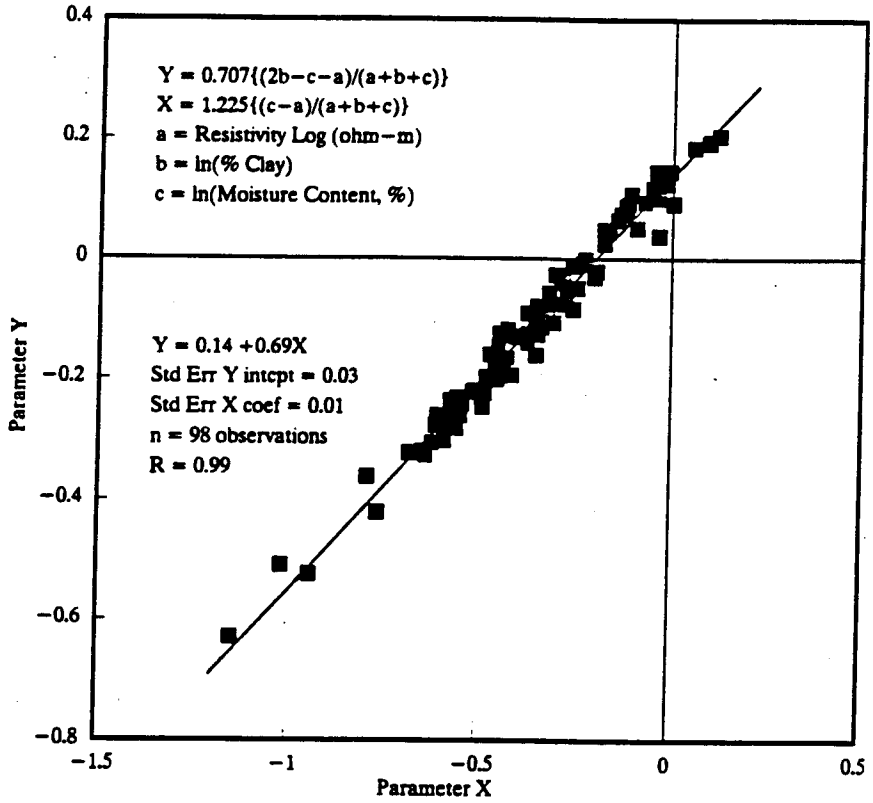

Figure F-10. Relationship between resistivity log, % clay and moisture content - Highvale, Big Valley & Syncrude data - sheet 2.

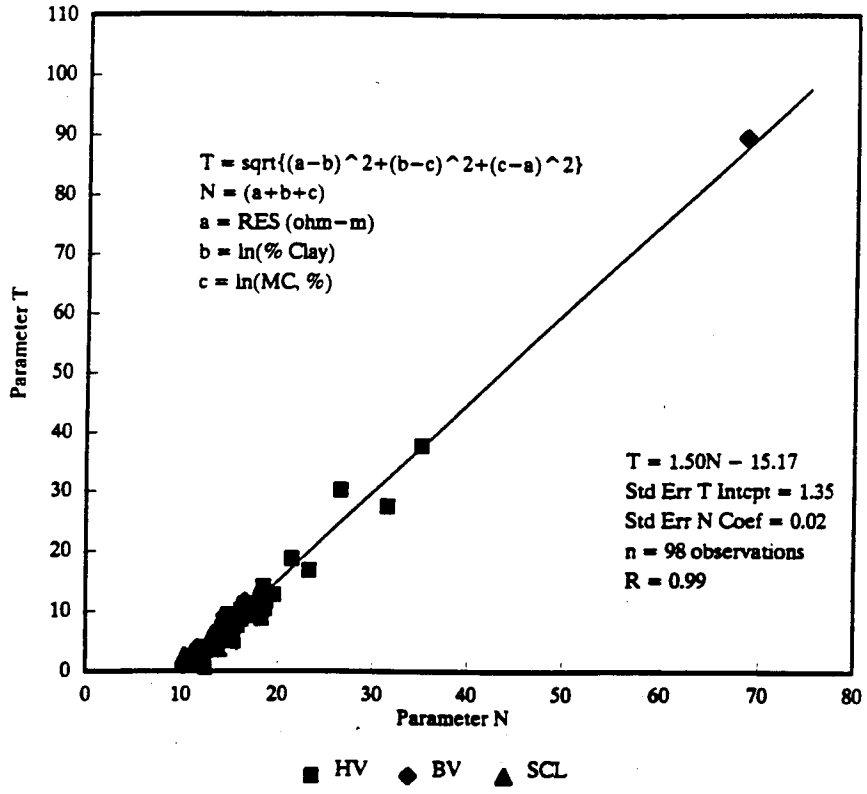

Figure F-11. Relationship between resistivity log, % clay and moisture content - Highvale, Big Valley & Syncrude data - sheet 3.

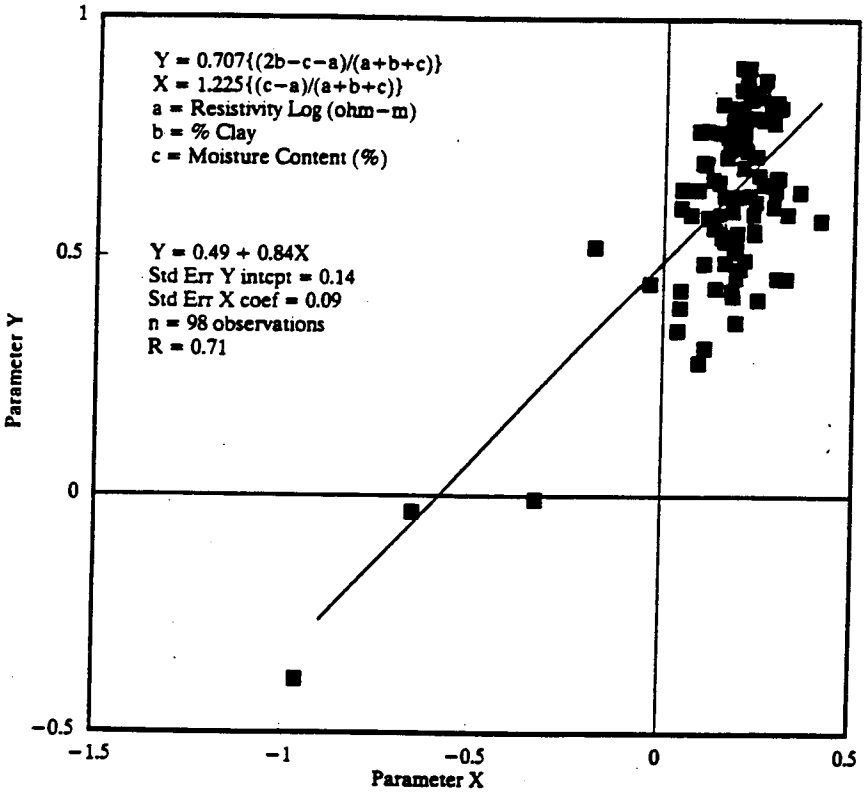

Figure F-12. Relationship between resistivity log, % clay and moisture content - Highvale, Big Valley & Syncrude data - sheet 4.

APPENDIX G

EXAMPLES OF POOR CORRELATIONS

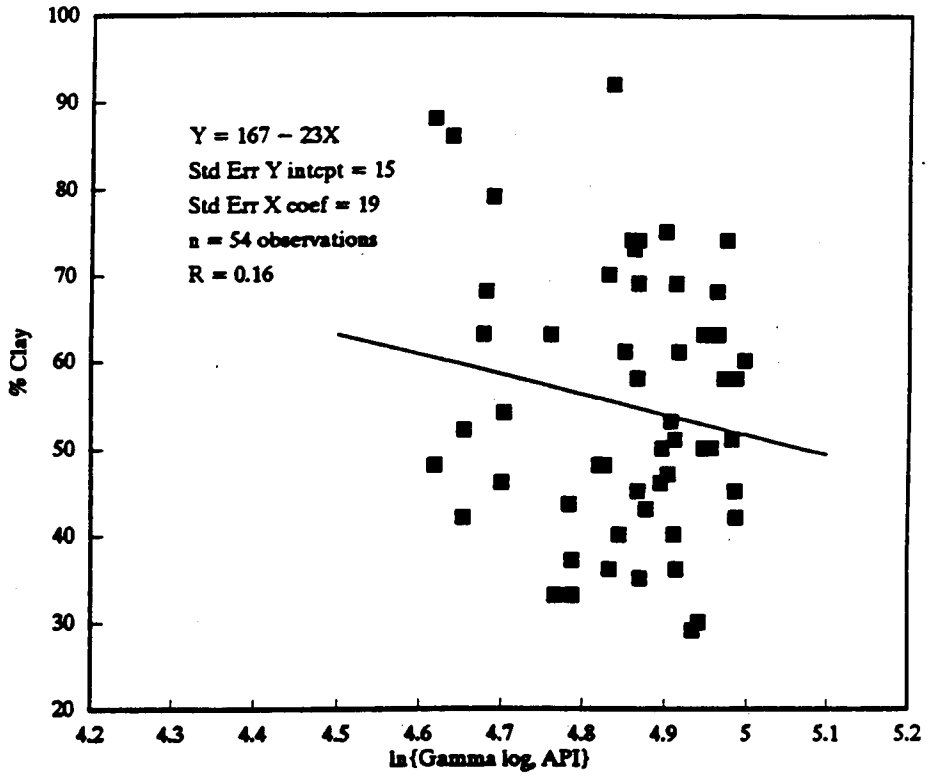

Figure G-1. % Clay vs gamma log - Syncrude hole 01.

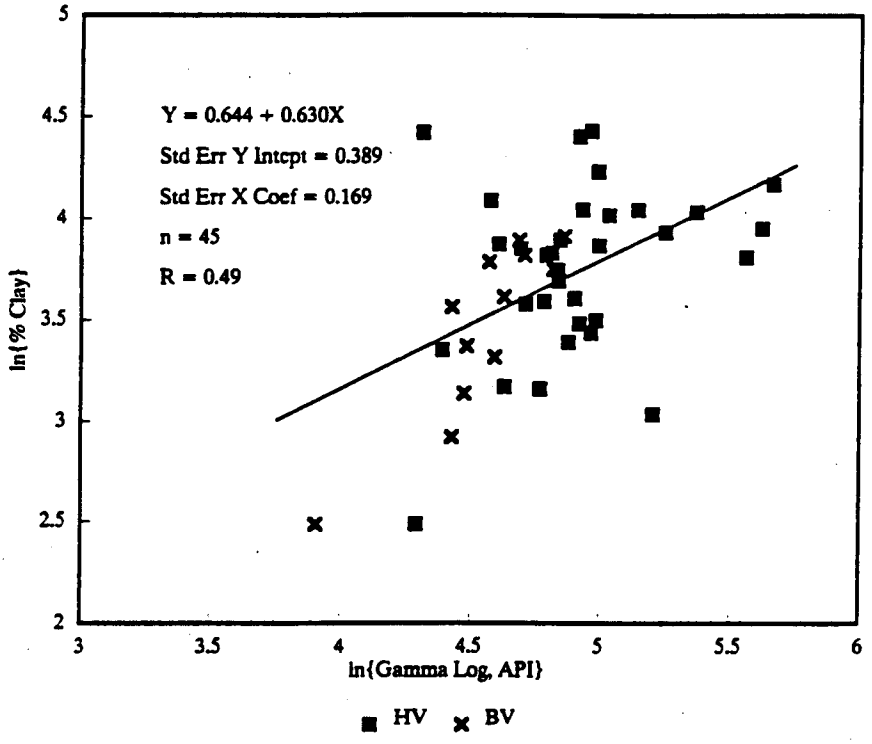

Figure G-2. % Clay vs gamma log - Highvale & Big Valley data.

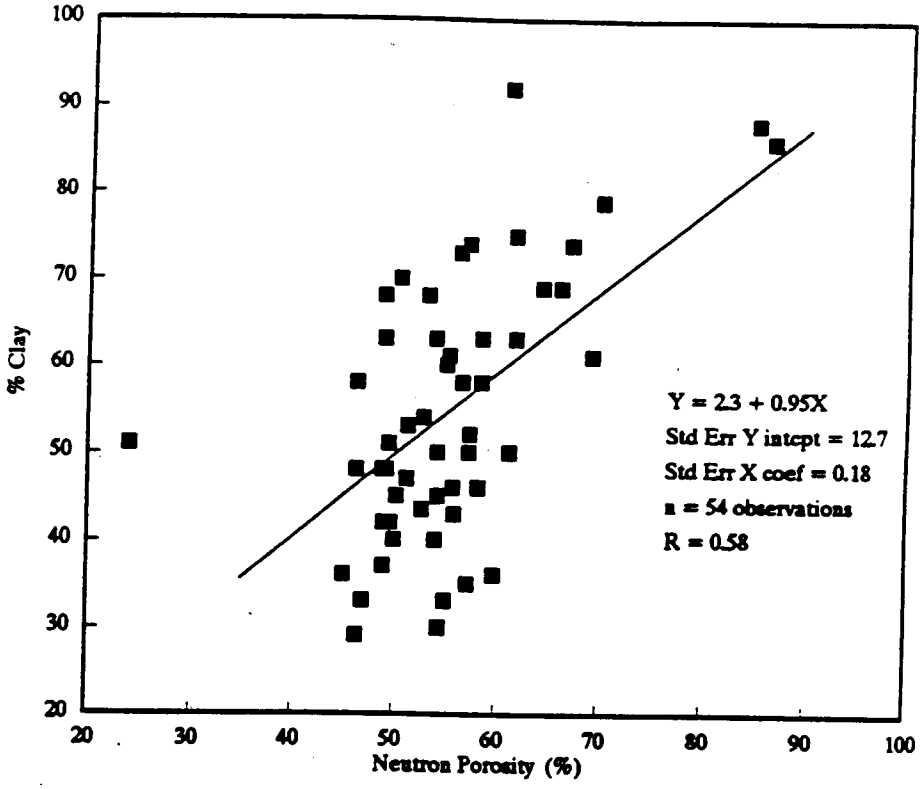

Figure G-3. % Clay vs neutron porosity log - Syncrude hole 01.

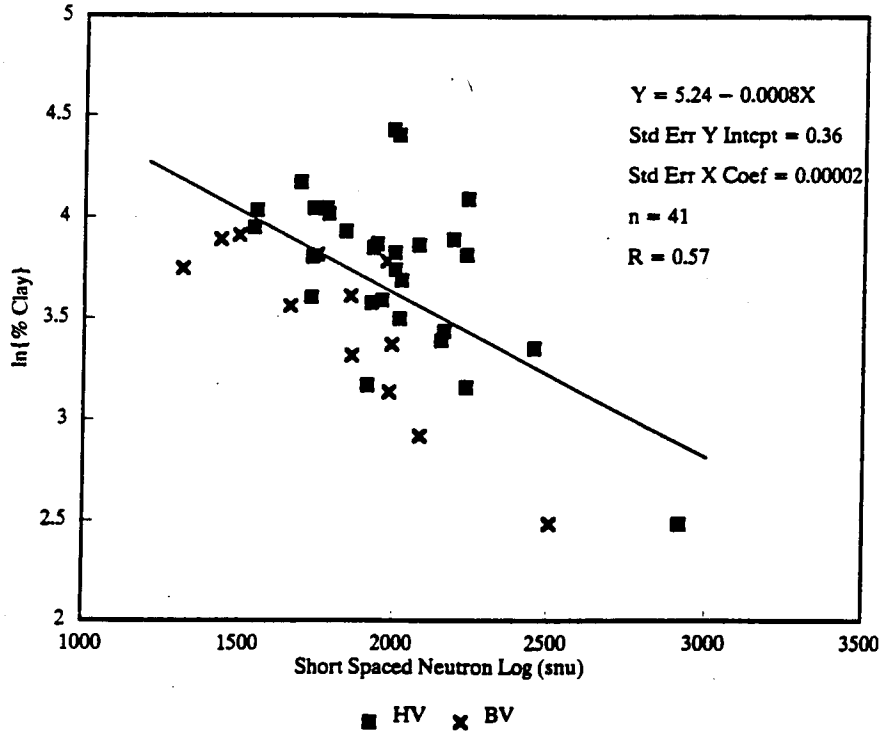

Figure G-4. % Clay vs neutron log - Highvale & Big Valley data.

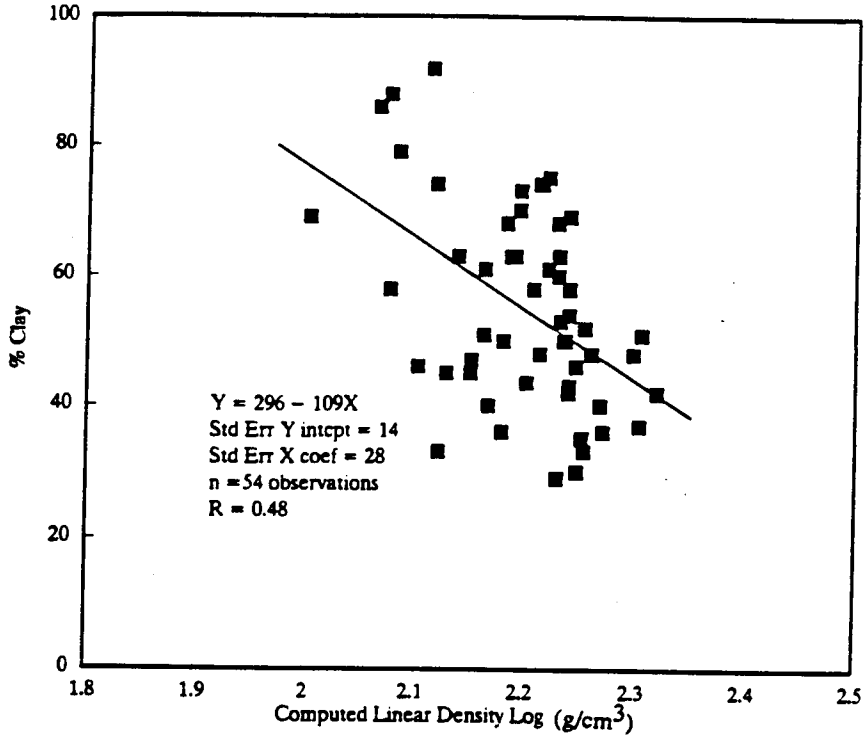

Figure G-5. % Clay vs computed density log - Syncrude hole 01.

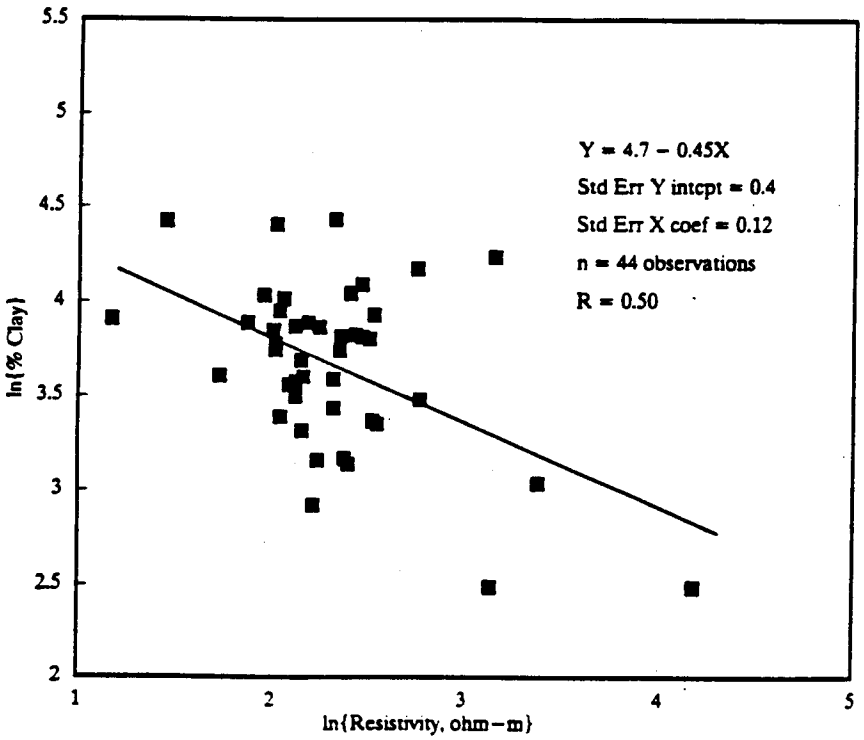

Figure G-6. % Clay vs resistivity - Highvale 1988-89 data.

APPENDIX H

DIGGABILITY PROGRAM

DIGGABILITY PROGRAM

This program will automatically extract and compute the depths and sonic travel time values of all troughs (i.e. lows) that occur on the sonic log signature for a given drillhole. These troughs correspond to hard bands.

In addition the average thickness of each hard band is determined by computing the width of the sonic trough along sonic grid lines at specified intervals.

The number and thickness of hard bands or difficult-to-dig strata are governed in part by equipment digging capacity, different levels of which can be accommodated by appropriate numeric adjustments in MACRO \D.

```
\A      /RNCX~BA4~/RNCA~B31~/RNCB~B32~/RNCD~C1~
        {BLANK D}{BLANK BA4..BC1000}
        {LET BP14,2}{LET X,130}/RNCE~BC4~{GOTO}BL1~
        {WINDOWSON}{WINDOWSOFF}
        {IF B="BLOCK"}{BRANCH AA20}
        {IF A="BLOCK"}{BRANCH AA20}
        {IF A-B>=0}{BRANCH AA7}
        {BRANCH AA8}
        {GOTO}B~/RNCB~{DOWN 2}~{GOTO}A~/RNCA~{DOWN 2}~
        {LET D,D+0.02}{BRANCH AA3}
        {IF A>=X}{BRANCH AA15}
        {GOTO}A~/C{RIGHT}~X~{DOWN}
        {IF @CELLPOINTER("type")<>"b"}{BRANCH AA15}
        {IF X=130}{BRANCH AA13}
        /CD~E~{BRANCH AA14}
        {BLANK D}{BLANK X}
        {GOTO}AY1~{BLANK D}{BEEP}{BEEP 4}{BRANCH CB1}
        {IF B="BLOCK"}{BRANCH AA20}
        {IF A="BLOCK"}{BRANCH AA20}
        {IF A-B<0}{BRANCH AA19}
        {BRANCH AA3}
        {GOTO}B~/RNCB~{DOWN 2}~{GOTO}A~/RNCA~{DOWN 2}~
        {LET D,D+0.02}{BRANCH AA10}
        {IF X=130}{BRANCH AA22}
        /CD~E~{BRANCH AA23}
        {BLANK D}{BRANCH AA19}
        {GOTO}E~/RNCE~{DOWN}~{GOTO}X~/RNCX~{DOWN}~
        {LET X,130}{BLANK D}{BRANCH AA19}

\B      /RNCC~A1~{LET C,0}/RNCS~A30..A8000~/MS~C30~{GOTO}B30~
        {IF @CELLPOINTER("type")<>"b"}{BRANCH E9}
        {BRANCH AA1}
        {IF @CELLPOINTER("contents")>=125}{BRANCH E16}
        {LET C,C+1}{DOWN}~{BRANCH E7}
        {IF @CELLPOINTER("type")<>"b"}{BRANCH E13}
        {BRANCH AA1}
        {IF @CELLPOINTER("contents")>=125}{BRANCH E15}
        {LET C,C+1}{DOWN}~{BRANCH E7}
        /RNDT~/RNCT~~{DOWN}~{BRANCH E17}
        BLOCK~{DOWN}~{BRANCH E11}
        {IF @CELLPOINTER("type")<>"b"}{BRANCH E19}
        /RNDV~/RNCV~{RIGHT}{END}{DOWN}~/MV~T~{BRANCH AA1}
        {IF @CELLPOINTER("contents")>=125}{BRANCH E21}
        /RNDV~/RNCV~{RIGHT}{END}{DOWN}~/MV~T~{GOTO}V~
        {BRANCH E14}{DOWN}{BRANCH E17}

\C      {GOTO}BN25~@NOW~/RV~BN1~{GOTO}A28~
        INPUT RANGE AND NAME OF SOURCE FILE
        {DOWN 2}/FCCN{?}~{?}~
        {GOTO}BL1~{LET BP14,1}~
        {WINDOWSOFF}{PANELOFF}{BRANCH E6}

\D      {GOTO}BC4~
        {IF @CELLPOINTER("type")="b"}{BRANCH AM6}
        /RNCZ~{RIGHT 5}~
        {RIGHT 6}@AVG(Z)~
        {GOTO}Z~{DOWN}/RNDZ~{BRANCH AM2}
        {GOTO}BC4~
        {IF @CELLPOINTER("type")="b"}{BRANCH AM12}
        {RIGHT 2}~/RNCU~{RIGHT 3}~
        {RIGHT 5}@AVG(U)~
        {GOTO}U~{DOWN}/RNDU~
        {LEFT 2}{BRANCH AM7}
        {GOTO}BN25~@NOW~/RV~BO1~
        {GOTO}AX1~{LET AX1,BO1~BN1}~{WINDOWSON}{PANELON}
        {BEEP}{BEEP 4}{BEEP}{QUIT}

\E      /RNCC~A1~/RNCF~BD4~{BLANK C}/RNCJ~A3~{LET J,115}{GOTO}BL1~
        {LET BP14,3}~{WINDOWSON}{WINDOWSOFF}
        /RNCW~BE4~{BLANK BD4..BJ1000}{GOTO}B31~
        {IF @CELLPOINTER("type")="b"}{BRANCH CB11}
        {IF @CELLPOINTER("contents")="BLOCK"}{BRANCH CB8}
        {IF @CELLPOINTER("contents")>J}{BRANCH CB7}
        {LET C,C+.01}{DOWN}{BRANCH CB3}
        {DOWN}~{BRANCH CB3}
        /RNDG~{DOWN}/RNCG~~
        /CC~F~{GOTO}F~/RNCF~{DOWN}~
        {GOTO}G~{BLANK C}{BRANCH CB3}
        {GOTO}AY1~
        {LET J,J~15}{GOTO}W~/RNDF~/RNCW~{RIGHT}~/RNCF~~
        {IF J=40}{GOTO}BL1~{LET BP14,4}{WINDOWSON}{WINDOWSOFF}{BRANCH AM1}
        {GOTO}B31~{BRANCH CB3}
```

```
{GOTO}BN25-@NOW-/RV-BN1-{GOTO}A28-
INPUT RANGE AND NAME OF SOURCE FILE
{DOWN 2}/FCCN{?}-{?}-
{GOTO}BL1-{LET BP14,1}-
{WINDOWSOFF}{PANELOFF}{BRANCH E6}
```

INPUT SOURCE DATA

```
/RNCC-A1-{LET C,0}/RNCS-A30..A8000-/MS-C30-{GOTO}B30-
{IF @CELLPOINTER("type")<>"b"}{BRANCH E9}
{BRANCH AA1}
{IF @CELLPOINTER("contents")>=120}{BRANCH E16}
{LET C,C+1}{DOWN}-{BRANCH E7}
{IF @CELLPOINTER("type")<>"b"}{BRANCH E13}
{BRANCH AA1}
{IF @CELLPOINTER("contents")>=120}{BRANCH E15}
{LET C,C+1}{DOWN}-{BRANCH E7}
/RNDT-/RNCT--{DOWN 4}-{BRANCH E17}
BLOCK-{DOWN}-{BRANCH E11}
{IF @CELLPOINTER("type")<>"b"}{BRANCH E19}
/RNDV-/RNCV-{RIGHT}{END}{DOWN}-/MV-T-{BRANCH AA1}
{IF @CELLPOINTER("contents")>=120}{BRANCH E21}
/RNDV-/RNCV-{RIGHT}{END}{DOWN}-/MV-T-{GOTO}V-{BRANCH E14}
{DOWN 4}{BRANCH E17}
```

STAGE 1

DELETES DATA WITH SONIC TRAVEL TIMES >120 AND SEPARATES PREDOMINANT TROUGHS INTO BLOCKS

```
/RNCX-BA4-/RNCA-B31-/RNCB-B32-/RNCD-C1-{BLANK D}{BLANK BA4..BC1000}
{LET BP14,2}{LET X,130}/RNCE-BC4-{GOTO}BL1-{WINDOWSON}{WINDOWSOFF}
{IF B="BLOCK"}{BRANCH AA20}
{IF A="BLOCK"}{BRANCH AA20}
{IF A-B>=0}{BRANCH AA7}
{BRANCH AA8}
{GOTO}B-/RNCB-{DOWN 2}-{GOTO}A-/RNCA-{DOWN 2}-{LET D,D+0.02}{BRANCH AA3}
{IF A>=X}{BRANCH AA15}
{GOTO}A-/C{RIGHT}-X-{DOWN}
{IF @CELLPOINTER("type")<>"b"}{BRANCH AA15}
{IF X=130}{BRANCH AA13}
/CD-E-{BRANCH AA14}
{BLANK D}{BLANK X}
{GOTO}AY1-{BLANK D}{BEEP}{BEEP 4}{BRANCH CB1}
{IF B="BLOCK"}{BRANCH AA20}
{IF A="BLOCK"}{BRANCH AA20}
{IF A-B<0}{BRANCH AA19}
{BRANCH AA3}
{GOTO}B-/RNCB-{DOWN 2}-{GOTO}A-/RNCA-{DOWN 2}-{LET D,D+0.02}{BRANCH AA10}
{IF X=130}{BRANCH AA22}
/CD-E-{BRANCH AA23}
{BLANK D}{BRANCH AA19}
{GOTO}E-/RNCE-{DOWN}-{GOTO}X-/RNCX-{DOWN}-{LET X,130}{BLANK D}{BRANCH AA19}
```

STAGE 2

EXTRACTS MINIMUM SONIC VALUES WITH CORRESPONDING DEPTHS FOR EACH TROUGH BLOCK

```
/RNCC-A1-/RNCF-BD4-{BLANK C}/RNCJ-A3-{LET J,115}{GOTO}BL1-{LET BP14,3}
{WINDOWSON}{WINDOWSOFF}/RNCW-BE4-{BLANK BD4..BJ1000}{GOTO}B31-
{IF @CELLPOINTER("type")="b"}{BRANCH CB11}
{IF @CELLPOINTER("contents")="BLOCK"}{BRANCH CB8}
{IF @CELLPOINTER("contents")>J}{BRANCH CB7}
{LET C,C+.01}{DOWN}{BRANCH CB3}
{DOWN}-{BRANCH CB3}
/RNDG-{DOWN}/RNCG--
/CC-F-{GOTO}F-/RNCF-{DOWN}-
{GOTO}G-{BLANK C}{BRANCH CB3}
{GOTO}AY1-
{LET J,J-15}{GOTO}W-/RNDF-/RNCW-{RIGHT}-/RNCF--
{IF J=40}{GOTO}BL1-{LET BP14,4}{WINDOWSON}{WINDOWSOFF}{BRANCH AM1}
{GOTO}B31-{BRANCH CB3}
```

STAGE 3

CALCULATES THE WIDTH OF EACH SONIC TROUGH ALONG SPECIFIED SONIC GRID LINES

```
{GOTO}BC4-
{IF @CELLPOINTER("type")="b"}{BRANCH AM6}
/RNCZ-{RIGHT 5}-
{RIGHT 6}@AVG(Z)-
{GOTO}Z-{DOWN}/RNDZ-{BRANCH AM2}
{GOTO}BC4-
{IF @CELLPOINTER("type")="b"}{BRANCH AM12}
{RIGHT 2}-/RNCU-{RIGHT 3}-
{RIGHT 5}@AVG(U)-
{GOTO}U-{DOWN}/RNDU-
{LEFT 2}{BRANCH AM7}
{GOTO}BN25-@NOW-/RV-BO1-
{GOTO}AX1-{LET AX1,BO1-BN1}-{WINDOWSON}{PANELON}
{BEEP}{BEEP 4}{BEEP}{QUIT}
```

STAGE 4

COMPUTES AVERAGE THICKNESS OF EACH HARD BAND USING RESULTS OF STAGE 3

APPENDIX I

NEUTRON MOISTURE PROBE

NEUTRON MOISTURE PROBE

INTRODUCTION

The neutron moisture probe, a downhole geophysical tool, is widely used in the soil sciences to measure moisture content profiles through the near-surface soil horizons (Black and Mitchell, 1986; Chanasyk and Mackenzie, 1986; Chanasyk and Nath, 1988; Holmes, 1966). This was the first test of the device within the plains coal industry. It was used at Big Valley to measure moisture content and density changes in sediment to depths of 10 m.

The instrument used for this study is a Campbell Pacific Nuclear (CPN) model 501DR Depthprobe, capable of measuring bulk density and volumetric moisture of subsurface materials (CPN Corp., 1984). The unit is lightweight (approximately 20 kg), self contained and very portable. Density measurements are made from a 10 mCi Cesium-137 gamma source and gamma detector. A 50 mCi Americium-241/B3 fast-neutron source and thermal neutron detector is used for moisture readings. The probe is 57 cm long and has a diameter of 4.7 cm. Data are transmitted to the surface recording instrument through a multiconductor cable. Additional specifications are available in the equipment specifications sheets attached at the end of this section.

The surface electronic assembly records and displays the density and moisture data, and also acts as a shield for the probe upon retraction from the hole. The assembly comes equipped with a 10 m long cable and moveable cable stops to secure the probe at preselected depths. Longer cable lengths are also available.

The probe requires operation in a dry close-fitting cased hole. An undersized pilot hole was first drilled to the target depth using a Brat22 auger drilling rig. The rig then pushed a single length of casing down the undersized hole to ensure a tight fit between casing and formation. The casing was constructed of 5.1 cm diameter schedule 40 aluminum tubing. Prior to insertion in the hole the end of the casing was plugged and all joints were welded together to provide a sealed, moisture-free hole.

The tool assembly was positioned onto the casing-head protruding 25 cm above ground surface. The probe was then lowered down the cased hole to the selected depth. Moisture and density readings were recorded after a counting time interval of 64 seconds. Measurements were taken at 15 cm depth intervals between surface and 4 m, and at 25 cm intervals below 4 m. Additional readings were taken at 5 cm intervals at zones of particular interest.

The December and January data from Site 1 are similar (Figure 1). Both the moisture and density decrease markedly in the upper 1.5 m. The principal differences between the December and January curves are the result of readings taken at additional depths during the January, 1989 measurements. The close correspondence between the two sets of data is demonstrated by the ratio of the December to January readings (Figure 1).

The data from Site 3 exhibits a similar internal consistency (Figure 2). The density readings are similar to those at Site 1 in that they decrease noticeably within the upper 1.5 m. The moisture however, does not show a similar trend. The spike in the January moisture data, about 6.2 m, is a correct reading as the probe was returned to that depth during the same visit and a similar high reading obtained. The absence from the December reading is because that exact depth was not sampled.

The December and January readings within each data type from each site show a strong reproducibility. Both the moisture ratios and the density ratios are generally within less than 0.05 of 1 (Figures 1 and 2, and Table 1).

	Mean	Standard Deviation	Minimum	Maximum
Site 1 Moisture	1.01	0.016	0.96	1.05
Site 1 Density	1.00	0.011	0.97	1.02
Site 3 Moisture	0.99	0.013	0.97	1.02
Site 3 Density	0.99	0.009	0.98	1.02

Table 1. Ratio of the December 1988 to January 1989 neutron probe moisture and density data for Site 1 and Site 3. The ratios are close to one showing probe readings are reproducible.

Comparison of Neutron Probe and Sample Data

Both the moisture and density data from the neutron probe were compared to that obtained from the samples (Figure 3). The correspondence between the two different data sets was relatively poor compared to similarity between the December and January neutron probe readings. There is however, a consistent relationship between the readings as shown in

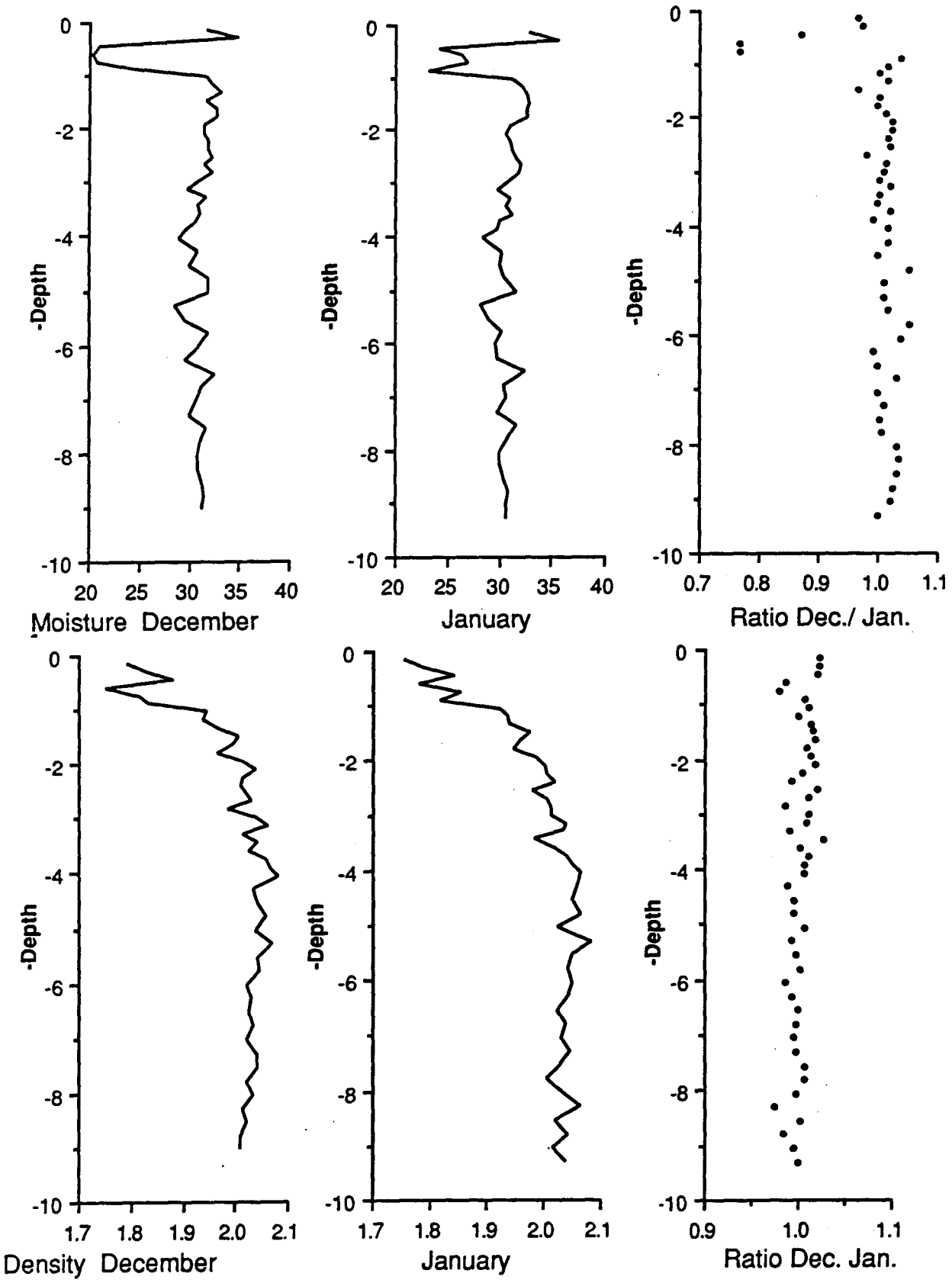

Figure 1. Site 1, comparison of December, 1988 and January 1989 data from neutron probe for volume percent moisture and wet density to demonstrate data reproducibility.

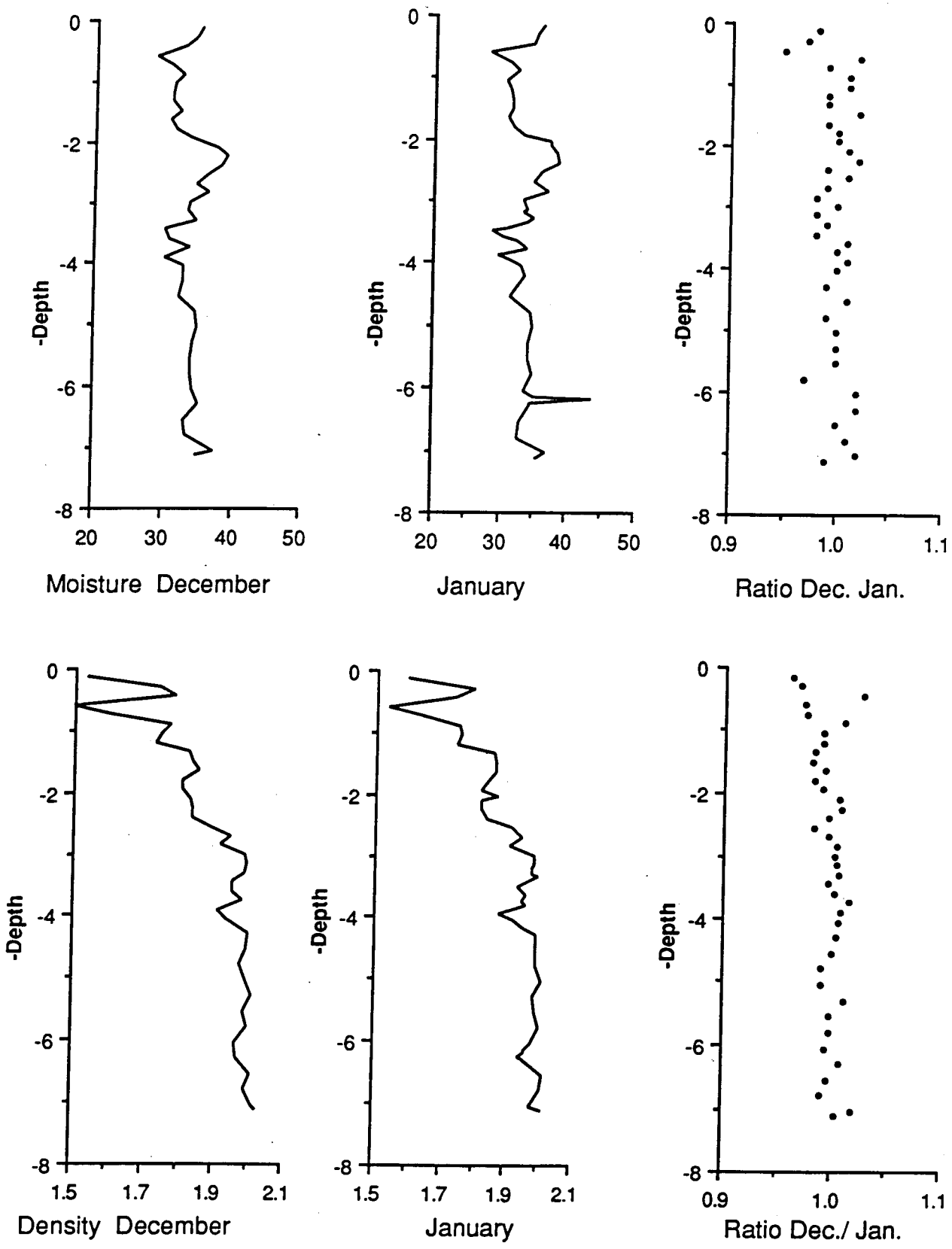

Figure 2. Site 3, comparison of December, 1988 and January 1989 data from neutron probe for volume percent moisture and wet density to demonstrate data reproducibility.

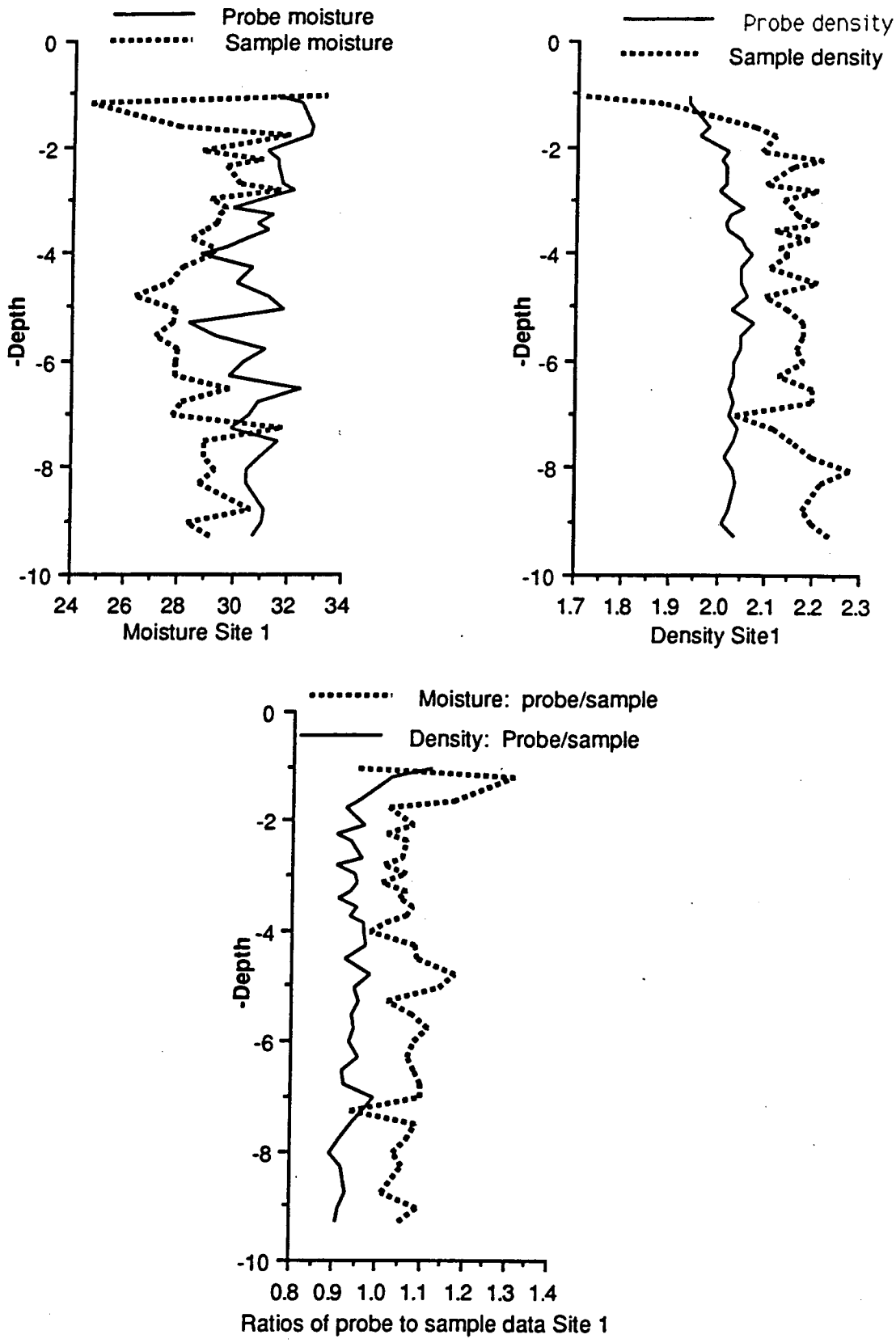

Figure 3. Comparison for Site 1, of moisture and density data from the samples and neutron probe.

Table 2. This is better illustrated by the ratio of the neutron probe reading (average of the December and January readings) to the sample data from the closest corresponding depth interval (Figures 3 and 4). The moisture readings from the probe are generally higher than those from the samples (Figure 3). The probe density readings are generally less than those from the samples.

The comparatively poor correspondence between the probe and sample readings may be the result of the probe reading a shorter interval than the "average" reading obtained from the 15 cm long samples. Certainly the spike shown on the January readings at about the 6 m depth interval (Figure 2) illustrated how a slight difference in probe depth could produce a major difference in the probe readings. Also the 6 m separation of the hole used for the neutron probe measurements and that from which the samples were taken may have contributed to this variability

	Mean	Standard Deviation	Range	Min.	Max.
Moisture					
Probe Site 1 (average)	31.07	1.03	4.63	28.4	33.03
Sample Site 1	28.90	1.50	8.74	24.6	33.61
Probe Site 3 (average)	34.01	2.71	14.9	29.0	43.9
Sample Site 3	32.51	4.04	20.3	22.7	43.1
Density					
Probe Site 1 (average)	2.02	0.032	0.14	1.93	2.07
Sample Site 1	2.15	0.092	0.57	1.72	2.29
Probe Site 3 (average)	1.93	0.072	0.28	1.73	2.02
Sample Site 3	1.99	0.100	0.44	1.71	2.15

Table 2. Comparison of neutron probe data, averaged for December and January readings, to the corresponding sample data for moisture and density.

The neutron probe enables the operator to make numerous readings within one hole and to return to collect subsequent data sets. This probe may be useful for long term monitoring of the moisture conditions within a mine site. The changes in moisture content and density could be related to changes in the sediment conditions with time such as the change in water table resulting from mining.

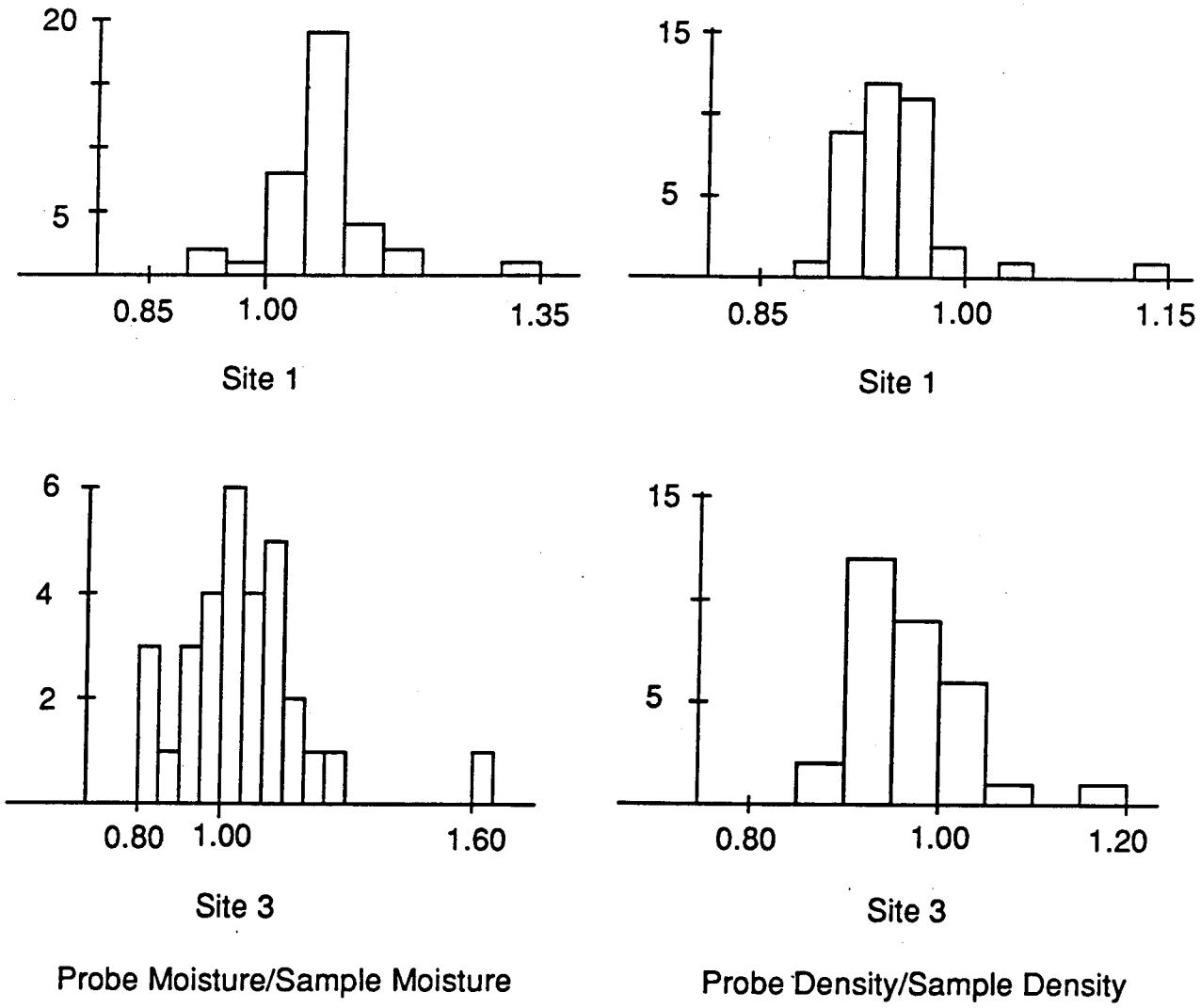

Figure 4. Ratios of probe to sample data. Probe data is average of the December and January readings.

Comparison of Geophysical Logs to Neutron Probe and Sample Data

This comparison was accomplished via three preliminary steps. The data from each of the geophysical logs had to be: (i) depth corrected, (ii) averaged for vertical resolution of the tool, and (iii) the data set thinned from the 1 cm spacing to that which matched the depths the neutron probe readings and/or sample data were collected. These steps consumed much of the time allotted for analysis of the data and therefore only the data from Site 3 were compared. The corrected geophysical logs for Site 3 are illustrated in Figure 5. The loss of data above 3 m for many of the logs severely reduces the amount of data left for comparison.

The densities from the geophysical log, neutron probe and sample analysis are plotted together in Figure 6 for preliminary comparison. The geophysical log density is generally higher than the density measured from samples, while the neutron probe curve is lower, suggesting that the coefficients used to calculate density from these radiation tools may differ from tool to tool. Preliminary comparison of the geophysical log data to the hydrogeological data from the neutron probe and sample shows only slight resemblance between the moisture data and that from the gamma and perhaps density. Additional analysis of these and other data sets is needed before the relationship between density and moisture from the neutron probe and samples can be related to the data from the geophysical log suite.

Water Table

The data from the samples and the neutron probe indicate the water table likely lies within 2 m of the surface (Figure 7). Final confirmation will be made after water levels stabilize in the piezometer wells. The difficulty in using other indicators to locate the water table in place of piezometers is in all likelihood due the high clay content to the sediment. Because of capillary action in the clays, a high percentage of water is retained in the sediment above the water table, thereby producing only a slight gradational change in moisture content that is difficult to detect by other means. Also the responses of geophysical logs are greatly effected by clay sediments, especially the neutron log which additionally measures mineralogically bound water (Keys and MacCary, 1971).

A water table above 2 m precludes any comparison with geophysical log data because the data from most of the logs, in the data sets provided to TSD, extends upward only to 2 or 3 m.

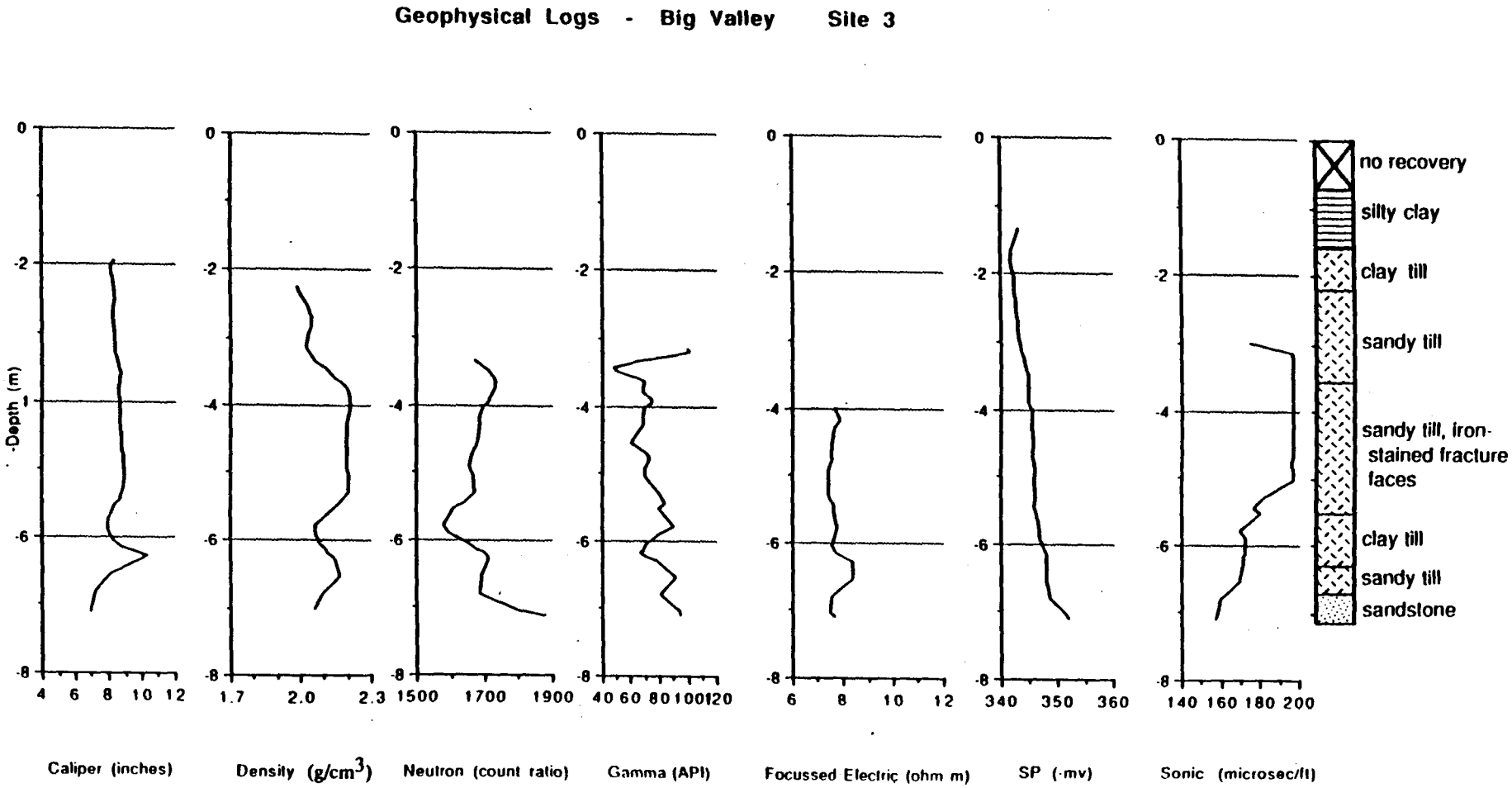

Figure 5. Plots of geophysical logs and lithology from Site 3, Big Valley.

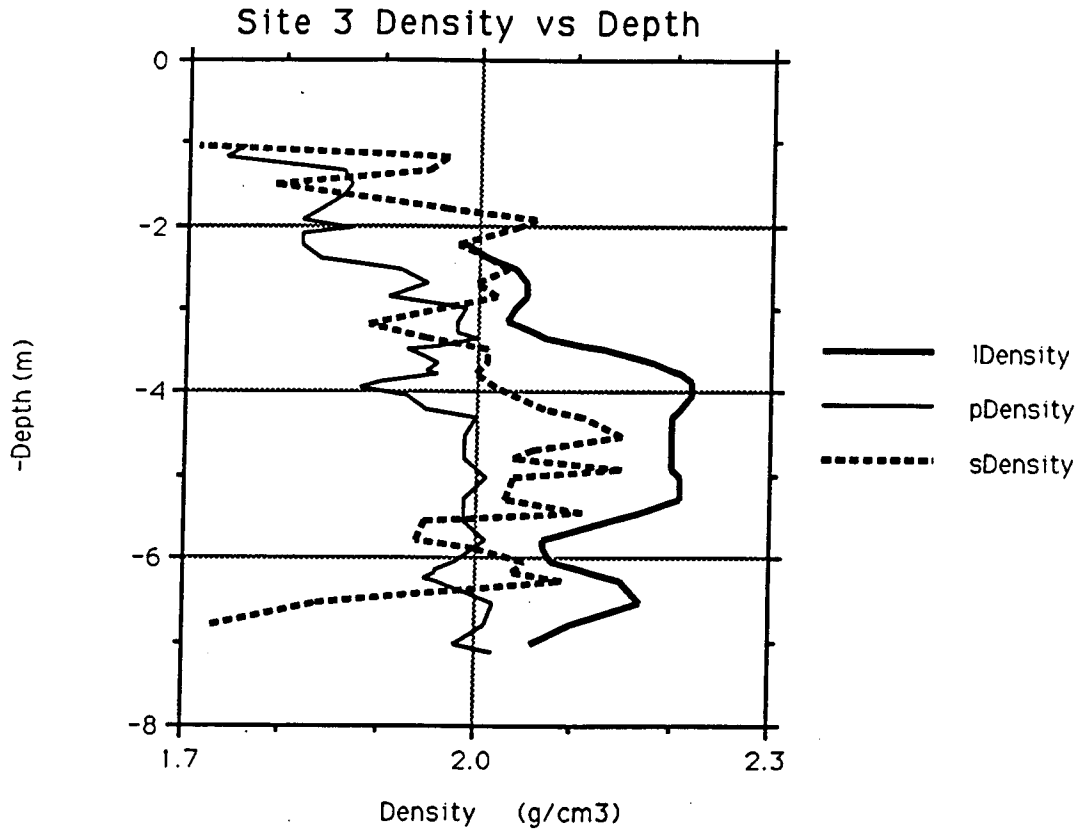

Figure 6. Comparison of bulk density values from the geophysical log, neutron probe and sample data of the upper 7 m from Site 3, Big Valley.

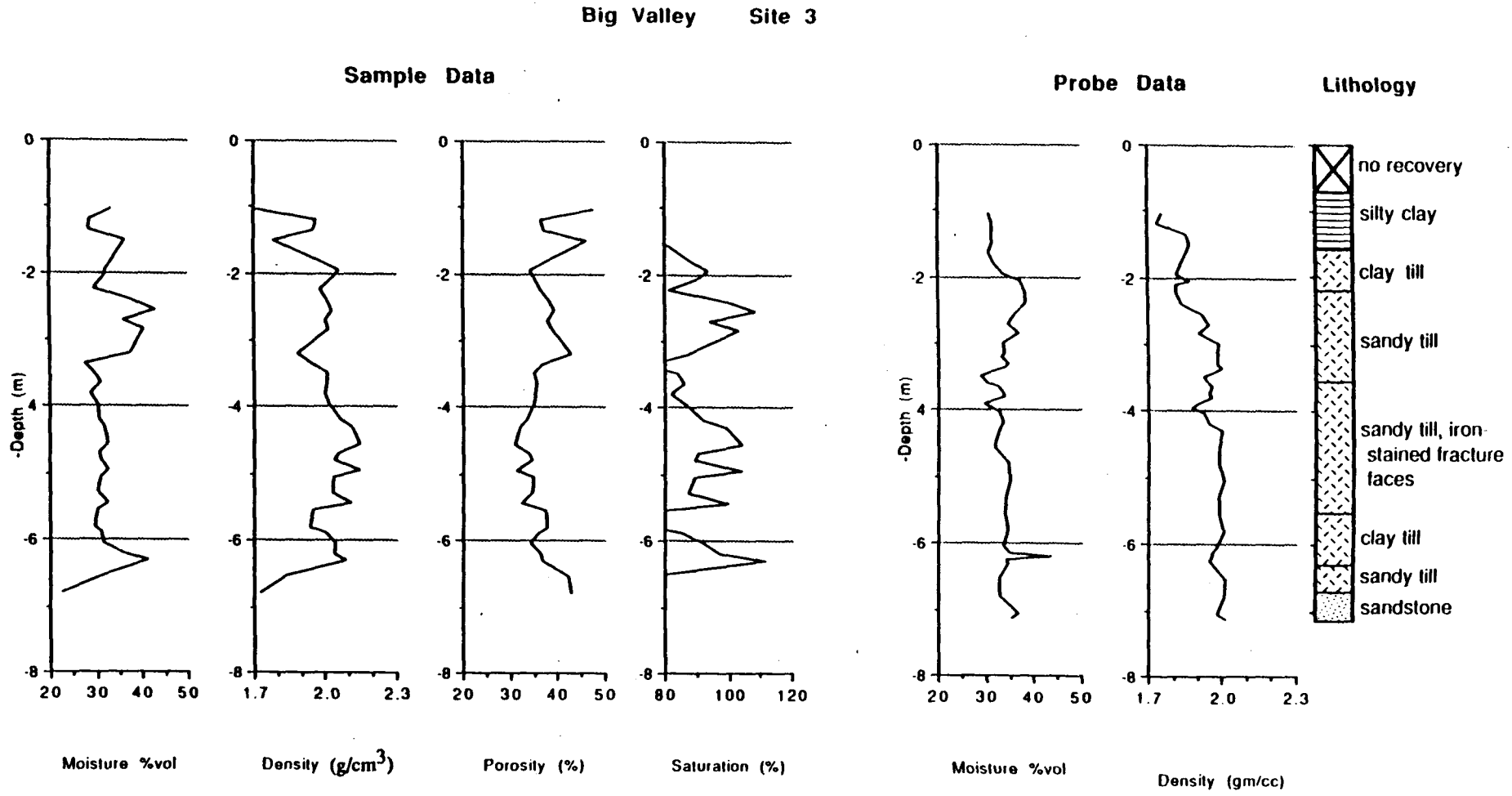

Figure 7. Plots of sample data, neutron probe data and lithology from Site 3, Big Valley.

APPENDIX I

NEUTRON MOISTURE PROBE

NEUTRON MOISTURE PROBE

INTRODUCTION

The neutron moisture probe, a downhole geophysical tool, is widely used in the soil sciences to measure moisture content profiles through the near-surface soil horizons (Black and Mitchell, 1986; Chanasyk and Mackenzie, 1986; Chanasyk and Nath, 1988; Holmes, 1966). This was the first test of the device within the plains coal industry. It was used at Big Valley to measure moisture content and density changes in sediment to depths of 10 m.

The instrument used for this study is a Campbell Pacific Nuclear (CPN) model 501DR Depthprobe, capable of measuring bulk density and volumetric moisture of subsurface materials (CPN Corp., 1984). The unit is lightweight (approximately 20 kg), self contained and very portable. Density measurements are made from a 10 mCi Cesium-137 gamma source and gamma detector. A 50 mCi Americium-241/B3 fast-neutron source and thermal neutron detector is used for moisture readings. The probe is 57 cm long and has a diameter of 4.7 cm. Data are transmitted to the surface recording instrument through a multiconductor cable. Additional specifications are available in the equipment specifications sheets attached at the end of this section.

The surface electronic assembly records and displays the density and moisture data, and also acts as a shield for the probe upon retraction from the hole. The assembly comes equipped with a 10 m long cable and moveable cable stops to secure the probe at preselected depths. Longer cable lengths are also available.

The probe requires operation in a dry close-fitting cased hole. An undersized pilot hole was first drilled to the target depth using a Brat22 auger drilling rig. The rig then pushed a single length of casing down the undersized hole to ensure a tight fit between casing and formation. The casing was constructed of 5.1 cm diameter schedule 40 aluminum tubing. Prior to insertion in the hole the end of the casing was plugged and all joints were welded together to provide a sealed, moisture-free hole.

The tool assembly was positioned onto the casing-head protruding 25 cm above ground surface. The probe was then lowered down the cased hole to the selected depth. Moisture and density readings were recorded after a counting time interval of 64 seconds. Measurements were taken at 15 cm depth intervals between surface and 4 m, and at 25 cm intervals below 4 m. Additional readings were taken at 5 cm intervals at zones of particular interest.

The December and January data from Site 1 are similar (Figure 1). Both the moisture and density decrease markedly in the upper 1.5 m. The principal differences between the December and January curves are the result of readings taken at additional depths during the January, 1989 measurements. The close correspondence between the two sets of data is demonstrated by the ratio of the December to January readings (Figure 1).

The data from Site 3 exhibits a similar internal consistency (Figure 2). The density readings are similar to those at Site 1 in that they decrease noticeably within the upper 1.5 m. The moisture however, does not show a similar trend. The spike in the January moisture data, about 6.2 m, is a correct reading as the probe was returned to that depth during the same visit and a similar high reading obtained. The absence from the December reading is because that exact depth was not sampled.

The December and January readings within each data type from each site show a strong reproducibility. Both the moisture ratios and the density ratios are generally within less than 0.05 of 1 (Figures 1 and 2, and Table 1).

	Mean	Standard Deviation	Minimum	Maximum
Site 1 Moisture	1.01	0.016	0.96	1.05
Site 1 Density	1.00	0.011	0.97	1.02
Site 3 Moisture	0.99	0.013	0.97	1.02
Site 3 Density	0.99	0.009	0.98	1.02

Table 1. Ratio of the December 1988 to January 1989 neutron probe moisture and density data for Site 1 and Site 3. The ratios are close to one showing probe readings are reproducible.

Comparison of Neutron Probe and Sample Data

Both the moisture and density data from the neutron probe were compared to that obtained from the samples (Figure 3). The correspondence between the two different data sets was relatively poor compared to similarity between the December and January neutron probe readings. There is however, a consistent relationship between the readings as shown in

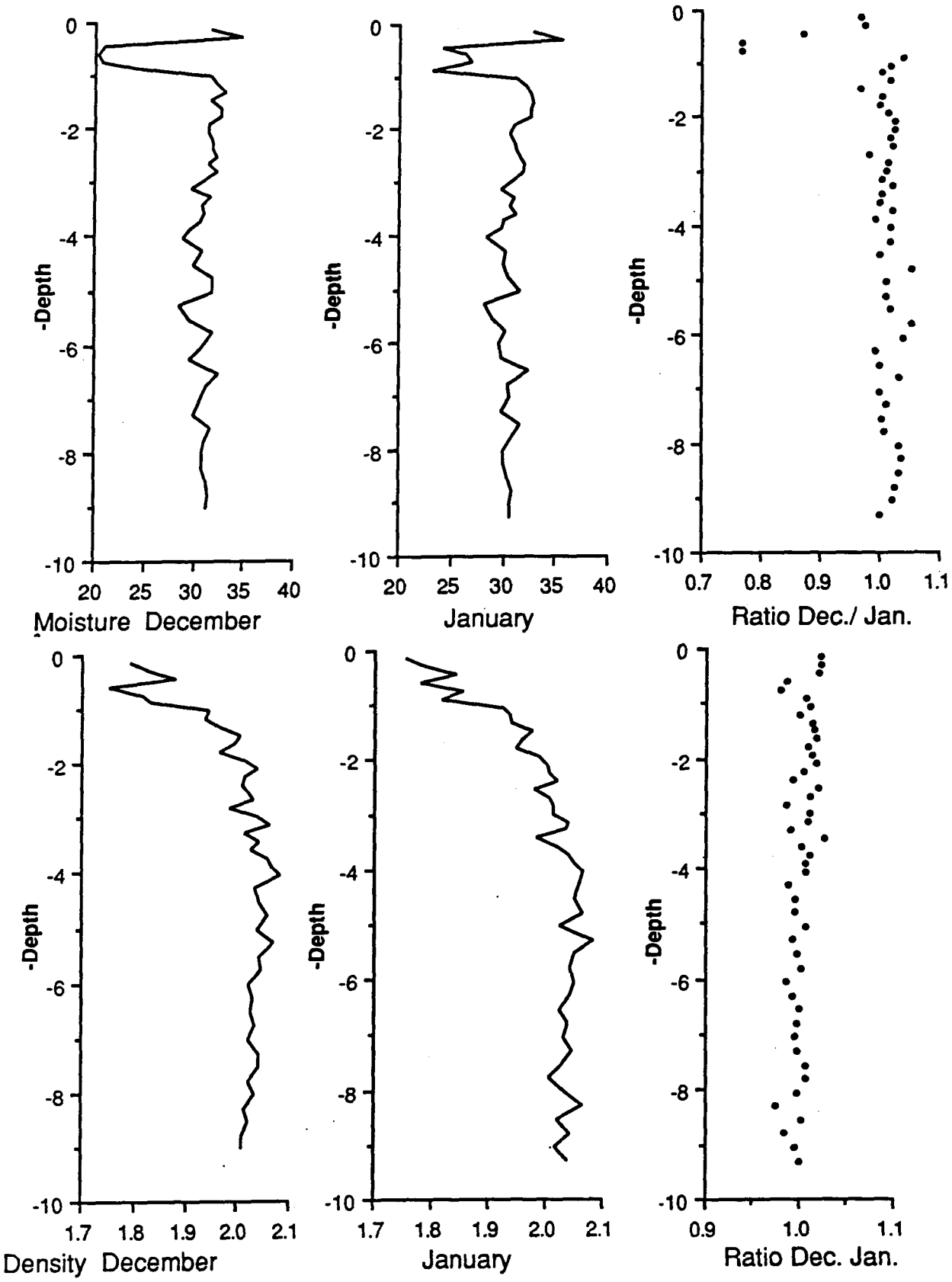

Figure 1. Site 1, comparison of December, 1988 and January 1989 data from neutron probe for volume percent moisture and wet density to demonstrate data reproducibility.

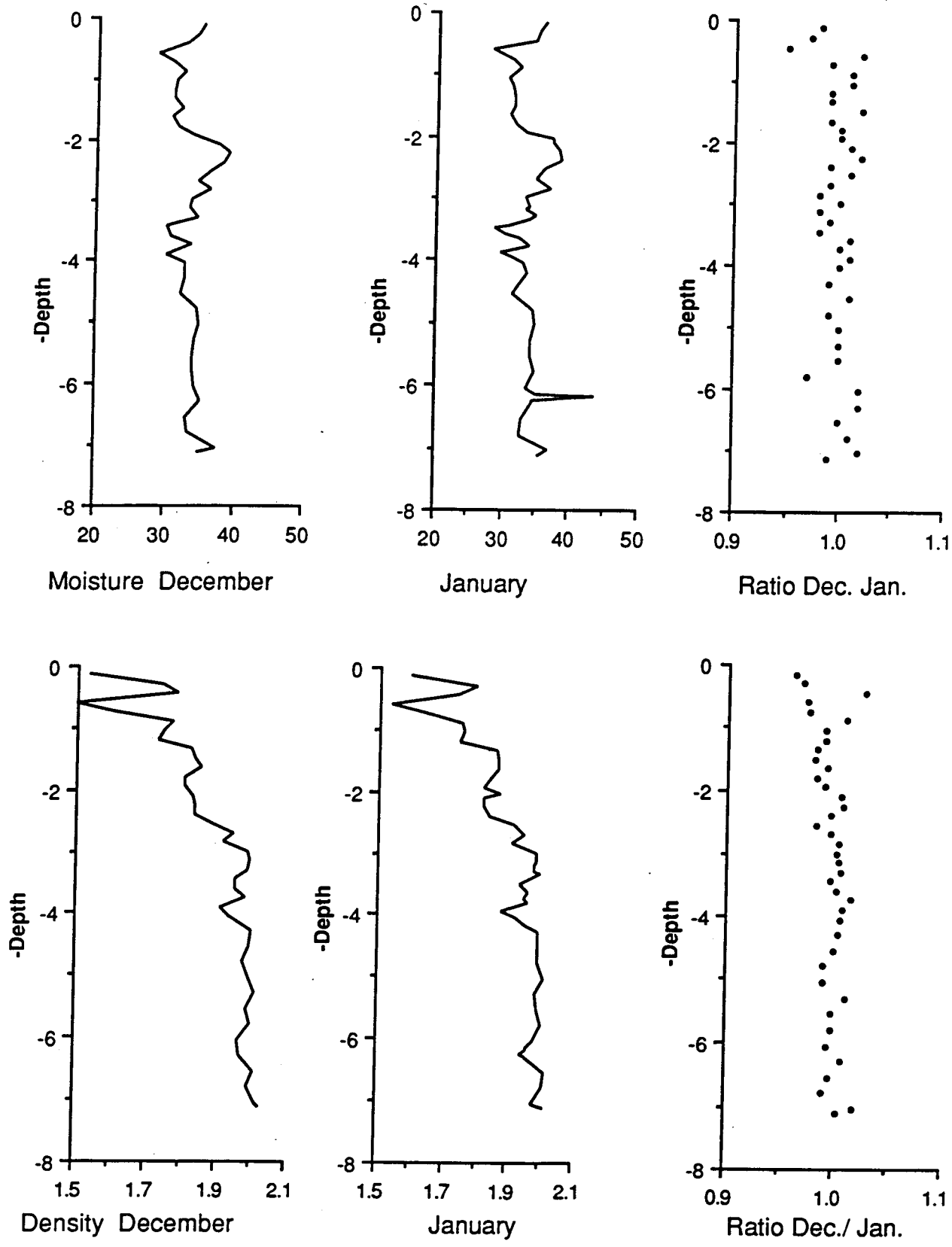

Figure 2. Site 3, comparison of December, 1988 and January 1989 data from neutron probe for volume percent moisture and wet density to demonstrate data reproducibility.

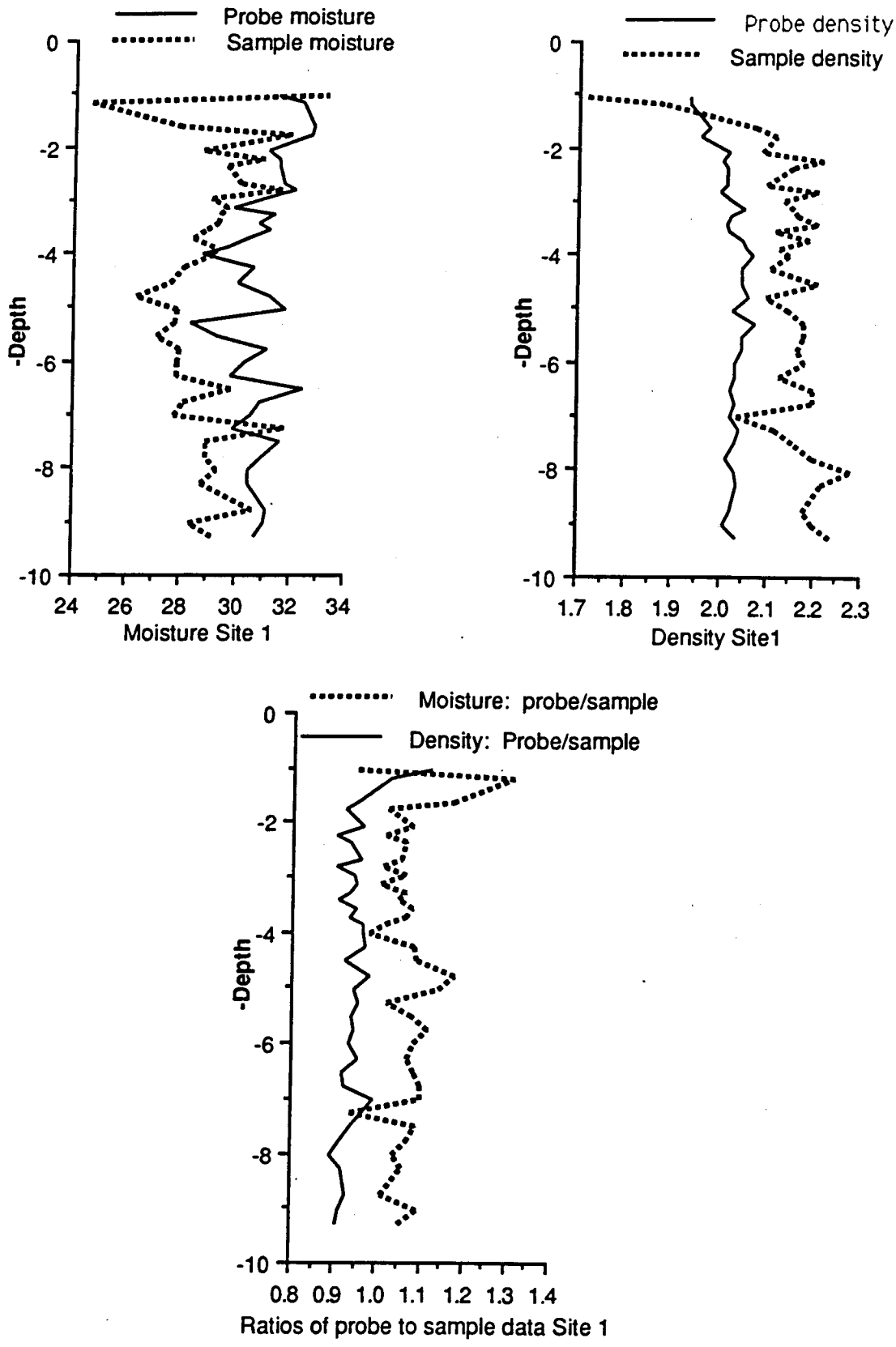

Figure 3. Comparison for Site 1, of moisture and density data from the samples and neutron probe.

Table 2. This is better illustrated by the ratio of the neutron probe reading (average of the December and January readings) to the sample data from the closest corresponding depth interval (Figures 3 and 4). The moisture readings from the probe are generally higher than those from the samples (Figure 3). The probe density readings are generally less than those from the samples.

The comparatively poor correspondence between the probe and sample readings may be the result of the probe reading a shorter interval than the "average" reading obtained from the 15 cm long samples. Certainly the spike shown on the January readings at about the 6 m depth interval (Figure 2) illustrated how a slight difference in probe depth could produce a major difference in the probe readings. Also the 6 m separation of the hole used for the neutron probe measurements and that from which the samples were taken may have contributed to this variability

	Mean	Standard Deviation	Range	Min.	Max.
Moisture					
Probe Site 1 (average)	31.07	1.03	4.63	28.4	33.03
Sample Site 1	28.90	1.50	8.74	24.6	33.61
Probe Site 3 (average)	34.01	2.71	14.9	29.0	43.9
Sample Site 3	32.51	4.04	20.3	22.7	43.1
Density					
Probe Site 1 (average)	2.02	0.032	0.14	1.93	2.07
Sample Site 1	2.15	0.092	0.57	1.72	2.29
Probe Site 3 (average)	1.93	0.072	0.28	1.73	2.02
Sample Site 3	1.99	0.100	0.44	1.71	2.15

Table 2. Comparison of neutron probe data, averaged for December and January readings, to the corresponding sample data for moisture and density.

The neutron probe enables the operator to make numerous readings within one hole and to return to collect subsequent data sets. This probe may be useful for long term monitoring of the moisture conditions within a mine site. The changes in moisture content and density could be related to changes in the sediment conditions with time such as the change in water table resulting from mining.

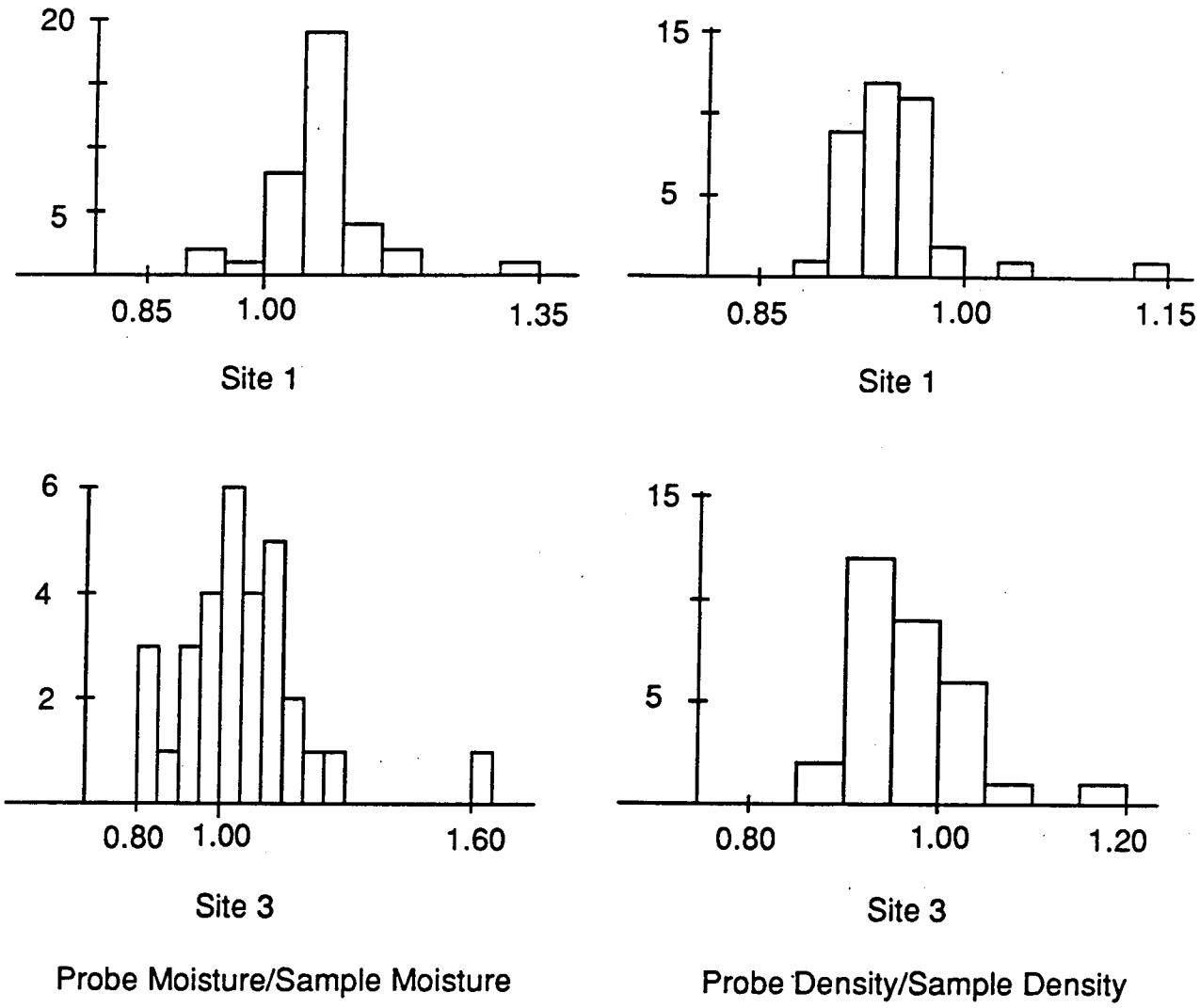

Figure 4. Ratios of probe to sample data. Probe data is average of the December and January readings.

Comparison of Geophysical Logs to Neutron Probe and Sample Data

This comparison was accomplished via three preliminary steps. The data from each of the geophysical logs had to be: (i) depth corrected, (ii) averaged for vertical resolution of the tool, and (iii) the data set thinned from the 1 cm spacing to that which matched the depths the neutron probe readings and/or sample data were collected. These steps consumed much of the time allotted for analysis of the data and therefore only the data from Site 3 were compared. The corrected geophysical logs for Site 3 are illustrated in Figure 5. The loss of data above 3 m for many of the logs severely reduces the amount of data left for comparison.

The densities from the geophysical log, neutron probe and sample analysis are plotted together in Figure 6 for preliminary comparison. The geophysical log density is generally higher than the density measured from samples, while the neutron probe curve is lower, suggesting that the coefficients used to calculate density from these radiation tools may differ from tool to tool. Preliminary comparison of the geophysical log data to the hydrogeological data from the neutron probe and sample shows only slight resemblance between the moisture data and that from the gamma and perhaps density. Additional analysis of these and other data sets is needed before the relationship between density and moisture from the neutron probe and samples can be related to the data from the geophysical log suite.

Water Table

The data from the samples and the neutron probe indicate the water table likely lies within 2 m of the surface (Figure 7). Final confirmation will be made after water levels stabilize in the piezometer wells. The difficulty in using other indicators to locate the water table in place of piezometers is in all likelihood due the high clay content to the sediment. Because of capillary action in the clays, a high percentage of water is retained in the sediment above the water table, thereby producing only a slight gradational change in moisture content that is difficult to detect by other means. Also the responses of geophysical logs are greatly effected by clay sediments, especially the neutron log which additionally measures mineralogically bound water (Keys and MacCary, 1971).

A water table above 2 m precludes any comparison with geophysical log data because the data from most of the logs, in the data sets provided to TSD, extends upward only to 2 or 3 m.

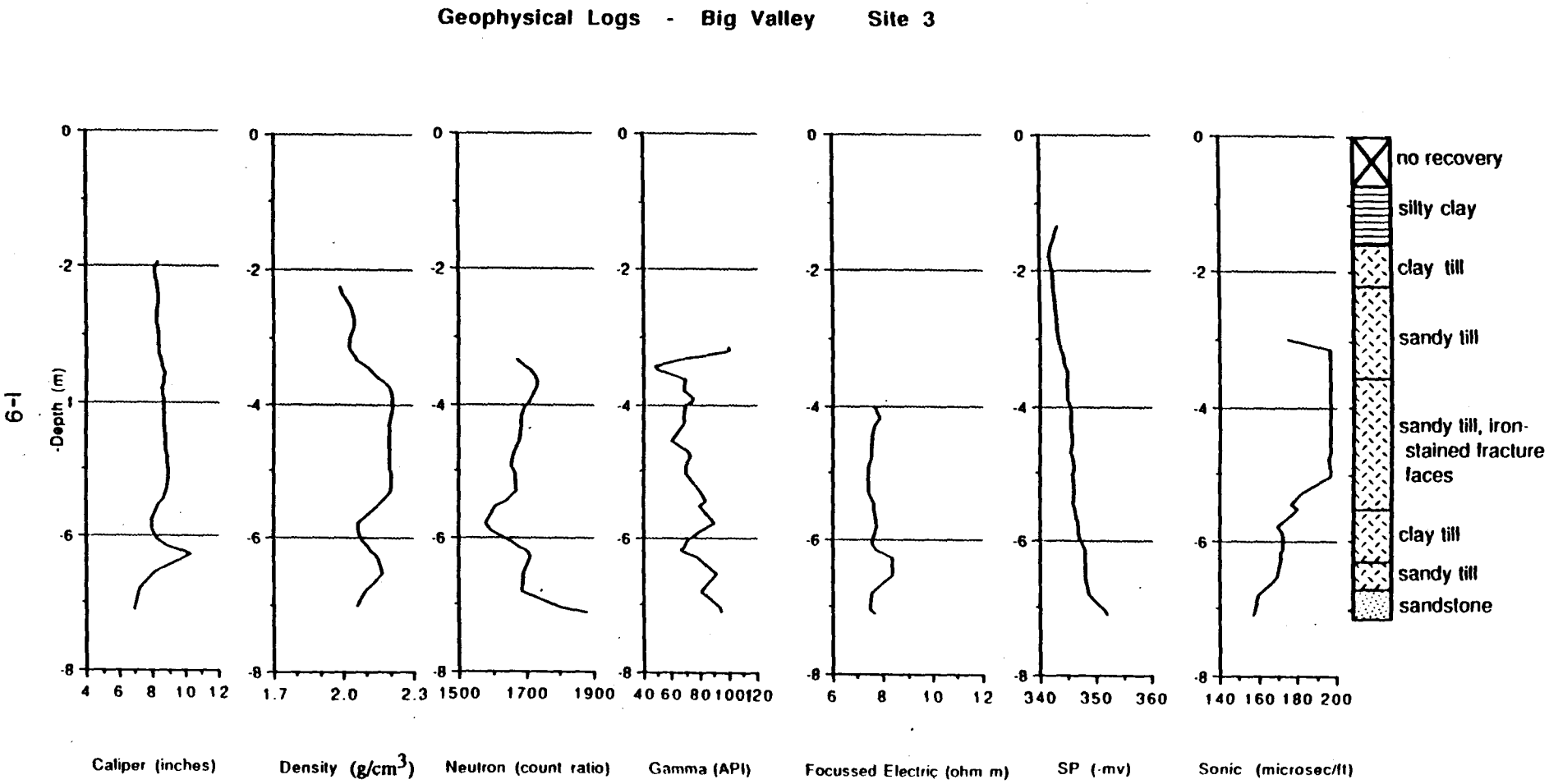

Figure 5. Plots of geophysical logs and lithology from Site 3, Big Valley.

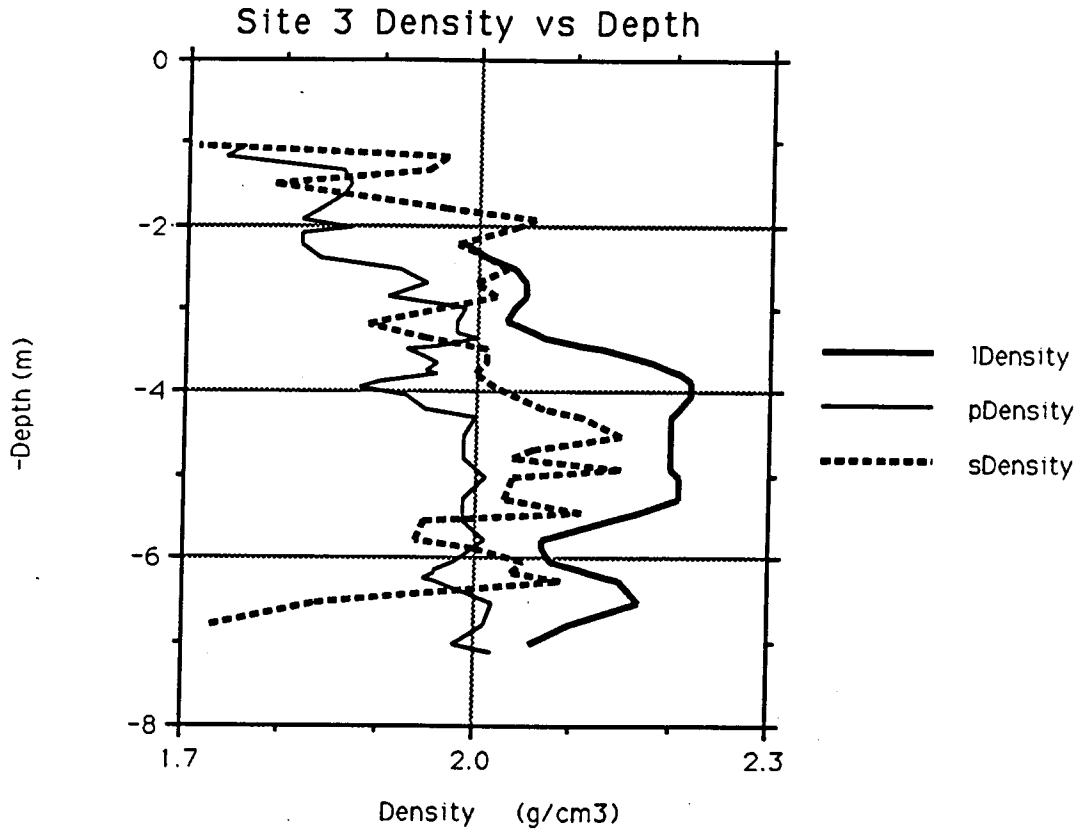

Figure 6. Comparison of bulk density values from the geophysical log, neutron probe and sample data of the upper 7 m from Site 3, Big Valley.

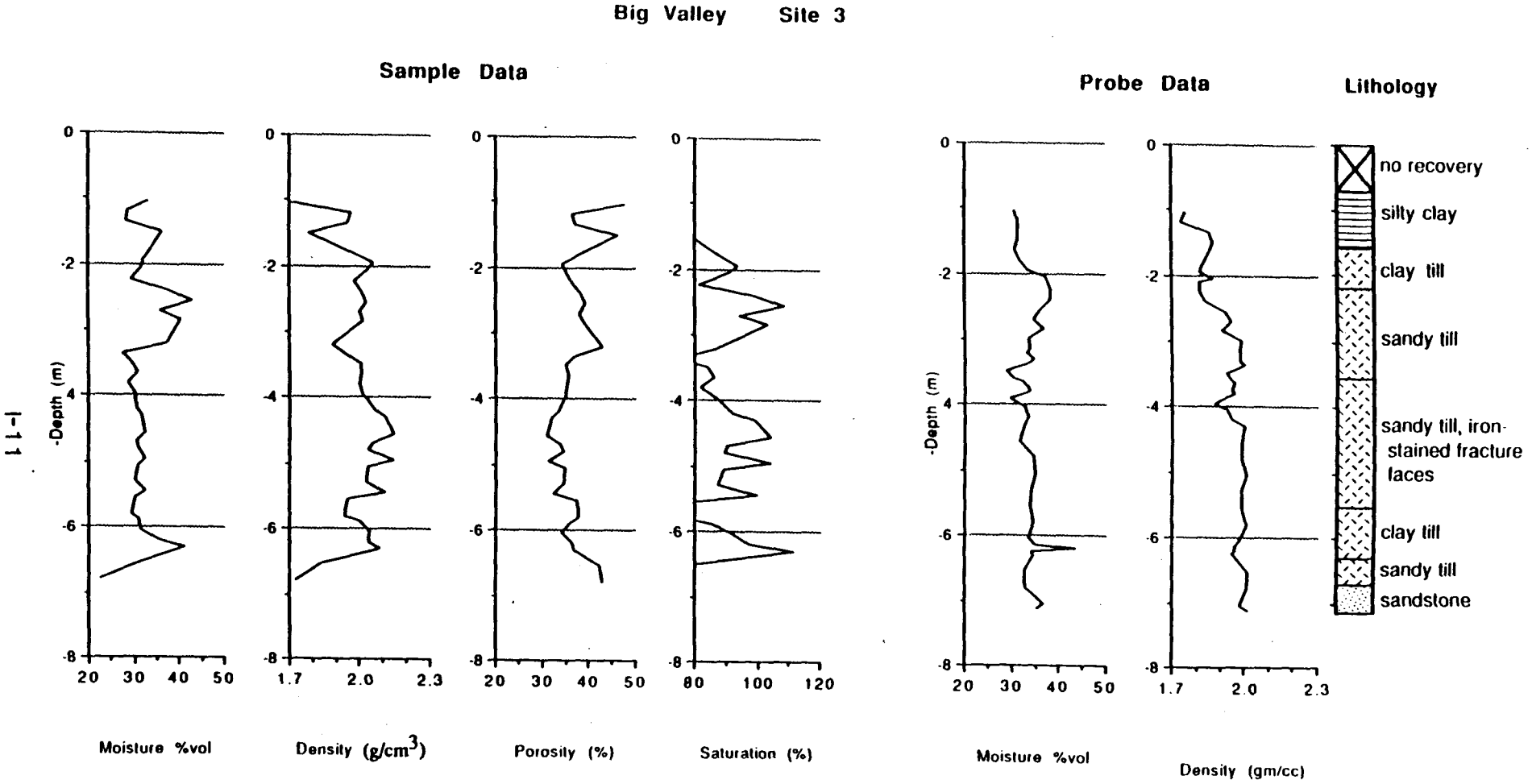

Figure 7. Plots of sample data, neutron probe data and lithology from Site 3, Big Valley.

NEUTRON MOISTURE PROBE - MODEL 501DR

SPECIFICATIONS

OPERATOR'S MANUAL

501DR DEPTHPROBE
MOISTURE DEPTH GAUGE

CPN CORP

130 SOUTH BUCHANAN CIRCLE PACHECO, CALIFORNIA 94553

PHONE (415) 687-6472 TELEX 171289 CPN CORP PACH

501 DR DEPTHPROBE
TABLE OF CONTENTS
(White Section)

SOFTWARE VERSION 50102 June 27, 1984

1.0 GENERAL

1.1 INTRODUCTION

The Model 501DR DEPTHPROBE, DEPTH DENSITY-MOISTURE GAGE measures sub-surface density and moisture in soil and other materials by use of a probe containing a gamma source and a GM detector for density and a fast neutron source and thermal neutron detector for moisture. The probe is lowered into a pre-drilled and cased hole to the depth of measurement. The density and moisture data are displayed directly in units of interest on an above-surface electronic assembly which is integral to the source shield assembly. The data is also stored for later dump to an off-line printer or computer.

The gage is supplied with a 10 meter (33 ft) cable and a moveable cable stop. The cable is marked at one meter intervals. Semi-permanent cable stops which can be placed at fixed positions and longer cable lengths are available as options.

Upon retraction of the probe into the shield, the probe locks automatically in place for transport.

The complete assembly is supplied with a plastic shipping and carrying container which contains: accessory items, cable, instruction manual, charger, and other materials which the operator may wish to carry.

1.2 SPECIFICATIONS

FUNCTION:	Sub-surface density and moisture measurements.
RANGE:	Density: 70 to 170 pcf, (1.12 to 2.723 g/cm3). Moisture: 0 to 80% vol, (0.80 g/cm3), (50 pcf), (9.6 in/ft).
PRECISION:	Density: 0.6 pcf at 125 pcf at one minute. (0.01 g/cm3 at 2.002 g/cm3) Moisture: 0.24% at 24% vol at one minute.
COUNT TIME:	1, 4, 16, 32, 64, and 256 sec.
TEMP:	0 TO 70oC operating.
POWER:	AA NICADS battery pack (0.5 Ah) 8 cells.
BATTERY LIFE:	500-1000 Charge-discharge cycles.
CONSUMPTION:	7.5 mA avg. (allows more than 3000 each 16 sec counts).
RECHARGE:	14 hours at C/10 via wall charger.
DISPLAY:	8 character alpha/numerical Liquid-Crystal Display. Easily readable in direct sunlight.
DATA STORAGE:	3070 cells of; counts, identifiers, or keyboard entry of auxiliary values. Format operator programmable. 0-15 key and 0-15 density-moisture count pairs per record
DATA OUTPUT:	RS232C serial dump to external printer, computer, CRT or coupler.
CALIBRATION:	8 ea user programmed (log for density, linear for moisture).
UNITS:	User selectable: Density: pcf, g/cm3, count and count ratio. Moisture: in/ft, pcf, g/cm3, % vol, cm/30cm, count and count ratio.
GAMMA SOURCE:	10 mCi Cesium-137
NEUTRON SOURCE:	50 mCi Americium-241/Be
ENCAPSULATION:	Double Sealed Capsules, CPN-131
SHIELDING:	Lead for gamma and silicon based paraffin for neutrons
SHIPPING:	Radioactive Material, Special Form, N.O.S., UN2974 Transport Index 0.1 YELLOW II Label USA DOT 7A, Type A Package
SPECIAL FORM:	USA/0115/S
CONSTRUCTION:	Aluminum with epoxy paint or hard-anodize finish. Stainless steel wear parts
SURFACE UNIT:	41.1#, 6.8"Wx7.0"Dx22.2"H (18.6),(172.7x177.8x563.9)
PROBE: Model -2	7.5#, 1.865" dia x 22.7"L (3.4), (47.4 dia x 576.6)
Model -1.5	7.0#, 1.500" dia x 22.7"L (3.14), (38.1 dia x 576.6)
CARRYING & SHIPPING:	76.0#, 28.5"Wx13.7"Dx16.0"H (33.7), (723.9 x 348 x 406.4)

APPENDIX J

FULLWAVE SONIC SONDE - BPB SPECIFICATIONS

FULL WAVE SONIC

Fully digitised, continuous waveform sonic logs have been available with oilfield equipment for a number of years. However it has been impractical and cost prohibitive to develop this measurement for a slimline application on a commercial basis.

A slimline Sidewall Sonic Sonde (SSL) has been developed by BPB Wireline Services which allows stationary waveform measurement to be taken in the borehole.

The SSL Sonde has two piezo electric transducers, with an 18 inch spacing between the transmitter and receiver. The tool is held sidewall by a caliper arm to increase the amount of S-wave energy input into the formation. A sonic pulse is fired from the transducer (Tx) and the waveform seen at the receiver (Rx) is transmitted to the surface.

Currently the waveforms are either photographed from the scope using a Polaroid scope camera, and interpreted manually, or digitized and held on floppy after which they can be interpreted interactively using special BPB software. The results are a delta t S and delta t P from which Poisson's ration can be calculated. With a density log, we can also calculate Young's moduli, Bulk Moduli or Shear Moduli. These mechanical properties are useful in excavation design and support design. They are also useful in comparison with bulk measurements made over a larger scale.

The values picked from the waveforms are:-

1) the time in microseconds from the transmitter pulse to the P-wave arrival;

2) the time in microseconds from the transmitter pulse to the S-wave arrival.

Sonic Measurements will become problematic in badly caved sections of the borehole or in unconsolidated (or other) formations where adequate acoustic coupling cannot be achieved. Slow P or S arrivals will be masked if they are later than the fluid arrival. Typical fluid arrivals are.

	Travel Time	Velocity
Pure water	207 s/ft	4,830 ft/sec
	680 s/m	1.5 Km/sec
200,000 ppm NaCl	180.5 ms/ft	5540 ft/sec
at 15 psi	592 s/m	1.7 Km/sec

GENERAL SPECIFICATIONS:

Length	-3.67m (12 ft.)
Weight	-20kg (44 lbs)
Diameter	-57mm (2 1/4 in)
Temperature	-up to 70 C (158 F)
Pressure	-up to 210kg/cm^2 (3000 psi)

OPERATING CONDITIONS:

Hole Depth	-to a max of 2000m (6500 ft)
Hole Diameter	-Open hole 75mm to 300mm (3 in to 12 in)
Logging Speed	-Stationary
Logging mode	-Sidewall Clamped, open fluid filled boreholes

When the S wave arrival is coincident with the fluid arrival it will not be seen. This is controlled by Poissons Ratio and for a particular formation it is possible to determine the maximum P-wave slowness that can be tolerated before the S-wave is lost. For example:-

$$\text{Poissons Ratio} \quad \text{Sigma} = \frac{(R^2 - 2)}{2\ (R^2 - 1}$$

$$\text{Where } R = \frac{\text{delta t shear}}{\text{delta t compressional}}$$

$$\text{and } 0 \leq \text{sigma} \leq 0.5$$

The largest delta t compressional is associated with sigma = 0 and under this condition R= 2 = 1.414. Assuming the fluid slowness is 189 microseconds per ft. (620 microseconds per metre), the maximum delta t compressional for sigma = 0 is 189/ 2 = 134 microseconds per ft. (438 microseconds per metre).

This figure is the absolute maximum. A more realistic minimum sigma is 0.1 corresponding to R=15 or a delta t compressional of 126 microseconds per ft. (413 microseconds per metre). We therefore do not expect to see a S-wave arrival if the P-wave velocity is slower than 126 microseconds per ft. (413 microseconds per metre).

SLIMLINE SERVICES

SS1 SIDEWALL SONIC SONDE (or 3DSVL)

FIELD INSTRUMENTATION

SUBSURFACE No.19

MEASUREMENTS:

SONIC TRANSIT WAVETRAIN

Two piezo electric transducers are clamped to the borehole wall with the eccentering caliper arm and operate in a direction normal to the borehole wall.
A sonic pulse is fired from the top transducer (Tx) and the waveform, seen at the reciever (Rx) is photographed on an oscilloscope or digitally recorded at the surface. This wavetrain can then be analysed to provide P and S wave velocities for the formation of interest.

GENERAL SPECIFICATIONS:

Length	— 3.67 m (12 ft.)
Weight	— 20 kg (44 lbs)
Diameter	— 57 mm ($2^1/_4$ in)
Temperature	— up to 70° C (158°F)
Pressure	— up to 210 kg/cm^2 (3000 psi)

OPERATING CONDITIONS:

Hole Depth	— to a max of 2000m (6500ft)
Hole Diameter	— Open hole 75 mm to 300 mm (3 in to 12 in)
Logging Speed	— Stationary
Logging mode	— Sidewall Clamped, open fluid filled boreholes

Sonic Measurements will become problematic in badly caved sections of the borehole or in unconsolidated (or other) formations where adequate acoustic coupling cannot be acheived. Slow P or S arrivals will be masked if they are later than the fluid arrival. Typical fluid arrivals are .

	Travel Time	Velocity
Pure water	207 µs/ft	4,830 ft/sec
	680 µs/m	1.5 Km/sec
200,000 ppm NaCl at 15 psi	180.5 ms/ft	5540 ft/sec
	592 µs/m	1.7 Km/sec

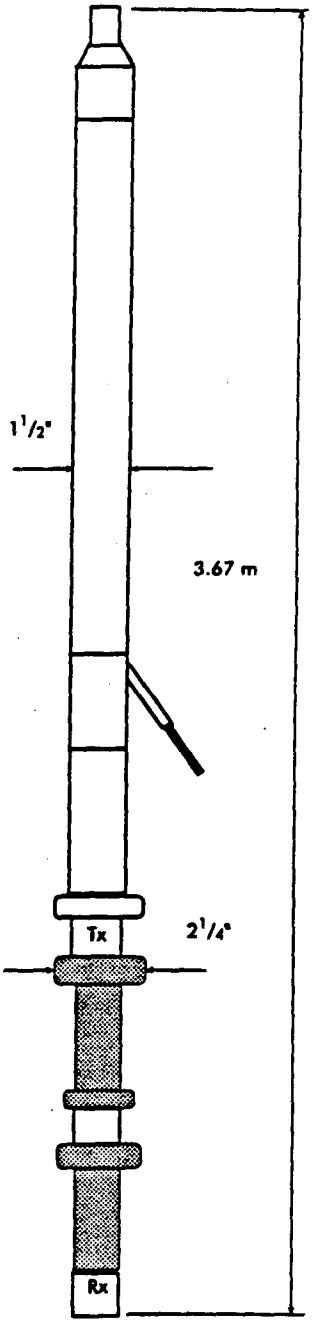

SS1 SCHEMATIC